PUB-5456

Report on
Ernest Orlando Lawrence
Berkeley National Laboratory

Laboratory Directed Research and Development Program

FY 1999

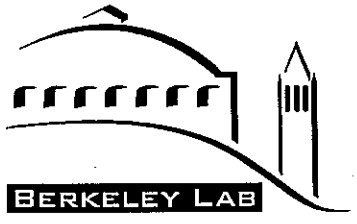

Ernest Orlando Lawrence
Berkeley National Laboratory
Berkeley, California 94720

Office of Science
U.S. Department of Energy

Prepared for the U.S. Department of Energy under Contract No. DE-AC03-76SF00098

Table of Contents

Introduction

The Ernest Orlando Lawrence Berkeley National Laboratory (Berkeley Lab or LBNL) is a multi-program national research facility operated by the University of California for the Department of Energy (DOE). As an integral element of DOE's National Laboratory System, Berkeley Lab supports DOE's missions in fundamental science, energy resources, and environmental quality. Berkeley Lab programs advance four distinct goals for DOE and the nation:

- To perform leading multidisciplinary research in the energy sciences, general sciences, biosciences, and computing sciences in a manner that ensures employee and public safety and protection of the environment.
- To develop and operate unique national experimental facilities for qualified investigators.
- To educate and train future generations of scientists and engineers to promote national science and education goals.
- To transfer knowledge and technological innovations and to foster productive relationships among Berkeley Lab's research programs, universities, and industry in order to promote national economic competitiveness.

Berkeley Lab's programs, all unclassified, support DOE's mission for "a secure and reliable energy system that is environmentally and economically sustainable" and for "continued United States leadership in science and technology," as enunciated in DOE's Strategic Plan. These efforts support the Comprehensive National Energy Strategy to "work internationally on global issues," to "improve the efficiency of the energy system," and to "expand future energy choices through wise investments in basic science and new technologies."

The *Berkeley Lab Laboratory Directed Research and Development Program* FY 1999 report is compiled from annual reports submitted by principal investigators following the close of the fiscal year. This report describes the supported projects and summarizes their accomplishments. It constitutes a part of the Laboratory Directed Research and Development (LDRD) program planning and documentation process that includes an annual planning cycle, projection selection, implementation, and review.

The Berkeley Lab LDRD program is a critical tool for directing the Laboratory's forefront scientific research capabilities toward vital, excellent, and emerging scientific challenges. The program provides the resources for Berkeley Lab scientists to make rapid and significant contributions to critical national science and technology problems. The LDRD program also advances Berkeley Lab's core competencies, foundations, and scientific capability, and permits exploration of exciting new opportunities. All projects are work in forefront areas of science and technology. Areas eligible for support include the following:

- Advanced study of hypotheses, concepts, or innovative approaches to scientific or technical problems;
- Experiments and analyses directed toward "proof of principle" or early determination of the utility of new scientific ideas, technical concepts, or devices; and
- Conception and preliminary technical analyses of experimental facilities or devices.

The LDRD program supports Berkeley Lab's mission in many ways. First, because LDRD funds can be allocated within a relatively short time frame, Berkeley Lab researchers can support the mission of the Department of Energy (DOE) and serve the needs of the nation by quickly responding to forefront scientific problems. Second, LDRD enables Berkeley Lab to attract and retain highly qualified scientists and supports their efforts to carry out world-leading research. In addition, the LDRD program also supports new projects that involve graduate students and postdoctoral fellows, thus contributing to the education mission of Berkeley Lab.

Berkeley Lab has a formal process for allocating funds for the LDRD program. The process relies on individual scientific investigators and the scientific leadership of Berkeley Lab to identify opportunities that will contribute to scientific and

institutional goals. The process is also designed to maintain compliance with DOE Orders, in particular DOE Order 413.2 dated March 5, 1997. From year to year, the distribution of funds among the scientific program areas changes. This flexibility optimizes Berkeley Lab's ability to respond to opportunities.

Berkeley Lab LDRD policy and program decisions are the responsibility of the Laboratory Director. The Director has assigned general programmatic oversight responsibility to the Deputy Director for Research. Administration and reporting on the LDRD program is supported by the Directorate's Office for Planning and Communications. LDRD accounting procedures and financial management are consistent with the Laboratory's accounting principles and stipulations under the contract between the University of California and the Department of Energy, with accounting maintained through the Laboratory's Chief Financial Officer.

In FY99, Berkeley Lab was authorized by DOE to establish a funding ceiling for the LDRD program based on 3.9% of Berkeley Lab's FY99 operating and capital equipment budgets. This funding level was provided to develop new scientific ideas and opportunities and allow the Berkeley Lab Director an opportunity to initiate new directions. Budget constraints limited available resources, however, so only $9.9 M was expended for operating and $0.7 M for capital equipment.

In FY99, scientists submitted 183 proposals, requesting over $27.8 M in operating funding. Eighty-five projects were funded, with awards ranging from $20 K to $368 K. These projects are listed in the Table of Contents.

Dynamics of Low-Emittance Electron Rings with Applications to High Energy Physics Colliders

Principal Investigators: John Corlett

Project No.: 99001

Project Description

This proposal represents a collaboration between the Accelerator and Fusion Research and Physics Divisions in the conceptualization of future high energy physics colliders. Consistent with the goals set by the recent HEPAP subpanel report "Planning for the Future of U.S. High Energy Physics" the project will develop and apply our existing and significant experience in low-emittance storage ring accelerator physics and engineering, and radiation-hardened electronics and novel controls systems for large accelerators.

We propose to develop the understanding and key technologies of low-emittance storage ring systems. This work will include optimizing lattice schemes for low-emittance and rapidly-damped beams, studies of impedance minimization and collective effects, and feedback systems to control residual beam motion. In collaboration with the Physics Division, we propose to utilize the existing expertise in radiation-hardened electronics to develop novel concepts in control system design, integrating radiation-hardened electronics located near the accelerator and incorporating complex algorithm's to allow efficient accelerator physics studies and manipulation of the beams in feedback and feedforward loops.

Accomplishments

We have begun studies of minimal impedance components for storage rings, most notably the accelerating radio frequency (rf) cavities, and fast-pulsed injection/extraction kickers. To take full advantage of low-emittance beams, it is important to operate below instability thresholds. Instabilities may be driven by electromagnetic fields coupling between particles within a single bunch, or by coupling through fields generated by a leading bunch and experienced by following bunches. In both cases, the dominant mechanism is wakefields produced in the vacuum chamber. Other instability mechanisms include coupling through ion clouds in the residual gas. The strength of the interaction between the beam and its environment is characterized by the beam impedance. Instabilities generally have a threshold current or impedance below which the natural damping mechanisms suppress the motion induced by the beam self-fields. Above threshold, the growth rate of the self-induced motion exceeds the damping rate, and beam quality degrades. Feedback and feedforward systems may help avoid instabilities by adding to the natural damping rate.

For the case of the rf cavities, a design using waveguide-damped structures has been conceptualized and modeled in 3-D electromagnetic simulation computer codes. The impedance appears to be suitably low, with cavity higher-order-modes reduced by several orders of magnitude. Since the rf cavities offer a very inviting geometry for accumulation of rf power, they are the dominant impedance in most rings, driving coupled-bunch motion in many modes. Clearly, suppression of this impedance is a goal to be strongly pursued. We have a sound conceptual design for the cavity, and are pursuing the design now by investigating more efficient and cost-effective means of absorbing the power deposited in higher-order-modes of the cavity. One concept is to connect waveguides to the cavity and absorb the rf power in resistive material inside the waveguide; an alternate approach is to convert from waveguide modes into coaxial modes, and then use commercially available high-power coaxial loads to absorb the power. Since the bandwidth required is large (approximately 1 to 8 GHz), we are currently favoring the waveguide load approach, and are developing 3-D computer simulations of wave propagation and power loss in waveguides loaded with lossy materials.

We have also begun to study an accelerating cavity design which operates in a mode optimized to reduce the interaction between cavity and beam.

This increases the stability of the rf system to beam loading transients, by virtue of its greater stored energy. This is unusual practice in cavity design, where one usually optimizes for a strong interaction in the accelerating mode. One consequence of this design is the increased power needed in order to provide the required operating electric field. The benefit is that the individual bunches in the trains of bunches in the ring will be equally phased along the drive rf waveform. In the case of strong beam-cavity interaction (beam loading) the energy deposited in the cavity by bunches at the head of a train can substantially change the field in the cavity for following bunches, resulting in a bunch-to-bunch phase shift along a bunch train. This phase shift may be detrimental to beam quality once the beam is extracted from the ring. A reduction of phase transients by a factor of about four or five is expected, allowing residual motion to be controlled with feedforward systems. Increasing the stored energy of the cavity requires changing its geometry, or the mode in which it operates. We have studied other possible operating modes and have concluded that the additional problems of having modes at both lower and higher frequencies than the operating mode are worse than the problem to be addressed. Thus, we have concentrated on geometry changes of TM_{011} mode cavities, to increase the Q-value of the mode.

In the Lambertson Beam Electrodynamics Laboratory at Berkeley Lab, we have performed beam impedance measurements using microwave measurement techniques of a prototype injection/extraction kicker. In order to inject beam into a storage ring, pulsed electromagnetic kickers are used to bend the trajectory of the incoming beam onto the stored-beam orbit. Fast rise and fall times are required in order that bunch trains may be injected or extracted without disturbing preceding or following trains. The kicker must switch on/off within the time interval between bunch trains (ideally as short as possible).

The results obtained so far will be used, in conjunction with estimated impedance of other components, to provide the basis for an impedance budget for a future low-emittance storage ring. We will compute collective effects and design feedback systems to control them. The nature of the interaction which produces the deflection in the beams also implies a strong coupling to the fields of the stored beam—characterized by the beam impedance. We seek to minimize this impedance, by allowing relatively unimpeded passage of the image current produced by the stored beam, and by minimizing resonant modes within the kicker structure. In our measurements, we found resonances trapped within the power feedthrough section of the kicker. Our work has helped in re-engineering the kicker, and we are pursuing other conceptual designs to eliminate this problem.

A technique used to store high-current beams is to produce many small bunches. Each bunch has a relatively modest current, which will not induce instabilities within a carefully designed storage ring. The large total current, however, may drive coupled-bunch instabilities, and these may be suppressed using fast feedback systems. By sampling the deviation of each bunch, we may derive a corrective kick term and apply it to the same bunch on each turn of the machine. The system bandwidth required is half the bunch rate, and may be a few hundred megahertz. Operating in the lowest modes, from kilohertz to hundreds of megahertz, is challenging, and we have proposed schemes which utilize higher frequency components. In this case the fractional bandwidth is much reduced and hardware is available, but the kickers required to impart the correction to each bunch become more difficult. We have conceptualized a kicker design which will provide a large impedance when operated at high frequency (in the gigahertz range), increasing the efficiency of the system and reducing costs of rf power. This kicker consists of several stripline plates connected with a pi/2 phase shift between each plate. As the beam passes through the structure, and the electromagnetic wave applied to the kicker by the feedback system propagates in the opposite direction, the beam experiences a transverse kick in one direction, as required. Several plates are needed to provide good efficiency, and this technique of connecting plates in series is unique in accelerator feedback systems.

In the design and optimization of low-emittance lattices, we have begun to analyze a theoretical minimum emittance design. While in the early stages of this analysis, we are hopeful that a machine with flexibility in operating point, and insensitivity to errors, can be achieved. A measure of the efficiency of a storage ring in capturing and containing beam is the dynamic aperture—the aperture within which a particle is bound inside the machine by the magnetic fields. A major contribution to the high-harmonic fields in the lattice, which may seriously decrease the dynamic aperture, is the wiggler. The wiggler is used to

increase the synchrotron damping rate of the machine, by forcing rapid bending of the beam back and forth; at each bend the beam emits synchrotron radiation which results in a natural damping process. To understand its properties, we have begun to study the basic lattice with an ideal wiggler. We will then incorporate a model of the real wiggler magnetic fields to ascertain their effects. Our analysis begins with a model generated in the Methodical Accelerator Design (MAD) code, which we convert to in-house codes to perform the more elaborate modeling studies.

Publications

T. Okugi et al., "Evaluation of Extremely Small Horizontal Emittance at the KEK Accelerator Test Facility," *Phys. Rev. ST Accel. Beams* **2**, 022801 (1999).

J.N. Corlett, et al., "The Next Linear Collider Damping Ring RF System," Particle Accelerator Conference '99, New York (March 29-April 2, 1999).

W. Barry and J. Corlett, "Coupled-bunch Feedback for ATF," International Study Group meeting, KEK, Japan (July 1999).

J. Corlett, "NLC Damping Rings RF Cavities," Linear Collider Workshop (submitted, October 1999).

C. Ng and J. Corlett, "NLC Damping Rings Longitudinal Broadband Impedance," Linear Collider Workshop (submitted, October 1999).

J. Corlett, "NLC Damping Rings Wiggler Straights," Linear Collider Workshop (submitted, October 1999).

R. A. Rimmer, J.Corlett, N. Hartman, D. Li, G. Koehler, J. Rasson, and T. Saleh, "RF Cavity R&D at LBNL for the NLC Damping Rings, FY 1999," *CBP Technical Note* **196** (November 1999).

J. Corlett, N. Hartman, K. Kennedy, G. Koehler, S. Marks, J. Rasson, and T. Saleh, "NLC Damping Rings Wiggler Studies 1999," CBP Technical Note (November 1999).

Laser-Driven Acceleration of Particles

Principal Investigators: Wim Leemans, Swapan Chattopadhyay, and Jonathan Wurtele

Project No.: 97002

Project Description

This LDRD is to conduct an experimental and computational study of a particle accelerator based on ultrahigh gradient (10's of GeV/m) laser-driven acceleration over long distances (1 to 10 cm) in plasmas. Experimental techniques are being developed to a) channel ultrahigh intensity laser pulses in cm-long, laser-produced plasmas, b) excite, probe, and control longitudinal wakes with multi-GeV accelerating gradients in these plasma channels and c) inject femtosecond (fs)-long electron bunches into the channel. Numerical tools and computational codes are being developed and integrated with the experimental program for fast and accurate modeling of the experiments. This work may lead to future compact accelerators using plasma or other advanced accelerator concepts.

Accomplishments

During FY99, experiments on laser guiding in plasma channels and production of femtosecond electron bunches through laser wakefield acceleration continued.

The laser guiding experiments have concentrated on the development of diagnostics for measurement of channel profiles and wakefields. The initial experiments (see FY98 report) used on-axis Mach-Zehnder interferometry to measure the plasma channel profile. Whereas this method was successfully used in diagnosing slab channel profiles, for round channels the guiding properties complicate the interpretation of the observed interferometric pattern. To have a direct measure of channel profile, we have implemented side-on folded-wave interferometry using a single beam which, after going through the plasma, is split and folded on top of itself to produce an interferogram. Phase retrieval algorithm and Abel inversion are

applied to infer the plasma density profile under the assumption of axisymmetry.

To measure the wakefield amplitude generated by the laser pulse propagating down the channel, we have studied the possibility of using Fourier domain interferometry. A novel holographic inversion method has been found and we are currently testing this technique experimentally. This measurement requires the use of two co-linearly propagating probe laser pulses, one behind and one ahead of the intense drive laser pulse. The two probe pulses are then allowed to interfere inside a spectrometer to produce a beat pattern. The modulation frequency of the beat pattern depends on the plasma wave amplitude and hence can be used to measure the properties of this wave.

To study the laser drive pulse evolution we have also begun to use a frequency resolved optical gating (FROG) system. The FROG system is capable of measuring the wavelength of a femtosecond laser pulse as a function of time. With this method we expect to measure the amount of coupling between the laser and plasma by measuring the redshifting of the drive laser pulse as energy is transferred from the laser photons to the plasmons.

An important aspect of the experimental implementation of these various methods was found to be beam pointing stability and movement during pump down of the vacuum chambers. Due to the small channel dimensions, tolerance for beam motion is on the order of 10 microns. This has been successfully obtained by strengthening the vacuum vessel.

The electron production experiments have succeeded in producing electron beams by propagating an intense ($I \leq 10^{19}$ W/cm^2), high power ($P \leq 12$ TW) laser pulse in a dense plasma ($n_e \leq 5 \times 10^{19}$ cm^{-3}). For such parameters, the laser pulse will become self-guided due to relativistic self-focusing and can undergo an instability which leads to a longitudinally modulated intensity profile with periodicity given by the plasma period and a large amplitude plasma wave. For sufficiently long propagation distances of the laser pulse in the plasma, the plasma wave can reach amplitudes comparable to the cold-wavebreaking limit, at which moment background electrons can be trapped and accelerated in the wave.

To achieve this parameter regime, an additional amplifier arm operating at 10 Hz and with average power of about 10 W (i.e. 1 J/pulse), a new target chamber and vacuum compressor system was designed, built, and commissioned. After amplification, the laser pulse was propagated through an evacuated beam pipe into a vacuum compressor where it was compressed to pulse durations on the order of 50 to 250 fs, depending on the compressor settings. The peak power for the shortest pulses was on the order of 10 to 12 TW. After compression, the laser pulse was focused on a Helium gasjet (backing pressure up to 1000 psi) using an F/4 off-axis parabola to a spot size on the order of 6 to 7 mm, resulting in peak intensities on the order of 10^{19} W/cm^2. Folded wave interferometry was used to measure the plasma density produced by ionization of the Helium gas plume by the front of the intense pulse. The plasma length was measured to be on the order of 1.2 to 1.5 mm. After interaction with the gasjet, an ultrathin mirror deflected the laser beam onto a single-shot auto-correlator and power meter. The mirror substrate was sufficiently thin to allow energetic electrons to pass through. The electron detection system consisted of a phosphor screen, protected by a 75-micron thick Al foil, which was mounted on the faceplate of a fiber-coupled 14-bit charge-coupled device (CCD) camera. The sensitivity of the camera was measured using Cs-137 and I-129 radioactive sources and found to be on the order of 3 to 4 electrons/count. The camera was surrounded by 8" thick lead shielding to reduce the amount of radiation inside the experimental cave.

By tuning the position of the gasjet and laser pulse duration, electrons were observed. These measurements constitute the first time electron acceleration has been achieved using ultrashort laser pulses produced by a Ti:Al_2O_3 laser system. All previously reported results were obtained using longer pulse (0.4 to 1 ps) Nd-glass laser systems. Furthermore, those systems operate typically at very low repetition rate (1 to 20 minutes between shots) compared to the 10 Hz system here at Berkeley Lab. A permanent magnet based bend magnet was used to distinguish between electron and x-ray/gamma-ray induced signals on the phosphor screen. Based on the sensitivity calibrations of the detection system, a total of greater than 10^9 electrons per pulse was measured. Experiments are currently underway to accurately measure the amount of charge using an integrating current transformer. A solenoidal magnet has been installed to allow focusing of the electron beam. An imaging bend magnet spectrometer is being designed to measure the beam energy and its spatial dependence. The expected

energy distribution is expected to be very broad (100%) with most of the electrons having energies on the order of 1 to 2 MeV and only a fraction having 10's of MeV energy.

To significantly reduce the energy spread and increase the mean energy, injection of two additional laser pulses is being implemented (see FY98 report). The additional laser pulses will provide the means to control the injection phase into the plasma wave by providing a time-gated electron trapping pulse.

On the theory side, significant progress has been made in providing analytic and computational tools to predict and analyze the experimental results. New results on laser propagation in plasma channels have been obtained by extending the conventional paraxial propagation model through the inclusion of non-paraxial terms. The new model allows for fast and accurate modeling of the self-modulated and Raman forward scattering laser instabilities, which are relevant to the experiment. A novel fluid code has been developed which allows laser and plasma evolution to be calculated self-consistently, under the assumption that no particle trapping occurs. To further extend our capabilities, we have implemented a collaborative effort with UC Berkeley and University of Colorado, on the use of particle-in-cell (PIC) codes for self-consistent modeling of the laser-plasma interactions, including particle trapping and acceleration.

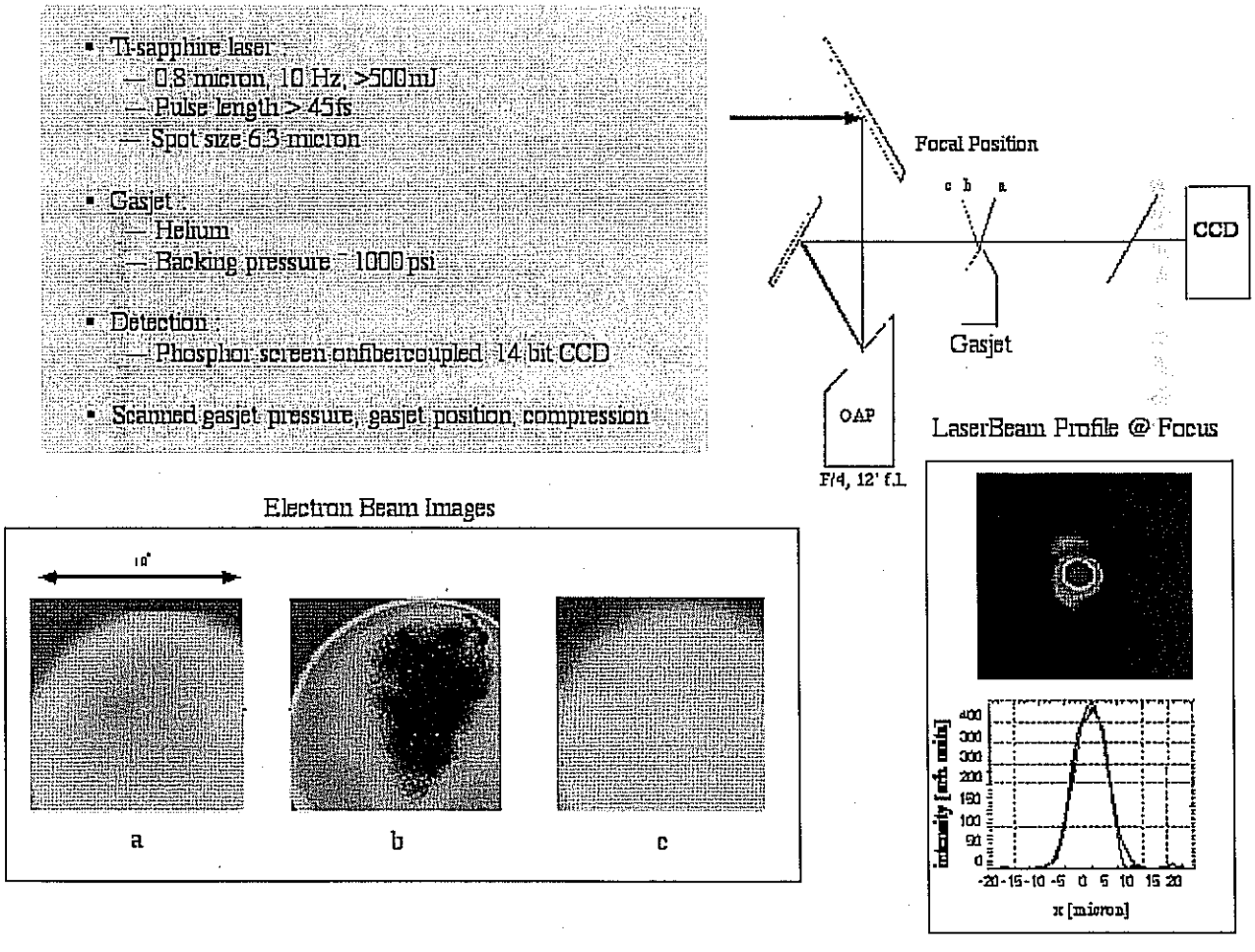

Figure 1. Experimental set-up, laser beam spot and line profile, and electron beam images on phosphor screen.

Publications

P. Volfbeyn, E. Esarey, and W.P. Leemans, "Guiding of Laser Pulses in Plasma Channels Created by the Ignitor-Heater Technique," *Phys. Plasmas* **6**, 2269 (1999).

E. Esarey and W.P. Leemans, "Non-Paraxial Propagation of Ultrashort Laser Pulses in Plasma Channels," *Phys. Rev. E* **59**, 1082 (1999).

C.B. Schroeder et al., "Generation of Ultrashort Electron Bunches by Colliding Laser Pulses," *Phys. Rev. E* **59**, 6037 (1999).

E. Esarey, C.B. Schroeder, W.P. Leemans, and B. Hafizi, "Laser-Induced Electron Trapping in Plasma-Based Accelerators," *Phys. Plasmas* **6**, 2262 (1999).

D. Bernard, F. Amiranoff, W.P. Leemans, E. Esarey, and C. Joshi, "Alternative Interpretation of Nucl. Instr. Meth. A 410 (1998) 357 (H. Dewa et al.)," *Nucl. Instr. Meth. A* **432**, 227 (1999).

E. Esarey, C.B. Schroeder, and W.P. Leemans, "Ultrashort Electron Bunches from Laser-Plasma Accelerators," High Field Science (Plenum, NY), p. 135 (1999).

W.P. Leemans, et al., "Channel Guiding for Laser Wakefield Accelerators," Proceedings of 1999 Particle Accelerator Conf., IEEE, Piscataway NJ p. 325 (1999).

E. Esarey and W.P. Leemans, "Scaling Laws for Laser Wakefield Accelerators," Proceedings of 1999 Particle Accelerator Conf., IEEE, Piscataway NJ, p. 3699 (1999).

P. Volfbeyn, E. Esarey, and W.P. Leemans, "Laser Wakefield Diagnostic using Holographic Longitudinal Interferometry," Proceedings of 1999 Particle Accelerator Conf., IEEE, Piscataway NJ, p. 3696 (1999).

E. Esarey, C.B. Schroeder, B.A. Shadwick, J.S. Wurtele, and W.P. Leemans, "Nonlinear Theory of Non-paraxial Laser Pulse Propagation in Plasma Channels," submitted to *Phys. Rev. Lett.* (1999).

W.P. Leemans, et al., "Femtosecond X-ray Generation through Relativistic Electron Beam-Laser Interaction," submitted to *Comptes Rendus a l'Academie des Sciences* (1999).

Time-Resolved X-Ray Measurements of Complex Magnetic Materials

Principal Investigators: Roger Falcone, Inuk Kang, Philip Heimann, Howard Padmore, and Zi Qiang Qiu

Project No.: 99002

Project Description

This project involves a time-resolved x-ray study of dynamical phase transitions of the colossal magnetoresistance (CMR) materials. The CMR materials exhibit extremely rich phase transition phenomena owing to strong electron-spin and electron-phonon interactions. Understanding the dynamical interplay of these two interactions in the CMR materials is one of the most important problems in condensed-matter physics. This project will use time-resolved x-ray diffraction to investigate the role of the electron-phonon interaction in the phase transitions, and will develop a new time-resolved x-ray magnetic circular dichroism (XMCD) measurement technique to probe the dynamics of the electron-spin interaction.

We will monitor the temporal evolution of the lattice and magnetic structure during the laser-induced phase transitions in the CMR materials. Laser systems producing light pulses synchronized with the Advanced Light Source (ALS) x-ray pulses permit us to do pump (laser)-probe (x-ray) measurements. The change of the lattice structure of the CMR materials during the laser-induced phase transitions can be monitored by measuring x-ray diffraction at different temporal delays between the laser- and x-ray pulses. Interrogation of element-specific magnetic dynamics requires development of a time-resolved XMCD technique. This XMCD capability will be developed at beamline 7.3.3 of the ALS. The x-ray measurement will be complemented by conventional magneto-optic techniques. The dependence of the laser-induced phase transitions on the composition of the materials, temperature, and magnetic field will be tested.

Accomplishments

We investigated the role of the Jahn-Teller interaction in the charge-ordered CMR materials by time-resolved x-ray measurements of the polaron dynamics. The formation and relaxation of the polarons, induced by photo-carriers, were observed for the first time in picosecond dynamics of the diffuse x-ray scattering. We monitored how the lattice structure of $Nd_{1/2}Sr_{1/2}MnO_3$ evolved after the material was irradiated with 150 fs, 800 nm laser pulses between 10 and 300 K. We implemented a low-temperature x-ray diffraction set up. The pump-laser wavelength overlapped with the broad Mn^{3+} to Mn^{4+} charge-transfer transition band. The lattice dynamics was probed with the time-resolved x-ray Bragg diffraction from the orthorhombic *Pbnm* (112) plane of a single crystal $Nd_{1/2}Sr_{1/2}MnO_3$. The experiment was performed at beamline 7.3.3 of the ALS. Strong diffuse scattering, indicative of a large lattice distortion, was observed to develop over ~30 ps and to relax in 300 ps. This diffuse scattering is similar to the diffuse scattering observed at the phase boundary between the charge-ordered and ferromagnetic states. We interpret this as the formation of local patches of new structural phases induced by the Jahn-Teller coupling of the lattice to the charge-transfer.

Publications

I. Kang, et al., "Time-Resolved X-ray Measurements of Polaron Dynamics of Charge-ordered $Nd_{1/2}Sr_{1/2}MnO_3$," ALS Users' Meeting (November 1999).

Ultrafast X-Ray Spectroscopy via Optical Gating

Principal Investigators: Thorton Glover, Philip Heimann, and Howard Padmore

Project No.: 98032

Project Description

Synchrotrons have provided valuable information about the static properties of materials important to the physical and life sciences. Their role in studying material dynamics, however, has been limited due to inadequate time-resolution. The ability to perform x-ray spectroscopy with sufficient time resolution to observe the fast (~100 fs) primary events which drive many interesting chemical reactions, phase-transitions, etc., will have an important impact on a number of fields in physics, chemistry, and biology. The goal of our research is to expand Advanced Light Source (ALS) capabilities for performing ultrafast x-ray spectroscopy by developing a fast (femtosecond) x-ray detector based on optical gating. Optical gating will be based on multiphoton processes driven by the combination of visible (laser) and x-ray (synchrotron) light. Such two-color experiments represent an interesting new direction for synchrotron-based research. From a fundamental perspective, x-ray/laser two-color experiments offer a means of studying novel structure and dynamics of matter exposed to intense, coherent (laser) radiation. From an applications perspective, x-ray/laser multiphoton processes can serve as the basis for a high time-resolution x-ray detector via optical gating.

In optical gating, a thin (temporal) slice of a long x-ray pulse is isolated using an x-ray/laser multiphoton process. Specifically, a short laser pulse will induce modifications to an x-ray photoelectron spectrum (XPS). Narrow-band synchrotron light is tuned to a core-level absorption edge and will produce a narrow photoelectron peak. When a laser pulse is present during the x-ray ionization event, additional peaks (spaced by multiples of the optical photon energy) will appear on either side of the primary x-ray peak. These additional peaks are due to absorption and emission of optical photons during the narrow window in time when a short laser pulse overlaps the longer x-ray pulse. For moderate laser intensity, the optical scattering peak amplitudes are linearly proportional to the flux contained within a thin slice of the x-ray pulse and can be used to record materials dynamics with time-resolution equal to the duration of a short laser pulse (as short as 5 to 10 fs for current lasers). The goal of this project is to demonstrate that such two-color processes can serve as a basis for an ultrahigh time-resolution x-ray detector.

Accomplishments

Experiments have been performed at the micro-x-ray photoelectron spectroscopy (XPS) endstation at beamline 7.3.1.2. X-rays at approximately 800 eV emit 2p core-shell electrons from silicon. The electron spectrum (Figure 1) indicates a 2p-photoemission line at 730.5 eV. When a laser pulse (800 nm, 1.55 eV photons) is present during the photoemission process, the Si 2p line is shifted to higher kinetic energy by ~250 MeV. This shift is due to laser-induced surface charge and is used to ensure that the x-ray and laser pulses are spatially and temporally overlapped on the Si target. We note that the dynamics of the laser-induced line-shift are determined by recombination processes at the Si surface so that picosecond and femtosecond time-resolved measurements of the Si 2p line position provide information about surface recombination dynamics. While such information can be obtained using optical gating, the Si line dynamics have not yet been mapped and we turn attention to our initial observations of optical gating.

We describe two (related) pieces of data which suggest that we have observed optical gating. First (Figure 1 left inset), an x-ray/laser cross-correlation curve and second (Figure 1 right inset), a laser-perturbed Si XPS. The data are obtained by measuring the Si photoelectron spectrum as a function of laser arrival time at the sample (for fixed x-ray arrival time). The left inset to Figure 1 shows that the electron counts (in the vicinity of 730.5+1.55 = 732 eV) are 4 to 5% above the baseline for a time-interval corresponding to ~100ps. This curve amounts to an x-ray/laser cross-correlation measurement of the x-ray pulse indicating an x-ray pulse duration of ~100ps. We note that the magnitude of the measured effect (4 to 5%) is approximately a factor of two larger than the calculated effect (2%). It is possible, however, that the calculation (performed for a single atom in

isolation) underestimates the optical scattering efficiency by not accounting for collisions within the solid. In the time-interval between ionization and photoemission from the surface, the photoelectron can undergo collisions and these collisions provide additional opportunities for scattering optical photons.

The right inset to Figure 1 shows the laser-perturbed XPS. The spectrum is obtained by taking a Si spectrum corresponding to coincident x-ray/laser arrival at the sample (-50 ps on Figure 1 left inset) and subtracting the spectrum corresponding to non-coincident arrival (-150 ps). The spectrum shows a peak at 732 eV, corresponding to the primary x-ray peak (730.5 eV) plus one optical photon (1.55 eV).

While these preliminary experiments suggest that we are indeed observing laser-induced continuum transitions, we note two reasons for caution. First, since the Si 2p line is shifting as a function of time (due to laser-induced surface charge and associated recombination dynamics), these line-shifting dynamics may distort the cross-correlation curve resulting from optical gating. A second, and related, issue is that the measured x-ray pulse (~100 ps) is longer than expected (~30 ps for ALS in normal mode). We note, however, that beam-damping was not operative for the data of Figure 1 and this may account for the discrepancy. Follow-up experiments are in progress.

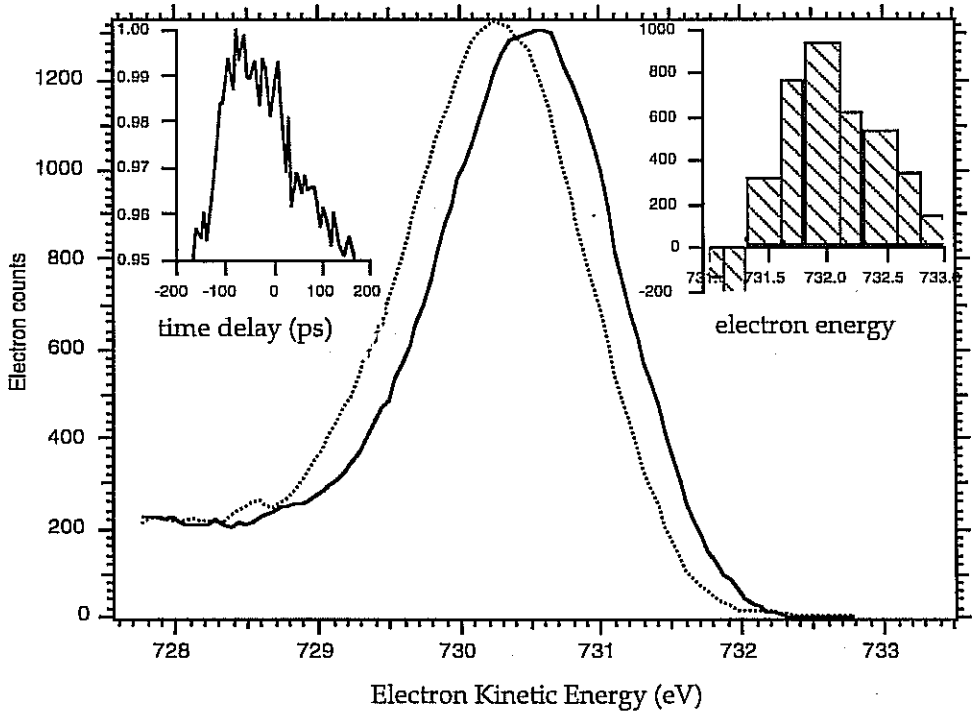

Figure 1. : Si 2p photoemission spectra with laser off (dashed line) and on (solid line). Left inset: Electron counts (arbitrary units) in the vicinity of 732 eV as a function of laser-x-ray time delay. Right inset: Si 2p spectrum at 0ps minus the Si 2p spectrum at –160ps.

Publications

T.E. Glover, G. D. Ackermann, H. W. Chong, P. A. Heimann, Z. Hussain, H. Padmore, R.W. Schoenlein, A.A. Zholents, and M. Zolotorev, "X-ray + Laser Multiphoton Processes: Ultrafast Detectors for Femtosecond Spectroscopy at Synchrotrons," presented at ALS User Meeting (1999).

Phase- and Amplitude-Contrast Tomography using Intermediate-Energy X-Rays: Research for 3-D Imaging of Complex Materials

Principal Investigators: Malcolm Howells, Alastair MacDowell, Howard Padmore, Robert Ritchie, and Wenbing Yun

Project No.: 99003

Project Description

The general goal of this project is to develop three-dimensional x-ray tomographic imaging techniques at high spatial resolution using intermediate-energy x-rays. The project will combine the high brightness of the Advanced Light Source (ALS) superbend sources with the high performance of x-ray imaging optics such as a zone plate. A prototype phase contrast microscope similar to that established in the soft x-ray region as well as in visible spectrum will be developed. The phase contrast microscope will have a spatial resolution better than 100 nm and detection sensitivity substantially better than absorption contrast. The outcome will address the needs of the materials science community, particularly in the study of crack initiation and propagation in microelectronic and structural materials. This includes metallic and polymer-based composites and bioceramics such as partially-stabilized zirconia and pyrolytic carbon. Other applications include imaging of bones, soils, Micro-Electro Mechanical Structures (MEMS) and Bio MEMs, laser fusion targets, and integrated semiconductor devices, all benefiting from the high spatial resolution and detection sensitivity of the microscope and the high penetrating power of x-rays.

Accomplishments

We have constructed a prototype full-field imaging x-ray microscope and deployed it on beamline 7.3.3 at the ALS. The instrument consists of a field aperture, the zone plate, a phase shifter (in the first case a simple zero order stop) and a detector consisting of a scintillator screen, visible-light imaging system and charge-coupled device (CCD) detector, and a high-precision mechanical system for alignment and sample manipulation. Most components can be aligned by remote control.

Imaging of many objects ranging from biological to materials objects has been done using either absorption or dark-field phase contrast, depending on the contrast type of the particular object. High quality images of objects ranging from lichen, bone joints, metal grid, human hair, a shark tooth, and semiconductor integrated circuits have been obtained. Figure 2 shows the images of part of an integrated circuit chip supplied by Dr. Neogi of Intel Corporation in collaboration with Dr. Levin of National Institute of Standards and Technology (NIST). The chip is made using the recent Cu technology for integrated devices. It consists of Cu interconnects at two layers connected by vias. All Si of the original integrated circuit (IC) chip was removed from the sample because it was originally prepared for low energy (~2 keV) imaging. A Si substrate of < 50 μm could have been left on the IC for the x-ray energy used in our experiment, without affecting the exposure time significantly.

Figure 2 shows clearly the image of the vias whose dimension is about 0.4 μm. Preliminary analysis indicates that the spatial resolution of the x-ray image is about 120 nm, which is considerably better than obtainable in optical microscopes. It is also interesting to note that the edges around the Cu interconnects are markedly darker than the rest of the interconnect, indicating stronger absorption at the edges. This resulted from 30-nm Ta liners used to prevent the diffusion of Cu into Si. The fact that the 30-nm Ta liners are clearly detected indicates that the feature that can be detected by the microscope is much smaller than its spatial resolution.

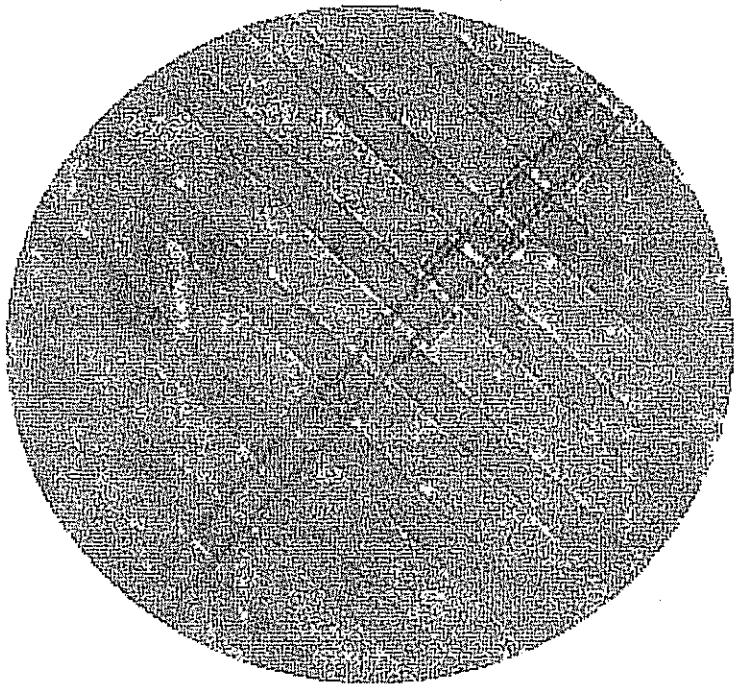

Figure 2. X-ray image of an integrated circuit showing images of vias connecting Cu wires in two different layers, shown as the small dots at the intersection between the thin and wide Cu wires.

Publications

W. Yun, M. R. Howells, J. Feng, R. Celestre, C-H Chang, A. A. MacDowell, H. A. Padmore, and J. Spence, "Hard X-ray Microscopy and Tomography at the ALS: Experiments and Plans," to be published in the proceeding of VI[th] International Conference on X-Ray Microscopy, August 1-6, 1999, Berkeley, California (in press).

W. Yun, M.R. Howells, J. Feng, R. Celestre, C-H. Chang, A.A. MacDowell, H.A. Padmore, and J. Spence, "A Zone Plate Based Hard X-ray Imaging Microscope," to be submitted to *Applied Physics Letter.*

High-Efficiency Electron-Spin Detector for Photoemission Experiments

Principal Investigators: Zahid Hussain and Zhi-Xun Shen

Project No.: 98033

Project Description

Over a decade after the discovery of high-T_c superconductors, neither the origin of the superconductivity nor the nature of the peculiar normal state in these materials is satisfactorily understood. The heart of this problem lies in the larger problem of understanding highly-correlated materials, which includes colossal magneto-

resistance materials, half-metallic ferromagnets, and Wigner crystals. Further understanding the nature of these materials depends on improved characterizations of their properties, in particular the discovery of new electronic states of matter.

Studies are currently underway at the Advanced Light Source (ALS) to study highly-correlated electronic materials, with emphasis on transition metal oxides (e.g., high-T_c superconductors), alloys, and compounds. The objective of this project is to build a high-efficiency electron-spin detector that will compliment the High-Energy Resolution Spectrometer (HERS) at ALS Beamline 10.0. This new spin detector will be mounted on the exit plane of a Scienta SES-100 analyzer. Initially the system will be used with a frequency doubling argon laser that can deliver up to 10^{16} photons per second. This will allow us to carry out ultrahigh energy and spin-resolved photoemission experiments of threshold electrons (low energy <2 eV) with an energy resolution comparable with KT (<20 meV). This has not been achieved before.

The first sample we plan to investigate with the new electron spin analyzer is CaB_6. This compound will meet two objectives. The first is as a test of the new electron-spin analyzer (ESA). Because CaB_6 is ferromagnetic and has a small work function, we will be able to use a laser to excite a large polarized photoelectron current suitable for testing. Our second reason for choosing this sample is the interesting physics recently found in measurements on electron-doped CaB_6 showing that the ground state is ferromagnetically polarized with a saturation moment of 0.07μB per electron. Surprisingly, the magnetic ordering temperature of this itinerant ferromagnet is 600° K, which is three times larger than estimates based on conventional band theory. The strong spin-spin correlation is expected to be responsible for such a high magnetic ordering temperature. We expect the new instrument to provide new correlation using spin-polarized photoemission.

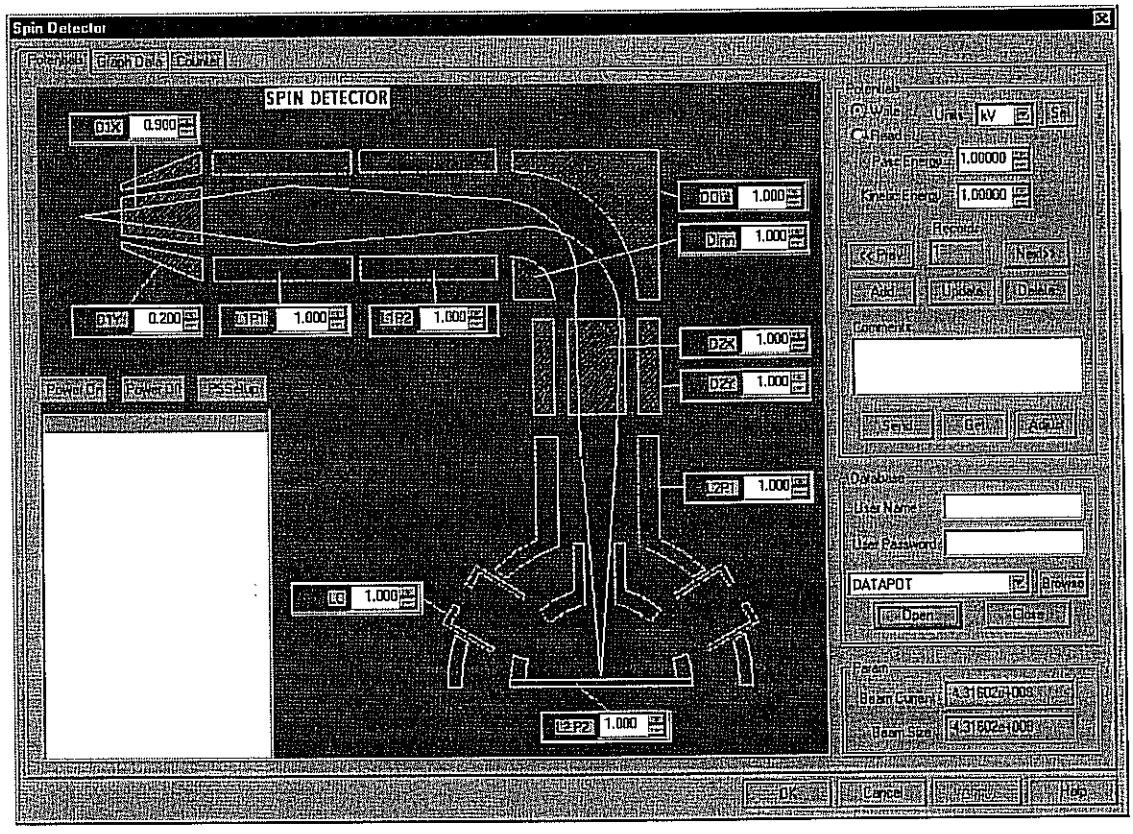

Figure 3. Spin-resolved detector control panel.

Accomplishments

Considerable progress has been made during the past year (FY99).

- The ESA has been fabricated and mounted on an ultrahigh vacuum chamber.
- A frequency-doubling Argon laser (contributed by Stanford University) was put together in a temporary laser laboratory at the ALS. The laser system has been successfully tested and is operational.
- All the necessary electronics for the ESA, including power supplies, have been tested.
- A sophisticated computer control and data acquisition system has been developed and is currently being tested. (Figure 3).
- A specialized, custom-made electron gun, which simulates the electron emission pattern from the exit slit of the electron energy analyzer, has been developed. It is being used to test and optimize the ESA.
- A Scienta SES-100 electron energy analyzer has been purchased and is being tested.

The completion and testing of the spin detector were accomplished and successful. With the follow-on program funding now received, we are ready to assemble all the components (each unit having been tested separately) and create a state-of-the-art capability that will enable spin-resolved photoemission experiments with unprecedented energy resolution.

Studies in Beam Dynamics and Operations with Superconducting Magnets at Critical Energy of 12 KeV

Principal Investigators: David Robin and Ron Scanlan

Project No.: 98034

Project Description

The concept of implementing superconducting magnets to enhance the capabilities of the Advanced Light Source (ALS) has been endorsed by the ALS Science Policy Board, the Workshop on Scientific Directions for the ALS, the ALS Science Advisory Committee and Department of Energy/Office of Basic Energy Sciences. A significant fraction of the ALS user community is interested in using high-brightness intermediate energy x-ray light from such superconducting magnets for applications such as protein crystallography, sub-micron spot size x-ray diffraction of heterogeneous materials, and sub-micron spot size x-ray absorption on environmental and earth sciences samples.

It appears likely that a magnet can be built with a sufficiently robust operating margin. The purpose of this project was to build and test a proof-of-principle model including tests of the cooling system and current leads. Also, accelerator physics simulations are being performed to study the impact of the machine performance (dynamic aperture) with the superbends.

Accomplishments

In FY98 a conceptual design for the superbend cryosystem was made based upon two key features: a Gifford McMahon cryocooler and high-temperature superconducting (HTS) leads. The Gifford McMahon cryocooler was chosen because it is regarded as more reliable than cryocoolers with Joule-Thomson circuits. HTS leads have a very low heat leak compared with normal conducting leads which is an essential for operation with such a low power cryocooler.

In FY99 a test cryosystem was built to test the performance of the cryocooler and the HTS leads. A 1.5 watt Sumitomo cryocooler and a set of American Super Conductor HTS leads were purchased. These were incorporated in a test cryostat that was constructed by Berkley Lab, in conjunction with Wang nuclear magnetic resonance (NMR). A picture of the test cryosystem can be seen in Figure 4.

In all aspects the system performed well. The cryocooler was very easy to set up and operate and it had sufficient capacity for cooling the superbend. Measured heat leaks from the leads were low and in agreement with the estimated heat leaks. The American Superconductor (ASC) leads (2223 with Ag alloy matrix) were found to be very stable and robust against temperature excursions. The results of these tests ensure us that the design concept for the cryosystem is sound and the system should perform reliably.

In addition to the cryocooler tests, a design package for the superbend magnet/cryosystem was completed incorporating the new cryosystem features. Also, accelerator simulations were done to study the effects of ramping and electron beam stability.

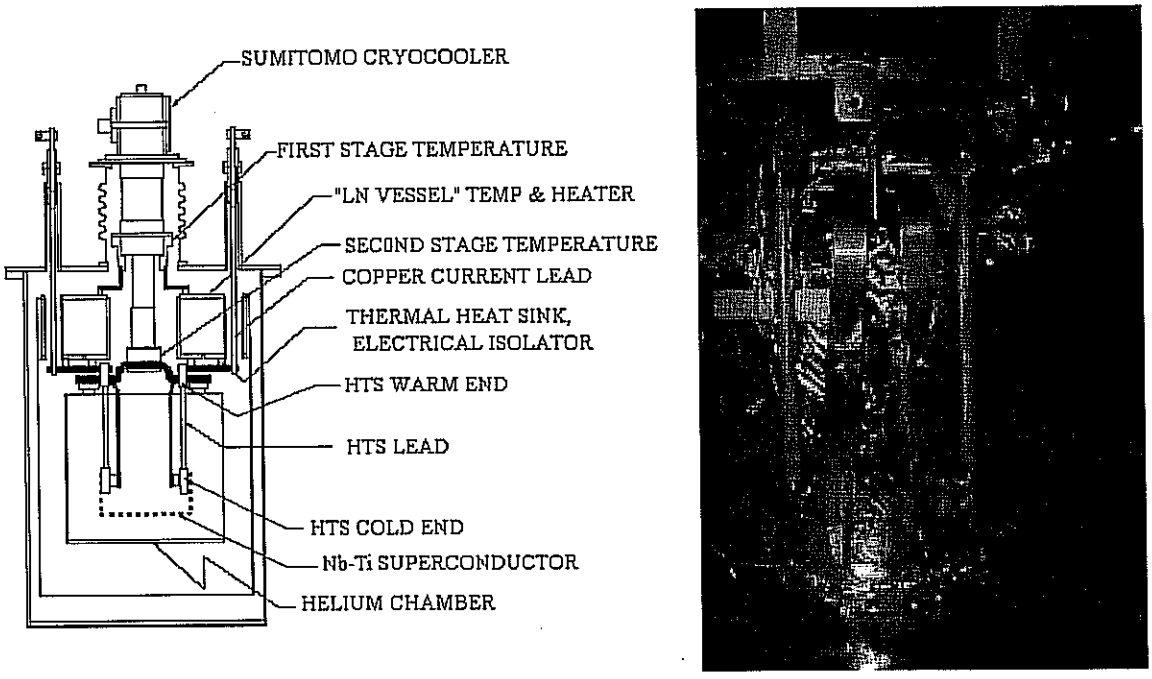

Figure 4. Diagram (left) and picture (right) of the test cryostat.

Numerical Treatment of Lepton Pair Production in Relativistic Heavy Ion Collisions using Parallel Processing

Principal Investigators: Ali Belkacem

Project No.: 97004

Project Description

The purpose of this project is to use the T3E supercomputer to numerically solve the momentum-space time-dependent Dirac equation that describes the production of electron-positron pairs in relativistic heavy ion collisions, as well as other atomic processes such as ionization, charge transfer, and excitation. The solution on a grid will give a direct visualization of the pair creation and excitation processes as the collision between the ions evolves in time. Such an approach has enormous advantages in that it provides a great deal of insight through the "animation" of the collision and also provides a powerful non-perturbative treatment for an inherently difficult problem. The goal is to apply this powerful non-perturbative method to study the dynamics of electron-positron pair production in heavy ion collisions. We also seek to apply the method to study ionization dynamics in the high fields generated by two highly charged ions.

Accomplishments

In FY99, we successfully implemented the main code on the T3E supercomputer. In its initial version the computer code scaled efficiently on up to 128 Processor Elements (PE's) but the scalability was lost beyond that. After analytically constructing wave packets representing electrons and positrons, we started a set of intensive production runs on the T3E. In these production runs, we limited the energy of the collision to up to 10 GeV/n where we have the best handle on the level of precision and time of integration of the code. We used the calculations output from the T3E to generate, on a desktop computer, the first animation showing the evolution of the collision over time.

We applied the calculation to two distinct situations. In the first, we study pair production by starting with a wave packet imbedded in the negative energy continuum and following, through visualization, the evolution of the wave packet in the extremely high field generated by the heavy ions. Here we choose bare gold ion impinging on bare uranium ion at 1 GeV/n and 10 GeV/n. The uranium ion is at rest in the laboratory frame. The comparison of the dynamics of the collision for different initial conditions constructed from the negative-energy continuum states shows a very striking behavior of the "quantum electrodynamics (QED) vacuum" in strong fields. Most of the electron density flows away from the two-center strong Coulomb field in circular patterns. However, toward the end of the collision, a sizable fraction of the electron density flows back to the center of the Coulomb field and remains localized around the uranium ion. This density is related to the probability for the electron to make a transition from the negative energy continuum to the positive bound states, changing the charge state of the uranium ion from U^{92+} to U^{91+}. A first analysis shows capture from pair production probabilities a few times larger than predictions of perturbative methods.

Furthermore, to study excitation and ionization mechanisms, we applied the method to a head-on collision between a bare Au^{79+} and a hydrogen-like uranium target at energy of 100 MeV/n. Figure 1 shows snapshots of the electron probability density in coordinate space at two different times. A narrow peak centered at the origin is associated with electronic excitations to the target bound states. An additional local maximum is clearly seen at the position of the moving ion, a signature of charge transfer from the target to the projectile. In order to unravel the specific features of the different excitation mechanisms, in the contour plots shown in Figure 1, we eliminated contributions associated with transitions to the target K-shell, which is the dominant reaction channel. Of particular interest are structures appearing in the contour plots in the region between the target and the projectile, where a local maximum separates into two distinctly

different ones, moving symmetrically and roughly perpendicular with respect to the beam direction. We interpret this as a new (and unexpected) ionization mechanism in which electrons are emitted with very high transverse velocities. Note that in contrast to the well-known saddle point emission, these electrons have velocities much higher than the projectile velocity. The results of this work are written and submitted for publication in *Physical Review Letters*.

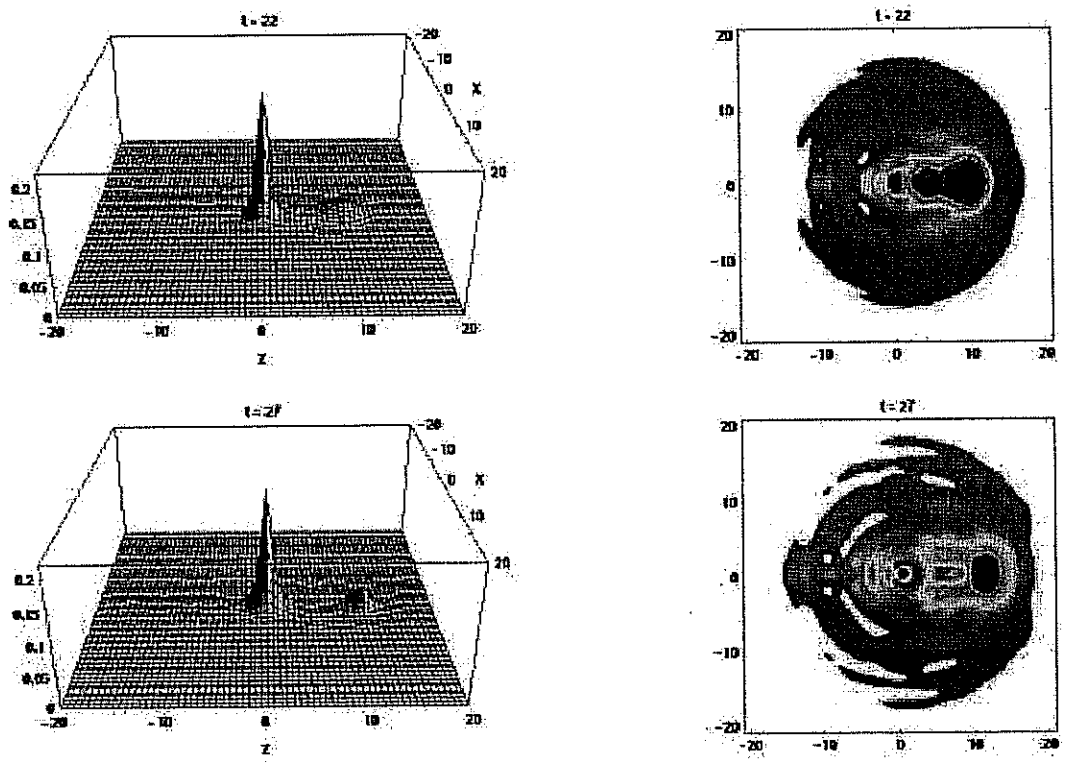

Figure 1. Time evolution of the electron density for the collision of Au^{79+} on a hydrogen-like uranium at 100 MeV/n. The snapshots shown here at time t=22 and t=27 are extracted from an animation rendered from the data calculated on the T3E. The projectile moves from left to right in both the 3-D plots and the corresponding contour diagrams.

Publications

D. C. Ionescu and A. Belkacem, "Relativistic Collisions of Highly Charged Ions," *Physica Scripta* **T80**, 128 (1999).

D. C. Ionescu and A. Belkacem, "Dynamics of Ionization Mechanisms in Relativistic Collisions Involving Heavy and Highly-Charged Ions," submitted to *Physical Review Letters* (October 1999).

New Approach to Efficient Large-Scale Conversion of Terminal Alkenes into Linear Alcohols and Linear Amines

Principal Investigators: Robert Bergman and Don Tilley

Project No.: 99004

Project Description

The conversion of simple hydrocarbon feedstocks such as alkenes into higher-value functionalized, organic compounds, such as alcohols and amines, is a primary goal of laboratory organic synthesis and large-scale industrial technology. Unfortunately there is at present no efficient way to convert terminal alkenes ("alpha-olefins") into primary amines and alcohols of the same carbon chain length. These materials are instead prepared by converting smaller alkenes into alcohols using hydroformylation/hydrogenation, which requires a carbon monoxide/hydrogen (CO/H_2) mixture that must, in turn, be prepared from petroleum or natural gas by a high-temperature, energy-consuming process. If terminal alkenes could be converted to primary alcohols and amines directly—by the addition of the N-H or 0-H bonds of ammonia, water, or other amines or alcohols across the carbon-carbon double bonds of the alkenes with the proper regiochemistry at ambient temperature—it would constitute an important advance in the efficiency with which these materials are made, and therefore a major saving in the energy required by the chemical industry. Classical methods for adding N-H or O-H bonds across alkene double bonds proceed with the wrong regiochemistry, leading to branched rather than linear amines and alcohols. Therefore the solution to this problem requires a method for N-H or O-H addition that takes place by a completely new approach or reaction mechanism.

In this proposal, we suggest a new approach to the catalyzed overall addition of O-H and N-H bonds to the carbon-carbon double bonds of terminal alkenes to convert them to linear alcohols and amines. This envisions initial catalytic conversion of the alkene to a three-membered ring intermediate—an oxirane (epoxide) in the case of hydration, and an aziridine in the case of hydroamination—followed by catalyzed rearrangement of this intermediate to the desired linear alcohol and amine. Several catalysts that should be useful in carrying out these steps are proposed.

Accomplishments

A major problem in the efficient industrial utilization of terminal or "alpha" olefins is the difficulty of converting them into linear alcohols or amines by the addition of the elements of H_2O or NH_3 to the carbon-carbon double bond. Our goal is to find a method to reverse the classical "Markovnikov" regiochemistry of this reaction and add the elements of H_2O and NH_3 to terminal alkenes using chemistry that will place the functional group at the terminal carbon atom.

Our new approach to the attainment of such "anti-Markovnikov" hydration and hydroamination envisions the initial conversion of the starting alkene to a three-membered ring intermediate (an oxirane in the case of hydration, and an aziridine in the case of hydroamination). This would be followed by ring opening of these intermediates with a regiochemistry that would result in the formation of linear alcohol or amine as the final product. Ideally, the system that we develop would allow us to carry out the three-membered ring formation and conversion to alcohol in the same reaction vessel. This requires not only identifying catalysts that can carry out each reaction efficiently, but also requires that the two catalytic systems be compatible (i.e., they cannot react irreversibly with one another).

We decided to focus on the alkene hydration problem first, and then apply any positive results we obtain to the amination. Our first goal was to identify reagents that would provide efficient epoxidation of alkenes under mild conditions. We carried out an extensive literature survey of these materials to obtain an evaluation of their efficiency. As a result of that survey, we decided to focus on two catalytic systems to use for the epoxidations. These are the CH_3ReO_3/H_2O_2/3-cyanopyridine system discovered recently in Herrmann's group and improved by Sharpless, and the Re_2O_7/silyl peroxide system described by Jackson and Sharpless. We have worked out analytical methods using vapor phase chromatography to carefully monitor the rate and yield of these reactions, and then carried out expoxidation reactions using both systems on 1-decene as a trial alpha-olefin. In these experiments we have confirmed that both catalyst systems can be used to efficiently convert 1-decene to the corresponding expoxide.

In more recent work, we have begun to investigate systems that can be used for converting 1-decene epoxide into the corresponding linear alcohol or to the corresponding aldehyde (which can be converted to the alcohol by catalytic hydrogenation). Once again, the Lewis acid isomerizations were subjected to literature analysis. It was decided that aluminum and nickel reagents offered the best potential for efficient isomerization rates and potential compatibility with the reagent used for epoxidation.

In work carried out near the end of our project year, we found that both $((CH_3)_2CHCH_2)_3Al$ and $(PPh_3)_2NiBr_2$ can be used for cleaving the three-membered ring in 1-decene expoxide, although we are still working on reproducing the efficiencies reported in the literature. Perhaps most significantly, our work with the aluminum reagents has generated a modified approach that should provide substantial improvement over the literature method for the epoxide-to-linear-alcohol conversion. The goal is to replace the alkyl groups on the aluminum reagent with alkoxy groups such as isopropoxy, giving $[(CH_3)_2CH\text{-}O\text{-}]_3Al$, and run the reaction in the presence of isopropyl alcohol as a hydrogen source. This should allow us to generate a working catalytic cycle. If this is successful, a similar approach to the amination reaction would employ aziridines in place of epoxides, and $[R_2N]_3Al$ complexes as catalysts.

This project was not renewed for a second year and continuation of the work is being explored with the Department of Energy.

Overcoming Computational Bottlenecks in the Simulation of Molecular Processes

Principal Investigators: David Chandler, Martin Head-Gordon, and William Miller

Project No.: 96030

Project Description

We have completed three years of research funded by LDRD and supported by the National Energy Research Scientific Computing (NERSC) Division at the Berkeley Lab. The common theme of this research has been to advance the possibilities for numerical simulation of molecular processes. Three major computational bottlenecks have been attacked with outstanding progress on all fronts.

- *The timescale bottleneck in molecular simulations.* Condensed-phase chemistry often occurs on timescales that are three-to-ten orders-of-magnitude longer than the nanosecond timescale of molecular simulations. Novel ways of following the crucial, infrequent events, which determine such reactions, are required.
- *The particle number bottleneck in electronic structure calculations.* All widely used electronic-structure methods show nonlinear increases in computational cost as molecular size increases. This translates into sublinear improvements in the size of systems that can be simulated for a given improvement in computer power. The development of new linear-scaling methods is the most direct attack on this bottleneck.
- *The dimensionality bottleneck in quantum reactive scattering.* Although first-principles quantum-mechanical calculations of chemical reaction rates are now a reality for small systems, the complexity of such exact calculations grows exponentially with the number of degrees of freedom. To permit reliable treatment of larger systems, new methods that circumvent this acute dimensionality dependence are needed.

Accomplishments

Overcoming the Time-Scale Bottleneck

To achieve simulation of rare events, it is necessary to focus computational effort on the fleeting passage between metastable states. In the past, this focus has been achieved within the framework of transition state theory—shooting trajectories from predetermined dynamical bottlenecks. This procedure is not applicable, however, in high dimensional systems with complex potential energy surfaces exhibiting a huge multitude of local minima and saddle points. Instead, we have developed a general computational method for finding the transition pathways for infrequent events, which requires no preconceived notion of mechanism or transition state. Called "transition path sampling," the method is

metaphorically akin to throwing ropes over rough mountain passes, in the dark. "Throwing ropes" in the sense that one shoots short trajectories, attempting to reach one stable state from another. "In the dark" because high dimensional systems are so complex, it is generally impossible to literally visualize the topography of relevant energy surfaces. In such cases, it is unlikely that the first throw of the rope will be successful, but one can learn from failures, and there should be an optimum algorithm, i.e., sequence of throws, with which success is efficiently obtained. We have discovered and demonstrated this type of sequence, and we believe it opens the way for many heretofore impossible computational studies of the dynamic pathways of chemical reactions in clusters and in condensed phases.

Transition path sampling is based upon the statistical mechanics of directed trajectories. We have derived the fundamental principles governing ensembles of stochastic and deterministic trajectories, including the concept of annealing and the isomorphism between free-energy calculations and time-correlation function calculations. We have derived efficient transition path sampling algorithms, "shooting" and "shifting," scaling linearly with trajectory length and number. We have further established statistical criteria, including principles governing separatrix distributions, for extracting and characterizing transition state ensembles from the ensembles of trajectories harvested by transition path sampling.

Overcoming the Particle-Number Bottleneck

To achieve simulation of very large molecules, it is necessary to develop electronic structure methods whose computational requirements rise only linearly with the number of particles; this is the so-called particle-number bottleneck of quantum chemistry. Most methods for achieving a linear scaling solution of either tight-binding or Kohn-Sham density functional theory Hamiltonians are based on exploiting the short-range character of the one-particle density matrix in large-gap systems. Such methods do not work (i.e. fail to yield linear scaling until the system size is absurdly large) for small gap systems with long range density matrix correlations. However, the long-range correlations may often be relatively smooth, and can therefore, in principle, be described in terms of a small number of judiciously chosen collective variables. In this project, we have pioneered a new method we call the Energy Renormalization Group (ERG) as a systematic tool for obtaining such variables. For the first time, we have been able to demonstrate near-linear scaling for several one- and two-dimensional metallic and small-gap model problems involving tight-binding Hamiltonians. These developments help to lay a basis for being able to leverage future advances in computer power directly into the ability to simulate proportionately larger systems. This scaleability with the number of particles is at least as important as the more commonly discussed issue of the scaleability of an algorithm with the number of processors.

Overcoming the Quantum Dynamics Bottleneck

Very significant progress has been made over the last year in developing the semiclassical initial value representation (SC/IVR) as a way for incorporating quantum effects into (otherwise classical) molecular dynamics simulations. Work is progressing along two fronts: one is the application of the SC/IVR approach to an increasingly wide range of dynamical phenomena to establish the limits of its validity, and the other is exploring new algorithms to make the SC/IVR calculations more efficient and thus capable of being applied to more complex molecular systems.

Some of the recent applications have been to inelastic scattering, to femtosecond pump-probe photodetachment of negative ions, and to the hydrogen atom transfer reaction in 7-azaindole dimers. This work demonstrates the broad applicability of the SC/IVR approach to a variety of dynamical phenomena.

The most important methodological development has been a "forward-backward" IVR. This expresses the two time-evolution operators, which appear in the quantum time evolution for a typical time correlation function, as a single phase space average over initial conditions of the classical trajectories. This approach gives promise for being able to incorporate quantum features into classical molecular dynamics with only a modest additional effort beyond a purely classical treatment.

Another interesting theoretical development showed how the SC/IVR expression for time correlations can be written in a form that makes the classical limit especially transparent in the limit as the classical dynamics become chaotic. The goal now is to see how one can incorporate this analytical observation into a computational algorithm to simplify calculations in this limit.

The evidence is mounting, therefore, that the SC/IVR model provides a useful description of quantum effects in essentially all aspects of molecular

dynamics. The appropriate (linearized) version of it is very easy to implement—not much more difficult than ordinary classical molecular dynamics—and is perhaps adequate for many purposes, while the full SC/IVR seems to be more generally accurate. We plan to pursue both of these directions.

Publications

C. Dellago, P. Bolhuis, and D. Chandler, "Efficient Transition Path Sampling: Application to Lennard-Jones Cluster Rearrangements," *J. Chem Phys.* **108**, 9236 (1998).

C. Dellago, P. Bolhuis, F. Csajka, and D. Chandler, "Transition Path Sampling and the Calculation of Rate Constants," *J. Chem. Phys.* **108**, 1964 (1998).

D. Chandler, "Finding Transition Pathways: Throwing Ropes Over Rough Mountain Passes, in the Dark," in *Computer Simulation of Rare Events and Dynamics of Classical and Quantum Condensed-Phase Systems – Classical and Quantum Dynamics in Condensed Phase Simulations*, edited by B.J. Berne, G. Ciccotti and D.F. Coker, p 51-66 (World Scientific, Singapore, 1998).

F. Csajka and D. Chandler, "Transition Pathways in a Many-body System: Application to Hydrogen-bond Breaking in Water, " *J. Chem. Phys.* **109**, 1125 (1998).

P. Bolhuis, C. Dellago, and D. Chandler, "Sampling Ensembles of Deterministic Transition Pathways," *Faraday Discussion Chem. Soc.* **110**, 421 (1998).

P. Geissler, C. Dellago, and D. Chandler, "Chemical Dynamics of the Protonated Water Trimer," *Phys. Chem. Chem. Phys.* **1**, 1317 (1999).

C. Dellago, P. Bolhuis, and D. Chandler, "On the Calculation of Reaction Rate Constants in the Transition Path Ensemble," *J. Chem. Phys.* **110**, 6617 (1999).

P.L. Geissler, C. Dellago, and D. Chandler, "Kinetic Pathways of Ion Pair Dissociation in Water," *J. Phys. Chem.* **B103**, 3706 (1999).

R. Baer, M. Head-Gordon, and D. Neuhauser, "Shifted Contour Auxiliary Field Monte-Carlo for Electronic Structure: Straddling the Sign Problem," *J. Chem. Phys.* **109**, 6219-6226 (1998).

E. Schwegler, M. Challacombe, and M. Head-Gordon, "A Multipole Acceptability Criterion for Electronic Structure Theory," *J. Chem. Phys* **109**, 8764-8769 (1998).

R. Baer and M. Head-Gordon, "Energy Renormalization Group Method for Electronic Structure of Large Systems," *Phys. Rev. B* **58**, 15296-15299 (1998).

R. Baer, and M. Head-Gordon, "Electronic Structure of Large Systems: Coping with Small Gaps Using the Energy Renormalization Group Method," *J. Chem. Phys.* **109**, 10159-10168 (1998).

C.A. White, and M. Head-Gordon, "Curvy Steps along Idempotent Paths for Density Matrix Based Energy Minimization," submitted *to J. Chem. Phys.*

H. Wang, X. Song, D. Chandler and W.H. Miller, "Semiclassical Study of Electronically Nonadiabatic Dynamics in the Condensed-Phase: Spin-Boson Problem with Debye Spectral Density," *J. Chem. Phys.* **110**, 4828-4840 (1999).

D. Skinner and W.H. Miller, "Application of the Semiclassical Initial Value Representation and Its Linearized Approximation to Inelastic Scattering," *Chem. Phys. Lett.* **300**, 20-27 (1999).

V. S. Batista, M.T. Zanni, B.J. Greenblatt, D.M. Neumark, and W.H. Miller, "Femtosecond Photoelectron Spectroscopy of the I2- Anion: A Semiclassical Molecular Dynamics Simulation Method," *J. Chem. Phys.* **110**, 3736-3747 (1999).

M.T. Zanni, V. S. Batista, B.J. Greenblatt, W.H. Miller, and D.M. Neumark, "Femtosecond Photoelectron Spectroscopy of the I2- Anion: Characterization of the Ã'2∏g,1/2 Excited State," *J. Chem. Phys.* **110**, 3748-3755 (1999).

X. Sun and W.H. Miller, "Forward-Backward Initial Value Representation for Semiclassical Time Correlation Functions," *J. Chem. Phys.* **110**, 6635 -6644 (1999).

V. Guallar, V. S. Batista, and W. H. Miller, "Semiclassical Molecular Dynamics Simulations of Excited State Double-Proton Transfer in 7-Azaindole Dimers," *J. Chem. Phys.* **110**, 9922-9936 (1999).

W.H. Miller, "Using Mechanics in a Quantum Framework: Perspective on Semiclassical Description of Scattering," *Theo. Chem. Accts.* (accepted).

H. Wang and W.H. Miller, "Analytic Continuation of Real-Time Correlation Functions to Obtain Thermal Rate Constants for Chemical Reaction," *Chem. Phys. Lett.* **307**, 463-468 (1999).

W.H. Miller, "Generalization of the Linearized Approximation to the Semiclassical Initial Value Representation for Reactive Flux Correlation Functions," *J. Phys. Chem.* **103**, 9384 (1999).

Selective Chemistry with Femtosecond Infrared Laser Pulses

Principal Investigators: C. Bradley Moore

Project No.: 99005

Project Description

The basic goal is to use the intense fields of 100 femtosecond (fs) infrared (IR) pulses to move a molecule from its equilibrium configuration to a desired transition state in a short time, compared to the time for vibrational energy randomization. In this way, it may be possible to carry out bond-selective and functional-group-selective reactions using IR photons.

Since the first experiments on infrared multiphoton dissociation (IRMPD) 25 years ago, chemists have wanted to be able to select specific reactions by using intense IR lasers to drive vibrational modes corresponding to the desired reaction coordinate. Attempts with nanosecond and microsecond lasers failed because intramolecular redistribution of vibrational energy (IVR) occurs on shorter timescales. Thus all modes are energized simultaneously. Inspired by the increasing availability of intense femtosecond IR pulses, a collaboration with Professor K.-L. Kompa and his group at the Max Planck Institute for Quantum Optics in Garching has been initiated. Initially, a single tunable IR frequency will be used to excite a molecule and products will be detected by standard methods. Ultimately, two tunable IR frequencies will be generated. Pulses of 100 fs duration are fast compared to many IVR processes. Theoretical and experimental studies on diatomic molecules suggest that substantial multiphoton vibrational excitation can take place at optical fields below that for which substantial non-resonant ionization takes place. In the event that selective reactions do not occur, time-resolved measurements of IVR rates may be carried out for individual modes and relaxation pathways identified. These experiments are just on the edge of feasibility with current technology and therefore it is critical to design the excitation schemes correctly the first time. The measurements of spectroscopic level widths and structures, of reaction rates and of picosecond IRMPD in our lab and dynamical calculations in Kompa's lab should allow the optimum conditions for these experiments to be defined in advance.

Initially, we will select unimolecular reactions with low energy thresholds that require only a few IR photons to activate. The hydrocarbon free radicals on which we have recently initiated dynamical studies in crossed laser and molecular beams are an ideal starting point:

$CH_3O \rightarrow CH_2O + H$

$CH_2CH \rightarrow HCCH + H$

Since the reaction coordinate involves simultaneous stretching of the CH bond and contraction of the C=O or C=C bonds, it will be possible to carry out part of the excitation using a nanosecond (ns) IR laser to excite long-lived CH stretching states. Then fs excitation at either the CH or C=O/C=C frequencies will take the molecule through the transition state to products. Products will be detected by Resonance Enhanced MultiPhoton Ionization (REMPI) or Laser-induced Fluorescence (LiF) in the molecular beam on fs or ns timescales.

A second approach heads more directly toward the interests of synthetic chemists. Here the collaboration includes Chemical Science Division's Professor Robert Bergman. Many important synthetic reaction steps have activation energies that correspond to a few IR photons. This chemistry happens mostly in solution where energy is dissipated to the solvent, as well as to other vibrational degrees of freedom within the molecule. Our first target is to stimulate reaction of diazo groups. Jake Yeston (a Bergman/Moore student) has been studying ultraviolet (UV) photolysis of diazo compounds using an excimer laser for photolysis and a continuous-wave (cw) IR diode laser for measuring concentration vs. time for products. The asymmetric stretch of the diazo group near 2150 cm^{-1} is almost identical to the reaction coordinate:

HRC=N=N $\rightarrow$ HRC + NN

where R is an alkyl or cyano group. If these reactions can be driven, we will look at molecules containing a second functional group with lower activation energy and see if the diazo can be driven to react without the normal thermal reaction occurring.

Accomplishments

An experimental apparatus for spectroscopic and dynamic studies of CH_3O has been completed and

double resonance (depletion of UV fluorescence by IR excitation) spectra of the fundamental and first overtone of methoxy isotopomers has been carried out. Dissociation is expected to occur at the energy of the second overtone. Experiments to record spectra by fragment detection and by fluorescence depletion are underway.

Appropriate diazo molecules have been synthesized and picosecond UV flash photolysis studies using the visible absorption of the carbene product have been initiated.

Study of Radionuclide-Bacterial Interaction Mechanisms

Principal Investigators: Heino Nitsche and Petra Panak

Project No.: 99006

Project Description

This project proposes to determine the influence of microorganisms on radionuclide transport in the environment. The goal is to develop a quantitative and mechanistic understanding of radionuclide interaction, in particular of the actinides neptunium and plutonium, with aerobic and anaerobic soil bacteria. The information from this study is important for improving reactive transport models for predicting the movement of neptunium and plutonium at contaminated sites and assessing the risk of potential nuclear waste disposal sites. Furthermore, the results will be transferable to possible biotechnology processes for stabilization and remediation of radionuclide-contaminated sites. This interdisciplinary study combines actinide chemistry, microbiology, and molecular environmental science.

The production and testing of nuclear weapons, nuclear reactor accidents, and accidents during the transport of nuclear weapons have caused significant environmental contamination with radionuclides. Due to their long half-lives and high chemical- and radio-toxicity, the actinides pose a significant threat to human health. Their migration behavior is controlled by a variety of complex chemical and geochemical reactions such as solubility, sorption on the geo-medium, redox reactions, hydrolysis, and complexation reactions with inorganic, organic, and biological complexing agents. In addition, microorganisms can strongly influence the actinides' transport behavior by both direct interaction (biosorption, bioaccumulation, oxidation, and reduction reactions) and indirect interaction (change of pH and redox potential), thus immobilizing or mobilizing the radioactive contaminant. Very little information is available about these processes. Our research focuses on the interaction of aerobic bacteria that are present in the upper soil layers and anaerobic bacteria that can be found in deeper geologic formations.

Accomplishments

We studied the interaction of Pu(VI) with two strains of *Bacillus sphaericus* (ATCC 14577 and ATCC 4525), *Bacillus subtilis* ATCC 6051, *Pseudomonas aeruginosa* ATCC 10145, and two strains of *Pseudomonas stutzeri* (ATCC 17588 and ATCC 51152), representatives of the main aerobic groups of soil bacteria present in the upper soil layers. The accumulation studies have shown that these soil bacteria accumulate high amounts of Pu(VI) in the concentration range examined (4-81 mg/l).

The sorption efficiency increases with increasing Pu(VI) concentration and depends on the amount of biomass in the sample. To study the biosorption efficiency as a function of biomass, we used *Pseudomonas stutzeri* ATCC 17588 and *Bacillus sphaericus* ATCC 14577. The biosorption efficiency decreases with increasing biomass concentrations. This is due to increased agglomeration of the bacteria at higher biomass concentrations, thus leading to a decrease of the total surface area and the number of available complexing groups. The spores of *Bacillus sphaericus* show very high biosorption at low biomass concentration, which decreases significantly with increasing biomass concentration. The vegetative cells of *Pseudomonas stutzeri* and *Bacillus sphaericus* display a very similar sorption behavior. They also show decreasing biosorption efficiency with increasing amount of biomass, but the decrease is less than for the *Bacillus sphaericus* spores. At higher biomass concentrations (> 0.7 g/l), the vegetative cells of both strains and the spores of *B. sphaericus* show comparable sorption efficiencies.

Information on binding strength and reversibility was obtained from extraction studies with 0.01 m ethylenediaminetetra acetic acid (EDTA) solution. For all biomass concentrations, the plutonium bound to

the biomass was almost quantitatively released. These results indicate that the plutonium is bound to the cell walls and is not transported to the inside of the cells. The complex formed with the functional groups of the cell surface is less stable than the EDTA-complex. We observed no significant differences of extraction behavior between the different strains or between the vegetative cells and the spores.

Using optical absorption spectroscopy, we found that the amount of Pu(VI) decreased with increasing concentration of biomass. The spectra also confirmed that no Pu(VI)-bacterial complexes were formed. Synchrotron-based x-ray absorption spectra [x-ray absorption near-edge structure (XANES)] and extended x-ray absorption fine structure (EXAFS)] revealed that the plutonium, initially present as Pu(VI), was reduced to Pu(IV), which was coordinated to phosphate groups of the bacterial cells. This is the first observation of actinide reduction by aerobic soil bacteria.

Publications

P. J. Panak and H. Nitsche, "Interaction of Aerobic Soil Bacteria with Hexa- and Pentavalent Plutonium," *Radiochim. Acta*, (draft).

High-Precision Arithmetic with Applications in Physics and Mathematics

Principal Investigators: David Bailey

Project No.: 99007

Project Description

For a growing number of investigators in mathematics, physics, and engineering, the standard computer hardware arithmetic (IEEE 64-bit) available on today's computer systems is inadequate. Some problems require twice this amount ("double-double precision"), while other problems require much more—hundreds or even thousands of digits. High-precision arithmetic of this sort is typically performed using software packages, one of which is the Principal Investigator's "MPFUN" package.

Some of the more interesting applications of high-precision arithmetic are the recent discoveries of new mathematical identities. In these studies, hundreds of new identities were discovered, using the "PSLQ" algorithm and high-precision arithmetic. Perhaps the most remarkable discovery of this general type is a new formula for the mathematical constant pi, which was found in 1997 by the Principal Investigator and two Canadian mathematicians. This formula, which eluded mathematicians for centuries, has the remarkable property that it permits one to determine the n-th hexadecimal or binary digit of pi, without computing any of the first n-1 digits, using a simple scheme that can be implemented on a workstation or personal computer. This is the first instance in history of a new formula for pi discovered by computer.

In the past two years, these results have been overshadowed by some remarkable discoveries by the British physicist David Broadhurst. Using a high-precision PSLQ program written by the Principal Investigator, he has found an impressive number of new results in quantum field theory. For example, he has shown that in each of the ten cases with unit or zero mass, the finite part of the scalar 3-loop tetrahedral vacuum Feynman diagram reduces to four-letter "words" in an alphabet of seven "letters."

This project proposes to develop new computer software for performing high-precision arithmetic, and to explore applications of this software. Some specific tasks include: (1) porting the MPFUN package to the C/C++ language; (2) developing portable software libraries to perform double-double and quad-double precision arithmetic, with related transcendental and utility routines; (3) designing a library of basic linear algebra subroutines (BLAS) utilizing double-double precision arithmetic; (4) developing parallel programs for performing the PSLQ algorithm, using very high-precision arithmetic; (5) developing a new package for arbitrary precision arithmetic, based on the properties of IEEE arithmetic; and (6) exploring some specific applications of this software that require very high precision arithmetic. One specific application that will be pursued is to investigate the phenomenon of vortex roll-up in fluid mechanics.

Accomplishments

Accomplishments in the first year of this project include:

- The MPFUN package has been converted from Fortran-77/90 to C/C++. This was done mostly in a complementary effort by Professor Sid Chatterjee and Hermann Harjono of University of North Carolina.
- A library of double-double precision routines, together with supporting routines for transcendental functions and binary-decimal conversion, has been completed and is available at the web site www.nersc.gov/~dhbailey.
- A library of basic linear algebra subroutines (BLAS) utilizing double-double precision arithmetic has been designed and is now mostly complete. This was done mostly in another complementary effort by Sherry Li of National Energy Research Scientific Computing (NERSC), together with several students working with Professor James

Demmel of University of California at Berkeley.

- A new variant of the "PSLQ" integer relation detection algorithm has been discovered that is well-suited for parallel programming. This new algorithm has now been successfully implemented on both a distributed shared memory parallel system (the SGI Origin 2000) and a highly parallel, distributed memory system (the SGI/Cray T3E).
- Using the new parallel PSLQ programs mentioned above, several very large integer relation computations have been performed. These include the identification of the fourth bifurcation point in the "logistic iteration" of chaos theory (a 121-dimensional integer relation search, requiring 10,000 digit arithmetic), the verification of a conjecture by Broadhurst regarding the dimension of Euler sum constants (a 145-dimensional integer relation problem, requiring 5,000 digit arithmetic), and the discovery of a relation involving the real root of Lehmer's polynomial (a 125-dimensional integer relation problem, requiring 50,000 digit arithmetic).

The computations mentioned in the last item are easily the largest integer relation computations ever performed. They clearly demonstrate that these computational tools can be used to discover new mathematical and physical principles, principles that are well beyond the reach of present-day theoretical techniques. Even more intriguing, these results suggest that there is an intimate relationship between quantum field theory and algebraic number theory in pure mathematics. The implications of these discoveries are currently being investigated by researchers in the U.S., Canada, and Great Britain.

Publications

D.H. Bailey and D.J. Broadhurst, "Parallel Integer Relation Detection: Techniques and Applications," LBNL-44639 (submitted to *Math. of Computation*, October 1999).

D.H. Bailey and D.J. Broadhurst, "A Seventeenth-Order Polylogarithm Ladder," LBNL-44640 (submitted to *Experimental Math.*, October 1999).

D.H. Bailey, "Integer Relation Detection," LBNL-44481 (to appear in *Comp. in Science and Engineering*, November 1999).

D.H. Bailey and J.M. Borwein, "Experimental Mathematics: Recent Developments and Future Outlook" LBNL-44637 (to appear as a chapter in upcoming book *Future of Mathematics*, November 1999).

Numerical Simulation of Turbulent Swirling Boundary Layers

Principal Investigators: John Bell and Alexandre Chorin

Project No.: 98005

Project Description

Numerical simulations of intense vortices interacting with the surface have been valuable tools in the study and analysis of phenomena such as tornadoes, waterspouts, and dust devils. In particular, numerical models have identified the importance of the no-slip boundary condition at the surface. It is the resulting strong radial inflow in the swirling boundary layer that allows tornadoes to achieve such high wind speeds. However, accurate simulations of this phenomenon at a high Reynolds number are difficult, due to the significant scale separation between the boundary layer and the larger vortex circulation.

Accomplishments

We have applied adaptive mesh refinement (AMR) to the simulation of an axisymmetric tornado-like vortex. Tornadoes are generally believed to form when rotating air near the earth's surface is forced to converge underneath a strong thunderstorm updraft. It is known from previous work that tornado-like vortices with remarkably realistic swirling velocity fields (as compared to observations) can be produced when a simple vertical forcing field is used to drive the convergence of rotating air.

To facilitate high-resolution studies of swirling boundary layers, we have developed a refinement criterion based on the cell Reynolds number. Statistically, numerical results with this new refinement criterion show excellent agreement

compared to uniform fine grid solutions, even for long time simulations. The results indicate that, at a fraction of the computational cost of a uniform grid, we can accurately predict mean maximum windspeeds in the tornadic vortex within one percent of those predicted by full-resolution simulations. AMR facilitates increased resolution in the boundary layer and allows us to expand the size of the domain to be several times larger than the tornado-like vortex under study, eliminating edge effects that can pollute computational results. An example of this is shown in the figure, which shows the azimuthal velocity field throughout a cylindrical domain four kilometers in height and four kilometers in radius. Each box indicates a region of refinement by a factor of two, and enclosed boxes indicate multiple levels of refinement. Regions of substantial refinement are mostly limited to the boundaries, with a few exceptions due to intense axisymmetric rolls in the interior of the domain. The maximum azimuthal velocity occurs in the lower left-hand corner, at a radius of 100 meters and a height of only 70 meters. A close-up of the swirling velocity field in the core of the tornadic vortex, shown in the inset in the figure, bears strong similarity to tornadic velocity fields recently observed with portable Doppler radar.

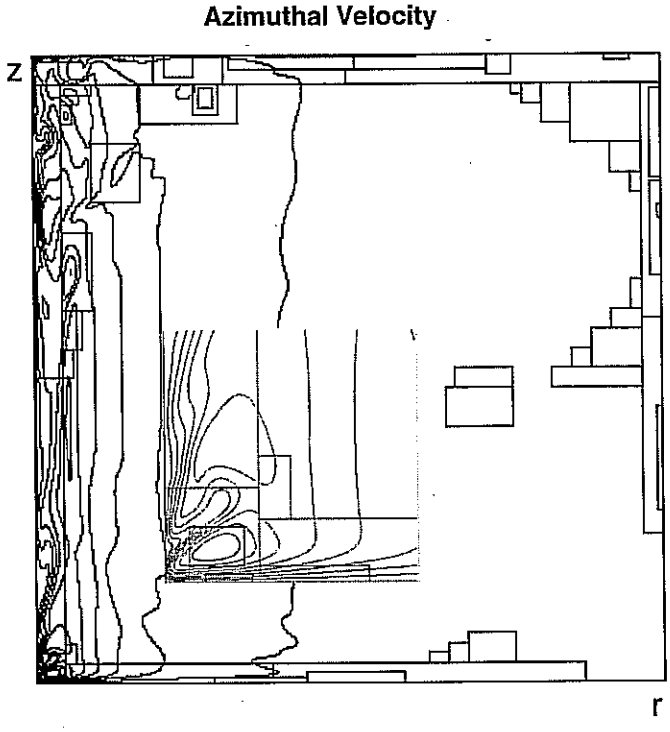

Figure 1. Numerical simulation of a swirling vortex in a four kilometer domain. Inset is a blowup of the lower portion of the lower left hand corner of the domain. The boxes shown are regions of mesh refinement.

Publications

D.S. Nolan, A.S. Almgren and J.B. Bell, "High Reynolds Number Simulations of Axisymmetric Tornado-like Vortices with Adaptive Mesh Refinement," submitted for publication to *Journal of the Atmospheric Sciences* (July 1999).

Agenda for Combustion Visualization

Principal Investigators: E. Wes Bethel and Terry Ligocki

Project No.: 99009

Project Description

The scope of this project was to perform basic research and development of scientific visualization processes, including working prototypes and recommendations for future work, as applied to combustion research.

Two fundamental challenges are encountered when considering scientific visualization of combustion simulation data. First is the problem of sheer data size. Second is the data modeling problem. Increasing computational and storage capacities have enabled undertaking simulations of higher resolution and complexity. Such simulations result in large data sets. The size of these data sets often necessitates careful consideration of data management issues. In some cases, the simulation is performed on a remote resource, and transferring the data to local storage is not feasible using existing Wide Area Network (WAN) technology. In other cases, the data will not fit onto the researcher's workstation, so processing and visualization must be performed remotely.

The data modeling challenge stems from the fact that combustion simulation codes and data models are built upon a software application programming interface (API) that supports dynamic adaptive grid refinement (AMR) with data storage and retrieval from opaque C++ objects. The data modeling infrastructure code is a large, complex and under-documented system, reflecting its heritage as an ongoing research effort. Current research efforts include development of techniques to extend the base data modeling system to accommodate new variables, including embedded boundary information, as well as face- and volume-fraction data. The existing data model assumes that all data is local.

Our goals for this project include developing an understanding of the issues involved with the end-to-end visualization process, developing some working prototypes of tools that would be of immediate use to combustion researchers, and identifying potentially fruitful research and development paths for future visualization efforts.

Accomplishments

Our efforts on this project were divided into two primary phases. First, we became familiar with the research data modeling infrastructure currently in use by local combustion researchers. Second, we undertook multiple visualization research and development paths for the purpose of producing working prototypes. Our efforts produced a better understanding of issues that will contribute to fruitful future research and development efforts in combustion visualization.

To become familiar with the existing combustion data modeling infrastructure, we first attempted to copy and compile the source code for the infrastructure. Among the snags encountered along the way, we discovered that the C++ compilers on our machines were either out-of-date or inadequate, as the data modeling infrastructure makes use of features in the C++ language that are not always implemented by vendors. Replacing or upgrading compilers is a challenging effort involving personnel from multiple groups.

We identified a three-tier approach for visualization of combustion data. First, we modified existing example code in the infrastructure to output grids that had been "flattened." Flattened grids are those that are structured and exhibit no local refinement. Contemporary visualization tools expect grids of this type. By flattening grids, we were able to quickly make use of existing tools for the purpose of simultaneously rendering combustion simulation variables as well as embedded boundary information.

In the future, there are two potential approaches that warrant further exploration. The first such technique involves visualizing and rendering data from the highest-resolution grid available at any point in space in the problem domain. In an adaptive grid model, any given point in space may be contained in multiple grids. Our suggestion is to first render all the coarse data, then the next finest level, and so forth, in a "painter's" type algorithm. The first improvement in this approach is to detect areas in coarse grids that are occupied by higher resolution grids, and perform processing only in areas not occupied by higher resolution grids. The next improvement involves actually "blending" the data between coarser and finer resolution grids. Multi-

resolution techniques that address this problem have been explored in other visualization systems tooled for terrain-style visualization. However, we feel that grid "zippering" must be addressed by the same code that performs the combustion calculations so as to not introduce error or other artifacts into the visualization process.

We also explored the possibility of a "protocol-based" interface to the research data modeling infrastructure. In contrast to a file-based interface (a flattened grid), or a direct programmatic interface (visualization tools compiled with the research data modeling interface), the protocol interface is like a transaction server. A remote client connects to a data server and requests information and data. The data server is by necessity built atop the research data modeling infrastructure. The client, however, has no such dependencies. This type of interface appears promising, especially for "browsing" a number of data sets that are remotely located from the researcher. We took this concept one step further, and designed a network-based application infrastructure around this concept. This project, called Image-Based-Rendering-Assisted Volume Rendering, is a scalable parallel volume rendering framework that combines computational, data modeling and visualization technology. This framework implements a client-server model, where the client is a viewer that runs on commodity grade graphics hardware, while the server is implemented using specific data modeling technology. The existing project shows the use of both combustion and Distributed Parallel Storage System data modeling technology.

We explored combining a research visualization tool and the research data modeling infrastructure at the programming language level. We learned that such an effort had been independently initiated by researchers at the National Center for Supercomputing Applications (NCSA). We obtained their tools and successfully combined them in our environment and were able to generate visualizations. Except for the data size limitations, this approach will be fruitful for rapid prototyping of visualization tools by combustion researchers.

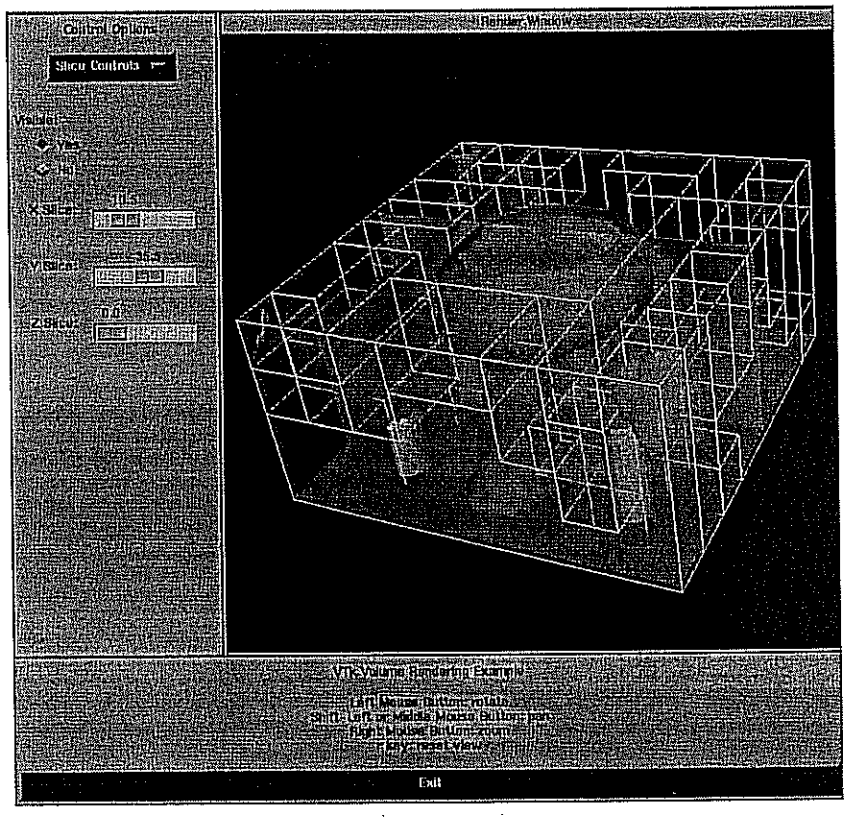

Figure 2. From an embedded boundary combustion simulation, this image shows direct volume rendering of density, false-colored density slices, an isosurface of density, embedded boundary geometry, and the adaptive grid outlines.

Numerical Methods for Time-Dependent Viscoelastic Flows

Principal Investigators: Grigory Barenblatt and Alexandre Chorin

Project No.: 98007

Project Description

Liquid crystalline polymers (LCPs) are inherently anisotropic. At rest, concentrated solutions and melts exhibit orientational texture, in which there is a local preferred orientation that extends over distances on the order of micrometers, but the sample is isotropic on a macroscopic scale. The texture is related to local orientational defects and is sometimes described as consisting of "domains." The texture evolves with shear and seems to vanish at high shear rates, but a texture always returns when the flow stresses have relaxed. Existing theories of anisotropic liquids predict the evolution of orientational structure in shear flow. However, the calculated textures are unlike those seen in liquid crystalline polymers, where the length scale of the texture appears to be independent of the macroscopic scale of the experimental equipment. It is generally believed that long-range interactions (elastic coupling) must be included in the nematic potential to generate a constitutive theory of liquid crystalline polymers that can accommodate defect textures. The first such proposal seems to be by Marrucci and Greco (MG).

Accomplishments

We have developed and studied a new model for LCPs under shear flow, which is an extension of the well-known Doi theory with an inter-molecular potential of MG type that accounts for long-range elastic coupling. To the best of our knowledge, our work is the first to have considered the full set of equations that couple the dynamics of the nematic structure tensor to the flow equations, via the stress tensor. Our model turns out to exhibit a remarkably rich spectrum of dynamics, even for the simplest case of highly symmetric shear flow; this richness results directly from the coupling between the flow and the nematic order. In particular, we discovered that the shear field may develop unsuspected discontinuities associated with the formation of defect lines, and strong vorticity "bursts" associated with the release of accumulated elastic energy. It is unclear at this stage whether the defect dynamics observed in our simulations are similar to the defects observed in experiments, but it is very likely that for the full range of dynamics to be observed one has to simulate the proposed equations in three dimensions.

We have also made progress on the formulation of models for polymeric solutions and melts at large strain rates, taking into account the fact that both materials are suspensions of aggregates whose bonds are stronger when the aggregates are of smaller size. At large strain rates the largest aggregates are destroyed. This explains the fact that the shear-stress-strain rate dependence is not monotonic. This does not lead to an instability of the solutions if one takes into account the finite time it takes the equilibrium microstructure of the fluid to form in response to a given non-steady strain rate. This leads to a model described by a nonlinear pseudo-parabolic equation of third order. We have performed numerical investigations of the initial value problem for this equation, and have observed the formation of steps in the velocity distribution across the flow, which we identify with mushy regions. The agreement with the data is better than in previous models. In the next stage of the work, we shall assume that the characteristic time of the microstructural transformation is a constant. We expect to eventually develop a more complete theory of kinetics of microstructural transformation.

Publications

R. Kupferman and M.M. Denn, "Emergence of Structure in a Model of Liquid Crystalline Polymers with Elastic Coupling," *J. Non-Newt. Fluid Mech.* (in press, 1999).

Integrated Systems and Network Resource Management

Principal Investigators: Bill Kramer

Project No.: 99010

Project Description

Scheduling work effectively in large computer systems traditionally focused on scheduling central processing unit (CPU) time, with only modest efforts made to schedule other resources. This made sense in the past, since CPU power was the most expensive resource and it was relatively straightforward to achieve high CPU utilization rates with Symmetric Multi-Processor (SMP) systems. Therefore, CPU oriented benchmarking often gave a good indication of the overall efficiency of a given computer system for scientific applications.

The advent of Massively Parallel Processing [e.g. the National Energy Research Scientific Computing (NERSC) T3E] and SMP cluster systems (e.g. the NERSC IBM SP) makes it more complex to manage systems in order to achieve a given level of effectiveness. Despite that, it is possible to develop software and system management procedures that allow highly effective system operation. An example is the effort to improve T3E utilization when NERSC, working closely with Cray Research, was able to improve utilization through the gradual introduction and exploitation of system software functionality. During the first 18 months in service, the T3E-512 utilization increased from approximately 55% to over 90% while still focusing most of the system resources on large jobs. This represents almost a factor of two in price performance increase for the system or, in other words, the equivalent (in 1999 costs) of $10.25M.

No single metric existed to either predict or help guide system managers in determining how effective a system could be or what functionality would have the most impact on effectiveness.

The purpose of this project was to address this shortfall in the measurement of modern computer systems.

Accomplishments

This LDRD contributed to the development of a meaningful metric of system-level effective performance. Designated the Effective System Performance (ESP) test, this metric attempts to distinguish the theoretical maximum system capability from measured system utilization. In particular, the ESP test measures the efficiency of the overall system and the ease with which the system can handle large configuration jobs and typical system management tasks.

The first implementation of the ESP test consists of a "mix" of individual jobs that are multiple copies and different sized versions of application programs. Two additional jobs are "full configuration" (FC), namely calculations that use the entire system. The mix is submitted at staggered times to the system in three "lots", with the composition of the "lots" and the order of the jobs random. The first of the two FC jobs is submitted at a certain predetermined time in the test. This job is to be run immediately upon submission. Immediately after the FC job is completed, the system is shut down and then rebooted. After the system has been rebooted, the mix is restarted, and eventually, the second FC job is submitted. The objective of the ESP test is to minimize the total elapsed wall clock time until all jobs are completed. The ESP test is illustrated in Figure 3.

The initial application of the ESP test had dramatic impact on four activities. First, an early version of the test was used as a key requirement in the recently completed NERSC-3 contract. It sets a baseline measure of system effectiveness for the NERSC-3 IBM SP. The test then will be used to measure improvements in system effectiveness. The contract has specific improvement goals for effectiveness based on ESP test results.

The second impact is in the Department of Energy "Valuation of Ultra-scale Computing Systems: A White Paper " report, developed by representatives of 12 major supercomputing sites and four computer vendors. The report states the following recommendation "Design benchmark suites and performance models to predict the effectiveness of the systems instead of solely measuring utilization after the fact. It is recommended that the results of the [LBNL] ESP effort mentioned in the previous section, for example, be brought to the attention of advanced platform managers in government, industry and at educational institutions."

The ESP test is part of a paper being prepared for submission by NERSC staff. Running the test on several more systems and configurations is currently underway. A draft of the paper can be found at www.nersc.gov/~dhbailey.

Finally, the concepts developed during the work on ESP were part of the well-regarded tutorial entitled "High Performance Computing Facilities for the Next Millennium," given by NERSC at SuperComputing '99. This tutorial was attended by 60 people from throughout the supercomputing community.

The work developed by this LDRD will continue in several different areas. NERSC staff are expanding the ESP concepts and developing simulation tests that provide a "prediction" of effectiveness before a test is run on an actual system. NERSC and several vendors will run the test in different environments and report results. One or more formal papers will be presented on the ESP test in FY00 and, of course, the ESP test will continue to influence the NERSC-3 contract to the benefit of Berkeley Lab and NERSC users. This work is also a key technical component in proposals for additional funding from Department of Energy and other sources.

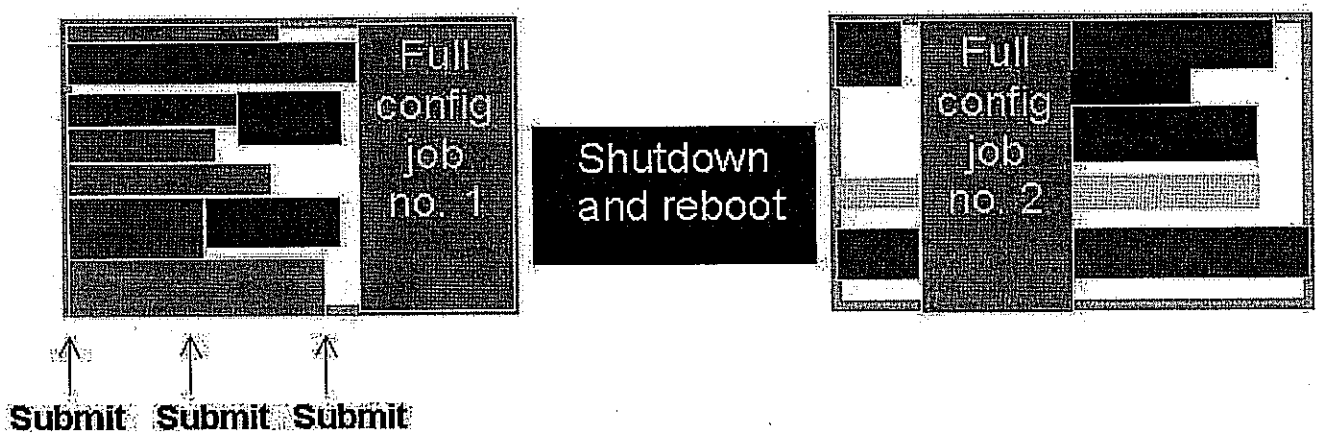

Figure 3. ESP Test Timeline

Once the test run is complete, a system effectiveness ratio E is computed as

$$E = \frac{p_1 t_1 + p_2 t_2 + \ldots + p_n t_n}{P\,(S+T)}$$

where

- p_i = Number of processors utilized by job i
- t_i = Wall clock run time in seconds required by job i on a dedicated system
- n = Number of individual jobs run during the test
- P = Total number of processors in the system
- S = Time required for shutdown and reboot
- T = Averaged wall clock run time (not counting shutdown and reboot)

Accurate Segmentation of Nuclei and Cells from Confocal Microscope Images using Geometric Methods

Principal Investigators: Ravi Malladi

Project No.: 98008

Project Description

If one is able to measure/quantify cell and tissue organization, and changes pertaining to it, using image cytometry, one will be able to characterize the changes that occur during carcinogenesis. Once those morphological changes have been characterized, one can start correlating them with other elements involved, such as genetic instability, the abnormal pattern of expression of some proteins, etc. This correlation will help one to understand the relationship between structure and cell function and could be clinically applied as a new marker for cancer diagnosis and prognosis. The two key technical capabilities required in such study are (a) cell and nuclei staining and imaging using a confocal microscope, and (b) efficient and reliable image analysis techniques that make denoising, segmentation, and measurement possible. In this project, we focussed on the latter aspect and built both models and code for reliable and fast image denoising and segmentation algorithms. The work should ultimately help address specific biological hypotheses; develop new algorithms to accurately segment whole cells and other structures inside cells, including those from 3-D x-ray microscope images; and develop measurement algorithms based on spatial statistics to study the internal and external organization of cells in tissue.

Accomplishments

Fluorescence-labeled Imagery

We have both devised schemes and built code to efficiently segment nuclei shapes from confocal microscope imagery of fluorescence-labeled cells. The core algorithms and techniques are borrowed from real-time image analysis work, due to Malladi and Sethian, which was tested extensively in the medical imaging setting (magnetic resonance imaging, computerized tomography, ultrasound, etc.). The idea is to exploit the strengths of both the automatic and interactive segmentation techniques, namely, (a) preprocess the 3-D image to reduce noise by paying close attention to edge-geometry, (b) an automatic segmentation method based on gradient-weighted thresholding, (c) regularization of the rough shapes describing the nuclei via curvature- and edge-based speed, and (d) finally, split the nuclear clusters that are sometimes found in cases where cells are structurally dominated by their nuclei.

Lamin Surface Markers

We also focussed on segmenting nuclei shapes from a different imaging technique. The fluorescence-labeled DNA does not necessarily extend out to the surface of the nucleus. Our collaborators therefore used specific nuclear surface markers (lamin antibodies) to delineate nuclear surfaces. However, these surface markers do not uniformly label the surface and the images are much noisier, presenting a more challenging segmentation task. Some results used a modified shock-based flow and a segmentation method utilizing the Fast Marching algorithm. More importantly, due to poor definition of cell boundaries, the adjoining cell shapes in a cluster tend to incorrectly merge into one. We used a multiple interface flow idea to handle this particular difficulty.

Publications

C. Ortiz, R. Malladi, S. Lelievre, and S. Lockett, "Segmentation of Nuclei and Cells using Membrane Related Protein Markers," submitted to *Journal of Microscopy* (January 2000).

A. Sarti, C. Ortiz, S. Lockett, and R. Malladi, "A Geometric Model for 3D Confocal Image Analysis," submitted to *IEEE Transactions on Biomedical Engineering* (September 1999).

Electron Collision Processes above the Ionization Threshold

Principal Investigators: C. William McCurdy and Thomas Rescigno

Project No.: 99011

Project Description

The computational prediction of the electronic *structure* of atoms and molecules has become a practical task on modern computers, even for very large systems. By contrast, sophisticated calculations on electronic *collisions* have been limited in terms of the complexity of the targets that can be handled and the types of processes that can be studied. Collision processes are, nevertheless, central to the problems of interest to the Department of Energy (DOE), playing a key role in such diverse areas as fusion plasmas, plasma etching and deposition, and waste remediation. The intermediate energy region, extending from the ionization threshold to a few hundred eV, presents the greatest challenge for *ab initio* theory, since the infinity of energetically accessible final states precludes one from writing down a wave function that describes all possible scattering events, and is simply a reflection of the fact that ionization persists as one of the fundamentally unsolved problems of atomic collision theory.

A practical route to solving the intermediate energy electron collision problem cannot rely on close-coupling approaches, but rather must be based on formalisms that allow the wave function itself to be computed without recourse to the explicit asymptotic form, and on methods that extract cross section information from the wave function without knowing its detailed asymptotic form. The purpose of this project is to develop such an approach for both atoms and molecules. The approach will build on the algebraic variational formalism we have previously developed to study electron-molecule scattering. The approach will be extended to include the scattered-wave, flux operator formalism, which we have developed, complex optical potential interactions, and a variety of techniques based on analyticity. For atomic ionization problems, we will carry out direct solutions of the Schroedinger equation on a (complex) numerical grid and use the projected flux operator formalism to extract total and differential ionization cross sections.

Accomplishments

There have been two major accomplishments during the past year:

- We completed and published a theoretical study of low-energy electron scattering by carbon dioxide. This is, significantly, the first *ab initio* calculation to obtain quantitative agreement with experimentally measured cross sections for this system.
- We produced the first essentially exact quantum mechanical results for low-energy electron impact ionization of an atom, a problem that has resisted accurate numerical treatment since the formal theory was set forth over thirty years ago.

CO_2 is an important atmospheric constituent and plays an important role in many gaseous electronics applications. Electron-CO_2 collisions are of fundamental and practical importance and continue to attract the attention of experimentalists and theorists. Using the complex Kohn variational method, we carried out a study of electron-CO_2 scattering from .25 to 10 eV. This is the first *ab initio* study to accurately reproduce the two dominant features observed in experiment, namely the dramatic rise in the integral cross sections below 2 eV and the resonance enhancement near 3.8 eV. We also obtained elastic differential cross sections that agree well with very recent experimental measurements. Previous theoretical studies have failed to achieve even qualitative agreement with experiments below 5 eV. These calculations show the importance of including a proper balance between electron correlation and polarization in the scattering wave functions. Our calculations also included a preliminary consideration of the effects of vibrational motion, which was found to be important in describing the cross sections in the resonance region. Further work on this problem is currently underway.

Our work on electron impact ionization of hydrogen, which is being published in *Science*, represents a breakthrough in quantum collision physics. An exact numerical treatment of the complete Coulomb three-body problem is a goal that

had resisted solution for over thirty years, since the problem was originally formulated. The key to our successful treatment was the use of a formulation that does not require us to know the detailed asymptotic behavior of the wave function, which is extremely complicated for three "free" charged particles. Our calculations required the solution of very large (~4 million) systems of complex linear equations to produce wave functions that contain complete information about the collision process, including probabilities for detecting final scattered electrons with specific energies and angles of ejection. Our results are in essentially perfect agreement with absolute measurements.

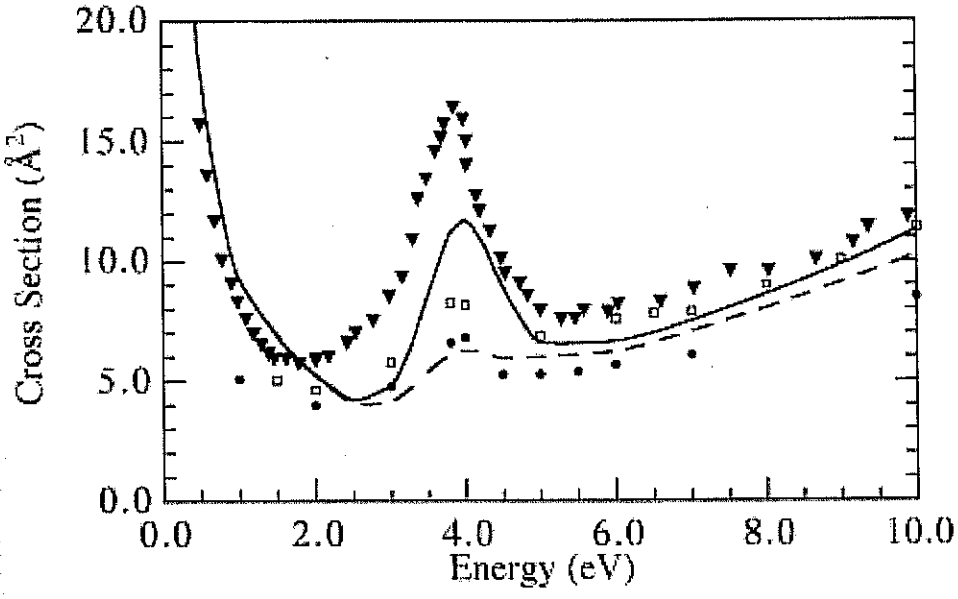

Figure 4. Total and vibrationally elastic e-CO_2 integrated cross sections. The theoretical results (solid and broken curves) are compared with several recent sets of experimental results.

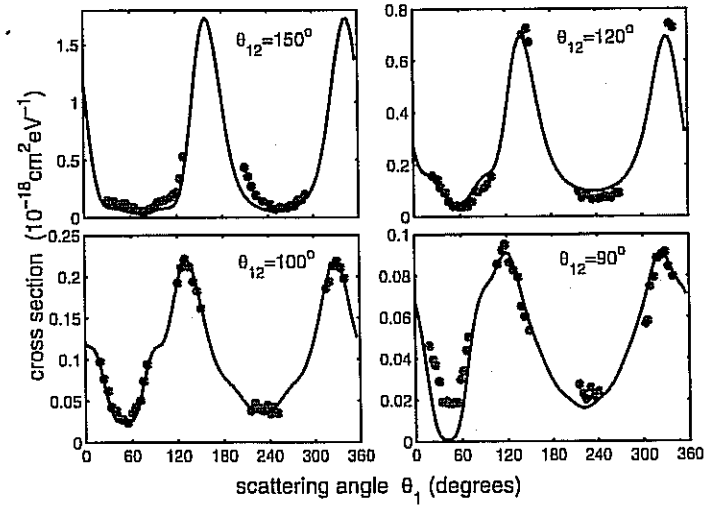

Figure 5. Triple differential cross sections for electron impact ionization of atomic hydrogen at 17.6 eV incident energy. θ12 is the angle between the two outgoing electrons, while θ1 is the angle between the incident electron beam and one of the detected electrons.

Publications

T. N. Rescigno, "Aspects of an *Ab Initio* Approach to Electron Scattering by Small Molecules," in "Supercomputers, Collision Processes and Applications," edited by D. Crothers and K. Taylor (Plenum, Yew York, 1999) p. 67.

M. Baertschy, T. Rescigno, W. A. Isaacs, and C. W. McCurdy, "Benchmark Single-Differential Ionization Cross Section Results for the s-Wave Model of Electron-Hydrogen Scattering," *Phys. Rev. A* **60**, R13 (1999).

D. A. Byrum, W. A. Isaacs, and C. W. McCurdy, "Theoretical Studies of Low-Energy Electron-CO_2 Scattering I: Total, Elastic and Differential Cross Sections," *Phys. Rev. A* **60**, 2186 (1999).

T. Rescigno, M. Baertschy, W.A. Isaacs, and C.W. McCurdy, "Collisional Breakup in a Quantum System of Three Charged Particles," *Science 286*, 2474 (1999).

T. Rescigno, C. W. McCurdy, M. Baertschy and W. A. Isaacs, "On the Use of Two-Body Close-Coupling Formalisms to Calculate Three-Body Breakup Cross Sections," *Physical Review A* **60**, 3740 (1999).

Feature Extraction from Observed and Simulated Data

Principal Investigators: Bahram Parvin and Qing Yang

Project No.: 99012

Project Description

The current generation of environmental satellites and numerical simulation models generates a massive amount of spatio-temporal data. These data represent different geophysical fields (such as sea surface temperature, wind stress, precipitation) at different spatial and temporal resolutions. For example, the NASA MODIS sensor could potentially generate 200 gigabytes of data per day, where 50-100 gigabytes of it are ocean products. Similarly, a 20-year ocean circulation model, with $O(5 - 10)$ km resolution, at 20-minute time steps produces about 4 terabytes of prognostic data. Such a vast amount of data poses serious performance, management, and comprehension problems. Furthermore, existing comparative analyses of climate codes are based on aggregate measures such as average temperature and raindrops, ignoring higher-level feature activities. Particular features of interest include vortices and saddle points. Ocean vortices are an important component of global circulation because they are an efficient transport and mixing mechanism for salt/freshwater, heat, plankton communities, nutrients, and momentum. Similarly, atmospheric vortices are important for meteorological studies, e.g., their frequency, strength, duration, and tracks. If vortices can be detected and tracked, pertinent questions can be asked about other sources of data. For example, how does the precipitation vary along these tracks, and how does precipitation vary for individual storms? What is the correlation between storm strength and sea surface temperature (SST)? How do the storms alter SST? Such an integrated knowledge-based system provides a detailed view of the air/sea interaction that goes beyond simple means. Thus far, our research has focused on a feature-based representation of spatio-temporal SST data for providing an intelligent summary of the underlying images and to facilitate correlation studies between different types of events (in different fields) for hypothesis testing, comparative analysis of numerical simulation and observational data, and efficient visualization of meaningful information. This is achieved by computing the feature velocities from the fluid motion and then computing pertinent features from the computed vector field. We have applied our methods to 12 years of sea surface temperature data. The data set has a spatial resolution of 9 to 18 km that is recorded by the Advanced Very High-Resolution Radiometry (AVHRR) sensor once every two days.

Accomplishments

Specific accomplishments include:

- *A novel formulation of flow field computation that incorporates an incompressibility constraint for tracking fluid motion.* The algorithm is then implemented through a multigrid representation for reducing the computational complexity. Computed flow of feature velocities are then compared with ground truth data in selected regions.
- *A robust approach for detection and tracking vortices and saddle points from the vector field representation.* Vortices are important in two

ways. First, they are an important component of the global circulations. Thus, their duration, direction, and localization are valuable to climatic studies. Second, they are singular events that provide a compact representation of the spatio-temporal images. Thus, they can be used as indices for representation and quick access.

- *Interesting climatic results indicating that the numbers of singular events (in SST data) are seasonally correlated and that they have a preferred localization.* This is observed by accumulating event features over a 12-year period and representing their occurrences as a probability density function. The result is shown in Table 1.

Year	Day 1-90	91-181	182-273	Day 274-365
1986	5194	3991	5126	4425
1987	4970	3881	5382	4455
1988	5119	3991	5241	4854
1989	5051	4303	5060	4230
1990	4933	4183	5298	4470
1991	5166	4133	5542	4870
1992	5254	4273	5446	4617
1993	4988	4043	5247	4171
1994	5057	3942	5071	3380
1995	5109	4212	5089	4419
1996	5283	4090	5210	4847
1997	5422	4280	5278	4519
1998	5095	4074	5133	4534

Table 1 shows the number of events (vortices and saddle points) for each year and each season. This table indicates (almost) equal number of events in each year. The number of events is higher in the first 90 days than the second 90 days. It rises again during the third 90 days and then drops during the fourth 90 days. This seasonal periodic effect has not been observed in the past due to lack of effective computational techniques.

Inter-annual observations indicate preferred localization of events at 40°S and 40°E during 1986-89, 1993, and 1998. Figure 6 shows preferred occurrences of events for a 12-year period (2190 images). The results clearly indicate preferred occurrences of events along the equator, Gulf Stream and to the north of it, and 40°S. These areas are the East Pacific instability region, the Gulf Stream vortices, the meander region, and the sub-polar front of the Southern Oceans.

Figure 6. Frequency of occurrence of vortices and saddle points, shown at 1° resolution, from 1986 to 1998.

Publications

Q. Yang and B. Parvin, "Detection and Tracking Vortices and Saddle Points in SST Data," *16th Internation Conference on Interactive Information and Processing Systems for Meteorology, Oceanography, and Hydrology* (to be published, January 2000).

Q. Yang and B. Parvin, "Feature Based Visualization of Large Scale Geophysical Data," (submitted to IEEE Conference on Computer Vision and Pattern Recognition, June 2000).

Q. Yang and B. Parvin, "Detection of Singular Events from SST Data," (submitted to Internation Conference on Pattern Recognition, September 2000).

Q. Yang, B. Parvin, A. Mariano, and R. Evans "Detection and Tracking of Vortices in SST Data," (submitted to *Journal of Geophysical Research Letters*).

Q. Yang, B. Parvin, A. Mariano, and R. Evans "Seasonal and Interannual Studies of Singular Events from SST Data (submitted to *Journal of Geophysical Research Letters*).

Berkeley Lab Distribution (BLD): Software for Scalable Linux Clusters

Principal Investigators: William Saphir

Project No.: 99013

Project Description

An exciting development in scientific computing over the past few years has been the demonstration that clusters of PCs can achieve performance of supercomputers for many problems of interest to DOE. Such clusters promise to greatly increase the impact of computation on science. Despite their promise, we believe that clusters are destined for only a minor role unless two critical barriers are overcome:

- Most existing and planned system software for clusters is not scalable, making infeasible large clusters that can be applied to DOE mission-critical applications.
- Cluster software is ad-hoc, poorly integrated, lacking in functionality, and difficult to use, making the setup and management of clusters very labor intensive, and limiting their flexibility.

We are designing, implementing, and integrating scalable system software and architectures for clusters. This software will form the basis of the "Berkeley Lab Distribution," or BLD, a complete package of plug-and-play software for configuring, managing, and using Linux clusters.

Accomplishments

In the first year of this LDRD, we have focused on understanding cluster requirements, developing basic infrastructure for the cluster, and building collaborations with other labs that will eventually form the basis for coordinated multi-lab system software development.

The building block for the BLD architecture is a subcluster consisting of a filesystem server and one or more compute nodes that perform computations. The compute nodes of the cluster boot from and mount their root file system over a private Internet Protocol (IP) network. Most existing clusters have not used such a "diskless boot" system because it is difficult to configure by hand, even though it has a number of technical advantages over local operating system installation.

We have developed software called BCCM (Berkeley Cluster Configuration Manager) that makes it significantly easier for a system administrator to set up the compute node root filesystems using a minimum amount of storage on the server, and also handles other tasks required to add a compute node to a cluster. BCCM is scalable, in that the effort and storage space required for an N-node cluster do not vary significantly with N. We do not have a testbed cluster large enough to determine the largest feasible N, but this limit must exist (because of NFS limitations) and clusters larger than N will build from N-node subclusters. BCCM is the first major step BLD project, which will eventually handle all important aspects of cluster administration.

We have established a strong collaboration with Los Alamos and Argonne National Labs to coordinate our cluster development efforts. This collaboration resulted in a full-day tutorial at Scientific Computing '99 on production Linux clusters.

We have developed an extensive collection of benchmark results for processors used in Linux clusters. These results have become an important and highly visible resource for the community.

Publications

Tutorial "Production Linux Clusters," presented at Scientific Computing '99 (LBNL-43738).

"Linux for Scientific Computing," presented at the Oreilly Linux Conference (August 1999).

Linear Algebra and Statistical Algorithms for Text Classification in Large Databases

Principal Investigators: Horst Simon

Project No.: 99014

Project Description

The goal of this research is to use high-performance computing to help understand and improve subspace-based techniques for information retrieval, such as latent semantic indexing (LSI). In the past, LSI has been used only on very small data sets. We are developing an environment and scalable linear algebra algorithms where LSI-based information retrieval can be applied to matrices representing millions of documents and hundreds of thousands of key words. The computational power of the T3E is required to accomplish this.

There are two main components to this: the retrieval accuracy and the efficiency of the algorithms used in retrieval algorithms.

To this end we hope to:

- Further develop our subspace-based model and gain deeper understanding of the effectiveness of LSI. We will also explore the possibility of extending the subspace-based model for handling image and multimedia retrieval problems.
- Develop more robust and computationally efficient statistical tests for the determination of the optimal latent-concept subspace dimensions. We will especially investigate methods based on cross-validation.
- Further explore the low-rank-plus-shift structures of the term-document matrices and develop fast and memory-efficient numerical algorithms for the computation of low-rank matrix approximations. We will also investigate linear-time partial Singular Value Decomposition (SVD) algorithms based on term and document sampling.
- Investigate a variety of statistical methods such as canonical correlation analysis and a generalized linear model for translingual text retrieval.

This project will be one of the first to compute decompositions of complete large term-document matrices. Other efforts have had to resort to sampling to keep things computationally tractable. As such, we are in a unique position to study how scale affects subspace-based retrieval techniques.

We also believe that the algorithms developed here will be of use not only in text retrieval, but in more complicated settings such as classification of image collections, and extraction of images with desired features from large collections. Combining effective search and classification algorithms for image problems with the compute and storage capabilities of future NERSC systems will also help the development of algorithmic techniques for the data and visualization corridors of the next decade.

Our computational approach is planned to explore the use of the SVD. In the future, other low-rank approximations to the document structure will be considered.

Accomplishments

First, we have been successful in porting MATLAB*P to the Cray T3E at National Energy Research Scientific Computing (NERSC). This tool provides the ability to manipulate both dense and sparse matrices stored on the T3E, using the popular MATLAB environment. The goal is to reduce the programming overhead in setting up our numerical experiments.

Preliminary experiments on a large collection with over 500,000 documents have demonstrated the feasibility of our software. We have been able to perform LSI on the complete collection where previous attempts have had to restrict their attention

to a smaller subset of the data. We are now in the process of interpreting the results and designing new experiments that will deepen our understanding of the techniques used.

Second, using a statistical interpretation of text retrieval, we were able for the first time to answer an open question about the optimal subspace dimension for LSI. The result was obtained using a maximum likelihood estimation technique and, for the first time, establishes an optimality criterion for a subspace.

Third, we investigated the question of computing approximate SVDs with possible applications to LSI. This resulted in a new algorithmic approach described in a series of two reports, which are available at www.nersc.gov/research/SIMON

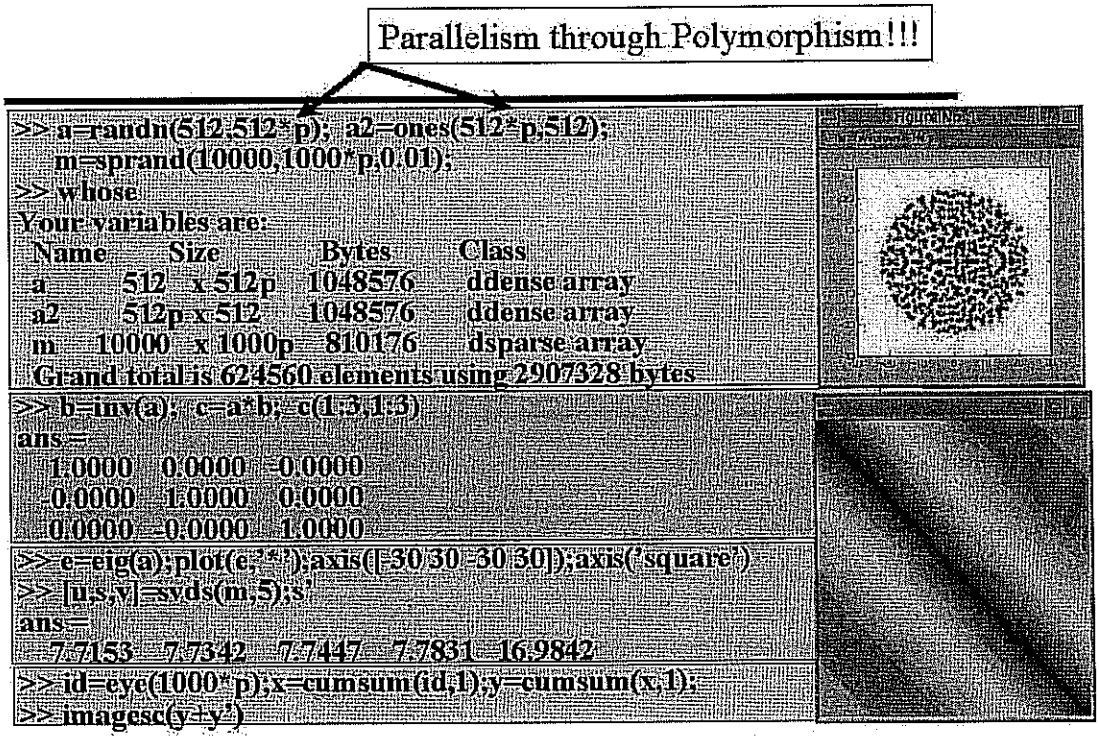

*Figure 7. MATLAB*P creates data structures on the parallel server (here the T3E). All MATLAB tools are available on the workstation.*

Publications

P. Husbands, C. Isbell, and A. Edelman, "MATLAB*P: A Tool for Interactive Supercomputing," Proceedings of the 9th SIAM Conference on Parallel Processing for Scientific Computing (1999).

H. Zha and H. Simon, "On the Updating Problems in Latent Semantic Indexing," *SIAM Journal of Scientific Computing* (1999).

C. Ding, "A Similarity-Based Probability Model for Latent Semantic Indexing." Proceedings of 22nd International ACM SIGIR Conference on Research and Development in Information Retrieval, Berkeley, California (1999).

Z. Zhang, H. Zha, and H. Simon, "Low-Rank Approximations with Sparse Factors I: Basic Algorithms and Error Analysis," LBNL-44003, (1999) (submitted to *SIAM Journal of Matrix Analysis).*

Z. Zhang, H. Zha, and H. Simon, "Low-Rank Approximations with Sparse Factors II: Penalized Methods with Discrete Newton-Like Iterations," LBNL-44217, (1999) (submitted *to SIAM Journal of Matrix Analysis).*

Z. Zhang and H. Zha, "Structure and Perturbation Analysis of Truncated SVD for Column-Partitioned Matrices," LBNL-43597, (1999) (submitted *to SIAM Journal of Matrix Analysis).*

Ocean Particulate Carbon Dynamics

Principal Investigators: Jim Bishop

Project No.: 98035

Project Description

There is an urgent need to devise strategies to stabilize the levels of carbon dioxide in the atmosphere. The purpose of this project is to carry out fundamental research into the dynamics of particulate carbon off the coast of California and in the world's oceans. The sedimentation of particulate organic carbon is the ultimate burial of atmospheric carbon, but particulate carbon dynamics is not well understood because of the difficulty and exorbitance of direct high-precision measurements of trace constituents in the water column. This project seeks to explore the development of an economical autonomous device that profiles particulate organic carbon (POC) and particulate inorganic carbon (PIC) concentrations in the water column on time scales fast enough (~diurnal) to capture biological variability. Biological formation of PIC produces CO_2 as a byproduct and therefore counteracts the CO_2 drawdown due to formation of POC. The device and sensors will be inexpensive enough to permit the first large-scale quantification of the geographic and temporal distribution of POC and PIC. We will also study existing samples of particulate matter collected by large-volume, *in situ* filtration from the North Pacific and other environments, and analyze them for compositional information that may yield insight into the processes of formation and removal of particulate organic and inorganic carbon.

Accomplishments

Our approach to understanding ocean particulate carbon dynamics will enable and refine strategies to meet targets for stabilizing carbon dioxide in the atmosphere.

- Development of autonomous vehicles for carbon system monitoring.
- Development of PIC and POC concentration sensors for the vehicles.
- Data/sample analysis synthesis and publication.

LDRD support in 1999 initiated three activities in the area of ocean carbon cycle research at Berkeley Lab. All activities strongly tie to the vision of the original LDRD proposal and several additional pending initiatives are likely to result in additional funding.

- We worked to implement an optical POC sensor and to develop and implement a PIC sensor (see below) on the Sounding Oceanographic Lagrangian Observer (SOLO) float. An autonomous profiling float developed at Scripps, SOLO is capable of 150 round trips between the surface and 1000 meters. Satellite telemetry of data after each surfacing permits real-time observational data to be obtained from remote locations. With twice-a-day profiling, SOLO can observe ocean carbon biomass variability for four months.
- LDRD support enabled studies to investigate environmental acceptability and effectiveness of different ocean carbon sequestration strategies. The emphasis is on understanding carbon cycle dynamics and on carbon cycle perturbations resulting from ocean fertilization with iron. The focus is also on the development of low-cost, but effective, autonomous monitoring technology required to evaluate ocean carbon sequestration strategies.
- The LDRD work also supported the preliminary design of an autonomously operating POC and PIC flux monitoring device based on the concept of SOLO floats and modified versions of the POC and PIC concentration sensors.

LDRD also supported the synthesis of data and samples on particulate matter dynamics, obtained during four recent oceanographic cruises to the subarctic northeastern Pacific Ocean.

Publications

J.K.B. Bishop, "Transmissometer Measurement of POC," *Deep-Sea Research I* **46(2)** 353-369 (1999).

J.K.B. Bishop, S.E. Calvert, and M.Y.-S. Soon, "Spatial and Temporal Variability of POC in the Northeast Subarctic Pacific," *Deep-Sea Research II* **46(11-12)** 2699-2733 (1999).

P.W. Boyd, N.D. Sherry, J.A. Barges, J.K.B. Bishop, S.E. Calvert, M.A. Charette, S.J. Giovannoni, R. Goldblatt, P.J. Harrison, S.B. Moran, S. Roy, M. Soon, S. Strom, D. Thibault, K.L. Vergin, F.A. Whitney and C.S. Wong, "Transformations of Biogenic Particles from the Pelagic to the Deep Ocean Realm," *Deep-Sea Research II* **46(11-12)** 2761-2792 (1999).

M.A. Charette, S.B. Moran, and J.K.B. Bishop "^{234}Th as a Tracer of Particulate Organic Carbon Export in the Subarctic Northeast Pacific Ocean," *Deep-Sea Research II* **46(11-12)** 2833-2862 (1999).

M. Eek, M.J. Whiticar, J.K.B. Bishop and C.S. Wong, "Carbon Isotope Composition of Alkenones along Line P - NE Pacific: Effects of pCO_2, Nutrients and Temperature," *Deep-Sea Research II* **46(11-12)** 2863-2876 (1999).

I.Y. Fung, S.K. Meyn, I. Tegen, S.C. Doney, J.G. John, and J.K.B. Bishop, "Iron supply and Demand in the Upper Ocean," *Global Biogeochemical Cycles* (in press, 1999).

D. Thibault, S. Roy, C.S. Wong, and J.K.B. Bishop, "The Downward Flux of Biogenic Material in the NE Subarctic Pacific: Importance of Algal Sinking and Mesozooplankton Herbivery," *Deep-Sea Research II* **46(11-12)** 2669-2698 (1999).

Quantitative Measures of Global Climate Change and Carbon Fluxes

Principal Investigators: Donald DePaolo

Project No.: 98009

Project Description

Bringing together scientists from Berkeley Lab and the newly formed Center for Atmospheric Sciences at University of California at Berkeley, this project carried out fundamental investigations that will help quantify the effects of global climate change.

Accomplishments

The Influence of Soil Minerals on Storage and Turnover of Soil Organic Carbon

The project on soil carbon sequestration focused on using isotopes to quantify the turnover time of soil organic matter and soil respiration rates. We investigated soil mineralogy, as originally envisioned, and also expanded the scope of the project to take advantage of a large global-change experiment that was established at the nearby Jasper Ridge Biological Preserve in Stanford, California.

Quantitatively important rates of C sequestration in soils have proven hard to detect with conventional methods due to the large initial stock and high variability. However, the combination of isotopic techniques and soil fractionation can greatly increase our ability to detect early changes in carbon cycling, by magnifying the signal for changes in carbon stocks and sources. In addition, the isotopic signature of C fluxes can be used to investigate root vs. microbial respiration, treatment effects on productivity and decomposition rates, and how these affect soil carbon storage. We added this suite of measurement approaches to elevated CO_2 experiments at Jasper Ridge, to develop new understanding of, and techniques for, ecosystem carbon cycling and global change

With the support of the FY99 LDRD, a global-change experiment at Jasper Ridge was outfitted for the study of the carbon cycling effects of elevated CO_2 alone and CO_2 plus warming, water, and/or nitrogen. The modifications included installing permanent soil chamber bases, soil gas probes, and litter bags. Laboratory capabilities were enhanced for this, specifically by development of an autosampler for stable isotope analysis of ^{13}C in soil respiration and soil leachate collected at the field site.

The second facet of work concerns sensitive detection of changes in soil carbon storage, using a combination of isotopic techniques and soil fractionation. We used soils from a previous Jasper Ridge experiment in which elevated-CO_2 consistently led to positive fluxes of carbon into the soil of the grassland ecosystem. Hungate et al. could not empirically 'find' this carbon, however, due to a large initial stock of soil organic carbon and high

spatial variability. This past year, a graduate student and the P.I. have chemically separated the labile vs. mineral-associated carbon fractions in soils collected from the last year of the experiment. Since the experiment was replicated on sandstone and serpentine parent materials, it provides the first long-term tracer experiment for investigating mineral influences on carbon turnover.

The isotopic content of soil respiration was used to estimate the proportion of CO_2 flux that is derived from root respiration and root exudates of the current growing season versus soil organic matter produced in previous years. The results are that by the end of the growing season (May 1999), approximately 70% of respiration was derived from the current year's photosynthesis (root respiration, fine root turnover, and exudates) and 30% was produced by microbial respiration of soil organic matter from previous years (Figure 1). There was no effect of nitrogen, warming, or water treatments on the contribution of roots to total soil respiration. Preliminary analysis of soil leachate indicates that the warming treatment increased the contribution of roots to dissolved inorganic carbon losses from soil. This is the first *in situ* experimental test of the influence of these environmental factors on root carbon cycling in either respiration or leachate.

In the soil organic matter study, the light (labile) fraction shows a detectable increase in soil carbon ($p<0.031$, $n=10$) in the elevated CO_2 treatment. The ^{13}C isotopic analysis confirms that the light fraction contains more labile carbon, and that the heavy fraction contains more of the older (i.e., more stable) mineral-associated carbon. The radiocarbon content of the heavy fraction of the sandstone and serpentine soils was used to estimate and compare the turnover times of mineral-stabilized C on these soil types, and the capacity of soils to stabilize organic C for long-term storage. We found that the turnover time of mineral-stabilized organic carbon in the top 15 cm of soil is 270 years in sandstone, and 450 years in serpentine.

The Atmospheric Budget of Methyl Bromide (CH_3Br)

Pure samples of CH_3Br were obtained from the three major industrial manufacturers (Albemarle, Dead Sea Bromine, and Great Lakes) for isotopic analysis. These companies manufacture approximately 82% of the world total CH_3Br used as a fumigant. The $\delta^{13}C$ signatures were measured on a Micromass Isoprime Gas Chromatograph-Isotope Ratio Monitoring Mass Spectrometer (GC-IRMS) at the Berkeley Lab Center for Isotope Geochemistry. GC-IRMS allows separation of CH_3Br from other gases, followed by in-line combustion to CO_2 and analysis by magnetic sector mass spectrometry. The method is selective, reproducible, and orders-of-magnitude more sensitive than traditional Dual Inlet Mass Spectrometry (DIMS). The $\delta^{13}C$ values measured by GC-IRMS for individual tanks typically had standard deviations of less than 0.1‰ and were indistinguishable from DIMS measurements made on CH_3Br following off-line closed-tube combustion.

The measured $\delta^{13}C$ values of industrially produced CH_3Br were all low, and there was variability both within and between manufacturers. The $\delta^{13}C$ measured values ranged from –66.4‰ to –43.5‰, and the mean for all measured tanks is –55.7‰ (±2.0‰ S.E.). There were differences in the $\delta^{13}C$ of CH_3Br from the various manufacturers, and thus a weighted mean $\delta^{13}C$ of CH_3Br released from industrial processes should be more accurate. Based on reported CH_3Br production the weighted mean value was –54.4‰, in good agreement with the mean of all measured tanks. The industrial CH_3Br source is isotopically light, probably because thermogenic methane is used as a carbon source for methanol, which in turn is the feedstock for manufacturing CH_3Br.

The results presented here demonstrate that industrially manufactured CH_3Br has a carbon isotopic signature ($\delta^{13}C = –55‰$) that is likely to be significantly different, and therefore readily distinguishable, from the major non-industrial sources. Isotopic measurements of the main CH_3Br sources and the atmospheric reservoir should therefore greatly improve our understanding of the CH_3Br budget, and of the biogeochemical processes controlling atmospheric CH_3Br. This approach could also provide an independent tool for assessing the effectiveness of recent amendments to the Montreal Protocol that call for the complete phaseout of CH_3Br by 2005 in industrialized nations.

Climate Records and Atmospheric Moisture Transport

The main goal of this part of the project is to begin to bridge the gap between basic one-dimensional Rayleigh models of isotopic composition in precipitation and three-dimensional General Circulation Models. We have extended advection-based Rayleigh models by adding evaporation and eddy-fluxes, without losing the simplicity of a

purely latitudinal description of the major features of the isotopic distribution in precipitation.

Based on the ratio of vertical exchange between the ocean and atmosphere, to the horizontal transport of atmospheric moisture, the Earth is divided into three regions: an Equatorial Evaporation-Dominated Zone, a Southern Distillation Zone and a Northern Quasi-Distillation Zone. The isotopic composition of evaporation in the Equatorial Evaporation-Dominated Zone controls the isotopic composition of precipitation in this region, and sets the initial value from which isotopic ratios in the two mid- and high-latitude regions follow. In the distillation zones, three parameters control the spatial $\delta^{18}O$ and δD gradients: 1) temperature through condensation temperature, 2) temperature gradient through water vapor gradient and 3) the Peclet number, the ratio of advective transport to eddy-flux transport.

We also use the model to simulate changes in several climate parameters to determine the temporal response of $\delta^{18}O$ and δD in precipitation. Temporal variations in the $\delta^{18}O$ (or δD) relationship with local surface temperature do not necessarily coincide with the present–day, observed local spatial relationship. All three of the controlling parameters can have an effect on the isotopic fluctuations with time, complicating interpretation of ice core records in terms of temperature. $\delta^{18}O$ and δD are increasingly sensitive to changes in all three parameters at locations distant from the ocean evaporation source. Interior Antarctic and Greenland sites exhibit larger $\delta^{18}O - T$ slopes than do coastal sites.

Evaporation processes are still not well understood, and our first attempt to include the physics of evaporation in the model have not produced precipitation simulations that agree well with the precipitation data. However, we feel that these results will be improved through further experimental study of the kinetic fractionation factor involved in the liquid to vapor transition. Contrary to the results of Johnsen, et al. and Jouzel, et al. results from our model show deuterium excess in Antarctic precipitation is not indicative of the conditions over the source region. The signature of low-latitude evaporation source is removed by molecular exchange over the Southern Ocean and therefore, deuterium excess in Antarctic precipitation appears to be determined by temperature and relative humidity over the Southern Ocean.

In the future, the model must be tested against data collected at mid and high latitudes. Vertical profiles of water vapor concentration, isotopic ratios in water vapor, precipitation data, and isotopic ratios of surface ocean water, all from the Southern Ocean between 50°S and the Antarctic coast, will place constraints on the model input parameters. In addition, the evaporation theory requires experimental determination of the kinetic fractionation factor and further research on how the values of this parameter, determined in the laboratory, apply to the ocean.

The model still has many applications for issues of more regional spatial scale and shorter time-scales. The model should next be incorporated in regional studies of the Northern Hemisphere. Two locations that might be useful in expanding the model are Greenland, where there is much data and interest in interpreting ice core records, and Western Canada, where water vapor transport is mainly in a west-to-east direction, which is ideal for the one-dimensional nature of the model. Input that has been averaged on time-scales shorter than one year provide simulations of the seasonal cycle in the hydrologic cycle and remove the wet season bias of precipitation that is inherent in studies of the average annual characteristics.

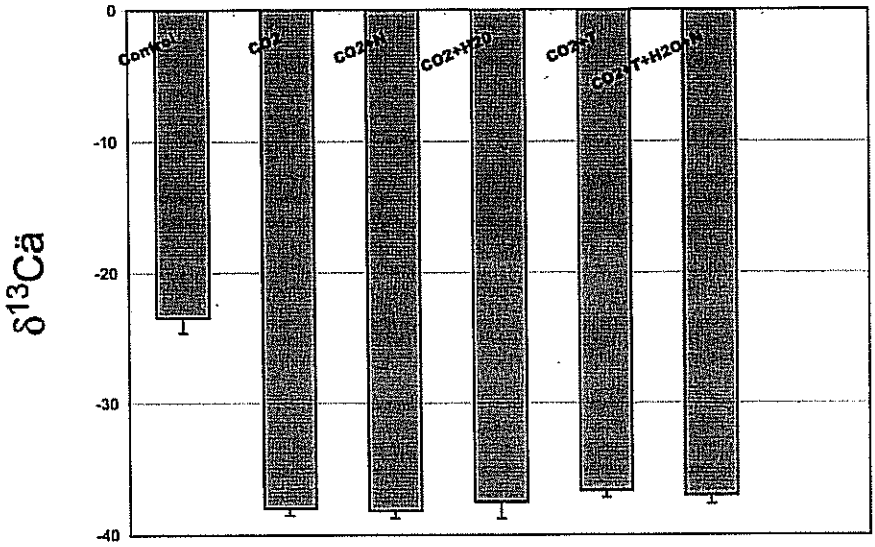

Figure 1. Isotopic signature of soil respiration from control, elevated CO_2, and CO_2 plus nitrogen, water, and/or warming. In all plots with elevated CO_2, root respiration and root exudates combined contribute 70% of total soil respiration, with no significant differences in root contribution among treatments. The percent root carbon was calculated by mass balance between the control ($\delta^{13}C$=-28‰) and elevated CO_2 ($\delta^{13}C$=-42‰) plant inputs.

Samples collected May 18-19, 1999 N=4 per treatment All regressions calculating signature, $R^2 > 0.9$

Publications

S.E. McCauley, A.H. Goldstein, and D.J. DePaolo, "An Isotopic Approach for Understanding the CH_3Br Budget of the Atmosphere," *Proceedings of the National Academy of Sciences*, **v. 96,** 10,006–10,009 (1999).

M. Hendricks, D.J. DePaolo, and R.C. Cohen, "Meridional Moisture Transport and the Global Pattern of $\delta^{18}O$ and δD in Precipitation: Space Versus Time Variations and Implications for Ice Core Paleotemperatures," *Global Biogeochemical Cycles* (in press, 1999).

M. C. Rillig, S.F. Wright, M.S. Torn, and C.B. Field, "Abundance of Glomalin, a Glycoprotein Produced by Arbuscular Mycorrhizal Fungi, along a Tropical Soil Chronosequence on the Hawaiian Archipelago," Proceedings of Soil Science Society of America Spring Meeting (1999).

E.S. Zavaleta and M.S. Torn, "Intermediate-cycling Soil Carbon Increased in Response to Elevated CO_2 in an Annual Grassland Ecosystem," *Bulletin of the Ecological Society of America*, Proceedings of Summer Meeting of Ecological Society of America (1999).

S. Davis, M.S. Torn, M.R. Shaw, and M. Conrad, "Application and Automation of Continuous Flow Analysis of Soil CO_2 and N_20 Stable Isotope Signatures, EOS," Proceedings of Fall Meeting of the American Geophysical Union, 1999 (in press).

M.S. Torn, E.S. Zavaleta, and C.B. Field, "Quantifying Soil C Dynamics with Elevated CO_2 Isotope Tracers and a Simple Model, EOS," Proceedings of Fall Meeting of the American Geophysical Union, 1999 (in press).

E.S. Zavaleta, M.S. Torn, and C.B. Field, Carbon Responses to Elevated CO_2 in Two Annual Grassland Ecosystems: a Stable Isotope Approach, EOS," Proceedings of Fall Meeting of the American Geophysical Union, 1999 (in press).

S. Davis, M.S. Torn, M.R. Shaw, and M. Conrad, "Application and Automation of Continuous Flow Analysis of Soil CO_2 and DIC Stable Isotope Signatures," (draft in preparation for submission to Soil Biology and Biochemistry, 2000).

E. S. Zavaleta, M.S. Torn, and C.B. Field, "Storage of Soil Carbon Due to Elevated CO_2 Detected by Stable Isotope Analysis," (draft in preparation for submission to Biogeochemistry, 2000).

Effects of 2xCO_2 Climate Forcing on the Western U.S. Hydroclimate Using the High-Performance Regional Climate System Model

Principal Investigators: Jinwon Kim, Norman Miller, and Chris Ding

Project No.: 99015

Project Description

Understanding the impacts of increased atmospheric CO_2 concentration on the regional climate, water resources, and socioeconomics is a growing concern (*Kyoto Protocol* 1997). The goal of this project is to study the climate and water resources in the western U.S. under a doubled carbon dioxide (2xCO_2) condition using recent General Circulation Model (GCM) projections as input to a high-performance Regional Climate System Model (RCSM.hp). Detailed objectives include: (1) investigate the effects of 2xCO_2 on the climate and water resources in the western U.S., (2) examine the Sensitivity Imposition Method (SIM) for downscaling GCM ensemble predictions, (3) contribute to the Intergovernmental Panel on Climate Change (IPCC) 2000 Regional Assessment Report and the U.S. National Assessment, and (4) develop the RCSM.hp.

We will investigate the effects of 2xCO_2 on the western U.S. climate using the RCSM.hp to downscale global climate data for the present-day and GCM-projected 2XCO_2 scenarios. The RCSM has been used in climate studies for the western U.S., eastern Asia, and northeast Australia with good results. We will calculate the regional climate sensitivity from the National Center for Environmental Prediction (NCEP) reanalysis (control simulation) and a 2xCO_2 climate projection from the Hadley Centre (sensitivity simulation). The sensitivity run will be made by modifying the present-day temperature and water vapor fields by the amount projected by the GCM. We will focus on precipitation, snow, soil moisture, and basin-scale hydrology for water-resource assessments. Development of the high-performance RCSM is a crucial part of this project, as climate simulations require a large amount of computational resources. A message passing method will be used for efficiency and portability across a variety of high-performance computing platforms. New techniques will be used to match cache-based processor architectures. Efficient schemes to improve data input and output will be developed.

Accomplishments

We have developed a prototype of the RCSM.hp. We have improved the code structure for better stability and ease of conversion. The modified code can be compiled on a CRAY T3E without special options, and code parameters are uniquely defined in a single place for better modularization. A parallelization strategy and implementation procedures, including communication patterns, 2D-decomposition and communication modules, have been designed and implemented. Speed-up of the prototype code on a CRAY T3E is presented in the figure attached. Based on the prototype RCSM.hp, we are building a more scalable version that can efficiently use new SP3 architecture.

During FY99, we have archived and processed the global data from the NCEP reanalysis and the Hadley Center 2xCO_2 climate projection for a hindcast and 2xCO_2 projection, respectively. We have tested the RCSM to evaluate model physics. This test is important as recent state-of-the-art convection schemes are generally "tuned" for specific geographical areas and climate regimes. Most tuning is based on data collected over the Great Plains-Oklahoma region or tropical oceans where the initiation of convection and storm structures are significantly different from the western U.S. Sensitivity tests showed that the simpler Anthesis scheme generally better simulated orographic convection than the more-sophisticated Simplified Arakawa-Schubert Scheme (SAS) in the western U.S.; however, the Anthesis scheme caused significantly more numerical point storms during summer than the SAS scheme. For an inter-annual regional climate simulation for the western U.S., we selected the SAS scheme. In addition to the convection schemes, improvements in land-surface parameters are being examined. Evaluation/improvements of model physics is one of our ongoing tasks in regional climate modeling.

A multi-year western U.S. regional climate hindcast using the RCSM has been completed for the 1988-1995 period. A preliminary evaluation suggests that wintertime precipitation was well simulated, but summer precipitation was somewhat overestimated

in the interior western U.S. Overall, simulated precipitation agrees well with observations, where correlation coefficients between observed and simulated monthly precipitation ranges from 0.6-0.9 for individual states. The multi-year hindcast is also used to study soil moisture. A preliminary analysis showed that snowmelt and vegetation cover play important roles in determining the spatial and temporal variation of soil moisture within the western U.S. A streamflow hindcast for the Hopland basin, the headwater of the Russian River in the northern California Coastal Range, also closely simulated monthly streamflow variation during the 8-year period.

We also completed a preliminary examination of the sensitivity imposition method (SIM) for $2xCO_2$ climate sensitivity studies. Analyses of the results suggested that the SIM, a method that utilizes a reduced set of widely available GCM outputs, can only generate qualitative assessments and needs further examination in comparison with full ensemble downscaling methods. Results from these simulations are reported in a special journal volume for U.S. National Assessment.

The RCSM's semi-distributed hydrologic model (TOPMODEL) was advanced with a deep ground water flux term, which controls the amount of soil-water flux into the deep ground. This term plays an important role in the total water budget for the near-surface soil, but it was not included in the original concept of this project and should be addressed in future work.

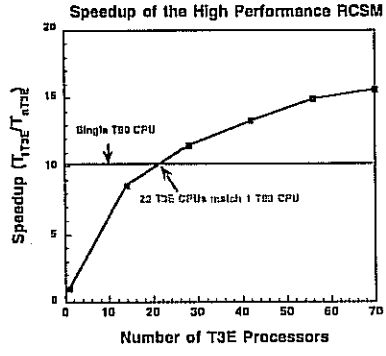

Figure 2. Speedup of the high performance RCSM as a function of number of T3E CPUs.

Publications

N.L. Miller, J. Kim, and Robert K. Hartman, "Downscaled Climate and Streamflow Study of the Southwestern United States," *Journal of American Water Resources Association* (in press, December 1999).

J. Kim, N.L. Miller, J.D. Farrara, and S.Y. Hong, "A Numerical Study of Precipitation and Streamflow in the Western United States During the 1997/1998 Winter Season," *Journal of Hydrometeorology* (under review, July 1999).

J. Kim, and N.L. Miller, "Hydroclimate modeling of the Western United States: A Hindcast and $2xCO_2$ Impacts," Presentation at Conference on Detection and Modeling of Regional Climate Change (June 1999).

N.L. Miller, and J. Kim, "Downscaled Hydroclimate and Streamflow Sensitivity Analysis of the Western United States," Presentation at Conference on Detection and Modeling of Regional Climate Change (June 1999).

J. Kim, N.L. Miller J.D. Farrara, D. Cayan, and K. Mo, "Winter Season Hydroclimate Study for the Western U.S. using the Regional Climate System Model (RCSM)," Presentation at 11th Conference on Applied Climatology (January, 1999).

N.L. Miller, J. Kim, J. D. Farrara, K. Mo, D. Cayan, "Short-term and Seasonal Streamflow Predictions for a California Coastal Basin during the 97-98 Winter," Presentation at 14th Conference on Hydrology (January, 1999).

Methane Hydrates: Resource Assessment, Production, and Role in Climate Change

Principal Investigators: Larry Myer, Raymond Jeanloz, Jen Blank, George Moridis, and Arlon Hunt

Project No.: 99016

Project Description

The purpose of this project was to conduct research on key scientific issues concerning the formation and possible production of methane hydrates as an energy resource. Methane hydrates are solids in which water forms a rigid lattice containing a guest molecule, methane. The concentration of methane per unit volume of water can be very large; 1 m^3 of fully saturated hydrate contains 164 m^3 of methane at standard temperature and pressure and only 0.8 m^3 of water. Methane hydrates occur ubiquitously along the continental shelves and slopes throughout the world as well as in on-shore permafrost regions. They thus constitute a huge potential energy resource, the amount of which may exceed the amount of combustible carbon available from all other fossil fuels. Use of methane as a fuel has environmental benefits. It has been estimated, for example, that conversion of existing coal-fired power generation to methane gas would reduce CO_2 emissions by 40 to 50%. However, the impact of methane as a greenhouse gas is perhaps as much as 10 times that of CO_2. Thus it must be produced and utilized without release.

To address these issues, improved understanding of hydrate formation mechanisms, thermodynamics, and kinetics is required. Numerical simulators incorporating these mechanisms are then required in order to perform resource assessment and evaluate potential safe production strategies.

Accomplishments

Three activities were undertaken. The first involved development of a method for preparing microcrystalline methane hydrate. The second activity was focused on study of kinetic reactions using Raman spectroscopy. The third activity, a new module including methane hydrate properties, was written for a general-purpose reservoir simulation code.

Several methods for preparing and analyzing microcrystalline methane hydrates were investigated. These included the production of water aerosols several microns in diameter in high-pressure methane and carbon dioxide environments (~10 ∞C; 700 to1200 psi). A specialized high-pressure system (Berkeley Lab's polarization-modulated multi-angle scatterometer) was developed to form clathrates and to monitor their physical properties in real-time using polarized light scattering. This system can determine the particle size and shape of various solid and liquid aerosols. When clathrates form from water droplets, they become non-spherical. This is a condition detected using the scatterometer. A method was developed to prepare a water aerosol in a high-pressure, temperature-controlled sample chamber equipped with low-birefringence windows for polarized scattering measurements. The vessel was successfully used to produce a water aerosol in both high-pressure CH_4 and CO_2environments, with drop sizes ranging from two to ten microns. Experiments are continuing to produce microcrystalline hydrates at temperatures above the freezing point of water. These experiments should elucidate the equilibrium and kinetics of clathrate formation and dissolution.

New experimental apparatus was developed to study equilibrium and kinetic reactions in the methane-water-hydrate system. The apparatus couples a hydrothermal diamond anvil cell (HDAC) with resistance heating and Raman spectroscopy. The apparatus was assembled and tested. Calibrations were carried out to allow real-time pressure determination from frequency shifts in the fluorescence of ruby grains located within the HDAC sample volume. A video monitor was also tested for use in photo-imaging of hydrate structure formed in the HDAC. Unique experiments in a pressure/temperature regime relevant to the deep marine/shallow crust environment can now be performed.

A new module, EOSHYDR, was completed and incorporated into the Earth Science Division's TOUGH2 general-purpose simulator for multicomponent, multiphase fluid and heat flow and transport in the subsurface. EOSHYDR is designed to model the non-isothermal CH_4 release, phase behavior, and flow under the conditions of the common methane hydrate deposits (i.e., in the permafrost and in deep ocean sediments) by solving

the coupled equations of mass and heat balance. As with all other members of the TOUGH2 family of codes, EOSHYDR can handle multidimensional flow domains and Cartesian, cylindrical or irregular grids, as well as porous and fractured media. Both an equilibrium and a kinetic model of hydrate formation or dissociation are included. Example simulations were performed. Results are presented for three test problems designed to explore different mechanisms and strategies for production from CH_4-hydrate reservoirs. These tests include thermal stimulation and depressurization under both permafrost and suboceanic conditions. The results of the tests tend to indicate that CH_4 production from CH_4-hydrates is technically feasible and has significant potential.

Publications

G. Moridis, J. Apps, K. Pruess, and L. Myer, "EOSHYDR: A TOUGH2 Module for CH_4-Hydrate Release and Flow in the Subsurface," LBNL Report 42386 (1998).

Numerical Simulation of Reactive Chemical Transport in Geologic Media

Principal Investigators: Karsten Pruess and George Brimhall

Project No.: 96031

Project Description

The purpose of this project is to develop a capability for detailed three-dimensional simulation of reactive chemical transport, and to study the geologic evolution of an actual ore deposit through reactive porous media flow, subject to unique geologic constraints. The site chosen for the analysis is the El Salvador mine, which is located in the Atacama Desert of northern Chile. El Salvador is operated by CODELCO, whose database of ore grades derived from 11,000 drill holes is available to this project.

The site-specific modeling effort will determine the interplay between paleoclimatic change, hydrogeologic conditions, erosion and uplift, and the mobilization and enrichment of massive amounts of copper-bearing minerals in response to spatially and temporally varying redox conditions. TOUGH2, Berkeley Lab's existing general-purpose, multiphase, multicomponent simulator, is being applied to model the evolution of hydrogeologic conditions over geologic time. The simulator is also being enhanced to describe the transport of chemical species subject to kinetic and equilibrium-controlled reactions, and is ported to advanced massively-parallel computing platforms.

Results from the project are expected to aid in future exploration efforts for porphyry copper deposits, and in the management of acid mine waters, leach dumps, mine tailings, waste disposal, and hydrothermal convection system. The reactive chemical transport capabilities will also be useful for assessing and remediating environmental contamination at Department of Energy (DOE) and industrial sites.

Accomplishments

We have developed a comprehensive numerical simulator, TOUGHREACT, which considers non-isothermal multi-component chemical transport in both liquid and gas phases. The coupled model is implemented by introducing reactive chemistry into the framework of the existing non-isothermal multi-phase flow code TOUGH2. A wide range of subsurface thermo-physical-chemical processes is considered. The model can be applied to one-, two- or three-dimensional porous and fractured media with physical and chemical heterogeneity. The model can accommodate any number of chemical species present in liquid, gas, and solid phases. A variety of equilibrium chemical reactions are considered, such as aqueous complexation, gas dissolution/exsolution, cation exchange, and surface complexation. Mineral dissolution/precipitation can proceed subject to either local equilibrium or kinetic conditions. The code was first developed on a PC, and then tested on VAX and UNIX systems. Later the simulator was ported to the Cray T3E at the National Energy Research Scientific Computing Center (NERSC), and a parallelized version was developed, resulting in significant improvement of computing efficiency.

As reported in the last year (1998) LDRD summary, the model has been successfully applied to supergene copper enrichment which involves oxidative weathering of pyrite (FeS_2) and chalcopyrite ($CuFeS_2$) and the associated acidification. This causes mobilization of metals in the unsaturated zone, with subsequent formation of enriched ore deposits chalcocite (CuS) and covellite (Cu_2S) in the reducing conditions below the water table. The alteration of primary minerals and the development of secondary minerals predicted by our model are consistent with observations in supergene copper deposits in the Atacama Desert.

The model has been qualified and applied in the Yucca Mountain nuclear waste disposal project, which is investigating whether Yucca Mountain, Nevada, is a suitable place for a nuclear waste repository. The TOUGHREACT model has been used to analyze and predict hydro-thermo-chemical behavior in heater tests and after emplacement of the nuclear wastes. A large number of aqueous species, minerals, and gases are considered in the simulation. Preliminary modeling results (Figure 3) indicate the importance of considering hydrochemical interactions between fracture and rock matrix for this type of system.

The model has also been used for analysis of rock alteration in geothermal fields, and is being applied in two new projects: (1) investigation of contaminant cleanup in the vadose zone at the Department of Energy's Hanford site; and (2) prediction and evaluation of coupled processes for CO_2 disposal in geologic formations.

In summary, the TOUGHREACT model is well suited for reactive transport in variably saturated porous and fractured media. The model allows us to understand the large space and time scale involved in the intricate web of interactions of fluids, chemicals, and rocks. This coupled model will be of wide interest to diverse fields including environmental geology, hydrology, economic geology, and sedimentary diagenesis, to name a few. The capabilities of the model have been illustrated with a few examples. The full potential is yet to be explored in the future.

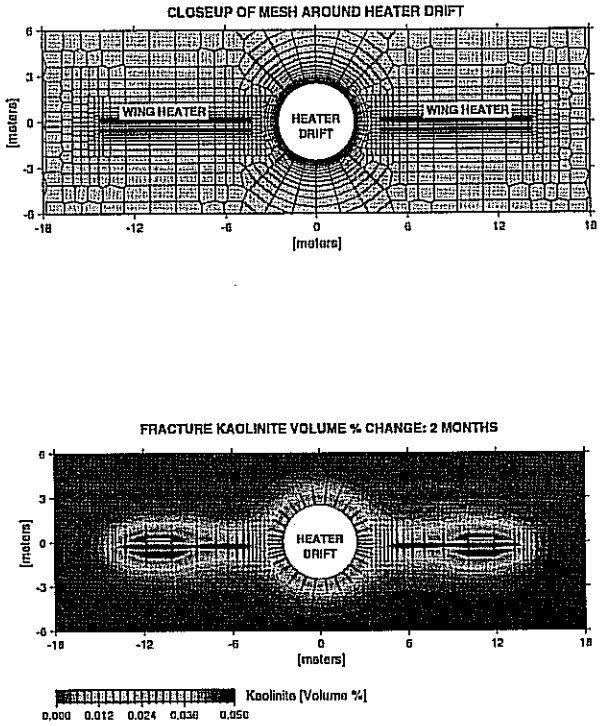

Figure 3. *Hydro-thermo-chemical modeling for drift scale heater test (top). Close-up view of mesh around heater drift (bottom). Results: change of mineral volume.*

Publications

T. Xu, K. Pruess, and G. Brimhall, "An Improved Equilibrium-kinetics Speciation Algorithm for Redox Reactions in Variably Saturated Flow Systems," *Computers & Geosciences*, **25(6)**, 655-666 (1999,v.).

T. Xu, S.P. White, and K. Pruess, "Modeling of Pyrite Oxidation in Saturated and Unsaturated Subsurface Flow System," *Transport in Porous Media*, (in press).

T. Xu, and K. Pruess, "Non-isothermal Multiphase Fluid Flow and Subsequent Geochemical Transport in Variably Saturated Fractured Rocks: 1. Approaches," submitted to *American Journal of Science*, (in revision).

T. Xu, E. Sonnenthal, N. Spycher, K. Pruess, and G. Brimhall, "Non-isothermal Multiphase Fluid Flow and Subsequent Geochemical Transport in Variably Saturated Fractured Rocks: 2. Applications," submitted to *American Journal of Science* (in revision).

T. Xu, and K. Pruess, "Hydrothermal Fluid Flow and Mineral Alteration in a Fractured Rock under Multiphase H_2O-CO_2 Mixture Conditions," submitted to World Geothermal Congress 2000, Kyushu-Tohoku, Japan (May 28 - June 10, 2000).

T. Xu, K. Pruess, and G. Brimhall, "Reactive Chemical Transport in Fractured Rock: Supergene Copper Enrichment," Proceedings of Dynamics of Fluid in Fractured Rocks, Berkeley, California, LBNL-42718, 397 pp. (February 10-12, 1999).

T. Xu, K. Pruess, and G. Brimhall, "Oxidative Weathering Chemical Migration under Variably Saturated Conditions and Sugergene Copper Enrichment," Lawrence Berkeley National Laboratory Report, LBNL-43129, 41 pp. (1999).

Development of Mixed Waste Bioremediation: Biodegradation of Complexing Agent, Ketone, and Heavy Metal Mixtures

Principal Investigators: William Stringfellow and Jennie Hunter-Cevera

Project No.: 97010

Project Description

The presence of complexing agents and ketones in mixed wastes directly and indirectly influences the migration of toxic metals and radionuclides from land disposal sites at Department of Energy facilities. The objective of this research is to gain fundamental information concerning the fate of mixed wastes in biologically active environments. In this research, it is hypothesized that biodegradation of organic components in mixed wastes will influence the biogeochemistry and mobility of co-contaminant actinides and metals. Results from this project will be used in support for larger, longer-term research projects examining the bioremediation of mixed wastes containing both heavy metals and actinides.

The approach taken has been to apply classic methods of microbial ecology and physiology to elucidate fundamental information needed for modeling the biogeochemistry and environmental fate of mixed wastes. The focus of this year's research is to examine the impact of metal-ethylenediaminetetra acetic acid (EDTA) complexes on the biodegradation of solvents found in mixed wastes. In order to identify the major variables of importance to modeling actinide migration in the subsurface, we will examine the impact of individual metal-chelates on microbial processes driving actinide biogeochemistry.

Accomplishments

The first year of study focused on the isolation and characterization of microorganisms capable of degrading the ketone solvents. The second and third year of study examined how biomass formed during ketone solvent degradation could adsorb actinides,

and how co-occurring contaminants found in mixed wastes at the Hanford site could impact biomass formation. In the third year, we also investigated the impact of metals and metal-EDTA complexes on ketone biodegradation, and evaluated biomass formation.

Mixed wastes at the Hanford facility contain high concentrations of nitrate. Nitrate was examined for its influence on ketone metabolism and bacteria growth under both oxygen-limited and anaerobic conditions. Under oxygen-limited conditions, nitrate stimulated the growth of the ketone-degrading mixed culture. Under strictly anaerobic conditions, nitrate did not serve as an electron acceptor for ketone degradation.

Metals and metals-EDTA complexes had a significant negative impact on ketone metabolism, depending on the metal in the complex. Copper-EDTA was the most toxic complex tested to date. Surprisingly, lead-EDTA was not inhibitory to ketone metabolism at the concentrations tested. The impact of metal complexes on biomass formation is being used to model how mixed wastes can influence biofilm formation and thereby plutonium migration in the subsurface.

Publications

W.T. Stringfellow, I. AlMahamid, and N. Hakem, "Biosorption of Plutonium and Neptunium by Solvent Degrading Bacteria," (in preparation for submission to *Environ. Sci. Technol.*).

W.T. Stringfellow, "Inhibition of Nethyl Iso-butyl Ketone (MIBK) Degradation by Metal Complexes Found at Mixed Waste Sites," (in preparation for submission to *Environ. Toxicol. Chem.*).

N. Hakem, I. AlMahamid, and W.T. Stringfellow, "Plutonium Behavior in the Environment," presented at American Chemical Society National Meeting, Anaheim, California (March 1999).

Development of High-Performance TOUGH2 Codes

Principal Investigators: Yu-Shu Wu, Karsten Pruess, and Chris Ding

Project No.: 99017

Project Description

TOUGH2, a general-purpose numerical simulation program for simulating flow and transport in porous and fractured geological media developed and maintained at Berkeley Lab, is now being used in over 150 organizations in more than 20 countries. The largest user community is within the U.S., where TOUGH2 is being applied to problems in geothermal reservoir engineering, environmental remediation, and nuclear waste isolation. TOUGH2 is one of the official codes selected by the Department of Energy (DOE) for its civilian nuclear waste management program to help evaluate the suitability of the Yucca Mountain site as a repository for nuclear wastes.

The largest and most demanding applications of TOUGH2 currently arise in the context of nuclear waste isolation work. Berkeley Lab is in charge of developing a 3-D, site-scale flow and transport model at the Yucca Mountain site for DOE. The model involves using unstructured computational grids of 100,000 blocks and more, and hundreds of thousands of coupled equations of water and gas flow, heat transfer and radionuclide migration in subsurface. These large-scale simulations of highly-nonlinear multiphase flow and multicomponent transport problems are being run on workstations and PCs, and are reaching the limits of what can be accomplished on those platforms.

The purpose of this project is to explore whether the TOUGH2 can be upgraded to take full advantage of modern supercomputing capabilities. This will be accomplished by the following steps:

(1) Analyze and restructure the TOUGH2 codes for implementing a parallel scheme.

(2) Develop a parallel scheme for partitioning grid blocks for processor sub-domains of simulated systems. This includes examining for load balance involving both the Jacobian

matrix element calculations and the later linear equation solution. We also need to investigate the suitability of the Metis partitioner software and integrate it into the codes.

(3) Restructure linear solver part to incorporate the AZTEC parallel solver into the codes, and investigate the solver suitability for large-scale problems.

(4) Enhance computational performance of TOUGH2 on the T3E, or on other multi-processor computers, by one-to-two orders of magnitude improvement both in size of problems to be solved (up to 105 - 106 grid blocks) and in CPU time required.

(5) Create a TOUGH2 computing environment on the T3E, and make it available to the TOUGH2 user community worldwide.

Accomplishments

In FY 1999, we accomplished the following:

(1) Entire TOUGH2 codes have been parallelized and verified for correctness, including:

- Jacobian matrix calculations are parallelized through domain decomposition using the Metis partitioner.
- Nonlinear equations are solved using the Newton method, which incorporates the AZTEC parallel solver.

(2) Systematical evaluation of the codes, convergence rate, and computational efficiency have been carried out using real Yucca Mountain field problems. The results have been summarized in two papers. The paralleled code is efficient—it solves 300,000 unknown equations with stiff-condition numbers in 0.5 seconds on 512 processors of T3E. The code scales well to large processors and large problems. For the 3-D 300,000-equation problem, the speedup on 512 processors is 489.

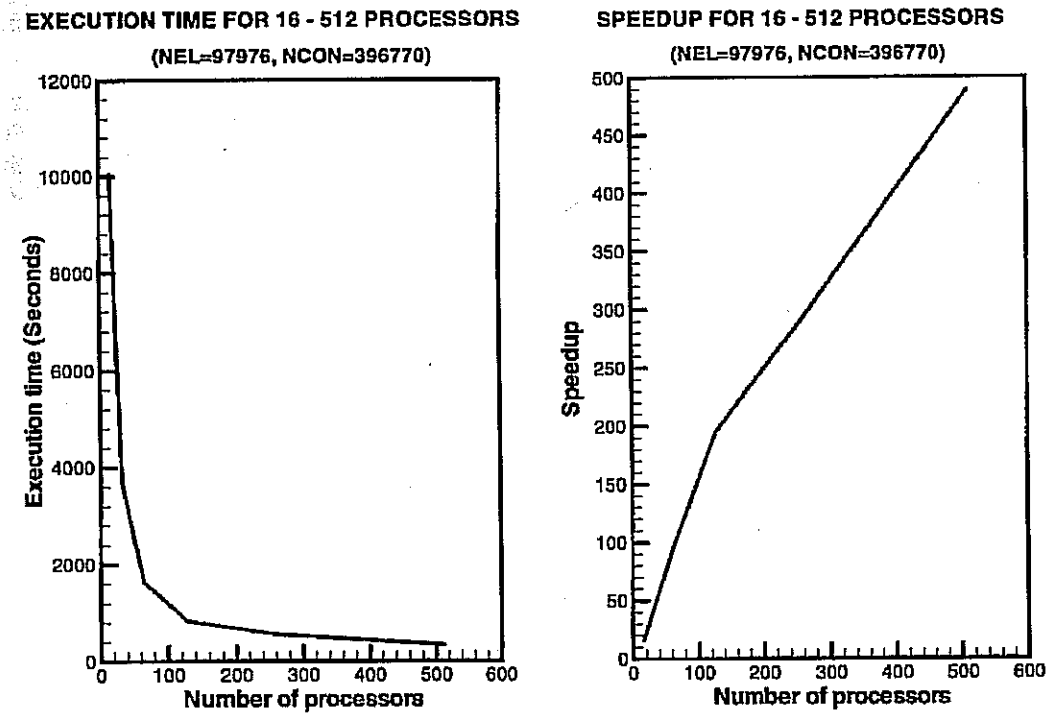

Figure 4. Execution time and parallel speedup on 3-D problem for 16, 32, 64, 128, 256 and 512 processors on the Cray T3E-900.

Publications

E. Elmroth, C. Ding, Y.-S. Wu, and K. Pruess, "A Parallel Implementation of the TOUGH2 Software Package for Large Scale Multiphase Fluid and Heat Flow Simulations," proceedings of Supercomputing '99, ACM (November 1999) LBNL-43385 (May 1999).

E. Elmroth, C. Ding, and Y.-S. Wu, "Higher Performance Computations for Large Scale Simulations of Subsurface Multiphase Fluid and Heat Flow," (submitted to *Journal of Supercomputing*, 1999).

Instrumentation for Sorting Individual DNA Molecules

Principal Investigators: Henry Benner

Project No.: 99018

Project Description

An ion detector, recently developed at Berkeley Lab and implemented in a new type of mass spectrometer, provides, for the first time, a way to measure the mass of individual ions nondestructively on-the-fly. The term "sorting," as used in this proposal, is the process of isolating one molecule out of many by first performing a measurement on a single molecule and then either choosing or eliminating it according to a predetermined selection criterion. The technological basis supporting our attempt to develop an instrument to sort individual molecular ions derives from the recent invention of charge detection mass spectrometry (CDMS). This proposal defines the design and fabrication of a new technique, based on this detector, to sort individual molecular ions according to their mass. The goal of the project is to evaluate how reliably individual ions can be sorted on demand.

This Berkeley Lab charge detection mass spectrometer will be modified to release individual molecular ions into collection wells. Initial evaluation of the procedure will be performed by sorting DNA ions. The polymerase chain reaction (PCR) replicates single target molecules. It will be used to confirm that individual ions can be guided into collection wells. Ion mobility will also be investigated as a way to select ions before they are sorted.

Accomplishments

Our initial goal for the current year's work was to evaluate several optics designs for deflecting ions having a predetermined mass into one or more collection wells. We proposed to develop a system to sort individual DNA molecular ions. DNA ions were chosen because they carry a large number of charges and because a biochemical technique sensitive enough to detect individual ions exists. In our system, DNA ions will be generated by electrospray, then weighed and gated into a collection well if they fall within a predetermined mass range. It is now an established procedure to detect single DNA molecules with the PCR. We planned to corroborate our ability to sort individual molecules by developing a single target molecule PCR assay, but the level of support we received did not allow us to develop this type of assay. As a consequence, we decided to design a system to detect sorted ions using a microchannel plate ion detector instead of PCR. In this alternative design, ions are weighed using charge detection mass spectrometry, then deflected towards a microchannel plate if they meet selection criteria. The issue is to determine if the system can sort individual ions or if contaminating ions interfere with the sorting procedure.

We have two ways of measuring the mass of ions with CDMS. We obtain the most precise measurements with a technique that relies on a matched pair of electrostatic ion mirrors to reflect ions back-and-forth through our image-charge detector tube. The reflections allow us to make multiple measurements of ion charge and velocity. This, of course, improves the precision of our mass measurements proportionally to the square root of the number of replicate measurements. The pair of mirrors is set to ground potential to receive an ion and then switched on when an ion enters the detector. A less precise measurement is obtained by our one-pass method, which does not rely on the ion mirrors and thus produces one measurement of the ion.

We evaluated our electrostatic trap for operation in a trap-and-release type of mode. We planned to trap ions for a fixed number of reflections and then release them into a collection well. We evaluated a number of computer algorithms for determining ion mass from the image-charge signal of a trapped ion. We determined that it was impossible with software running on a 400 MHz computer to process the signal fast enough to determine on-the-fly if the ion fell into a predetermined mass range. For example, our fastest algorithm requires about 50 ms of processing time to calculate ion mass from a 1 ms trapped ion waveform digitized at 10 MHz. This problem could be solved with DMA data transfer technology but was beyond

the scope of our immediate focus. We then evaluated the use of the less precise one-pass method for measuring mass. The evaluation of the potential for using this measurement method along with ion deflection led to the design of a reasonable system. We constructed a switched power supply that will produce the necessary signals. We are currently in the process of installing and writing the signal processing software and testing the combined operation of on-the-fly mass measurements and control of ion gating.

Publications

W. Henry Benner, G. Rose, E. Cornell and E. Jackson, "Mixtures of High Mass Electrospray Ions Analyzed with a Gated Electrostatic Ion Trap," Proceedings of the 47th Am. Soc. Mass Spectrom. Conference on Mass Spectrometry and Allied Topics, June 1999 (in press).

Biosensor Development

Principal Investigators: Mark Alper, Yann Chemla, John Clarke, Helene Grossman, Joseph Jaklevic, William Kolbe, Yan Poon, Garry Rose, and Raymond Stevens

Project No.: 98015

Project Description

There is an increasing need for the development of a variety of sensors to detect environmental contaminants, biohazards, and disease-causing agents (including bacteria, viruses, and toxins and biological and chemical-warfare agents). The project will examine three approaches for the rapid and sensitive detection of biological agents. The methods are based on: chemiluminescent detection of analyte species captured on magnetic beads; fiber optic sensing using fluorescent labels; and the sensitive detection of dynamic effects on reagent binding to magnetic beads, using an ultra-sensitive Superconducting QUantum Interference Device (SQUID) for magnetic field measurements.

Accomplishments

The project for FY99 focused on the completion of earlier preliminary studies using the three methods. In the case of the electrochemiluminscent (ECL) detection, the sensor had been well characterized and the reaction chemistry is established. The strengths of this system are: parts-per-billion (ppb) sensitivities; adaptability to a wide range of antibody-antigen pairs; compact size; "hands off" operation; high-multi-channel throughput; and minimized risk of exposure to users by complete containment and post-detection denaturation of the analytes, which can include biotoxins and viruses. Earlier work demonstrated the ability to develop a multi-channel, flow-through approach for ECL detection of antigen binding reaction on derivitized magnetic beads. However, preliminary studies indicated the need for a robust system in which engineering issues impacting precision and reliability would be addressed.

Experimental studies targeting these problems were carried out and a second-generation ECL system with improved precision and reduced measurement times was developed. A key component of the system is a positive displacement flow system. In the positive displacement system, all samples are driven through the detection cell by incompressible liquids, removing the flow variability observed when using compressed air. To provide precise control over sample flow rates, a 96-channel positive displacement pump driven by a stepper motor was developed. The system is completed and has entered the testing phase. All initial tests lead to the conclusion that this system will boast a large improvement in measurement accuracy and a significant decrease in sample detection time.

Fiber optic sensors are widely utilized in the field of biosensors due to their versatility of design and use. Our fiber optic system has undergone initial testing, and considerable progress has been made in optimizing the geometries of the sensing end of the fibers. Fiber optic sensors boast many of the same advantages as ECL, but also provide for: remote sensing; custom design of the fibers for varying environments; miniature size; ease of production; low cost; and adaptability to any detection scheme that results in light emission near the fiber surface. Our detector is intended to become a platform for an increasing array of bio-detection schemes and development/discovery of antibody-antigen related interactions to further the scope of detectable bio-agents.

The fiber optic sensor is being evaluated for routine use. The optical fiber etching robot, which allows for uniform etching of fibers to specific geometries, is allowing for fine-tuning of the fiber-sensing instruments. The fiber optic system is a useful tool to

facilitate the development of antibody-antigen pairs needed in the biosensor field. Fiber optics also lend themselves to detection in environments that are remote, spatially confined, or hostile to other detection techniques. As opportunities present themselves, this sensor will find applications in some of the more unique and exotic applications.

On a model system, appropriately tagged liposomes are placed above the SQUID and immersed in a solution of superparamagnetic nanoparticles. A magnetic field pulse aligns the magnetic moments of the nanoparticles parallel to the SQUID. Subsequently, the SQUID is used to detect the decay of the remnant magnetization of the magnetic nanoparticles—identifying the presence of the tagged liposomes. Unbound magnetic nanoparticles do not contribute to the signal, so the assay can be carried out without a washing step.

The tagged liposomes generate a strong, reproducible signal whereas controls give only small background signals. Although experiments to determine the sensitivity of the system are incomplete, we estimate that fewer than 10^4 targets can be detected. The response is linear with both magnetic particles and target liposomes. These results demonstrate conclusively the validity of this approach. Continuing work will be required to demonstrate its applicability to the detection of specific targets.

Publications

We expect to have the first paper on SQUID technology prepared for submission within a month or six weeks.

Fundamental Research on Lean Premixed Combustion for Gas Turbine Technology

Principal Investigators: Robert Cheng

Project No.: 98010

Project Description

Lean premixed (LP) combustion is an emerging environmental energy technology that is being developed to reduce the emissions of undesirable combustion byproducts from gas turbines. LP combustion emits only one-tenth to one-twentieth the amount of oxides of nitrogen (NOx) as conventional methods, but development of LP gas turbine combustors presents many engineering and technical challenges. Under gas turbine conditions of high pressures and elevated inlet temperatures, LP flames are prone to instabilities and blow-off. The scientific objective of this project is to improve our understanding of LP combustion in gas turbines by elucidating the fluid mechanic processes pertaining to stability, flame propagation, and emissions. Such basic scientific knowledge is essential to guide the design of gas turbine combustors as well as the development of software tools for engineering designs.

The LDRD fund supports the design and construction of a laboratory-scale experimental setup that allows the use of advanced laser diagnostics to probe turbulent LP flames at elevated inlet temperatures and high pressures.

Accomplishments

The objective of this project is to design and construct a research capability that supports lean premixed (LP) flame experiments under high pressures. It will be used for fundamental research on flame characteristics at the idling and mid-load conditions of a small gas turbine combustor. This experimental setup is designed to operate up to 15 atmosphere with preheat inlet temperature of 200° C. The first phase (FY98) was to construct the combustion chamber and test its operation up to 5 atmosphere. The second phase (FY99) is to upgrade the setup to operate at 20 to 30 atmospheres. The centerpiece is a stainless steel combustion chamber that mounts on top of a premixed burner. The combustion chamber is fitted with four 25.4 mm thick, 101.6 mm round sapphire windows to allow direct optical access to the flame. The burner has a 25.4 mm round exit port and can be adapted to generate different flame configurations. This setup includes computer controls to accurately set the fuel and air streams, monitor chamber pressure and surface temperatures, and analyze combustion byproducts. To supply the compressed air at 30 atmosphere requires the installation of a dedicated air compressor and an auxiliary air-tank in the combustion laboratory. In addition, equipment and controls for de-pressurizing and cooling the exhaust stream, igniting the flame, safe guarding the users from accidental release of energy from the high-pressure system are necessary.

In FY99, we have completed testing of the flow controllers at room temperature and high pressure. Software for controlling the experiments and gathering performance and exhaust gas data has been developed, tested, and refined. These include protocol for start-up, shut-down and emergency shut-off. The experimental setup is being commissioned for high-pressure flame operation. Typical conditions for these initial tests have flow velocities between 1 to 3 meters/second at 5 atmospheres for fine-tuning the flow control protocol, rehearsing the emergency shut-off procedure and evaluating the integrity of the safety interlocks. However, we have encountered some difficulty in igniting the flames. Our original idea was to ignite using an electronic spark to the flame stabilizer. This method was found not to be very effective because the pressure surge after ignition prevents the flame from attaching to the stabilizer. Similar problems were encountered when using a heated coil for ignition. From discussion with our industrial colleagues at Solar Turbine, we learned that ignition in a high pressure combustion facility is a common challenge. Upon their recommendation, we are constructing a pilot flame that will be used for igniting the premixed

flame. This is a standard practice in the industry and is a more reliable ignition source.

We have secured funding from DOE's Office of Industrial Technology to continue research on high-pressure premixed combustion for applications to gas turbines. Some of this new funding will be used to complete the construction of this experimental setup in FY00.

Air Pollution and Mortality: Significance of the Chemical Composition of Particulate Matter

Principal Investigators: Joan Daisey

Project No.: 98011

Project Description

The objectives of this investigation were to: (1) determine if there is any evidence that daily mortality, which has been associated with airborne particulate matter (PM) in a large number of recent epidemiological studies, is related to the mass concentration and chemical composition of the PM; and (2) determine if a new methodology which we developed for obtaining exposure metrics would elucidate relationships with PM chemical composition.

We hypothesized that by adding information on PM chemical speciation and source apportionment to the typical PM health epidemiological analysis, we would be able to identify and evaluate the impact of those PM sources that cause adverse health effects. Previous PM health studies have generally used PM mass or a single PM component, such as sulfate, as exposure metrics. In our approach, factor analysis (FA) is used first to convert multiple, highly correlated chemical speciation variables, such as trace metals, to a smaller number of linearized sums of the individual variables, i.e., a smaller number of factors. The factors, which are related to the sources of the PM via chemical markers, are then used as exposure metrics in Poisson Regression (PR) with weather variables included for confounder control.

The FA/PR method was applied to a unique PM data set with extensive chemical speciation, including measurements of nine trace metals, sulfate, and meteorological data made in three New Jersey cities (Camden, Newark, and Elizabeth) from 1981 to 1983. Mortality data for total, cardiovascular, and respiratory causes of 1981-1983 were retrieved from the mortality data tapes from the U.S. Department of Health and Human Services. Accidental deaths and homicides were excluded from the total mortality. In addition to FA/PR, we also investigated the relationship between mortality and single PM-mass related exposure metrics including inhalable particulate mass (IPM) ($d_{50} \leq 15$ μm), fine particulate mass FPM ($d_{50} \leq 2.5$ μm) and sulfate (SO_4^{2-}).

Using FA, we obtained four factors that were common to all three cities: oil-burning, motor vehicle emissions, secondary sulfate aerosol, and geological sources (e.g., wind-blown dust and re-suspended street dust). In each city, information on local PM emission sources with known tracers (and emissions profiles of such sources) were used to interpret the results of FA, especially the industrial sources. In addition to the sources common to the three cities, for Newark and Elizabeth, factors for industrial sources, traced by zinc and cadmium (a large zinc smelter) and by copper (e.g., fabricators, platers and illegal wire recovery operations), respectively, were also obtained. In Camden, a factor for sources traced by copper (incinerators) was obtained in addition to the other four factors.

Accomplishments

The results of FA/PR show that statistically significant associations (p-value ≤ 0.10) between daily mortality and several of the FA-derived PM factors/sources. In Newark, Oil burning sources (tracers: V and Ni), industrial sources (tracers: Zn and Cd), and sulfate aerosol showed positive relationships with total daily death (TDD). For cardio-respiratory daily death (CRDD), only sulfate was a significant factor in Newark. In Camden, oil-burning and motor vehicle emissions were two important sources for TDD; sources traced by copper showed a negative association with TDD. Three PM sources were significant predictors for CRDD in Camden: oil burning, motor vehicles, and sulfate. In Newark and Camden, there were statistically significant associations between total mortality and the factor related to oil burning. Cardiovascular death was also significantly related to oil burning in Camden. In Newark, the

two industrial sources and sulfate also had statistically significant associations with total mortality and cardiovascular mortality. The motor vehicle emissions source was a significant predictor of cardiovascular death only in Camden. For Elizabeth, no statistically significant relationships were found between total mortality and any of the source emissions metrics. This lack of association may be due to the higher socioeconomic and health status of the Elizabeth population in comparison to those of Newark and Camden. PM from geological sources (tracers: Mn and Fe) or other industrial sources (tracers: Cu and Pb) were not significantly associated with increased mortality based on our analyses.

The results of using single PM mass as exposure metrics are as follows: In Newark, significant associations were found between three single exposure metrics—IPM, FPM, and sulfate—and TDD and CRDD. In Camden, IPM and FPM were significantly associated with TDD and three single PM exposure metrics (FPM, IPM, and sulfate) were all significantly associated with CRDD. In Elizabeth, none of the three PM metrics was significantly associated with TDD or CRDD.

Using the FA/PR method, we have obtained the first epidemiological evidence indicating that chemical differences play a role in PM-induced health effects and that risks posed are not the same for various PM sources. Using this method, PM sources associated with mortality were oil burning, certain industrial sources, secondary sulfate aerosol, and motor vehicle emissions. The relative risks for the FA/PR model are higher than those obtained for simpler PM exposure metrics including inhalable and fine PM mass without consideration of sources, suggesting that this may be a more powerful method for examining the associations of PM and adverse health effects.

Publications

F. Tsai, M.G. Apte, and J. M. Daisey, "An Exploratory Analysis of the Relationship between Mortality and the Chemical Composition of Airborne Particulate Matter," *Inhalation Toxicology* (in press).

UV Disinfection: Field Test of a Small-Scale System

Principal Investigators: Ashok Gadgil

Project No.: 98036

Project Description

Berkeley Lab has developed a low-cost, robust, and energy-efficient ultraviolet (UV) technology, UV Waterworks, to disinfect drinking water in developing countries. This technology has passed careful tests in ten laboratories in five countries. Long-term field tests in real-world settings must be undertaken, however, to identify and correct any unforeseen shortcomings in this technology, its long-term performance, and its ability to disinfect the full annual range of challenge-water parameters. The goal of this project is to undertake a 12-month field test at one site in South Africa to determine the functioning of the unit under field conditions and its performance in disinfecting the annual range of challenge water.

Accomplishments

Work on this project was to identify (and correct) any unforeseen shortcomings in the UV Waterworks ("UVW") technology, its long term performance, and its ability to disinfect the annual range of water quality at a selected site. We also wanted to test the functioning of various electrical components of UVW when powered by a photovoltaic (PV) panel at the site, and identify snags or shortcomings in the design.

After initial assessments of two sites, we set up a site at the Greenock Health Clinic near Dundee in KwaZulu Natal province in South Africa. This clinic serves a remote community outside the small town of Dundee. The local community built the clinic by contributing labor, with hardware and building materials donated by charity. There is no electricity, but a Scandinavian charity has donated a PV system and a borewell pump with a tank that provides the water to the health clinic and also provides water to the community through a standpipe located just outside the fence of the clinic. Another international charity installed a deep drop toilet, unfortunately only about 30 feet

from the borehole. Our UVW installation would disinfect the water initially for the clinic, and eventually at the standpipe for the community.

The installation was completed and commissioned in early 1999. However, we have made very slow progress owing to two unexpected problems. The PV power line to the UVW was vandalized a few times. We now run the line through a galvanized iron pipe. The vandalism also led to poor repair, and consequent failure, of a few electrical components in the UVW, which we have replaced. The second problem has been with poor responsiveness in e-mail and fax communication from the local field engineer responsible for our site. We obtained only four data sets on water quality tests, by the time we should have obtained 20. Of the missing 16, nine could be attributed to power or component failure—the other five are owing to poor responsiveness from the field personnel. In response, we have appointed a manager to oversee the site operation, who gets paid upon Berkeley Lab's receipt of the scheduled report. We are hopeful that these measures will allow us to obtain useful data from the field site. The Department of Energy has funded the continuation of this effort, which we expect to complete in FY00.

Semiconductor Processing Technology for Energy-Efficient Lighting

Principal Investigators: Stephen Johnson and Michael Vella

Project No.: 98012

Project Description

The purpose of this project was to demonstrate new energy-efficient miniature high-intensity discharge (mini-HID) light sources and to demonstrate cost effective, wafer-based manufacturing adapted from a subset of semiconductor process tools. Compared with common incandescent sources, mini-HIDs will: have equivalent luminous output; fit within the same glass envelope; and be four times more energy efficient. They will also be significantly smaller and less expensive than comparable compact fluorescent sources.

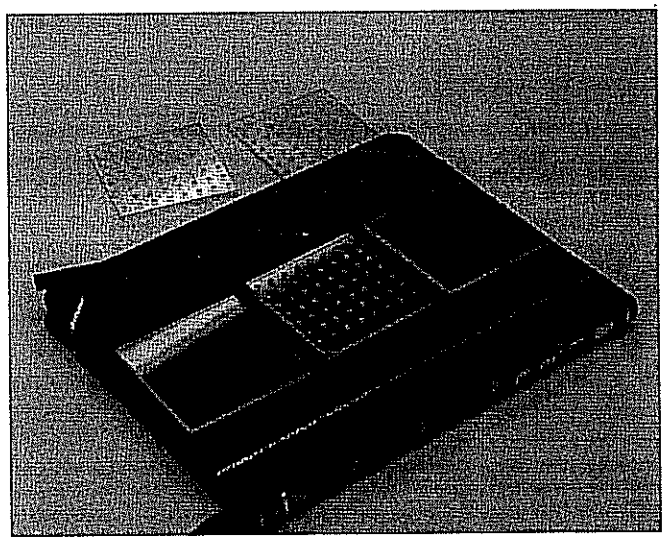

Figure 1. Polished quartz plates patterned with 3-mm diameter holes prior to bonding in a sandwich of 5-mm plates.

Accomplishments

Based on the experience developed last year with lamps made at Berkeley Lab, small batches of Argon/Mercury lamps were made to our specification by a commercial vendor, Galaxy Glass. These miniature lamps were constructed with electrodes and operated in arc discharge mode. The dimensions of the lamps were varied to investigate the effects of arc length and diameter. Those lamps having the best performance had a short arc length, an operating voltage of 40 to 60 volts at low frequency, and demonstrated a positive voltage/current characteristic. Under these operating conditions, lamps having a discharge length greater than or equal to the tube diameter resulted in the degradation of the quartz discharge vessel and the formation of cinnabar (mercury oxide) deposits on the walls. Utilizing these results, dimensions for patterning quartz plates were developed.

Thick quartz plates, 5 mm and 9 mm, were patterned with 3-mm diameter holes and polished in the Berkley Lab lens shop for bonding. Although the smoothness was acceptable for bonding, satisfactory bonds could not be obtained. The plates were too thick for the standard wafer-bonding techniques available at UC Berkeley, which rely

on wafer deformation at the bond front. Thin (0.5 mm) plates with a 0.5 mm hole pattern have been fabricated and polished with chemical mechanical polishing (CMP). These will be bonded at UC Davis, where a wafer-bonding tool is available that can bond wafers in a controlled gas pressure environment. After mercury insertion into the cavity, the wafers will be bonded in helium or neon atmospheres and operated in radio frequency (rf) mode for characterization. After characterization of these lamps, outside follow-on funding will be sought.

Electrocatalysis of Biological Processes for Remediation of Contaminated Soils

Principal Investigators: John Kerr

Project No.: 98014

Project Description

The aim of this project is to develop understanding of the effects of electrokinetic soil remediation on intrinsic microbial activity for accelerated *in situ* biodegradation of organic contaminants; and accelerated metals removal by biosorbent organisms. Electrokinetic soil treatment is a potentially powerful tool for enhancing bioremediation (see Figure 2). It provides a mechanism to efficiently deliver energy and nutrients to indigenous organisms in soil. If the conditions can be properly controlled, naturally occurring organisms can be encouraged to rapidly degrade organic contaminants in the soil and ground water. However, it is equally important to avoid misapplication. Therefore, a thorough understanding of the effects on indigenous biological activity is necessary. This project is designed to provide such knowledge by application of advanced chemical and biological methods. Contaminants to be studied are chosen in order to provide experience with common environmental problems so that the knowledge may be rapidly applied to the field.

Accomplishments

A total of six complete electrokinetic cell systems have been built and tested to provide a significant testing facility. Schematics of the laboratory system were shown in the FY1998 report.

Experiments were carried out with contaminated soil samples from a variety of sources. These included samples from a commercial site in Berkeley, California, that was heavily contaminated with transmission oil and garden soil samples, contaminated with lead from paint residues. Pyrene was added to soil samples to provide a more controlled contaminant distribution and provide a simpler analytical problem. Soil samples from Ft. Ord firing range in Monterey County, California, were also examined as these are contaminated with explosives such as TNT, RDX and HMX. For all of these systems, complex analytical methods must be developed to provide a complete picture of the evolution of the soil ecology. For this project, only the most pertinent analyses could be carried out. One particularly useful analytical method was developed as a result of these efforts. A capillary electrophoresis method was developed for detection of trace amounts of transition metal ions in a background matrix containing large amounts of iron. Since iron is a common soil constituent, this was an important development.

Initial results indicated that enhanced biological activity occurs due to the heating effect of the current. Comparisons between AC and DC current operation demonstrated that heat was a major factor in promoting biological activity. The electrokinetic process is an effective method for evenly heating soil, particularly in clay soils, where other hydraulic methods are ineffective. The electrokinetic method is therefore complementary to many methods currently deployed in the field. However, it was noted that after several days of operation, the soil samples were flooded. Analysis of the microbial activity revealed considerable spore formation, which indicated that the organisms were inhibited rather than activated. The electrokinetic process changed the soil environment quite drastically, resulting in saturation, anaerobic conditions and an increase in salinity and acidity. Since the indigenous organisms have evolved to cope with different conditions, the observed response is understandable.

These problems were addressed by the use of ion exchange membranes around the electrodes to

control the water flow into the soil. The cells could be operated in an unsaturated mode thereby preventing flooding and ensuring an adequate supply of oxygen. Solid polymer electrolyte electrolysis cells were added to the electrolyte management systems to provide much better control of pH and salinity. Although these methods did not completely solve the problems, they allowed the electrokinetic treatments to be carried out under conditions that were more hospitable to the natural organisms. Since electrokinetic treatments have been mostly successful in saturated, high-salt conditions, these improvements have widened the potential applicability of the method to more soil types, including more of the soils found in the U.S.

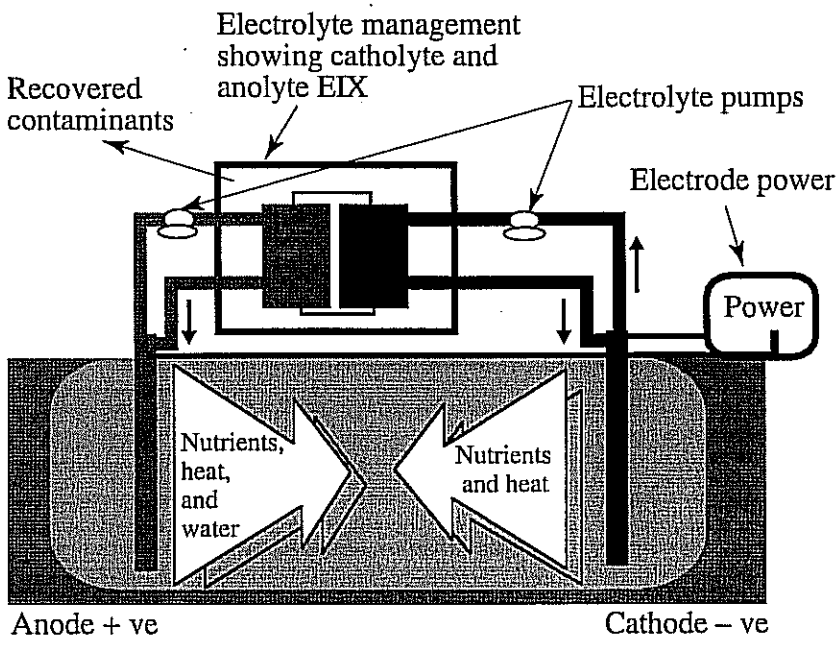

Figure 2. Schematic of the "Pool" Process (US Patent 5,433,829) for use with bioremediation in soil.

Publications

J.B. Kerr, F. Rabbi, W.T. Stringfellow and R. Clarke., "Electrokinetic Acceleration of Bioremediation of Metal Ion and Organic Pollutants In Soil," presented at ACS Anaheim National Meeting (March 1999).

J.B. Kerr, F. Rabbi, G. Klunder and W.T. Stringfellow, "Application of Capillary Electrophoresis to Monitor Metal Ion Content and Biological Activity in Contaminated Soils Under Accelerated Bioremediation," (in preparation).

Real Time System Control and Reliability Market Simulation for Restructured Electricity Industries

Principal Investigators: Mark Levine

Project No.: 99041

Project Description

This project is intended to advance Department of Energy public-interest research and technology development in electric power system reliability. Work has been initiated in the design and operation of electricity markets, focussing on the consequences of dispersed electricity systems on electric system reliability.

To extend the current state-of-the art requires efforts in the following areas:

- Methods to fully exploit new electric system measurement and data analysis technologies (PGP-based, time tagged phasor, and spectral measurements across wide geographic area);
- New control techniques from hybrid system analysis to optimally utilize continuous acting feedback with grid switching and protective breaker action;
- Data extraction methodologies that allow high-volume data to be converted to higher-level, but lower-volume information in order to streamline the process of state evaluation;
- New distributed agent control methods for network flow control using flow-gate (or FACTS) devices. This includes optimal placement and utilization of flow control resources;
- Evaluation of the impact and optimal control uses for large-scale power electronics, including flexible alternating current (ac) transmission (FACTS) and power-conversion technologies for distributed and alternative generation resources; and
- New on-line intelligent agents for predicting and mitigating impending threats to system security under volatile operating and generating market conditions.

Accomplishments

Work focused on developing the control systems that will be necessary to operate the future electricity supply system, and to simulate the effects that dispersed electricity resources (DER) will have on existing power systems. Changes in the economics of power production, transmission, and distribution suggest that future electricity generation will, at least in part, come from large numbers of small, dispersed sources, many of them using renewable fuels. These dispersed generation sources, together with smart end-use technologies, form DER. This configuration cannot be reasonably controlled by the centralized control structures of today, which have been developed under the paradigm of small numbers of large generating stations rather than large numbers of small ones.

This LDRD provided initial support for conceptualizing a control structure for a power system consisting of weakly-networked disperse nodes that are both sources and sinks. This is in contrast to the current system of strongly networked nodes that are either concentrated sources or dispersed sinks. In this new type of power system, coordination between system agents is likely to evolve from the command regime of today to control based on price signals established in open markets. We assume a decentralized control scheme in a hierarchically organized power system (DER site, local low-voltage feeder, and a classic high-voltage grid). That is, each DER site attached to the feeder behaves independently and its generation and/or consumption is driven by its own objectives, subject to prevailing prices. These prices reflect the status of the overall power grid and stimulate the agent to deliver appropriate products into it. These products are both energy and the various ancillary services, such as back-up generation, that are required to keep the total system balanced, stable, and reliable. The grid consists of weakly-connected microgrids that can function independently of the grid as islands and that are linked at nodes that separate the centrally-controlled, high-voltage grid.

The approach has been to explore the wider computer science literature on autonomous agents, identify concepts relevant to the DER control problem, and to outline a code design for a DER autonomous agent simulator. The simulator will replicate the behavior of a group of agents that control a diverse set of distributed energy resources. These resources, in particular, are sited along a specific electricity distribution feeder (15 km long) of a California distribution company. Predicted operation of the DERs can be simulated in this way, and the effect of their resulting pattern of generation and consumption on the feeder analyzed.

Publications

C. Marnay and B. Smolinski, "Autonomous Control of Small, Dispersed Electricity Resources," (in preparation).

Ion-Beam Thin-Film Texturing: Enabling Future Energy Technologies

Principal Investigators: Ron Reade and Paul Berdahl

Project No.: 99042

Project Description

Ion-beam assisted deposition (IBAD) processes have shown great potential for fabricating template buffer layers for epitaxial crystalline thin film growth without the need for expensive single-crystal substrates. However, current IBAD processes are very slow and thus too expensive for industrial application in cost-sensitive energy technologies such as high-temperature superconductor tapes. We are testing and developing a new concept for much more rapid processing—ion-beam thin film texturing (ITEX). In order to further develop ITEX processing, a better understanding of the fundamental mechanisms of ion-beam crystalline texturing processes is needed. The purpose of this project is to experimentally probe these mechanisms, and utilize this information to improve the fabrication processes for energy technologies. A new Reflection High Energy Electron Diffraction (RHEED) system, installed in our pulsed laser deposition system, will provide *in situ* information on film surface crystallinity and texture.

Accomplishments

A new RHEED system was purchased, and our Pulsed-Laser Deposition (PLD) system was modified for its installation. This system also has an ion beam source. The new RHEED capabilities were tested by generating beautiful diffraction patterns from the 311 surface of a high-purity germanium single crystal obtained from Eugene Haller.

The magnets in the ion source inside the PLD system bend and distort the electron beam from the RHEED system. We have implemented a temporary solution by reducing the number of magnets in the ion source, partially shielding the magnetic field, and placing a compensating magnet across from the ion source. This allows us to proceed with the initial experiments, but a more permanent solution will be needed to reduce the distortion of the electron diffraction patterns and allow accurate analysis of the ITEX-induced texture.

Another experimental issue is the chamber pressure and its effect on the RHEED images. During the ITEX process, the pressure rises and the RHEED images degrade. For the present, we are acquiring RHEED images mainly after stopping the processing. However, improvements to the differential pumping system (evacuating the electron gun) should allow improved imaging during the processing.

The ITEX film texturing method was applied to an yttria-stabilized zirconia (YSZ) film. YSZ is a key material used as a textured-template layer for YBa2Cu3O7 (YBCO) superconductor deposition on stainless metal substrates. The new RHEED images (though distorted by the magnetic field problem) clearly show that the surface is crystalline and in-plane oriented. In particular, when the sample is rotated about its surface normal, the RHEED pattern exhibits the desired four-fold symmetry. This is the first direct observation of surface texture of an ITEX film. Next, the effects of variations in process parameters such as time, temperature, and oxygen partial pressure on film quality will be investigated. When we are satisfied with the results, we will deposit a YBCO layer and measure its critical current density.

Publications

P. Berdahl and R. Reade, "Ion-Beam Texturing Mechanisms by Oblique Ion Beams Impinging on Metal Oxides," submitted to MRS Spring Meeting, April 2000.

Virtual Building Laboratory: Lighting Simulation Tool

Principal Investigators: Stephen Selkowitz, Nancy Johnston, and Stephen Lau, Jr.

Project No.: 97013

Project Description

The goal of this LDRD is to develop the first operational module of the Virtual Building Laboratory, a suite of tools that will serve as the building science research testbed and as a prototype for design tools of the future. The computational engine for the first module is Radiance, a lighting simulation tool using ray tracing developed by Environmental Energy Technologies Division (EETD) staff.

Radiance produces physically accurate renderings of the luminous environment in buildings by accurately modeling the effects of lighting and the surface interreflections. Although it generates accurate renderings, the amount of computation required precludes interactive walkthroughs in real time. The project attempts to achieve real-time rates by parallelizing Radiance and by developing a system of pixel reuse. We anticipate to reduce the amount of computation required to generate each frame by exploiting the frame-to-frame coherency during real-time walkthroughs.

The eventual goal of the project is to allow a user to virtually walk through a scene, using an appropriate input device, without having to stop and run different programs at different points. By achieving this rapid frame rate and interactivity through optimization, Radiance will be useful for energy-efficient building design, other industrial and governmental applications (e.g. FAA) and for providing the tools and techniques needed to better serve National Energy Research Scientific Computing (NERSC) remote users.

Accomplishments

This year was a continuation of last year's Radiance LDRD work. The same multi-divisional and multi-disciplinary team that was formed between NERSC and EETD for last year's project was used in this year's project. We built upon the achievements and work accomplished in the previous year. The primary goals of this year's LDRD were to increase the interactive rates of parallelized Radiance, decrease the amount of time required for image generation when incorporating ambient light, and to interactively display the Radiance calculations at a remote location.

Last year, we had parallelized Radiance on a Silicon Graphics Origin 2000 multi-processor machine as well as on a Cray T3E. The NERSC remote visualization server was used as the front end to display the rendered images and as a user interface. A prototype user interface for controlling the eye-position and direction-of-view of the user was also developed and used. Although the parallelization of the ray-tracing portion of Radiance decreased the amount of time required to calculate each frame, it was still not enough for interactive rates. We developed a point cloud method for pixel reuse and tested it out with the parallelized portion of Radiance. The pixel reuse method was run on the remote visualization server, communicating with the NERSC T3E to determine which pixels need to be recalculated in each frame.

The ambient component of the Radiance lighting calculations is computationally expensive. Without ambient lighting, a single image generated from a viewpoint requires the calculation of between one to twenty-five million rays. With ambient lighting, hundreds of millions of rays need to be calculated for an accurate rendering. As one of the goals of this year's LDRD, we increased the interactive rates for a Radiance calculation that incorporated ambient lighting.

When a Radiance calculation incorporated ambient lighting, one Processor Element (PE) served as the ambient master process controlling the sharing of ambient calculation results among processors in order to reduce the number of rays cast. All other PE's, the workers, were dedicated to ray tracing. Each worker PE kept track of how many ambient values it had generated, and when a certain number of values had been produced, it communicated them to the ambient master processor. The ambient master processor then returned to the sending worker any results accumulated from other processors. The sending worker added these new values to its ambient cache. For better load balancing, the number of values to accumulate

before sending was kept small. The sharing of ambient calculation greatly reduced the amount of time required to generate images incorporating ambient lighting.

Another goal for this year's LDRD was to increase the interactive rates of a remotely displayed Radiance calculation. When displaying over a wide area network, the amount of time it takes to transmit an image to the remote site becomes significant. A 640x480 32bit image requires a minimum of a tenth of a second to be transmitted over a high-speed FDDI network. It became obvious that to achieve interactive rates over a wide area network, we would need to decrease the amount of data being transmitted for each frame. One of the options we explored was the use of data compression. We incorporated JPEG compression to reduce the amount of data sent over the network. The images were compressed prior to transmission and then decompressed on the receiving end. Unfortunately the decompression of the images on the receiving end is fairly CPU intensive. More than one processor on an SGI Origin was necessary to decompress an image fast enough to make a difference when an FDDI network was available.

A cross-country demonstration of Radiance was conducted in August 1999, which showed the ability to both remotely control and interact with a real-time parallelized Radiance that incorporated ambient lighting.

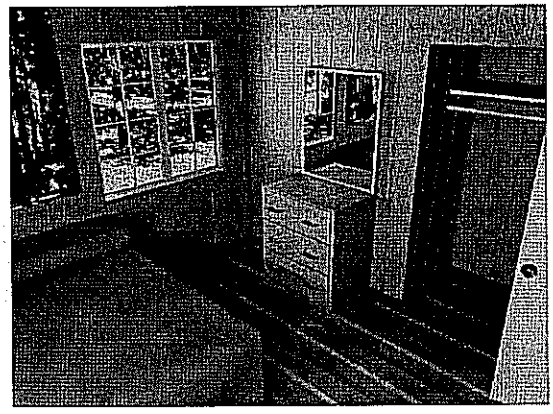

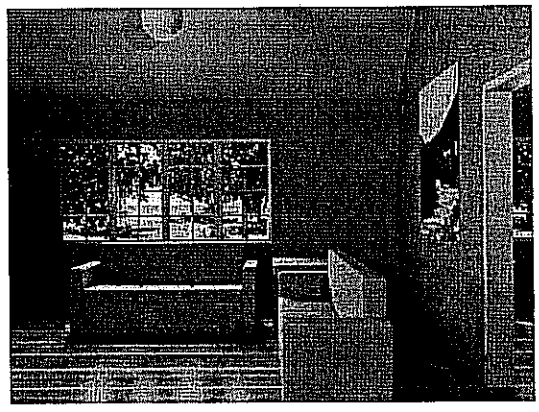

Figure 3 and 4: Generated with Radiance on the T3E showing two views of a cabin

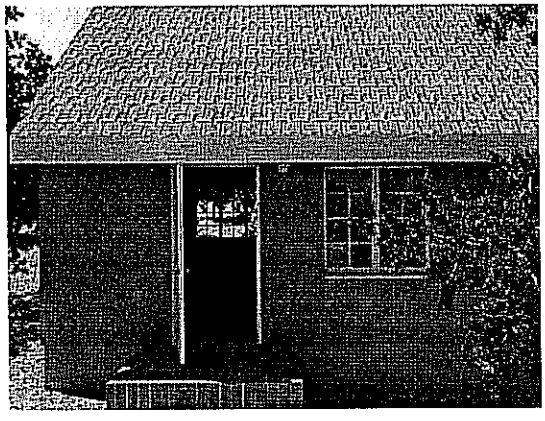

Figure 5. Rendering with ambient lighting

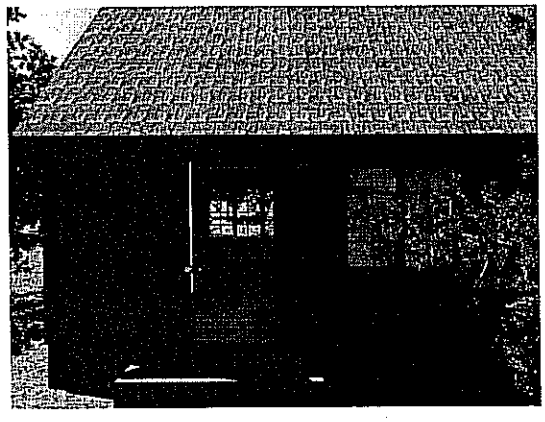

Figure 6. Rendering without ambient lighting

Publications

D. Robertson, K. Campbell, S. Lau, T. Ligocki, "Parallelization of Radiance for Real Time Interactive Lighting Visualization Walkthroughs," SuperComputing '99, Portland, Oregon (November 1999).

Genomic Approaches to Understanding Cell Genotype and Phenotype

Principal Investigators: Judith Campisi, Paul Kaufman, and Kunxin Luo

Project No.: 98017

Project Description

Cell phenotype is defined by all of the genes expressed by a given cell under a specific biological circumstance. Until recently, it has been impossible to know how various stimuli alter cell phenotype—or the pattern of gene expression—to any degree of completion. However, recent advances in genome research make it now possible to embark on an unprecedented, genomic-scale approach to defining and understanding cell phenotype.

This proposal aims to make accessible genomic scale approaches to biological questions that are unanswerable by conventional techniques. To do so, we proposed to establish a cell genotyping/phenotyping capability. This effort will need to acquire specialized equipment, develop streamlined procedures, and tailor state-of-the-art techniques to specific biological problems. We proposed to implement two technologies: DNA sequencing for gene identification and vector verification, and complete gene expression profiling serial analysis of gene expression (SAGE); and hybridization to microarrayed DNA and cDNA sequences, principally for analyzing patterns of gene expression.

The long-term goal is to offer high-quality, competitive DNA sequencing and gene expression profiling, and continue developing state-of-the-art methods for applying genomic scale approaches to biological problems.

Accomplishments

During its first year, the project evaluated and acquired specialized equipment items needed for the cell genotyping/phenotyping setup. This includes ABI-377 and 373 automated DNA sequencers, a Bio-Rad Cyclone imager, several thermocyclers and related equipment, and the computer hardware and software needed for data management and image analyses. New personnel include sequencing assistant and molecular biologist. Efforts have included exploring and evaluating a variety of sequencing and microarray technologies, and establishing the most suitable sequencing-based and hybridization-based gene expression profiling techniques.

The first technical accomplishment was to establish and optimize individual plasmid sequencing procedures. The sequencing effort has been extremely successful. Between October 1998 and June 1999, nearly 1000 DNA samples were sequenced, with an overall success rate of just over 83%. In addition, methodology was established for sequence-based gene profiling (SAGE). SAGE entails the construction of highly specialized cDNA libraries, which can now be constructed. A trial library was constructed from human mammary gland RNA, and preliminary sequencing showed it to be of high quality. The library is available for complete sequencing, and technical support is available for making and sequencing additional libraries.

The second technical accomplishment was to evaluate and establish gene expression profiling methods. Currently, gene expression profiling using filter hybridization can be done, but other methods are being evaluated and will be offered as the technology matures. The cDNA labeling and hybridization protocols and optimized conditions for maximizing resolution and reproducibility of the hybridization signals have been standardized. We have obtained the imaging hardware and computer software for detecting and analyzing the hybridization signals, and developed reliable methods for analyzing the microarray signals and organizing and displaying the data.

Structural Cell Biology of Multi-Component Protein Complexes Essential for Genomic Stability

Principal Investigators: Priscilla Cooper and John Tainer

Project No.: 99019

Project Description

A major challenge in structural cell biology concerns the structural chemistry of large multicomponent protein complexes. We propose the development and application of structural and computational technologies for characterization of such complexes via a closely coordinated range of approaches involving molecular and cell biology, biochemistry, electron microscopy, crystallization, and x-ray diffraction. The research will initially focus on complexes that are essential for maintaining genomic integrity through two critical processes: transcription-coupled DNA repair of oxidative damage, and DNA double-strand break repair. The techniques developed for characterizing these will be applicable to defining the structural biology of other critical multicomponent complexes. Thus, an overall goal is to provide the technical basis for structural characterization of large complexes in contrast to the biophysical chemistry of single proteins.

This research will provide over-expression and purification of component proteins involved in transcription-coupled base excision repair and double-strand break repair complexes. It will also address their biochemical characterization, atomic resolution x-ray diffraction structures of individual components, and cryo-electron microscopy characterization of the complexes, including diversity and conformational states. It will advance current barriers for x-ray crystallography and begin filling the gap between high-resolution structures for individual proteins and medium resolution electron microscopy (EM) of multiprotein complexes. Initially, we will make and characterize the complexes and develop the technical tools for linking EM and x-ray structures, including beamline design for low- and high-resolution data collection on crystals of multi-component complexes. The follow-on goal is for combined EM and diffraction studies of the components and complexes, with results linked to coupled cell biology studies in an experimental cycle in which each builds on information from the other.

Accomplishments

This research involves development of techniques to bridge the size and resolution gap between electron microscopy of biological assemblies and x-ray diffraction structures of separate proteins in order to advance the interpretative framework for molecular and cellular biology. The focus is on two complexes that are essential for maintaining genomic integrity. In the first year, we have achieved (1) successful expression of XPG, a key protein in transcription-coupled repair (TCR) of oxidative damage, and of the hMre11/hRad50 DNA double-strand break (DSB) repair complex, (2) crystallizations and structure determinations of human apurinic/apyrimidinic endonuclease (APE) enzymes that couple with XPG, and (3) crystallizations of thermostable archael homologs of Mre11 and Rad50. These accomplishments provide the essential material for small angle x-ray scattering (SAXS) diffraction studies key to Advanced Light Source (ALS) beamline tests during the second year of the project, and cryo-electron microscopy (EM) reconstructions.

For studies of the TCR complex, we have explored several different expression systems for XPG and are now purifying significant quantities of enzymatically active XPG from insect cells using a Baculovirus system. In addition, we have succeeded in expressing in *E. coli* at very high levels the full-length XPG carrying a C-terminal hexa-His tag as a fusion construct with maltose binding protein (MBP) at its N-terminus. We have also cloned and expressed a domain of XPG that is predicted by several lines of evidence to be involved in important protein-protein interactions. By addition to this "R domain" of a recognition sequence for heart muscle kinase, we are able to label the recombinant protein with ^{32}P. We have used the labeled protein as a probe in both Far Western and slot blot studies to search for specific interactions with other proteins in HeLa cell whole-cell extracts and to test purified candidate proteins for specific interactions with XPG. Thus far we have identified such specific interactions with hNTH1, hAPE, and hMutS-β. These results taken together suggest that

involvement of XPG in TCR of oxidative damage may be mediated through interactions of the R domain. We will therefore pursue crystallization trials with this protein, which we are able to make in quantity. For the XPG partner APE1, enzyme:DNA co-crystals and diffraction data sets were obtained with recombinant human APE and ds-DNA substrates with a central abasic-site analog. We have solved three structures of APE1:DNA complexes.

Substantial progress has been made in our studies of a key complex for DNA double-strand break repair. Successful production of hMre11, hRad50, and p95 individually and in pair-wise and three-component complexes using a Baculovirus insect cell system is providing the key material for cryo-EM and biophysical characterizations of the complex including BIAcore kinetics and affinities, SAXS, and crystallization experiments. In keeping with our general strategy of parallel research on human proteins and their thermostable archael homologs, our expression of thermostable Mre11 and Rad50 archael homologs will allow comparative studies and, importantly, the potential to trap functional intermediates at low temperatures. For Rad50, we co-expressed the N- and C-terminal components of the ATPase domains. We crystallized the complex and determined its structure to (at present) 2.2 Å resolution (the crystals diffract to 1.5 Å resolution). The structure shows that both half-domains tightly interact to form a 35kDa ATPase domain with striking similarity to the functionally unrelated ABC transporter family of ATPases. In addition, binding of ATP to the Rad50 ATPase domain induces dimerization or a large conformational change as measured by dynamic light scattering (the hydrodynamic radius changes from 2.7 to 3.5 nm). We also co-crystallized the ATPase domain with various ATP analogs (ATP, ATPγS, AMPPNP) and with DNA. Co-crystals diffract to 2.4 Å resolution and the cell dimension suggests a dimer in the asymmetric unit.

Mre11 has nuclease/phosphatase motifs of the calcineurin family in the N-terminal part and DNA binding motifs in the C-terminal part of the molecule. Removal of the 60 C-terminal residues improved solubility without affecting activity and gave crystals that diffract beyond 2.5 Å resolution at a synchrotron x-ray source. To determine interaction sites between Mre11 and Rad50 and determine a "minimal core" for crystallization of an Mre11-Rad50 complex, we co-expressed various Rad50 truncation constructs with Mre11 and probed for complex formation by co-purification assays. Incorporating ~50 amino acids of the coiled coil adjacent to the ATPase domain resulted in a tight complex of the ATPase domain with Mre11. These data suggest that Mre11 binds to Rad50 in the coiled coil region adjacent to the ATPase domain. Crystallization trials with this "minimal" complex are currently being pursued.

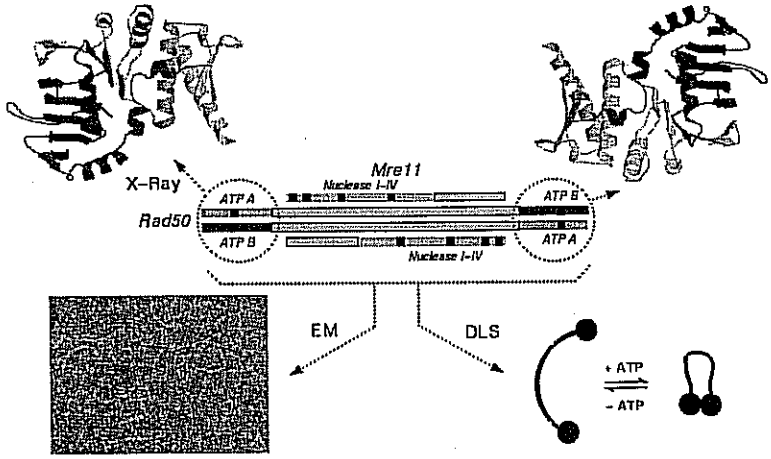

*Figure 1. **The Mre11/Rad50 DNA double-strand break repair complex.** Schematic sequence regions (center); EM results and schematic model of the full-length complex and ATP-driven conformational change (bottom); and crystal structure of the novel assemblies of the N- and C-terminal ATPase components formed by dimerization of Rad50 (top).*

Publications

C. D. Mol, T. Izumi, S. Mitra, and J.A. Tainer, "Structures and Mutants of APE1 Reveal How Abasic DNA Binding Stages DNA Repair," *Nature* (in press).

M. Pique, C.D. Mol, S. Parikh, and J.A. Tainer, "Dancing with the Elephant: Envisioning the Structural Choreography Coordinating DNA Base-excision Repair," internet video for *Nature* (in press).

DNA Microarray Analysis of Metabolic Regulatory Genes in the Mouse

Principal Investigators: Ronald Krauss

Project No.: 99020

Project Description

The overall goal of this project has been to delineate patterns of cellular gene expression in response to specific genetic and environmental perturbations as a means of determining the functions of these genes. Metabolic regulation in response to altered environmental conditions requires the coordinated expression of many genes. Analysis of the global pattern of gene expression following exposure to specific nutritional or metabolic environments provides information bearing on the functions of these genes. Microarray technology provides new tools for investigating the regulation of gene expression on a genomic scale.

Mice are useful experimental organisms for investigating patterns of gene expression. The mouse genome is being sequenced in parallel with that of the human, and a large number of expressed sequences is available for microarray analysis. Moreover, the availability of a variety of mouse strains with specific natural and induced mutations allows study of factors influencing gene expression in a variety of defined regulatory settings.

In the first year of this project, we have implemented and refined cDNA microarray methodology to establish the feasibility of this approach for studies of metabolic regulation in higher organisms. Our preliminary results have indicated that we can use this system to identify genes with increased or decreased expression in response to important metabolic perturbations in two mouse models:

- Mice with genetic inactivation of hepatic lipase (HL), a key enzyme involved in plasma lipoprotein metabolism.
- A mouse strain with insulin resistance, a condition associated with susceptibility to diabetes, obesity, and heart disease.

Accomplishments

Development of a Procedure for Normalizing Expression Data from cDNA Microarrays

The final goal of a cDNA microarray experiment is to achieve a quantitative measurement of the expression levels of a given gene under test and control conditions. The individually labeled samples are co-hybridized to the microarray to avoid potential artifacts arising from different hybridization conditions in different experiments. However, after fluorescence intensities are collected, adjustments must be made to correct artifactual sources of differences in the intensities, such as different amounts of RNA in the test and control sample, different efficiency of incorporation of the Cy3 and Cy5 labels and different hybridization affinity of the probes containing the two different labels, and finally, different fluorescent yields of the two labels. All of these factors are corrected by normalizing the intensity readings of one label, customarily Cy5. This is based on the assumption that, in any given experiment, only a few of the genes will change levels of expression while the vast majority will be unchanged, and their expression level should therefore be equal to 1. However, a single normalization factor cannot be used across the full range of genes—from those expressed at low levels to ones expressed at high levels—because genes expressed at low levels tend to show a bias towards the Cy3 label. That is, the majority of these genes appear to be consistently expressed more strongly in the control (Cy3) than in the test sample.

Similarly, genes expressed at high levels show a Cy5 bias. To correct for this non-linear label bias, we have developed a procedure that allows the data to be normalized locally and not across the whole intensity range. The microarray intensity data are first ranked from lowest to highest, and the logarithm of the raw expression ratio is calculated.

Each given gene is assigned to a set comprising its 100 lower and higher neighbors. The intensities of this set follow a normal distribution, the mean of which should be zero according to the assumption that the expression levels of the majority of the genes in the set should be unchanged. The mean of the distribution is therefore used as a normalization value and subtracted from the log ratio, and the process repeated for all the data. This approach has the added advantage that it contains a statistical measure of the degree of change of any given gene. In fact, every distribution has an associated standard deviation that can be used to measure how much a given expression ratio differs from the mean expression ratio. This is achieved by normalizing the gene's expression ratio by the standard deviation of its distribution, so that all the genes will have a value (shown in column 4 in the table below) indicating how many standard deviations they differ from the average expression ratio.

In this way, we can decide to analyze all the genes that change, for example, 1 or 2 or 3 standard deviations. Given the properties of the normal distribution, it can be expected that about 32% of the genes will differ 1 standard deviation from the mean expression ratio, 4.5% will differ 2 standard deviations and 0.3% will differ 3 standard deviations. Therefore, the probability that a gene differs by 2 or more standard deviations in "n" different experiments, by chance, will be 0.045n, which, for three experiments, is equal to $P<0.0001$.

Gene Expression Analysis in Hepatic Lipase Knockout Mice

In preliminary studies we have examined the impact of the lack of HL on gene expression of two tissues likely to be affected. Livers and both visceral fat pads were collected from male HL knockout mice on a FVB background and wild-type littermates, all between 16 to 18 weeks of age and these organs were immediately frozen in liquid nitrogen and stored at –80°C until used. The total RNA fraction was isolated and 50 µg was used to synthesize oligo dT-primed cDNA. The fluorescent labels Cy3 and Cy5 were incorporated in the control and HL cDNA, respectively. The labelled probes were hybridized overnight to a microarray containing approximately 3500 elements. Following hybridization, the arrays were washed and dried, and data for each individual spot collected by a confocal dual-laser scanner. The data were analyzed as described in more details in the next section. Analysis of gene expression in the liver did not reveal any changes consistent over several animals. Furthermore, little variation was observed between different animals, indicating that animal-to-animal variability is not a major source of experimental noise. On the contrary, analysis of visceral adipose-tissue gene expression revealed several interesting changes, summarized in the following table. The data are for three HL knockout mice compared to three wild-type.

The first column contains the name of the cDNA, or of the gene with the closest match to the cDNA, printed at a given spot. All of the genes presented in the table have been sequence-verified to make sure that the name assigned to each spot is correct. The second column (Green) shows the fluorescence intensity reading for the Cy3, or control, sample. The third column (Red) shows the fluorescence intensity reading for the Cy5, or test, sample, following normalization, carried out as described above. The fourth column represents a measure of how much that gene changes compared to the normal behavior of the bulk of the genes present on the array. The last column shows the ratio of test vs. control, a standard measure of change in gene expression levels.

Of particular interest are the first three groups of genes in the table. The first pair represents two different DNA sequences identifying lipoprotein lipase (LPL), which appears to be up-regulated about 1.6 fold in the HL knockout mouse. The observation that two independent sequences show a similar behavior on the microarray is an indication of the validity of the measurement. This finding is particularly interesting because a similar increase in LPL enzymatic activity has been measured in the plasma of these mice. LPL shares with HL the ability to hydrolize triglyceride, but LPL prefers large, triglyceride-rich lipoproteins as a substrate. The two following groups identify the adipocyte and the epidermal fatty acid-binding protein (FABP), respectively, two members of the FABP family. Again, three independent cDNA identify each of these genes, corroborating the finding. Adipocyte FABP, also known as aP2, is a major marker of adipocyte differentiation. Epidermal FABP, so called because it was first identified in epidermal tissue, is also expressed in adipose tissue, and has been reported to be up-regulated to compensate for the lack of aP2. These two proteins can bind fatty acids in the cytoplasm, but their function has never been clearly defined.

The following group of cDNAs represents genes involved in various steps of lipid metabolism. The presence of an expressed sequence tag (EST) similar to phosphatidylethanolamine-binding protein is intriguing, because this is the preferred phospholipid substrate of HL.

Finally, there are ten cDNAs for which no match could be identified in the database. These genes are expressed at different levels, and defining their function represents the next challenge of gene expression analysis.

Microarray Analysis of an Insulin-resistance Mouse Model

We used a cross of two mouse strains, C57BL/6J (B6) and BTBR, to study the changes in gene expression that take place in insulin-resistant mice. The male F1 offspring of this cross shows severe insulin resistance when fed a moderately (15%) high-fat diet, while the female F1, as well as the parental strains, do not. After two weeks on high-fat diet, male and female F1, 11 weeks of age, were injected with 0.75U insulin/kg body weight, and sacrificed at 0, 45 and 120 minutes after insulin injection. Their livers, visceral adipose tissue and skeletal muscle were collected, total RNA prepared, and cDNA microarray hybridization carried out as described above. The male and female F1 were used as the test and control sample, respectively. Analysis of gene expression in the liver of six pairs of animals revealed a highly significant (>10-fold) up-regulation of the glutathione S-tranferase gene (an enzyme that plays an important role in detoxification by catalyzing the conjugation of many hydrophobic and electrophilic compounds with reduced glutathione), and a 4-fold down-regulation of cholesterol 7a-hydroxylase (the enzyme catalyzing the rate-limiting reaction in bile acid biosynthesis in the liver). This latter finding is of particular interest since we have found that mice with knockout of this enzyme develop insulin resistance and obesity. Taken together, these findings indicate for the first time that cholesterol 7a-hydroxylase is a critical determinant of insulin action. We are currently expanding our analysis to other insulin-sensitive tissues, and breeding the two parental strains to determine whether observed changes are merely due to the sex difference or are truly relevant to the insulin-resistant phenotype.

Expected Outcomes

The wealth of new information that has come from these preliminary studies supports the value of microarray-based studies of gene expression in the discovery of genetic mechanisms involved in metabolic regulation. This work will be further developed with a projected National Institutes of Health grant, currently in preparation.

In addition, this research program will become an important component of a new Center for Nutritional Genomics that is being developed in conjunction with the College of Natural Resources, the School of Public Health, and the Department of Molecular and Cell Biology of University of California at Berkley. The mission is to identify the effects of nutritional environment on the expression and function of genes responsible for maintaining biologic homeostasis in humans and model organisms, and to determine the influence of interindividual genetic variation on nutritional requirements for optimal health.

NAME	Green	Red N	Err Ratio	RedN/ Green
EST, Highly similar to LIPOPROTEIN LIPASE PRECURSOR [Rattus norvegicus], lipid-UG	10167	16810	2.16	1.65
Mouse lipoprotein lipase mRNA, 3' end, lipid-UG	4887	7866	1.93	1.61
3T3-L1 lipid binding protein, lipid-Img	2344	4842	2.56	2.07
EST, Highly similar to FATTY ACID-BINDING PROTEIN, ADIPOCYTE [Bos taurus], lipid-UG	3992	7106	2.01	1.78
lipid binding protein-like, lipid-Img	6012	10914	2.41	1.82
psoriasis-associated fatty acid binding protein, lipid-Img	2992	6563	2.71	2.19
FATTY ACID-BINDING PROTEIN, EPIDERMAL, lipid-UG	749	1705	2.35	2.28
EST, Moderately similar to FATTY ACID-BINDING PROTEIN, EPIDERMAL [Mus musculus], lipid-UG	1719	4345	2.96	2.53
SCP2, lipid-UG	3800	8822	3.41	2.32
NCEH, lipid-Img	1025	1897	2.06	1.85
HB2, lipid-Img	5607	3281	2.15	0.59
EST, Weakly similar to PHOSPHATIDYLETHANOLAMINE-BINDING PROTEIN [Homo sapiens], lipid-UG	2185	941	2.83	0.43
Metallothionein1	1179	429	2.98	0.36
5' similar to gb:V00835 Mouse gene for Metallothionein-I (MOUSE)	949	344	2.88	0.36
MDB1105	471	1029	2.20	2.19
MDB1294	1332	593	2.27	0.45
5'. gi | 2187041 | gb | AA462150 | AA462150 [2187041]	1240	591	2.07	0.48
5'. gi | 1287063 | gb | W13005 | W13005 [1287063]	1503	515	3.16	0.34
5'. gi | 1287130 | gb | W12952 | W12952 [1287130]	825	334	2.44	0.40
5'. gi | 1287076 | gb | W13039 | W13039 [1287076]	2213	667	3.97	0.30
5'. gi | 1287593 | gb | W13556 | W13556 [1287593]	2256	5534	2.91	2.45
Unk	5799	10885	2.55	1.88
Unk	3425	1291	3.11	0.38
Unk	590	1440	2.64	2.44

Protein Distribution in Human Mammary Epithelial Cells using Soft X-Ray Microscopy

Principal Investigators: Carolyn Larabell

Project No.: 99021

Project Description

The purpose of this project is to examine the distribution of specific proteins using soft x-ray microscopy at the Advanced Light Source (ALS). Whereas the amount of certain proteins often remains the same in normal and tumor cells, the distribution is frequently altered. For example, it has recently been shown that the protein beta-catenin is located at the cell surface of normal cells but in the nucleus of tumor cells. In fact, an increasing number of proteins have recently been found in the nucleus of tumor cells, where it is believed they activate or repress gene transcription. The distribution of proteins is typically determined using immunolocalization analyses, but spatial resolution within the nucleus is difficult to determine using light microscopy. We will examine the distribution of proteins in normal human mammary epithelial cells and tumor cells, using soft x-ray microscopy to obtain higher resolution information. This requires a three-dimensional analysis that can only be accomplished with a cryo-tilt stage that can image specimens at multiple angles.

Human mammary epithelial cells will be grown on silicon nitride windows and fixed at various time intervals. They will then be incubated in the specific primary antibodies, followed by the gold conjugated secondary antibodies. The gold particles will then be enhanced with silver until approximately 45 to 50 nm in size. The hydrated, labeled cells will then be examined using the soft x-ray microscope at the ALS. The precise three-dimensional localization of these proteins, however, depends on the ability to obtain three-dimensional information from either stereo or tomographic images.

Accomplishments

For this project we utilized our existing technology to examine whole, hydrated cells in the x-ray microscope at high spatial resolution (35 to 40 nm). We used the silver-enhanced, gold-labeling protocol to examine the distribution of proteins believed to be involved with the structural organization of the nucleus. In addition, we compared the subcellular distribution of proteins known to be components of the *Wnt* signaling pathway in normal and tumor cells.

The prototype for a cryofixation apparatus and cryostage was developed by the Center for X-ray Optics during the past year. We tested the use of this instrument for examining a variety of specimens, including unfixed whole, hydrated cells. A monolayer of cells was grown on silicon nitride windows, rinsed, then rapidly frozen and examined in the microscope. These cells, which had not been exposed to chemical fixatives or contrast enhancement reagents, revealed remarkable preservation of ultrastructural details. The nuclear membrane surrounding the nucleus was well preserved and cytoplasmic organelles that were not seen in chemically fixed cells were easily discerned. The fine, elaborate filopodial extensions characteristic of the leading edge of cells were also clearly visualized. The details seen in these images of rapidly frozen cells demonstrate the power of soft x-ray microscopy to examine whole cells at unparalleled resolution. Additional improvements of this instrument will be made during the next year and will increase the capacity of the x-ray microscope for examining cells.

Publications

C. A. Larabell, D. Yager, and W. Meyer-Ilse, "Localization of Proteins and Nucleic Acids using Soft X-ray Microscopy," XRM99 – VIth International Conference on X-ray Microscopy," (August 1999, in press).

Analysis of Cellular Factors that Activate Transcription from the Major TGFβ Responsive Element in the Plasminogen Activator Inhibitor Type-1 Gene

Principal Investigators: Kunxin Luo

Project No.: 98018

Project Description

The transforming growth factor-β (TGFβ) family of cytokines has a wide range of biological functions in many cellular processes including tumor suppression, extracellular matrix production, embryonic development, hematopoiesis, and immune and inflammatory cell responses. How does a single molecule initiate such diverse and complex cellular events? Are they mediated by different signaling pathways? The goal of this proposal is to characterize the signaling pathway of TGFβ receptors leading to extracellular matrix production at the level of transcriptional activation. This proposal will allow for the identification and purification of cellular transcription factors that activate specific gene expression in response to TGFβ stimulation.

The signaling receptors for TGFβ include TβRI and TβRII, the type I and II receptors for TGFβ, which are members of the first known transmembrane serine/threonine kinase family and share 40% homology between their kinase domains. TGFβ1 binds directly to TβRII, allowing the formation of heteromeric complexes of TβRI and TβRII, and the transphosphorylation of TβRI by the constitutively active TβRII. It has been suggested that phosphorylation of TβRI activates its kinase activity and allows it to phosphorylate downstream substrates such as Smad2 and Smad3. The phosphorylated Smad proteins then translocate to the nucleus and subsequently activate downstream events. However, little is known about how the Smad complex activates the transcription of TGFβ-responsive genes. Recently, *Drosophila* Smad protein was found to bind to a DNA sequence present in the promoter region of Dpp-responsive genes. This finding suggests that Smad proteins could activate transcription by binding directly to TGFβ responsive elements.

We decided to analyze the signaling pathway leading to transcriptional activation of TGFβ-responsive genes using the PAI-1 promoter, because it has been well documented that TGFβ stimulation results in a fifty-fold induction of PAI-1 gene transcription. The promoter region of the PAI-1 gene has been well characterized, and a major TGFβ-responsive region has been mapped to a 258 bp sequence between –804 and –546 upstream of the initiation site. Although the sequence contains an AP-1-like motif, cellular factors that may interact with this region and activate transcription have not been identified. By overexpressing dominant negative and constitutively active Smad mutants in some cell lines, Smad proteins have been shown to be involved in the activation of PAI-1 transcription. However, the molecular basis of PAI-1 activation by Smads is not clear. Since human Smad4 shares a considerable homology with *Drosophila* Smad, and *Drosophila* Smad can bind DNA directly, we hypothesize that human Smad4 may also activate PAI-1 transcription by direct binding to specific sequences in the PAI-1 promoter. Using electrophoretic mobility shift assays (EMSA), we will investigate the mechanism by which Smad proteins activate PAI-1 transcription.

Accomplishments

Smad proteins are critical signal transducers downstream of the receptors of the TGFβ superfamily. Upon phosphorylation and activation by the active TGFβ receptor complex, Smad2 and Smad3 form hetero-oligomers with Smad4 and translocate into the nucleus, where they interact with different cellular partners, bind to DNA, regulate transcription of various downstream response genes, and cross-talk with other signaling pathways. Last year, we showed that Smad proteins play an important role in mediating TGFβ-induced transcriptional activation. To further understand the molecular mechanism of Smad action, we began to identify cellular proteins that interact with the Smad proteins using biochemical approaches. This is based on the hypothesis that Smad proteins must interact with different cellular partners in order to mediate diverse TGFβ -induced signals. Using epitope tagging and affinity purification methods, we have identified two nuclear proteins, SnoN and Ski, that associated with Smad2, Smad3 and Smad4 through the C-terminal domains of the Smads on the

TGFβ-responsive promoter. Ski and SnoN are two proto-oncogene products that when overexpressed, can transform mammalian cells. Elevated levels of Ski expression have also been detected in multiple types of human cancers. However, the molecular mechanism whereby Ski and SnoN transform cells is not clear. The identification of the tumor suppressor Smad proteins as the cellular partners for Ski and SnoN suggests that Ski and SnoN may cause oncogenic transformation by blocking the growth-inhibitory function of the Smad proteins.

We showed that Ski can directly interact with Smad2, Smad3, and Smad4 on a TGFβ-responsive promoter element and repress their abilities to activate transcription through recruitment of the nuclear transcriptional co-repressor N-CoR and possibly its associated histone deacetylase complex. Overexpression of Ski in a TGFβ-responsive cell line renders it resistant to TGFβ-induced growth inhibition and defective in activation of JunB expression. This ability to overcome TGFβ-induced growth arrest may be responsible for the transforming activity of Ski in human and avian cancer cells. These results have been summarized into a paper published in *Genes & Development.*

Similarly, the SnoN oncoprotein was found to interact with Smad2 and Smad4 and repress their abilities to activate transcription through recruitment of the transcriptional co-repressor N-CoR. Immediately following TGFβ stimulation, SnoN is rapidly degraded by the nuclear accumulation of Smad3, allowing the activation of TGFβ target genes. By two hours, TGFβ induces a marked increase in SnoN level, resulting in termination of Smad-mediated transactivation. Thus, SnoN maintains the repressed state of TGFβ-responsive genes in the absence of ligand and participates in negative feedback regulation of TGFβ signaling.

In summary, our work during the last year has demonstrated for the first time an important role of the Ski family of nuclear oncoproteins in regulation of TGFβ signaling. Future work will build on this project to investigate how an oncoprotein interacts with the tumor suppressors to regulate cell growth and carcinogenesis.

Publications

S.L. Stroschein, W. Wang, and K. Luo, "Cooperative Binding of Smad Proteins to Two Adjacent DNA Elements in the Plasminogen Activator Inhibitor-1 Promoter Mediates TGFβ -induced, Smad-dependent Transcriptional Activation," *J. Biol. Chem,* **274**, 9431-9441 (1999).

K. Luo, S.L. Stroschein, W. Wang, D. Chen, E. Martens, S. Zhou, and Q. Zhou, "The Ski Oncoprotein Interacts with the Smad Proteins to Repress TGFβ Signaling," *Genes & Development* **13**, 2196-2206 (1999).

S.L. Stroschein, W. Wang, S. Zhou, Q. Zhou, and K. Luo, "Negative Feedback Regulation of TGFβ Signaling by the SnoN Oncoprotein," *Science* **286**, 771-774 (1999).

Signal Transduction and Cytoskeleton

Principal Investigators: Mohandas Narla

Project No.: 98019

Project Description

Two new areas of research were developed as part of this project:

Functional Characterization of Homologues of Red Cell Membrane Proteins in Non-Erythroid Cells

Recent studies from our group and from a number of other groups have shown that homologues of red cell membrane cytoskeletal proteins spectrin, ankyrin and protein 4.1 are also present in a number of non-erythroid cells including epithelial cells, fibroblasts, endothelial cells, and neuronal cells. However, there is currently no knowledge of the function of these proteins in these cells. The project began the detailed characterization of different homologues of red cell protein 4.1R and the functional characterization of this protein family in non-erythroid, especially neuronal, cells.

Understanding the Role of Cytoskeleton in Signal Transduction and Erythroid Cell Differentiation

Erythropoiesis, which is responsible for generation of 2.5 million red cells per second in humans, is an excellent system for studying cell differentiation. Although the critical roles for the hormone erythropoietin and its receptor in erythroid

differentiation have been well delineated, the downstream signaling pathways are yet to be defined. We studied a congenital disorder, Diamond-Blackfan anemia, in which there is completely lack of red cell production in newborns, to explore the signal transduction process.

Accomplishments

During the two years of LDRD funding we made substantial progress in both of our proposed research areas. For the first, we cloned, sequenced and characterized the cDNA of three human homologues of red cell protein 4.1R—4.1G, 4.1N and 4.1B. 4.1G gene product is ubiquitously expressed in all tissues, the gene product of 4.1N is expressed in all neurons, and 4.1B is expressed predominantly in the brain. Having completed the detailed molecular biologic characterization of these three new human homologues of red cell protein 4.1R, we explored the function of these proteins. During the course of these studies we made an important observation that immunophilin FKBP13 interacts with 4.1G. We also focussed our efforts on defining the function of various protein 4.1 gene products in neuronal cells (in collaboration with Dr. Sol Snyder's group at Johns Hopkins University) and in kidney epithelial cells.

The second research area we pursued involved the defining of the molecular basis for the congenital disorder, Diamond-Blackfan anemia, in which there is a complete lack of red cell production in newborns. We successfully characterized one of the genes responsible for this human red cell disorder. We demonstrated that mutations in the ribosomal protein RPS19 account for this disease phenotype in 30% of the affected children. This turned out to be the first human disease proven to be caused by mutations in a ribosomal protein. We pursued studies to determine how mutations in a ribosomal protein can account for the lack of red cell production. This finding opened up an exciting new area of investigation for our research.

Publications

L. Peters, H.G. Weier, L.D. Walensky, S.H. Snyder, M. Parra, N. Mohandas, and J.G. Conboy, "Four Paralogous Protein 4.1 Genes Map to Distinct Chromosomes in Mouse and Man," *Genomics* **54**, 348-350 (1998).

M. Parra, P. Gascard, L.D.Walensky, S.H. Snyder, N. Mohandas, and J.G. Conboy, "Cloning and Characterization of 4.1G, A New Member of the Skeletal Protein 4.1 Gene Family," *Genomics* **49**, 298-306 (1998).

L.D.Walensky, S. Blackshaw, D. Liao, C.C. Watkins, H.G. Weier, M. Parra, R.L. Huganir, J.G. Conboy, N. Mohandas, and S.H. Snyder, "A Novel Neuron-enriched Homologue of the Erythrocyte Membrane Cytoskeletal Protein 4.1," *J Neuroscience* **19**, 6457-6467 (1999).

M. Parra, P. Gascard, L.D. Walensky, J.A. Gimm, S. Blackshaw, N. Chan, Y. Takakuwa, T. Berger, G. Lee, J.A. Chasis, S.H. Snyder, N. Mohandas, and J.G. Conboy. "Molecular and Functional Characterization of Protein 4.1B, A Novel Member of the Protein 4.1 Family with High Level Focal Expression in Brain," *J Biol. Chem.* (in press).

L.D. Walensky, P. Gascard, M.E. Fields, S. Blackshaw, J.G. Conboy, N. Mohandas, and S.H. Snyder, "Immunophilin FKBP13 Interacts with a Novel Homologue of the Erythrocyte Membrane Cytoskeletal Protein 4.1," *J Cell Biology* **141**, 143-153 (1998).

N. Draptchinskaia, P. Gustavsson, B. Andersson, M. Pettersson, T.N. Willig, I. Dianzani, S. Ball, G. Tchernia, J. Klar, H. Mattsson, D. Tentler, N. Mohandas, B. Carlsson, and N. Dahl, "The Ribosomal Protein S19 Gene is Mutated in Diamond-Blackfan Anemia," *Nature Genetics* **21**, 169-175 (1999).

T.N. Willig, N. Draptchinskaia, I. Dianzani, S. Ball, C. Niemeyer, U. Ramenghi, K. Orfali, P. Gustavsson, E. Garelli, A. Brusco. C. Tiemann, J.L. Perignon, C. Bouchier, L. Cicchiello, N. Dahl, N. Mohandas, and G. Tchernia, "Mutations in Ribosomal Protein S19 Gene and Diamond-Blackfan Anemia: Wide Variations in Phenotypic Expression," *Blood* **94**, 4294-4306 (1999).

Cryo-Electron Microscopy Studies of the Eukaryotic Transcription Basal Factor TFIID

Principal Investigators: Eva Nogales

Project No.: 99022

Project Description

The accurate and regulated transcription of protein coding genes in all eukaryotic organisms requires the assembly of a complex molecular machine at specific promoter elements that includes a cadre of general transcription factors in association with RNA polymerase II (RNA pol II). Recognition of core promoter DNA sequences by TFIID is followed by the assembly of a fully activated pre-initiation complex that contains TFIIA (IIA), TFIIB (IIB), TFIIE, TFIIF, TFIIH and RNA pol II. In the absence of activators bound to enhancer elements, this core transcription complex is capable of accurately initiating basal levels of RNA synthesis. In the presence of gene selective enhancer and promoter binding activators, dramatically elevated levels of transcription initiation can be achieved. A key step in the multi-step process of gene activation is the recruitment and subsequent assembly of the TFIID-IIA-IIB complex at the TATA DNA element found in many core promoters of eukaryotic genes. The TBP subunit and some of the TAF_{II} subunits (TAF_{II} 250, TAF_{II}150, TAF_{II} 70) make specific protein: DNA contacts with the TATA box and other core promoter elements including initiator (INR) and downstream promoter elements (DPE). Other TAF_{II}s of the multi-subunit TFIID complex, such as TAF_{II} 130, 100, 55, 32, 30, and 28 are thought to serve as targets of activation domains involved in the recruitment and stabilization of TFIID at core promoters by upstream enhancer binding factors.

The binding of TFIID to the core promoter is coordinated with the assembly of an active pre-initiation complex that includes IIA and B. Thus, one of the initial steps in the formation of an activated transcription complex is binding of the TFIID-IIA-IIB supra-molecular assembly to the template DNA. X-ray diffraction and nuclear magnetic resonance (NMR) studies have revealed the structures of various sub-domains and truncated fragments of IIA, IIB, and of subunits contained within TFIID. For example, the high-resolution structures of TATA Binding Protein (TBP) bound to TATA DNA and either domains of IIA or IIB have been determined. However, both the size of the TFIID complex as well as the inherent difficulties in obtaining large quantities of purified holo-TFIID, IIA, and IIB have precluded conventional x-ray diffraction studies of the full complex. Consequently, the overall shape and relative position of the components within this essential multi-subunit assemblage remain unknown. As a first step toward determining the structure of the intact native human TFIID, we have employed electron microscopy and single-particle image analysis. This technique does not require crystallization, can deal with very small quantities of the sample and, to a large degree, even with sample heterogeneity, and can be applied to samples of almost unlimited size in the molecular scale (i.e. several million Dalton). As a result, we have obtained the structure of TFIID and its complex with full length IIA and IIB at 35 Å resolution.

Accomplishments

Electron microscopy (EM) grids of TFIID (~45 ng/μl) were prepared and stained with uranyl acetate (4%). We collected image pairs of tilted (32°) and untilted (0°) samples using the random conical tilt method. A total of 4418 particle image pairs were used for further processing. Untilted images were subjected to reference-free alignment and merged by performing in-plane shifts and rotations into 25 classes defined by K-means clustering (the large number of classes chosen reflects the fact that TFIID orients almost randomly on the carbon film). 3-D structures for each of the 25 classes were calculated by back-projection using the paired tilted images. Twenty-four of the classes showed excellent correlation ($R > 0.85$), thus a single 3-D structure was obtained using the single particle tilted images from these 24 classes. This initial structure served as a reference for angular refinement. The final angular refinement was performed by generating 5088 reference projections from the newly obtained structure with an angular step of 2°. The reconstruction has a resolution of 35 Å based on the 0.5 Fourier shell correlation criteria.

The structure of TFIID is horseshoe-shaped with dimensions of roughly 200 Å x 135 Å x 110 Å. It is dominated by three main lobes connected by narrow bridges (~20 Å wide) arranged around a 65 Å diameter cavity. The lobes are roughly equal in size

(~60 Å diameter) but differ in structural detail. The central cavity and its 40 Å open channel at the bottom of the horseshoe could easily accommodate a 20 Å diameter strand of double-helical DNA.

We next studied the structure of the TFIID-IIB and TFIID-IIA-IIB complexes. The 3-D reconstruction of the binary complex, TFIID-IIB, was obtained by mixing the two factors in equimolar concentrations and incubating them for one hour at 4°C. Sample preparation, data collection, and image analysis was as described for holo-TFIID. Four thousand individual particle images were aligned in 3-D by reference to the refined 35 Å structure of naked TFIID. Once Euler angles were assigned, the new particle images were back-projected to generate a structure of the TFIID-IIB complex that was used as reference for further angular refinement to a resolution of ~35 Å. The structures of TFIID and the TFIID-IIB complex were then normalized according to the TFIID protein density, scaled, and subtracted to generate a difference map corresponding to the density of IIB [green (G) in Figure 2]. The difference density is positioned mainly on lobe B, but very close to the ~15 Å bridge connecting it with lobe C. The 3-D structure of the ternary complex, TFIID-IIA-IIB, was obtained following the same procedure as for the TFIID-IIB complex. The difference map obtained between TFIID and TFIID-IIA-IIB contains two distinct regions of density; one corresponding to the location of the difference obtained in the presence of IIB alone [green (G)], and a second one in lobe A consisting of a cluster of differentiated densities [magenta (M)]. This result confirms the position of IIB, and identifies the location of IIA.

The known crystal structure of TBP bound to IIA and IIB suggested that TBP should bind in the central domain C, between these two general factors. To test this hypothesis, we employed a monoclonal antibody raised against TBP. TFIID-antiTBP binding and preparation for EM was performed as described for the TFIID-IIB complex using a 5:1 antiTBP:TFIID ratio. More than 9000 particle images of the TFIID-antiTBP complex were used to obtain a reconstruction at ~30 Å resolution. Figure 2C indicates in yellow (Y) the position of the bound antiTBP obtained in the difference map applying the same methodology we used to find the IIA and IIB binding positions. The binding site of antiTBP indicates that TBP resides at the top of the cavity within the central domain, C, and faces the cavity in a position between IIA and IIB.

The EM studies presented here reveal a model for the structure of TFIID complexed to both IIA and IIB in the absence of DNA. Our findings provide a 35 Å structure of TFIID, and the binding locations of IIA and IIB in relation to the larger TFIID. Antibody mapping of TBP within TFIID strongly suggests the binding position of DNA at the top of the central cavity within the TFIID complex. The horseshoe shape of TFIID and its trilobal structure suggest conformational flexibility around the narrow contact regions, and regulation of the orientation between the lobes by transcriptional factors, with consequent effects in the shape of the central cavity and on the binding to DNA. Transcription factors IIA and IIB reside on opposite sides of TFIID and are likely to stiffen the structure of TFIID by bridging different lobes. In particular, IIA binds across the 25 Å channel near the surface of the central cavity. Thus, IIA could increase the surface available for DNA binding and thus affect the affinity between DNA and the TFIID-IIA complex that has been observed in DNA binding studies.

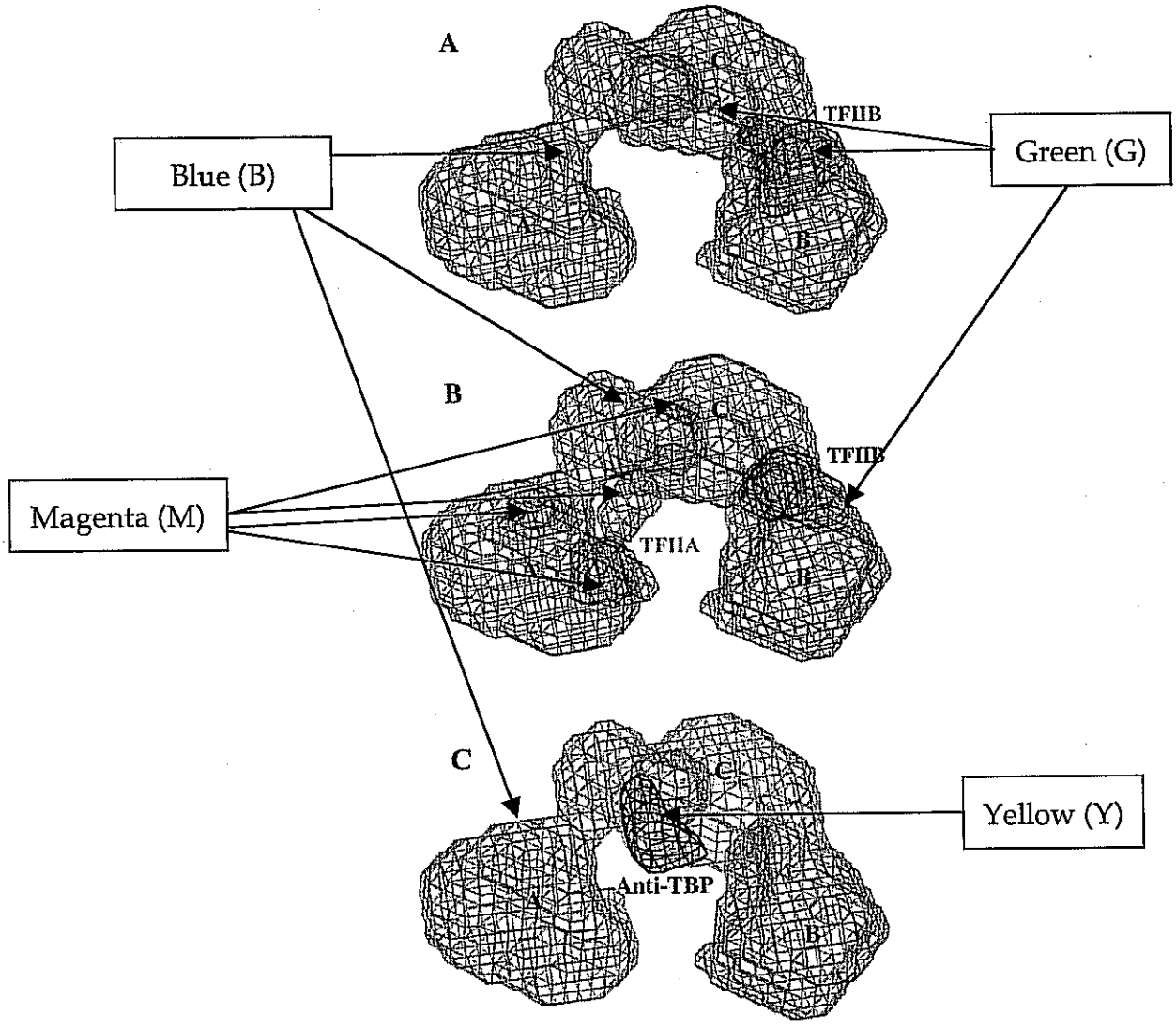

Figure 2. Position of TFIIB and TFIIA on the TFIID structure and mapping of the TBP. The blue (B) mesh corresponds to the holo-TFIID with the A, B and C lobes indicated. (A) The green (G) mesh corresponds to the density difference between the holo-TFIID and the TFIID-IIB complex. (B) The magenta (M) and green (G) meshes show the density difference between the holo-TFIID and the trimeric complex TFIID-IIA-IIB. The density depicted in light green (G) can be attributed to TFIIB by comparison with (A), with the magenta (M) density therefore corresponding to TFIIA. (C) The yellow (Y) mesh shows the density difference between the holo-TFIID and TFIID bound to the TBP antibody.

Publications

F. Andel III, A. G. Ladurner, C. Inouye, R. Tjian, and E. Nogales, "Three-Dimensional Structure of the Human TFIID-IIA-IIB Complex," *Science* (in press, 1999).

Semiconductor Nanocrystals as Probes for Biological X-Ray Microscopy at the Advanced Light Source

Principal Investigators: Shimon Weiss and Paul Alivisatos

Project No.: 99023

Project Description

The goal of this proposal was to develop the use of semiconductor nanocrystal probes for high-resolution biological x-ray microscopy. X-ray microscopes are capable of five-fold better resolution than the best confocal light microscopes, and this improved resolution could prove to be of great utility in the imaging of biological specimens. A major current approach is to obtain contrast in the x-ray microscope by staining the biological tissue with inorganic nanocrystals, for instance gold or silver particles. This proposal was directed towards using semiconductor rather than metallic particles for staining. When excited with visible light, the semiconductor particles emit light, and the color of the emission depends upon the particle size. We proposed to determine if light emission from the semiconductor particles could be observed following excitation with x-rays. Thus, if successful, a specimen labeled with semiconductor particles could be imaged with both conventional optical fluorescence and x-ray microscopy. In addition, different parts of a specimen could be labeled with different sizes of particle, providing multi-color ability.

This project was a follow-up to our earlier work in which we demonstrated the application of semiconductor particles in visible light microscopy.

Accomplishments

We regret that this project did not find the anticipated results. We were not able to detect any visible luminescence from the nanocrystals when they were excited with x-rays, even though the dots showed high yields when excited optically. We believe we now understand the physics underlying this difference. When an x-ray is absorbed several electron-hole pairs are created in the nanoparticle. Because the volume of the particle is small, and the number of electron-hole pairs is large, the rates of non-radiative, many-body relaxation pathways, such as Auger scattering, are greatly enhanced. In Auger scattering, one electron-hole pair is annihilated imparting extra kinetic energy to a third particle. This third particle can be ejected from the nanocrystal, ionizing the dot, and rendering it "dark." Unfortunately, this leads us to conclude that, while the semiconductor particles are excellent labels for optical microscopy of biological specimens, they are not well suited as x-ray labels.

Determining Macroscopic Materials Properties from Microscopic Calculations

Principal Investigators: Andrew Canning, Daryl Chrzan, Marvin Cohen, Steven Louie, and John Morris, Jr.

Project No.: 96041

Project Description

The goal of this research is to exploit advances in computer hardware and computational techniques, advances in the fundamental theory of bonding in solids, and advances in the theory of plastic deformation to construct new predictive models of the properties of real materials.

This is a collaborative project to compute the macroscopic properties of materials *ab initio*, by combining modern methods in theoretical solid state physics and materials science, and exploiting the advanced computational facilities at Berkeley Lab. The *ab initio* component involves electronic structure calculations similar to those the investigators

performed in the past, but rephrased to exploit new computational methods that take advantage of parallel processing. Using only the atomic numbers and masses of constituent atoms, it is now possible to compute electronic, vibrational, structural, and thermodynamic properties of, and dynamic processes in, materials. These fundamental calculations are used to develop scaling formulae to determine the macroscopic properties of complex materials and define in-out parameters for property simulations. Systems investigated include fullerene base solids, semiconductor clusters, and hard materials. The final nine months of this project were devoted to the study of hard materials, and the results stemming from the most recent work are reported here.

Accomplishments

Hard Materials

The upper limit of strength of a material is determined by elastic instability, which can be computed using *ab initio* electronic-structure, total-energy techniques. The most important limits on the strengths of metals concern their deformation in shear. During the past year, we have computed and analyzed the ideal shear strengths of Al, Cu and W. The calculations are the first to compute the (true) limits of shear strength in the fully relaxed case. Analysis of the results led to several new insights into the mechanical behavior of these prototype materials. Perhaps the most striking was the virtual identity of the strength of body centered cubic (bcc) tungsten for shear in the <111> direction on three different slip planes, {110}, {112}, and {123}. This behavior was shown to have its origin in the basic symmetry of the sheared bcc structure, and provides a theoretical foundation for the important, unexplained phenomenon of "pencil glide" in bcc crystals.

Dislocation Core Structures

In the final nine months of this project, we continued to study the stability of dislocation cores using total energy techniques. In addition, we developed a means to calculate the total elastic energy of dislocations, using isotropic elasticity theory. Comparison of the results of the two calculation techniques allows identification of the proper choice of core radius and shear modulus for larger scale models. In addition, we are able to calculate the stress state on the dislocations as a function of parameters chosen for the unit cell. This capability provides the ability to systematically study the structure of the dislocation cores as a function of the stress state. We have applied this technique to two systems.

First, we studied the stability and structure of the 90-degree, partial dislocation core in diamond, using *ab initio* methods. These studies established that for a broad range of stress states, the recently proposed period-doubled core is more stable than the commonly assumed single-period core. Further, these same studies indicated that the proper choice of small-scale cutoff for the dislocation in question is 0.4 Å. The shear modulus arising from the calculations is in excellent agreement with experimental values. These results prove that *ab initio* total energy techniques may be applied effectively in deducing dislocation properties.

For a second study, we began to explore the stress state dependence of the 90-degree partial in Si using empirical potentials. These calculations suggest that the stable core structure may be shear-stress dependent. If so, this result holds profound implications for researchers wishing to model the plastic deformation of Si. However, the energy differences calculated using the empirical potentials are quite small, and further work using more accurate total-energy techniques is required before drawing more firm conclusions.

Publications

D. Roundy, C.R. Krenn, M.L. Cohen, and J.W. Morris, Jr., "Ideal Strength of bcc Tungsten," submitted to *Phil. Mag. A*, (1999).

C.R. Krenn, D. Roundy, J.W. Morris, Jr., and M.L. Cohen, "The Nonlinear Elastic Behavior and Ideal Shear Strength of Al and Cu," *Mat. Sci. Eng. A*, (in press, 1999).

D. Roundy, C.R. Krenn, M.L. Cohen, and J.W. Morris, Jr., "Ideal Shear Strengths of fcc Aluminum and Copper," *Phys. Rev. Lett.* **82**, 2713-2716 (1999).

K. Lin and D.C. Chrzan, "Kinetic Monte Carlo Simulation of Dislocation Dynamics," *Phys. Rev. B*, **60**, 3799-3805 (1999).

X. Blase, K. Lin, A. Canning, S.G. Louie and D.C. Chrzan, "Structure and Energy of the 90 Degree Partial Dislocation in Diamond: A Combined *ab initio* and Elasticity Theory Analysis," submitted to *Phys. Rev. Lett.*

C.R. Krenn, D. Roundy, J.W. Morris, Jr., and M.L. Cohen, "Theoretical and Experimental Upper Bounds of Shear Strength," presented at MRS Spring Meeting (1999).

C.R. Krenn, D. Roundy, J.W. Morris, Jr., and M.L. Cohen, "The Nonlinear Elastic Behavior and Ideal Shear Strength of Al and Cu," presented at TMS Spring Meeting (1999).

C.R. Krenn, D. Roundy, J.W. Morris, Jr., and M.L. Cohen, "Ideal Shear Strengths of fcc Aluminum and Copper," poster presented at MRS Fall Meeting (1998).

K. Lin and D.C. Chrzan, "Kinetic Monte Carlo Simulation of Dislocation Dynamics," poster presented at MRS Fall Meeting (1998).

Atomically Resolved Spin-Polarized Imaging Using Superconducting STM Tips

Principal Investigators: J.C. Séamus Davis

Project No.: 99024

Project Description

The goal of this proposal is to create techniques of scanning tunneling microscopy using superconducting tips, which will allow imaging of the spin polarization, and thus the magnetic moment, of individual atoms on a surface.

A combination of the superconducting tip, very low temperatures, and high magnetic fields will allow us to create a 100% spin-polarized source of electrons in the tip by using the Zeeman splitting of the quasiparticle density of states (DOS) at the gap edge of the superconductor. The polarization is possible when $\mu_B B >> k_B T$. With the available magnetic field of up to 7.25 Tesla in our Scanning Tunneling Microscope (STM) cryostat, we should easily be able to achieve this condition and thus split the spin polarization states completely. The peaks in the DOS then occur at voltages given by $V_+ = (\Delta + \mu_B B)/e$ and $V_- = (\Delta - \mu_B B)/e$ where Δ is the energy gap of the superconducting tip, and e is the charge on the electron. Tunneling at bias V_+ uses only electrons of one polarization, and tunneling at V_- only those of the other. Using this Zeeman polarized superconducting tip, in combination with an atomic resolution STM, will give us a unique opportunity to create the first spin sensitive imaging technique at the atomic scale. Should this be achieved, it will revolutionize the way that magnetic materials are studied on the atomic scale.

Accomplishments

To realize atomic resolution controllable spin-polarization contrast STM three elements are required: (1) atomic resolution STM, (2) magnetic field and temperature such that $\mu_B B >> k_B T$, (3) superconducting STM tips, and (4) appropriate conducting samples which have spin-polarized surface states. We have recently succeeded in the first use of Nb superconducting tips with atomic resolution. We have also successfully integrated a high field magnet with our atomic resolution STM and 250° mK refrigerator. We are currently studying highly correlated electronic materials in magnetic fields with conventional tips to help choose appropriate spin polarized surface state systems. Following is a more detailed description of the steps taken.

Integrated Magnet with STM Cryostat—Demonstrated Atomic Resolution STM at 7 Tesla and 250° mK

We demonstrated the operation of our STM system at temperatures down to 250° mK and in magnetic fields up to 7.25 Tesla with high spatial and energy resolution. Our test results have shown that, at the base temperature, this instrument has better than 0.5 pm z-direction resolution in imaging mode, and better than 20 μV energy resolution in spectroscopy mode while at 7.25 Tesla.

Demonstrated the Use of a Superconducting Tip in STM Imaging

We achieved vacuum tunneling of superconducting quasiparticles from an atomically sharp Nb tip onto both gold and superconducting samples.

Discovered Atomic Scale Quasiparticle Scattering Resonances (QPSRs) in $Bi_2Sr_2CaCu_2O_{8+\delta}$

While studying magnetic properties of $Bi_2Sr_2CaCu_2O_{8+\delta}$, since it is the type of cuprate-oxide perovskite that is a potential target for spin-polarized STM, we discovered the existence of large

numbers of identical regions with diameter ~3 nm that have a relatively high density of low energy quasiparticle states. Their spatial and spectroscopic characteristics are consistent with theories of strong quasiparticle scattering from atomic scale impurities in a d-wave superconductor. As this first observation of QPSRs was in nominally undoped material, we then studied BSCCO doped with a known impurity, Zn, and found a similar phenomena but this time showing a clear four-fold symmetry, as shown in the figure.

Imaging and Spectroscopy of Magnetic Vortices in $Bi_2Sr_2CaCu_2O_{8+\delta}$ - Discovered Core States

While studying the magnetic properties of BSCCO in high magnetic fields another new observation was made. Previous studies of magnetic properties of $YBa_2Cu_3O_{7-\delta}$ have found localized quasiparticle states within the magnetic vortex cores. Similar studies of $Bi_2Sr_2CaCu_2O_{8+\delta}$ (BSCCO), on the other hand, found no evidence of localized cores states. During high-field STM test experiments on BSCCO we demonstrated for the first time the existence of localized core states in BSCCO. We also showed that atomic scale scattering centers, for example, single atom impurities or atomic sized defects, can influence vortex structure by pinning vortices. Such pinning not only leads to a disordered vortex solid, but also to a large overlap of previously reported scattering resonances and magnetic vortices.

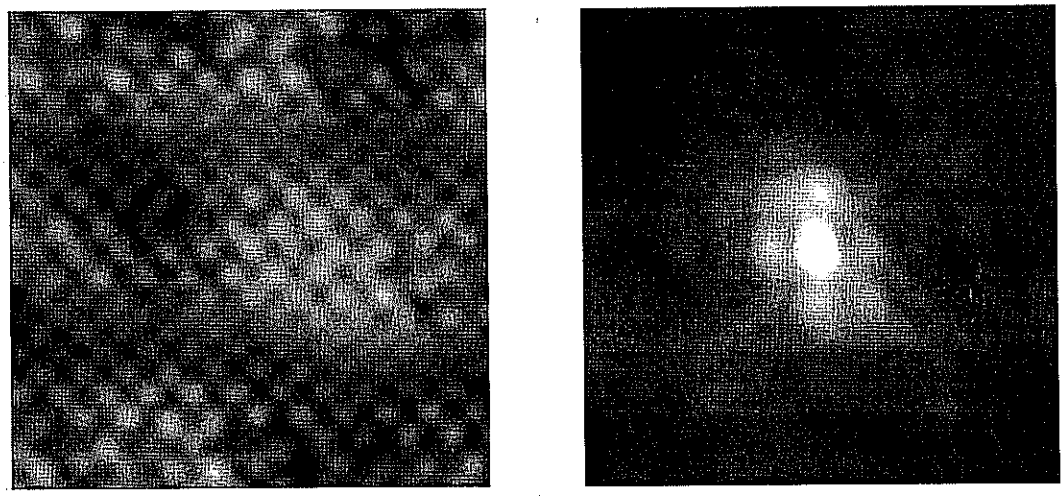

Figure 1. 64Å image of the topography (left) and simultaneously obtained local density of states (right) for a single Zn atom in BSCCO. The inner bright cross is oriented with the nodes of the D-wave gap in agreement with theoretical predictions of scattering from an impurity in a high T_c superconductor.

Publications

S.H. Pan, E.W. Hudson, and J.C. Davis, "He Refrigerator Based Very Low Temperature Scanning Tunneling Microscope," *Review of Scientific Instruments* **70**, 1459-63 (1998).

E.W. Hudson, S.H. Pan, A.K. Gupta, K-W Ng, and J.C. Davis, "Atomic Scale Quasiparticle Scattering Resonances in $Bi_2Sr_2CaCu_2O_{8+\delta}$," *Science* **285**, 88-91 (1999).

S.H. Pan, E.W. Hudson, K.M. Lang, H. Eisaki, S. Uchida, and J.C. Davis, "Imaging the Effects of Individual Zinc Impurity Atoms on Superconductivity in $Bi_2Sr_2CaCu_2O_{8+\delta}$," (accepted for publication in *Nature*, 1999).

S.H. Pan, E.W. Hudson, A.K. Gupta, K-W Ng, and J.C. Davis, "STM Imaging and Spectroscopy of Vortex Core States in $Bi_2Sr_2CaCu_2O_{8+\delta}$," (in preparation for *Phys. Rev. Letters*).

Development of Atomic-Resolution X-Ray Fluorescence Holography for Materials Analysis

Principal Investigators: Charles Fadley, Thomas Earnest, Zahid Hussain, Rupert Perera, Abraham Szöke, and Stephen Cramer

Project No.: 98021

Project Description

This project is to assist the development of x-ray fluorescence holography at the Advanced Light Source (ALS) as a novel probe of atomic structure with sub-Angstrom resolution. This newly discovered technique has been shown in a few prior experiments to be capable of providing local atomic structure information around a given elemental constituent of a material, without the need for macroscopic single-crystal samples. This method developed from the initial suggestion of Szöke in 1986 for using localized atomic emission events as sources of outgoing reference waves for holography. This was first realized experimentally with photoelectrons in 1990, then achieved with fluorescent x-rays in 1996, and finally seen with gamma rays via the Mössbauer effect in late 1997.

Our focus here is on x-ray fluorescence holography (XFH), in which the diffraction modulations of x-ray intensity are only of order ~±0.1%, but for which the holographic images are expected to be much more accurate than those obtained with the more strongly scattering photoelectrons. X-rays also provide a probe that can reach into the bulk of a sample, expanding the areas of application from surface science to materials science and ultimately the biosciences. In the simplest form of XFH, the modulations of a given single fluorescent energy are measured over a large solid angle above a sample surface, and a Fourier-transform-like operation is performed on this data to directly yield atomic images in three dimensions. Prior work in other laboratories has applied this method to inorganic solids (e.g. Fe metal, Sr in $SrTiO_3$, and Cu and Au in Cu_3Au) and a semiconductor dopant (Zn in 0.02 wt. % doped GaAs).

Beyond this approach, the Fadley group has been involved (in collaboration with Materlik et al. in Hamburg) in developing a more powerful form of XFH that has been termed multi-energy x-ray holography (MEXH). In this approach, the incident radiation beam is used as the reference wave, and the angle-integrated outgoing fluorescence is used only to measure the wavefield strength at a given emitting atom type. In this way, holograms at 5 to10 incident energies can in principle be measured, with the analogous Fourier-like inversion providing more accurate atomic images free of twin images and less affected by image aberrations. This type of measurement has so far been applied to two transitions metal oxides (Fe_2O_3 and CoO), but it is ideally suited for further exploitation at third-generation synchrotron radiation sources such as the ALS. We have thus proposed to build up the capability for carrying out both single-energy and multiple-energy x-ray holography experiments at the ALS in order to exploit the full potential of this exciting new probe of atomic structure. The very small percent effects involved make these very challenging experiments, and so our first attempts have been proof-of-principle in nature, with more concrete experiments and applications to more complex systems to come in the future. The project makes use of several unique resources at Berkeley Lab:

- *ALS Beamline 9.3.1*, which yields high-brightness x-rays up to ~7.0 keV in energy (or down to 1.8 Å in wavelength) and with total usable fluxes at the sample of ~4×10^{10} s^{-1}.
- *Multi-element semiconductor detectors*, which consist of approximately 12 to 30 working elements spanning areas of 2" to 3" radius, each of whose elements can, in principal, count with ~200 eV resolution at a rate of ~90 kHz (loaned by the Cramer group for this project).
- *A high-accuracy sample goniometer*, which is capable of rotating samples over a large solid angle in measuring holograms (loaned by the Earnest group, and assembled into a special sample chamber for this project).

Accomplishments

An X-ray Fluorescence Holography (XFH) endstation was constructed with assistance provided by several groups. This instrument consists of a vacuum chamber and support stand, a dual axis goniometer, a multi-element germanium detector manufactured by Canberra Instruments

(13 elements, but with electronics to drive only four elements during our experiments), pulse processing electronics, and a data acquisition system. Special data acquisition software was also written by M. Legros as part of the project.

Preliminary measurements have been performed on Beamline 9.3.1 to determine endstation function and to evaluate the count-rate capability of the detector and its pulse processing electronics. Experiments were carried out on a titanium polycrystalline sample and a nickel oxide (NiO) single crystal. The titanium polycrystal, from which Ti K_α radiation at 4.5 keV is emitted, should show no holographic features, and it was used as a reference to evaluate system stability, count-rate capability, and noise levels, while the NiO sample, from which Ni $L_{\alpha,\beta}$ radiation at 0.85 to 0.86 eV is emitted, was used to test the feasibility of recording a hologram via these much lower energy Ni L-edge emission lines.

A key requirement for any XFH experiment is the precise measurement of the normalized fluorescent x-ray flux from the sample. Ideally the overall stability should be 0.01% or 1 part in 10^4, although somewhat less than this is probably tolerable. Such precision counting must be effected while the fluorescent flux varies by as much as 30 to 50% due to the decay of the electron beam in the storage ring and changes in sample self-absorption as the sample is rotated with respect to the incoming beam. The beam-decay normalization procedure was evaluated by fixing the sample orientation and measuring the normalized Ti K_α x-ray fluorescence signal over the lifetime of a storage ring fill. Determining the normalized flux by taking the ratio of the x-ray fluorescence signal to the photocurrent from the titanium sample and allowing also for the appropriate dead-time correction as obtained from the acquisition software, showed that this signal varied by ~1 part in 10^3. Some improvement is thus needed in measuring the incident flux, with two future possibilities being to rotate the sample back to a fixed reference position periodically during a holographic scan; and to use an avalanche photodiode to record the magnitude of the scattered flux from a thin plastic foil placed close to the sample. Another count-rate limiting problem was the rate-dependent pulse pileup characteristics of the Canberra Instruments detector and electronics. This instrument could count at a maximum throughput of 9×10^4 cps per channel with a dead time of 35%, with the dead-time correction showing marked nonlinearity with input count rate. This borrowed unit is thus far from state-of-the-art regarding high rate, high precision spectroscopy, and we will in future pursue using much higher count-rate semiconductor detectors fabricated at Berkley Lab.

The measurement of MEXH holograms at the Ti L-edge, while novel and worthwhile, proved very challenging. The main problem was the large elastic scatter peak, which dominated the low energy fluorescence signal. To be successful, this experiment requires a more sophisticated detector technology, such as a next generation tunnel-junction-based spectrometer incorporating some kind of high energy prefilter to remove high-energy scattered radiation.

Overall, the basic endstation and control software worked well and the system constructed in this project should provide an excellent development platform for future XFH experiments. Beamline 9.3.1 will continue to be a useful source to evaluate each system upgrade, and the flux from the beamline has not been a limitation in any experiments to date, which are at present detector-rate limited. We have begun to address the detector and interference issues, and we have performed preliminary measurements using custom high-throughput pulse shaping electronics designed by the Engineering Division Measurement Science group.

Electron-Electron Interactions and Optical Properties of Materials

Principal Investigators: Steven Louie and Marvin Cohen

Project No.: 99025

Project Description

This project consists of two major components:

Quantum Coherence in Semiconductor Heterostructures

An experimental and theoretical study of coherent dynamics of light and excitons in a semiconductor heterostructure is performed. The key ingredient is the exciton-exciton correlation, which affects the coherent spin dynamics of excitons. This study of the basic physical processes of optoelectronics and magneto-optoelectronics may be relevant to future

device applications which involve coherent quantum control.

A fundamental theory of exciton-exciton correlation in terms of memory function, developed by L. Sham, T. Ostreich, and K. Schonhammer, is used by Ostreich and Sham to study further the coherent exciton dynamics at low densities. Emphasis is placed on understanding the intrinsic dephasing due to the exciton-exciton scatterings and the nonlinear optical processes beyond the third-order in the exciting field. The understanding of dephasing is crucial to the application of quantum coherence in semiconductors, and the theories which have been developed are either phenomenological or concerned with the mechanism of the electron-phonon interaction or disorder. The memory function theory of exciton-exciton correlation enables us to calculate the intrinsic dephasing beyond the second Born approximation. A Gross-Pitaevskii like equation of the coherent dynamics of exciton polarization has been established, which includes a correlation term. The equation is then solved to study the time and spatial evolution of the optically excited spin-dependent exciton coherence. As input, both the non-perturbative computation of the exciton memory function in a lattice model (with Hubbard and long-range interaction) and model constructions of the memory function satisfying a number of sum rules are used. The latter has the simplicity that makes it promising as a tool for interpreting experiments.

In collaboration with the experimental group of Daniel Chemla, the higher order (in exciting electromagnetic field) effects on nonlinear optical processes, including pump-and-probe and six-wave mixing are studied. The nonlinear processes in a microcavity where the photon-exciton interaction is enhanced by photon confinement have also been explored.

Strongly Correlated Semiconductors

Another activity is the exploration of possible electronic ferroelectrics and other related semiconductors with strong electron correlation.

Massimo Rontani performed a comparative study of the current across the interface between a normal metal and a strongly correlated semiconductor (a Kondo insulator or an electronic ferroelectric) and between a normal metal and an ordinary semiconductor. He studied the effect of both the density of states and the wave function coherence on the I-V characteristics and on the thermoelectric properties. The effects of model defects in the interface region have also been examined.

Po-Chung Chen, Thomas Ostreich and Lu Sham worked on solutions of the Falicov Kimball model beyond the mean-field approximation. The model contains interaction between a broad band of mobile electrons and a narrow band of localized electrons, as well as the strong Hubbard repulsion between two localized electrons on the same atom. In the mean-field approximation, the model is known to lead to a ferroelectric state. Other workers' observations that the localized electrons may be treated as a configuration of charges to provide a classical potential for the broad band electrons had led to computations of exact ground states. These ground states provided no coherent features of an exciton condensate and seemed to contradict the results of the mean-field approximation. Sham's current analytical and numerical solutions of the model show that in the spin one-half case, with either the broad band either half-filled and the localized electrons singly occupying all available sites or with the broad band completely filled and no localized electrons, the ground state may be an excitonic insulator.

Accomplishments

Quantum Coherence in Semiconductor Heterostructures

The Gross-Pitaevskii equation, including correlation, was constructed. An important result of the first-principles computation of dephasing is that in GaAs the intrinsic dephasing time is of the same order as found by experiment. From this, it is inferred that the intrinsic dephasing time is of the same order as the dephasing due to extrinsic causes. From the numerical simulations of the time-development of the optically excited exciton polarization we discovered an oscillation, which we showed by analytical solution of small oscillations about a slowly varying nonequilibrium decay to be the high frequency branch of the collective modes of the exciton branch. The low frequency branch is the Goldstone mode. There is also a corresponding spin oscillation mode. Thus, the exciton polarization may be inferred as behaving like a Bose-Einstein condensate.

Professor Chemla's group has utilized the strong exciton binding in ZnSe to study the exciton

interaction effects in a series of experiments. (1) They have found coherent oscillations in a pump-and-probe experiment of a single quantum well. This can be explained in terms of a bound biexciton using the average-polarization model, which can be obtained from the memory function by a single frequency spectrum. (2) When the ZnSe quantum well was placed in a microcavity, the experimentalists found direct evidence of antiparallel biexciton as a third peak in the pump-and-probe spectrum, in addition to the two polariton peaks. The spectrum is in good agreement with theory. (3) The experimentalists have also measured strong six-wave mixing signals in various configurations of polarizations of the excitation and test laser beams. Theory is used to sort out the contributions from all possible polarization configurations to fifth and seventh order in the exciting field. Experimental results show that seventh order terms are present, but there are quantitative discrepancies in the frequency spectra in some key polarization configurations between experiment and computation, which uses a decoupling approximation exact to third order in the exciting field (but does possess some of the higher order terms). This exciting finding shows, in particular, an important six-particle correlation unaccounted for by current theory.

Strongly Correlated Semiconductors

The effort on the thermoelectric properties of junctions between metal and strongly correlated semiconductors has shown that the electronic ferroelectric and the Kondo insulator show thermoelectric behavior distinct from the ordinary semiconductor. They have high thermoelectric figure of merit and are less affected by interface defects than ordinary semiconductors of comparable band gaps.

Chen, Ostreich and Sham carried out both analytical and numerical exact solutions of the Falicov-Kimball model. It is shown that in the spin one-half model, the exact ground state is an electronic ferroelectric for two cases: (i) with the broad band either half-filled and the localized electrons singly occupying all available sites and (ii) with the broad band completely filled and no localized electrons. In case (i), the divergence in the electric susceptibility, which leads to the ferroelectricity, has the same physics as the Fermi edge singularity (the Mahan effect). In case (ii), it is just a special case of the excitonic insulator.

Publications

L.J. Sham, "Theory of Spin Coherence in Semiconductor Heterostructures," *J. Magnetism and Magnetic Materials* **200**, 219-230 (1999).

T. Ostreich and L.J. Sham, "Collective Oscillations Driven by Correlation in the Nonlinear Optical Regime," *Phys. Rev. Lett.* **83**, 3510-3513 (1999).

L.J. Sham and T. Ostreich, "Exciton Interaction and Spin Dynamics in Semiconductor Heterostructures," Proceedings of International Conference on Luminescence 1999, Osaka, Japan, J. Luminescence (in press).

U. Neukirch, S.R. Bolton, L.J. Sham, and D.S. Chemla "Electronic Four-particle Correlations in Semiconductors: Renormalization of Coherent Pump-probe Oscillations," *Physical Review B* (in press).

U. Neukirch, S.R. Bolton, N. Fromer, L.J. Sham, and D.S. Chemla "Polariton-Biexciton Transitions in a Semiconductor Microcavity," submitted to *Phys. Rev. Lett.*

S.R. Bolton, U. Neukirch, V.M. Axt, L.J. Sham, and D.S. Chemla "Higher Order Exciton Correlations from Six-wave Mixing," abstract submitted to QELS 2000.

M. Rontani and L.J. Sham, "Thermoelectric Properties of Junctions between Metal and Strongly Correlated Insulator," (draft).

L.J. Sham, P.-C. Chen, and T. Ostreich "Coherent Ground State in the Spin-dependent Falicov-Kimball Model," (in preparation).

Presentations by L.J. Sham

"What we Know about the Density Functionals," invited speaker, Workshop on Density Functional Methods, Laguna Beach, California (March 26-28, 1999).

"Strongly Correlated Insulators," Seminar, Department of Physics, University of California, Berkeley (April 5, 1999).

"A Theory of Exciton Correlation and its Observable Effects," invited speaker, Optical Society of America, Topical Meeting on Quantum Optoelectronics, Snowmass, Aspen, Colorado (April 12-16 1999).

"Optical and Spin Coherence in Semiconductors," Seminar, Department of Physics, Georgetown University (April 28, 1999).

"Strongly Correlated Semiconductors," Seminars, National Taiwan University, Taipei, Taiwan (May 11, 1999).

"Optical Coherence and Exciton Correlation in Semiconductor Heterostructures" and "Strongly Correlated Semiconductors (Electronic Ferroelectrics and Kondo Insulators)," Seminars, National Center for Theoretical Sciences, Taiwan (May 12-14, 1999).

"Exciton Interaction and Spin Dynamics in Semiconductor Heterostructures," invited speaker, 1999 International Conference on Luminescence and Optical Spectroscopy of Condensed Matter, Osaka, Japan (August 23-27, 1999).

"Theory of Exciton Correlation and Optical and Spin Coherence in Semiconductor Heterostructures," September 9. "Exciton Condensation in Solids," September 16, NTT Lectures on Exciton Interaction: NTT Research Laboratories, Atsugi, Japan (1999).

"Exciton Condensation in Solids," Seminar, University of Tokyo (September 17, 1999).

"Exciton Correlation Effects," invited speaker, Autumn Meeting of the Physical Society of Japan, Morioka, Japan (September 24-27, 1999).

Infrared Spectroscopy of Complex Materials

Principal Investigators: Joseph Orenstein

Project No.: 99026

Project Description

Infrared (IR) spectroscopy is a powerful probe of new materials, enabling, for example, the discovery of gap-opening phase transitions and "pseudogaps" above the transition temperature. The goal of this project is to establish a capability for IR reflection and transmission measurements at the Advanced Light Source (ALS) and initiate the first experiments. IR spectroscopy will function synergistically with the angle resolved photoemission spectroscopy (ARPES) program at the ALS. ARPES is a powerful, but time intensive, technique. Characterization by IR spectroscopy can dramatically shorten the time for discovery of materials with the most exciting and useful properties.

Synchrotron-based IR beamlines are considerably brighter than conventional (thermal) IR sources. At present Beamlines 1.4.2 and 1.4.3 make use of the high brightness of the ALS to perform room temperature IR micro-spectroscopy using a Bruker IFS 66v/S spectrometer. We propose acquisition of a cryostat, reflection optics, and a visible-light interferometer to enable variable-temperature reflection and transmission spectroscopy as well. In collaboration with Janis Research Company we will use a liquid helium refrigerator designed to meet the demands of IR reflection spectroscopy. It will allow vertical positioning of up to three samples (typically one reference and two samples), as well as rotational alignment of the sample with respect to the IR beam. To measure reflectivity accurately, the reference mirror and the sample surface must be precisely coplanar. An external interferometer will permit precise alignment and coplanarity of the sample and reference.

Accomplishments

The beginning of this project in FY99 accomplished the following:

- Successfully recruited student Chris Weber, who has extensive experience in far-IR spectroscopy, to work together with Michael Martin on the project.
- All the component parts have arrived and have been tested: cryostat, cryostat-spectrometer interface, He-cooled bolometer, and sample mounts.
- Detailed characterization of the substrates that the thin film samples will be grown on has been performed. The substrates were found to be sufficiently transparent to permit transmission measurements from 20cm^{-1} to 200 cm^{-1}, which is the region of interest.
- Chris Weber and Michael Martin have begun to perform transmission spectroscopy on oxide materials, namely the bismuth-based high-T_c superconductor and $SrRuO_3$, which is a ferromagnetic ruthenate.

Publications

Weber, Martin, Orenstein, Dodge, Reiner, "Non-Fermi Liquid Charge Dynamics in Strontium Ruthenate," (in preparation).

Investigation of Quantum Well States in Magnetic Nanostructures

Principal Investigators: Zi Qiu

Project No.: 98041

Project Description

Quantum Well (QW) states plays an important role in many fascinating phenomena. In layered structures, QW states manifest as the film thickness shrinks into the scale of electron wavelength. Because of the short wavelength of electrons in metals, film thickness in a metallic nanostructure has to be controlled on the atomic scale to realize well-defined QW states. While such a short length scale challenges experimentalists to realize metallic QW states, it produces QW energy separations greater than the room-temperature thermal energy. This property has important technological application potential as the ideal device-working-temperature is room temperature.

Photoemission is currently the most direct experimental technique for QW study, as QW states can be easily identified as peaks in the photoemission spectrum. To have a systematic photoemission study of metallic QW states at the atomic scale, we performed photoemission on wedged sample, which can control film thickness continuously. Wedged sample, however, requires a local probe, which is not common in photoemission. The Beamline 7.0.1.2 at the Advanced Light Source (ALS) has the capability of fine photon beam size (~50 to 100μm) with high brightness (>10^{12} photons/sec at resolution power of 10,000). This unique capability makes it possible to perform photoemission experiments on wedged sample.

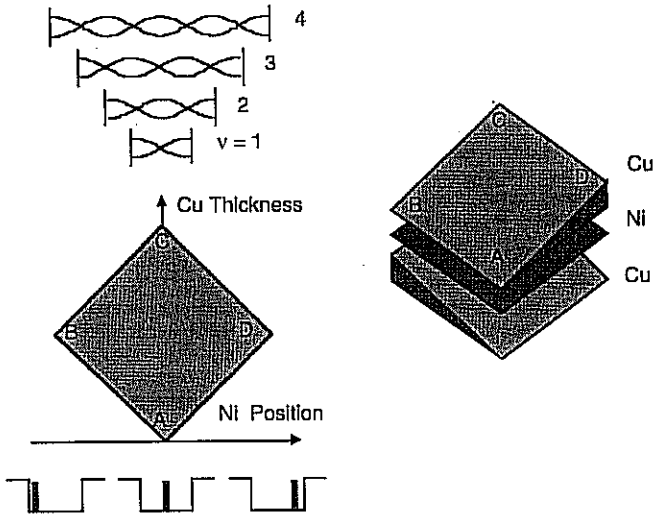

Figure 2. A double-wedged sample which allows the independent variation of the Cu thickness and the Ni position inside the Cu.

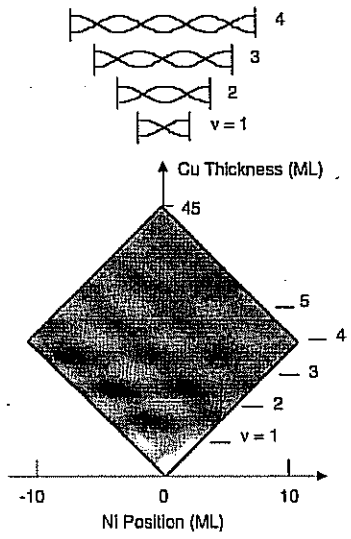

Figure 3. Photoemission from the double-wedged sample in Figure 2. Nodal structure of the QW states can be clearly seen.

Accomplishments

Current investigation on QW states in metallic nanostructures focuses on the peak positions in an energy-thickness plane. To have a deep understanding of the QW nature, it is crucial to obtain the depth profile of the QW wavefunction. We performed such experiments at the ALS to reveal the nodal structure of QW states in Cu thin film grown epitaxially on Co(100).

The idea is similar to the case of probing the nodal structure of a vibrating string. With a finger sweeping through the string, the standing wave will respond differently as the finger touches the node and antinode, respectively. In our experiment, the standing wave of the string is the QW wave of the electrons inside a Cu film. Because this "string" is only ~one nanometer long, we employed one layer of Ni atoms as a thin "finger" to play this QW "string." To systematically sweep the Ni "finger" across the nanometer-long Cu QW, we created a double wedged sample as shown in Figure 2. Two identical Cu wedges were created at 90-degrees with a one monolayer Ni film inserted in between. This sample geometry has the advantage of varying the Ni position while fixing the Cu thickness (along BD, see Figure 2) or varying the Cu thickness while fixing the Ni position (along AC, see Figure 2). Photoemission at the Fermi level is shown in Figure 3. Along the AC direction, we observe the intensity oscillation with a periodicity of 5.6 ml Cu thickness. This is the QW states observed before. Along the BC direction, we observed the QW nodal structure revealed by the Ni probe layer.

Publications

R. K. Kawakami *et al.*, *Nature* **398**, 132 (1999).

Result of this work was reported as an invited talk in the 1999 International Conference on Magnetics, and will also be presented as an invited talk in the 2000 APS March Meeting.

Spatially-Resolved Residual Stress Characterization at Microstructural Dimensions

Principal Investigators: Robert Ritchie and Howard Padmore

Project No.: 99027

Project Description

There is a wide variety of problems in materials science that have eluded full understanding due to an inability to experimentally characterize the local residual stresses at spatial dimensions comparable to, and below, microstructural size-scales. These stresses are important as they are additive to any applied stresses, and thus critically affect any local defect mobility, deformation, and fracture behavior. As no techniques to date have been capable of quantifying the magnitude and gradient of such residual stresses over micron-sized dimensions, this

work is focused on the development of experimental methods and analysis for this purpose through the use of ultrahigh-brightness, x-ray micro-diffraction techniques at the Advanced Light Source (ALS), and the application of such techniques to several critical problems in materials engineering. The ALS provides the unique ingredient here due to its ability to produce high photon fluxes over spot sizes of micron dimensions, thus permitting stress and strain measurements within a single microstructural feature.

The approach has been to establish and calibrate (against known standards) the experimental setup and procedures, and then to apply the technique to a wide range of applications. During the past year, we have investigated the problem of residual stresses in the immediate vicinity of impact sites due to foreign object damage. Future applications will include such projects as the identification and quantification of (1) processing-induced residual stresses in the nanometer-thick grain-boundary films in ceramics, (2) defect structure transport in Al-Cu interconnects in integrated circuits, and (3) local stress gradients at matrix/reinforcement interfaces in composite materials.

It is believed that the ability to measure the magnitude of peak residual stresses over microstructural dimensions, and to quantify the gradient of such stresses near specific microstructural features, would provide new mechanistic insight into the local and global structural properties of a wide class of materials.

Accomplishments

The quantification of residual stresses is difficult at any dimension. However, over microstructural size-scales, existing experimental techniques are severely limited in spatial resolution. For example, the most common procedure, that of x-ray diffraction, typically suffers in this respect from a lack of brightness. Conventional systems utilize a photon flux of ~10^5 to 10^6 ph/sec, but over a spot size on the order of millimeters; these techniques can be modified for micro-diffraction with spot sizes down to ~50 μm, but then are limited by a very low photon flux. These limitations in the ability to characterize local stresses can be readily overcome by employing diffraction measurements using a focused ultrahigh brightness source of x-ray radiation, such as that provided by the Advanced Light Source (ALS). The ALS is capable of producing high photon fluxes (~10^9 ph/sec) over micron-dimension spot sizes, such that measurement of residual stress gradients over micron-sized dimensions, and within individual microstructural entities such as a grain or precipitate, are now a real possibility. To aid in the development of the techniques and experimental procedures to effect such measurements, and to apply them to the characterization of residual stresses affecting defect behavior, deformation and fracture events *at microstructural size-scales* has been a major objective of this work.

Our initial studies have focused on the problem of measuring the local gradients in residual stresses in impact damaged Ti- and Ni-base alloy turbine blades subjected to foreign object damage. This has involved the development of comprehensive calibration techniques on well-defined standards to establish the validity of the technique, and refinement of this technique to the problem of impact damage. To this end, initial synchrotron experiments have been conducted at the Stanford Synchrotron Radiation Laboratory (SSRL).

The calibration technique involves an *in situ* straining jig mounted in an x-ray diffractometer, capable of applying strain to a known standard, where the amount of applied strain is measured directly from a strain gauge mounted to the standard. At each applied strain level, the corresponding peak shift in the diffraction pattern can be compared to the unstrained peak position and the x-ray determination of strain can be compared to the strain gauge measurement (Figure 4a). In the current setup, the applied strain (as well as the strain measured by the strain gauge) is perpendicular to the surface normal strains measured by x-ray diffraction and hence the comparison must include the proper Poisson's scaling ratio. These studies on the calibration technique have indicated the strain resolution is ~10^{-4}, which is more than adequate to characterize failure-critical stress gradients.

Foreign object damage (FOD) is an acute problem in gas-turbine blades, where small particles ingested by gas-turbine engines can result in local microstructural damage on the blades, leading to the initiation of fatigue cracks and eventual failure of the engine. This is currently a major, if not the leading, cause of engine failures in high-performance gas turbines. To simulate FOD, a damage site was created by firing a 3.1-mm diameter Cr-hardened steel ball onto a specimen of titanium blade alloy, Ti-6Al-4V, at velocities of 200 to 300 m/s using an automated, high-velocity,

compressed air gun facility. This damage site was then probed using the available macro-diffraction beamline 2-1 at SSRL. A coarse x-ray beam, 1 mm wide, was used to probe next to the 2 mm diameter crater left by the impact (Figure 4b). The probe was stepped incrementally away from the edge of the crater in increments of 0.5 mm. When compared to peaks from the back side of the same specimen (in the unstrained condition), the peaks from the foreign object damage show both compressive and tensile residual strain fields depending on the position of the probe (Figure 4c). This very interesting result indicates that not only does the magnitude of the corresponding stresses change across the gradient, but that the sign of these stresses change as well. This finding was verified using finite-element analysis of the residual deformation associated with the indentation. Experiments and analysis indicate that within the gradient of the field left by the indent, there exist local regions of both tensile and compressive stress. Specifically, we find three primary regions of local tensile stress: at the base of the indent, at the edge (rim) of the indent, and a short distance away on the surface. Subsequent experimental high-frequency fatigue testing of FOD-damaged samples indicated that these were precisely the regions where fatigue cracks were initiated. These results provide critical insight into the conditions that cause crack formation and eventual failure due to foreign object damage. While the relatively crude 1 mm spot size available at SSRL was useful as an initial probe of this phenomenon, the need for a well-resolved delineation of these stresses is apparent. The microdiffraction capability being set up at the ALS will provide the pivotal role in this regard.

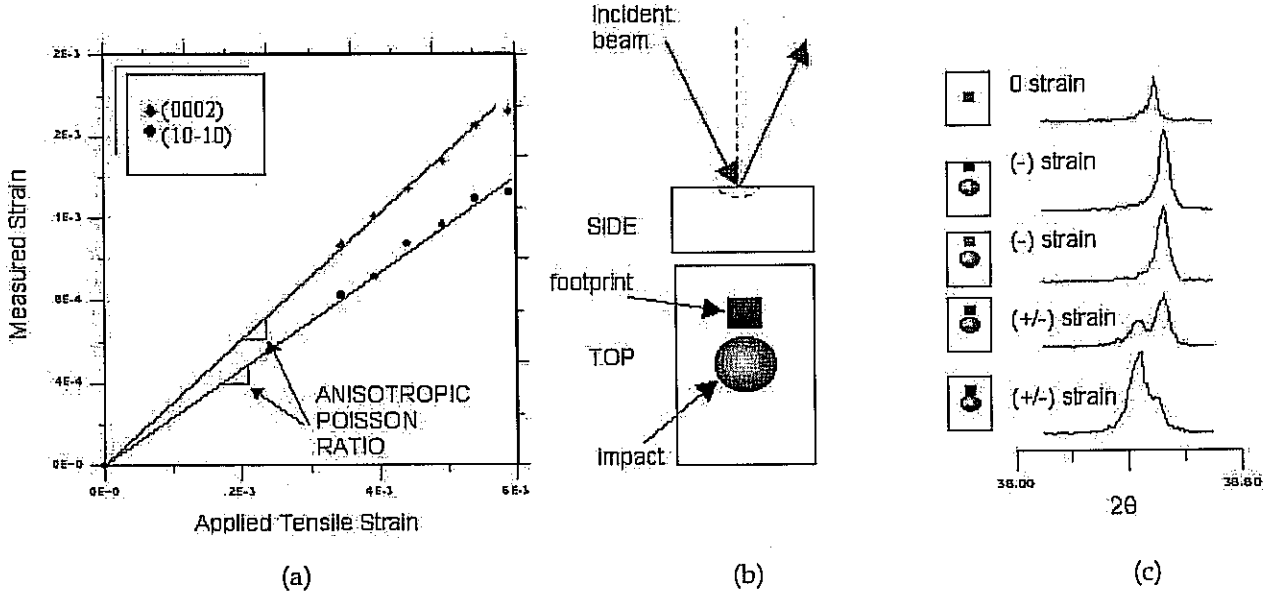

Figure 4. (a) Calibration technique showing resolution, (b) FOD interrogation, and (c) bifurcation of the (0002) peak.

Publications

B.L. Boyce, A.W. Thompson, O. Roder, and R.O. Ritchie, "Measurement of Residual Stresses in Impact-Damaged Ti-6Al-4V," Proceedings of the Fourth National Turbine Engine High Cycle Fatigue (HCF) Conference (1999).

Electron Spectroscopy of Surfaces under High Pressure Conditions

Principal Investigators: Miquel Salmeron, Zahid Hussain, and Charles Fadley

Project No.: 99028

Project Description

The goal of this project is to build a special environmental chamber to perform studies at the liquid-gas and solid-gas interface at high pressures (up to 20 torr), using the high beam intensity of the synchrotron radiation at the Advanced Light Source (ALS). In its first phase, it will be applied to the study of the surface structure of ice near the melting point. The existence of a liquid-like layer on the ice surface at temperatures well below its triple point plays an important role in a wide variety of phenomena, such as ozone depletion in the upper stratosphere, acid rain, and the reduced friction of ice near its melting point. In another important application, the chamber and spectrometer should be invaluable in studies of catalysis, biological, and environmental sciences where surfaces are exposed to high pressure of gases or liquids. Until now, surface electron spectroscopy could only be performed in high vacuum conditions.

Accomplishments

First, an environmental cell to perform environmental studies of water adsorption on solid substrates has been built. Near Edge X-Ray Absorption Fine Structure (NEXAFS) studies of the absorption of water on mica have shown the presence of a peak in the total electron yield (TEY) spectra that is characteristic of the water monolayer in equilibrium with the vapor up to 4.5 torr. This peak allowed us to study equilibrium adsorption isobars and isotherms.

Second, we have obtained the first fluorescent yield NEXAFS spectra of liquid water and liquid-like water on ice in equilibrium with water vapor at 0.09 torr. The different coordination of water in the disordered liquid state is reflected in the presence of a distinct peak near the threshold, which is not present or much weaker in crystalline ice. The thickness of the liquid-like layer is seen to increase as the temperature approaches 0°C.

Third, we have designed and constructed a unique lens system that serves also as a differentially pumped stage for the performance of x-ray photoemission spectroscopy (XPS) at high pressures (up to ~10 torr). The system is currently in its testing stage at the ALS.

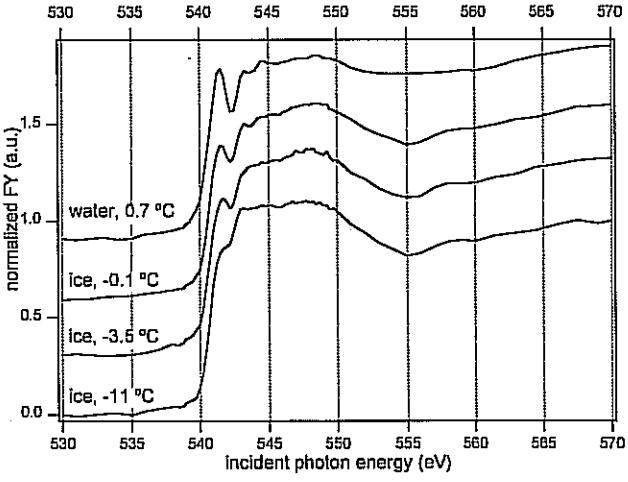

Figure 5. Fluorescent yield NEXAFS spectra of water and ice at normal incidence of the x-ray beam and grazing fluorescence

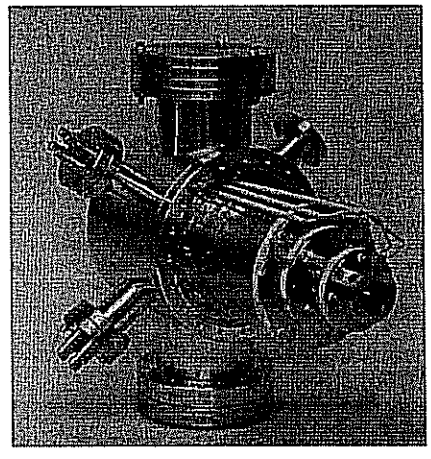

Figure 6. Photograph of the differentially pumped electron lens system. The picture was taken from the sample side of the lens system.

Direct Measurement of the Force Field Between Mesoscopic Objects and Single Atoms

Principal Investigators: Miquel Salmeron and D. Frank Ogletree

Project No.: 99029

Project Description

The aim of this project is to develop techniques for the direct measurement of forces and force gradients acting between a mesoscopic object and single atoms or molecules adsorbed on various substrates. The mesoscopic object is the sharp tip (of nanometer dimensions) used in scanning tunneling microscopy (STM) and atomic force microscopy (AFM). The forces are responsible for the attraction, repulsion, energy transfer, and dissipation processes that govern chemical bonding, friction, magnetic properties, etc. Measuring these forces will help to understand the mechanism for manipulation of matter at the atomic and nanometer scales.

Accomplishments

An analog electronic, phase-locked loop control for the detection of the amplitude, phase, and frequency shifts of an oscillating AFM/STM tip due to tip-surface forces has been constructed. With this prototype, several experiments were performed in air and also in ultrahigh vacuum. These experiments have helped to understand and to determine basic parameters of the new operation mode in non-contact AFM. The results of the experiments are being used in simulations to optimize the design for the next generation of totally digital instrument now under construction.

Secondly, we performed measurement in dc mode of the tip-surface force acting on the STM tip while imaging. The force at step edges and over adsorbates was found to change by a few nanonewtons and is thought to originate from electrostatic dipolar fields localized around step and adsorbate atoms. This is the first time that the forces acting during STM imaging have been measured directly.

Finally, we have developed a Runge-Kutta simulation of the oscillation of a tip in proximity to a surface, and used the simulated photodetector signal as the input to a separate simulation of the demodulator circuit. The demodulator simulation is capable of locking into the resonance frequency of the cantilever, and tracking variations of the resonance frequency and oscillation amplitude. The simulation is also capable of controlling either the oscillation amplitude or the oscillation phase. In addition, the recorded signal of a real lever has also been used as the input to the demodulator simulation, with similar results. The demodulator simulation is a software replica of the digital demodulator that can be built into hardware. The software algorithms that are used to implement feedback can be directly applied to digital signal processor (DSP) hardware.

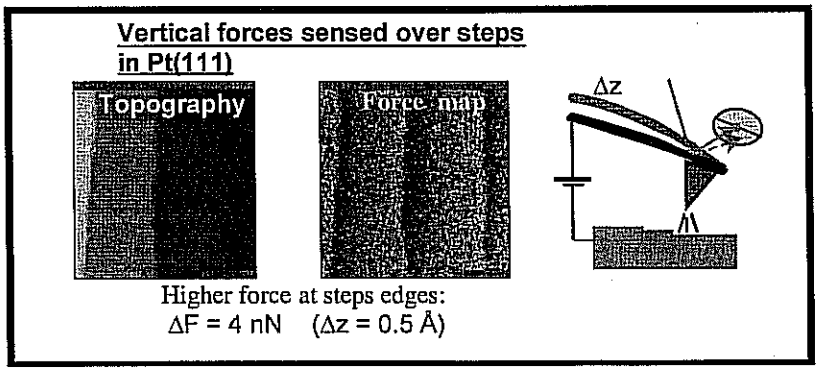

Figure 7.

Publications

Article on direct measurement of forces over Pt(111) steps and adsorbates (in preparation).

Single Molecule Protein Dynamics

Principal Investigators: Shimon Weiss, Peter Schultz, Carlos Bustamante, and Phil Dawson

Project No.: 99030

Project Description

This project seeks to study conformational changes and folding/unfolding pathways of single macromolecules by novel single molecule fluorescence spectroscopy techniques. Fluorescence resonance energy transfer (FRET), which measures the proximity between two fluorophores, is used to measure distance changes, and therefore conformational dynamics, between two points on a macromolecule. This distance serves as a reaction coordinate for folding/unfolding, denaturation, and charge screening reactions. Performing such measurements on the single molecule level has important advantages over conventional ensemble measurements, since they resolve and quantitatively compare distinct sub-populations of conformational states, otherwise invisible at the ensemble level; and resolve dynamic conformational changes, otherwise hidden at the ensemble level because of lack of synchronization.

Two kinds of molecules have been investigated: single stranded DNA (ss-DNA) and the protein Chymotrypsin Inhibitor 2 (CI2). In the first experiment, ss-DNA is used to study the statistical and dynamical properties of a short polymer, with only very few Kuhn segments. While the conformational statistics of long single and double stranded DNA have been studied extensively using traditional methods such as sedimentation velocity, light scattering, and optical tweezers, these methods are inadequate for the studies of polymers on the 100Å scale, far from the infinite chain limit. Properties such as the persistent length and the characteristic ratio of DNA oligonucleotides in this distance range (15 to 60 bases in length) change significantly with increasing chain length. While models have been proposed to calculate the end-to-end distance distributions and scaling properties in such oligonucleotides, they have not been systematically tested experimentally. Such scaling issues and the effects of solvent environment on the polymer conformational properties are being studied.

The molecule CI2 is used for single-molecule protein folding experiments. The problem of protein folding is of great significance from both fundamental and practical points of view. The question of how a relatively unstructured protein in its unfolded state finds its way through a huge conformational space to a small ensemble of structures that is the native state is one that has fascinated physicists, chemists, and biologists for many decades. Furthermore, the current effort in genome research is producing massive quantities of protein sequence information that needs to be converted into structural and functional information. A detailed understanding of protein folding mechanisms is therefore a very important piece of this puzzle. Although much has been learned about the issue, especially in the last decade, the complexity of protein structure precludes detailed studies from being carried out using ensemble methods. These methods lose a lot of the dynamic and stochastic information that is both fascinating and crucial to the understanding of the physics of protein folding mechanisms.

Accomplishments

ss-DNA:

We used computer simulations to design first-generation constructs and experiments. We synthesized various ss-DNA constructs and site-specifically labeled them with donor and acceptor dyes. Single pair FRET (spFRET) experiments were performed and polymer mean end-to-end distances were extracted. We are currently comparing the results to theoretical models used in the simulations.

Computer modeling: The means and distributions of end-to-end distances in ss-DNA are sensitive to the conformations of the chain monomers and intrastrand interactions. Simulations have been carried out using a rotational isomeric state model to predict the effects of numbers of monomeric units on the end-to-end distance means and distributions. Based on these calculations, we have chosen to study poly(dT) strands in the 15 to 60 base range. (Thymine was chosen as the base in order to minimize secondary structure within the strand and for synthetic considerations.) The theoretical models also assist in analysis of the effects of changes in the constructs on the observed distances.

Synthesis of oligonucleotide constructs: These experiments require ss-DNA site-specifically labeled

with donor and acceptor dyes. Oligonucleotides with two orthogonal reactive groups, a thiol and an amine, were synthesized using standard oligonucleotide synthesis techniques. TMR, the donor, and Cy5, the acceptor were attached to the thiol and amine respectively.

Single molecule experiments: While mean FRET efficiencies can, in principle, be measured using ensemble fluorescence methods, donor-only impurities in the samples skew the numbers. In the case of the ss-DNA samples, the purification efficiency is dependent on the number of monomeric units. Hence, even measurements of mean end-to-end distances of the series of DNA molecules are complicated at ensemble resolution. In single molecule measurements, however, donor-only impurities are seen as a separate peak with a FRET efficiency close to zero, allowing "electronic purification" of the sample.

Diffusion sp-FRET measurements were carried out on the ss-DNA molecules as a function of polymer length (number of bases) and salt concentrations. Here, both the scaling properties and the effects of counter-ion screening on the DNA conformations are being investigated. Initially, $(dT)_{20}$ and $(dT)_{30}$ were studied, and changes in the FRET distributions were observed as a function of salt and polymer length. The measurements for $(dT)_{20}$ and $(dT)_{30}$ clearly show that ss-DNA is a polymer that spends most of its time in a disordered form, and that it is becoming stiffer as the polymer gets shorter (the persistent length gets longer as the polymer gets shorter). We also find that the ionic strength dependence of the persistent length for short ss-DNA is different from that of a double stranded DNA.

CI2:

We chose CI2, a well-studied two-state folder, as a model system for single-molecule protein folding experiments. We generated site-specifically donor-acceptor labeled protein for single molecule FRET studies and carried out preliminary experiments using diffusion spFRET methodology. We are currently developing non-perturbative surface immobilization methods, which will allow us to perform spFRET folding studies of immobilized molecules.

Protein molecules: Chymotrypsin Inhibitor 2 has been studied extensively using ensemble experimental methods (Fersht and coworkers) and theory. It shows relatively simple two-state behavior. Its stability can be changed conveniently by single changes in the sequence (point mutations), and it is small enough to be conveniently made using semi-synthetic methods. The protein was made using ligation methodology, the donor was incorporated during the synthesis, and the acceptor attached using the single cyteine at position 40. Site-specific labeling was confirmed using mass spectral analysis. The structure of the protein construct and location of donor and acceptor are shown in Figure 8a.

Diffusion spFRET experiments: The donor-acceptor labeled protein was studied at single molecule resolution, using the ratiometric diffusion spFRET technique that was recently developed in our lab. This method minimizes the perturbations due to surface interactions, a problem that is commonly encountered in single molecule experiments. Fluorescence bursts from single, freely diffusing, donor-acceptor labeled protein molecules in solution are analyzed to identify and quantify folded and unfolded protein sub-populations as a function of guanidine concentration. Sample FRET histograms are shown in Figure 8b. These data were used to calculate a denaturation curve, which is shown in Figure 8c. A destabilized mutant of the protein was also examined; the observed changes in the folded/unfolded sub-populations with denaturant concentration and protein stability are consistent with literature ensemble measurements. The first two moments of the FRET distributions of folded and unfolded sub-populations were analyzed (peak position and width) and pair distances and potentials for folded and unfolded sub-populations were extracted. These measurements seem to indicate that the unfolded population has a broader distribution and more extended conformation at higher and higher guanidine concentration. We are currently analyzing the experimental distributions to separate out contributions from factors extrinsic to the folding process itself (such as relative dye orientations and photophysical properties of the dyes).

These studies demonstrate the feasibility and the power of single molecule techniques for the study of protein folding. They provide benchmark single-molecule folding data and give confidence in exploring other methods such as experiments on single immobilized protein molecules.

Immobilization methods: We are currently exploring two options for protein immobilization—surface and gel immobilization. For this, both confocal scanning and charge-coupled device (CCD) camera

imaging methods are being used. For gel immobilization, experiments are being carried out to determine optimal gel materials (polyacrylamide, agarose, etc.), gel pore size, etc. For the surface immobilization, new surface chemistries are being developed to achieve protein attachment, while still minimizing non-specific interactions between the protein and the surface. An attractive possibility is to use a mono-layer of polyethylene glycol on the glass surface, which has been previously shown to prevent protein adsorption. A low concentration of reactive groups on the surface will be used to attach handles for protein immobilization. Fast mixing techniques have been developed to initiate folding/unfolding in this immobilized format.

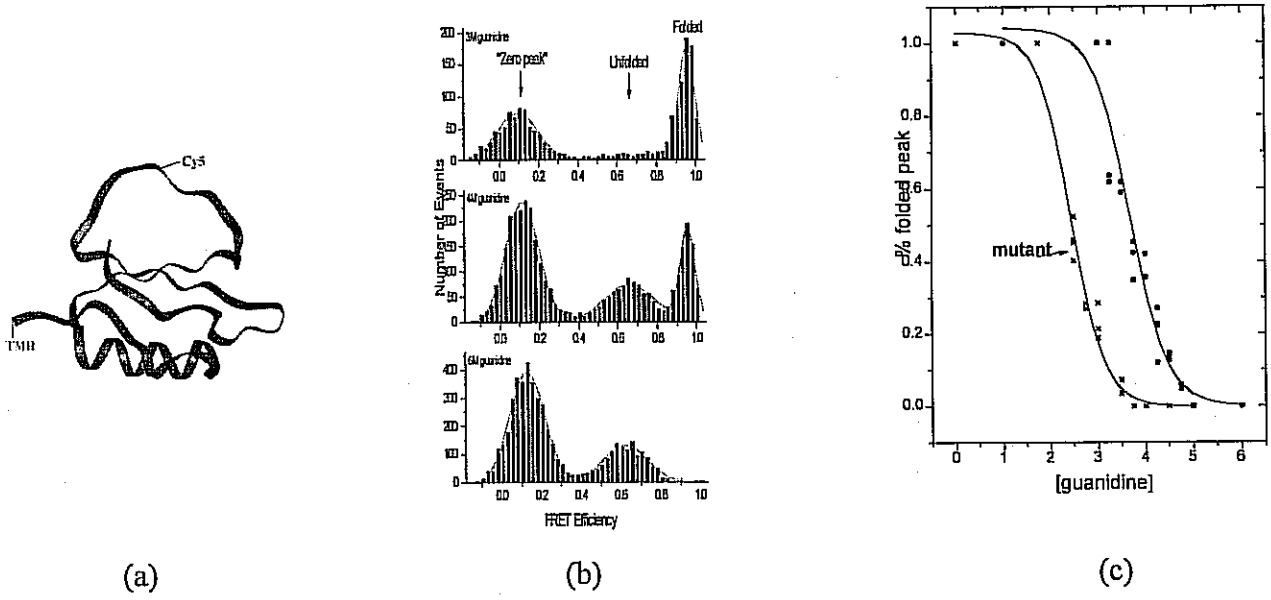

(a) (b) (c)

Figure 8. (a) Crystal structure of CI2 and points of attachment for donor and acceptor. (b) spFRET histograms for 3 guanidine concentrations. Folded and unfolded distributions are clearly seen. (c) Denaturation curves obtained from FRET distributions as in (b) for wild-type and destabilized mutant of CI2..

Publications

S. Weiss, "Single Molecule Fluorescence Spectroscopy of Reacting Biomolecules," invited paper, *Science*, **283**, 1676 – 1683 (1999).

T. Ha, A.Y. Ting, J. Liang, W.B. Caldwell, A. Deniz, D.S. Chemla, P.G. Schultz, and S. Weiss, "Single Molecule Fluorescence Spectroscopy of Enzyme Conformational Dynamics and Cleavage Mechanism," *Proc. Natl. Acad. Sci. USA*, **96**, 893 - 898 (1999).

A.A. Deniz, M. Dahan, T. Ha, J. Grunwell, A. Faulhaber, D.S. Chemla, S. Weiss, and P.G. Schultz, "Ratiometric Single Pair FRET on Freely Diffusing Molecules—Observation of Förster Distance Dependence and of Sub-populations," *Proc. Natl. Acad. Sci. USA*, **96**, 3670 – 3675 (1999).

T. Ha, A.Y. Ting, J. Liang, A.A. Deniz, D.S. Chemla, P.G. Schultz, and S. Weiss, "Temporal Fluctuations of Fluorescence Resonance Energy Transfer between Two Dyes Conjugated to a Single Protein," invited paper, *Chem. Phys.*, **247**, 107-118 (1999).

M. Dahan, A. Deniz, T. Ha, J. Grunwel, P.G. Schultz, D.S. Chemla and S. Weiss, "Ratiometric Identification and Separation of Single Molecules Diffusing in Solution," invited paper, *Chem. Phys.*, **247**, 85-106 (1999).

T. Ha, T. Laurence, A.Y. Ting, P.G. Schultz, D.S. Chemla, and S. Weiss, "Polarization Spectroscopy of Single Fluorescent Molecules," invited paper, *J. Chem. Phys. B*, **103**, 9839-6850 (1999).

Possibility of Very High Temperature Superconductivity using Cage Molecules

Principal Investigators: Alex Zettl

Project No.: 99031

Project Description

This project will explore the possibility of high temperature superconductivity in a carbon cage molecular solid C_{36}. Theoretical predictions suggest that very high T_cs are possible in this pure-carbon system. Other cage-based systems, such as those based on carbon/nitrogen, will also be synthesized.

The approach is to synthesize, and form into a solid, a small-cage molecule based on carbon (or carbon together with, for example, boron or/and nitrogen), with sufficient curvature and density, and with appropriate quantum states, to yield high-T_c superconductivity. To many organic chemists, this idea may appear outlandish, as the C_{60} cage molecule is already a highly strained molecule and is the smallest pure-carbon molecule that satisfies the "isolated pentagon rule." Pentagons introduced into the (originally flat) hexagonal structure of a graphite sheet generate finite curvature, and with 12 pentagons a closed cage structure is possible. The lowest strain energy results if the pentagons are isolated, i.e. each pentagon is surrounded only by hexagons. Going below 60 carbon atoms invariably results in the energetically unfavorable condition of some pentagons adjacent to one another. Consequently, it has generally been accepted in the carbon cluster community that carbon cage molecules smaller than C_{60} are not stable.

A method recently developed by the P.I. for the synthesis of C_{36} molecules will be scaled up to produce bulk quantities of purified C_{36} and related materials. These materials will be characterized via structural, optical, electronic, and other means, including Advanced Light Source-related spectroscopies.

Accomplishments

The properties of a new carbon molecular solid, C_{36}, have been investigated. A method has been developed which charges C_{36} molecules in the solid (via alkali doping) and reduces the binding energy between molecules. This is an important development for C_{36} evaporation and further characterization. The magnetic and transport properties of C_{36} powder have been determined via high-sensitivity Superconducting QUantum Interference Device (SQUID) and electrons in response (ESR) measurements, thin film resistivity, resistivity under hydrostatic pressure in a diamond anvil cell, and resistivity for alkali doped films. Some of the transport measurements below 50° K are anomalous and suggestive of high-temperature superconductivity. Further tests are needed before definitive conclusions can be reached.

The electronic structure of C_{36} molecules and clusters has been investigated by scanning tunneling spectroscopy; and comparisons to theoretical predictions have been made.

Publications

C. Piskoti and A. Zettl, "The First Stable Lower Fullerene: C_{36}," *AIP Conference Proceedings 442, Electronic Properties of Novel Materials: XII International Winterschool*, H. Kuzmany *et al.* eds. (The American Institute of Physics, Woodbury, New York, 1998) p. 183.

P. Collins, J.C. Grossman, M. Cote, M. Ishigami, C. Piskoti, S.G. Louie, M.L. Cohen, and A. Zettl, "Scanning Tunneling Spectroscopy of C_{36}," *Phys. Rev. Lett.* **165** (January 1999).

A. Zettl, C. Piskoti, Jeffery C. Grossman, Marvin L. Cohen, and Steven G. Louie, "Effect of Alkali Doping on the Structural Stability of Solid C_{36}," *Electronic Properties of Novel Materials– Science and Technology of Molecular Nanostructures*, H. Kuzmany, J. Fink, M. Mehring, and S. Roth, eds. (AIP Conference Proceedings **486**, American Institute of Physics, Melville, New York 1999) p. 183.

J. C. Grossman, C. Piskoti, and A. Zettl, "Molecular and Solid C_{36}," *Fullerenes and Nanotubes*, R. Ruoff, ed. (in press).

A. Zettl, "New Carbon Materials," *McGraw Hill Yearbook of Science & Technology* (McGraw Hill, 1999) (in press).

Improved Temporal Resolution in Femtosecond X-Ray Spectroscopy

Principal Investigators: Robert Schoenlein, Alexander Zholents, Max Zolotorev, and Philip Heimann

Project No.: 98023

Project Description

We propose a novel technique for generating femtosecond x-ray pulses from the Advanced Light Source (ALS). This will improve the temporal resolution available at an existing bend-magnet beamline from 30 ps to ~250 fs. The availability of ultrashort x-ray pulses from a synchrotron source will open new areas of research in physics, chemistry, and biology by allowing the motion of atoms in materials to be directly probed on the time scale of a vibrational period which is the fundamental time scale for structural dynamics, chemical reactions, phase transitions, etc. High-brightness femtosecond x-rays will allow researchers to combine powerful x-ray structural probes such as diffraction and extended x-ray absorption fine structure (EXAFS), with ultrafast pump-probe techniques. In addition to being a significant capability enhancement of the ALS, this proposal is an important first step toward the development of a fourth-generation synchrotron light source providing two-to-three orders of magnitude improvement in time resolution over existing synchrotron sources. The main components (femtosecond laser system and modifications to the ALS storage ring) are already in place, and considerable progress has been made toward the development of the source. This project seeks to complete the development and characterization of the femtosecond x-ray source. We expect that a successful demonstration of this source will serve as the basis for proposing construction of a beamline specifically for femtosecond x-ray science at the ALS.

The temporal duration of synchrotron light pulses is determined by the duration of the stored electron bunches, typically >30 ps. We propose to reduce the duration of the x-ray pulses by more than two orders of magnitude by selecting radiation which originates from a short (~100 fs) temporal slice of the electron bunch. Such a slice can be created through the interaction of a femtosecond laser pulse co-propagating with an electron bunch in an appropriate wiggler. The high electric field of the laser pulse modulates the energy of a slice of the electron bunch. The accelerated and decelerated electrons are spatially separated from the main electron bunch by a bend-magnet. Femtosecond x-rays will be generated at an existing beamline by imaging the synchrotron radiation from the displaced femtosecond electron slice. Initial measurements of the pulse duration will be made by cross-correlating visible light from the beamline with laser pulses in a nonlinear crystal.

Accomplishments

We have demonstrated, for the first time, the generation of femtosecond synchrotron pulses from a storage ring. We have developed sensitive diagnostics for monitoring the interaction between the laser and the electron beam. The strength of the interaction is evaluated by measuring the gain experienced by the laser beam passing through the wiggler, equivalent to the single-pass gain in a free-electron-laser (FEL). The agreement between the measured gain and theoretical predictions (based on known parameters of the electron beam) demonstrates that the interaction between the laser and the electron beam is nearly optimal. We have made detailed measurements of the femtosecond time structure created in the stored electron bunch by a femtosecond laser pulse, and manifest in the synchrotron radiation from an ALS bend-magnet beamline. This was accomplished by cross-correlating visible light from the beamline with ~50 fs pulses from the laser in a nonlinear crystal. Figure 9 shows two such cross-correlation measurements. The first measurement (Figure 9a) uses only the central $\pm 3\sigma_x$ region of the synchrotron beam, and reveals the femtosecond hole or dark pulse that is created due to energy modulation of the electrons by the laser pulse. Electrons with $\Delta E<0$ follow a shorter path to the bend-magnet and give rise to the transient increase in synchrotron radiation which precedes the femtosecond dark pulse. Similarly, electrons with $\Delta E>0$ contribute to the bump, which follows the dark pulse in time. Because the bend-magnet radiation is collected from a dispersive region of the storage ring (in which the horizontal beam size is primarily determined by the electron energy), synchrotron radiation from the energy-

modulated electrons appears at different horizontal positions corresponding to the electron energy. Figure 9b shows a cross-correlation measurement in which synchrotron light is collected over only the $+3\sigma_x$ to $+8\sigma_x$ region (corresponding to electrons with $\Delta E < 0$). This measurement reveals the femtosecond pulse of synchrotron radiation, which is created in the spatial wings of the main synchrotron beam by the energy-modulated electrons. The solid lines in Figure 9 are from a model calculation of the electron distribution. The pulse duration (~300 fs) is determined by the time-of-flight stretching of the electron bunch as it propagates from the wiggler to the bend-magnet beamline (1/8th of a storage ring orbit). The agreement between model calculations and experimental measurements of the time structure gives us confidence that for an optimally-placed beamline (immediately following the wiggler), synchrotron radiation pulses of 100 fs duration may be generated using this technique.

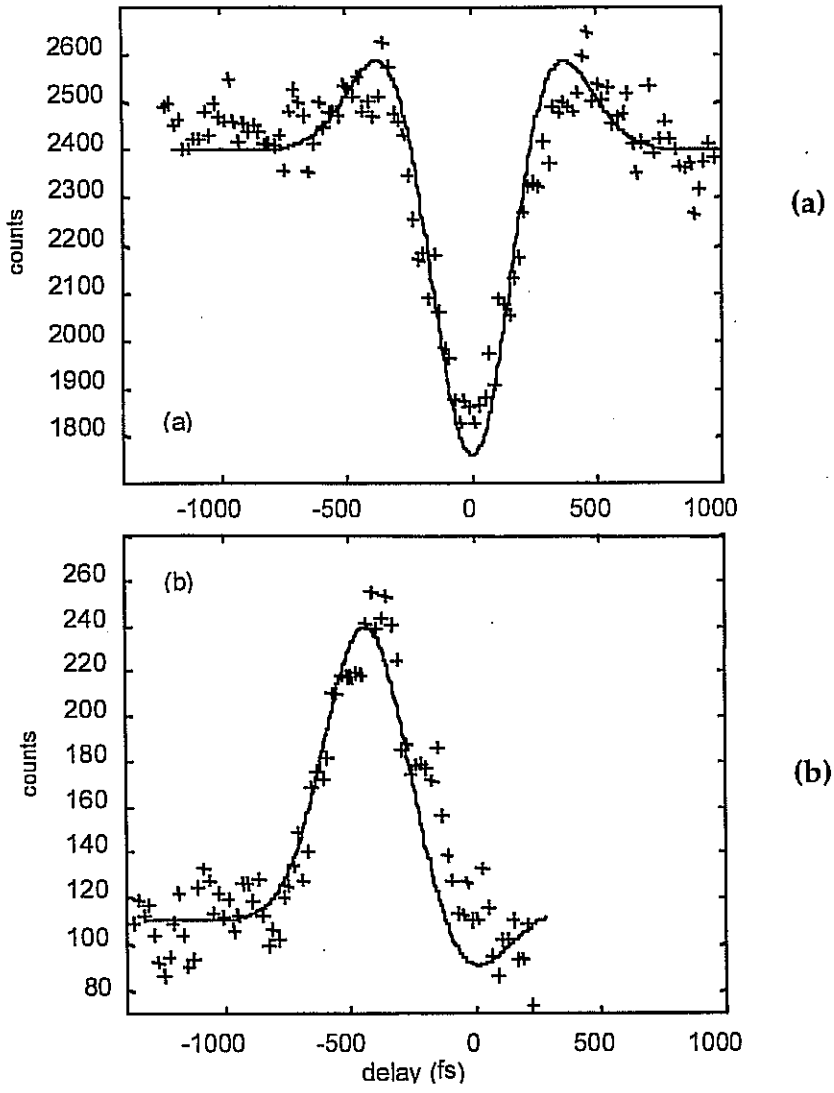

Figure 9. Cross-correlation measurements between a delayed laser pulse and synchrotron radiation originating from an energy-modulated electron bunch. In (a), synchrotron radiation from the central core ($\pm 3\sigma_x$) of the electron bunch is selected. In (b), synchrotron radiation from the horizontal wings ($+3\sigma_x$ to $+8\sigma_x$) of the electron bunch is selected. Solid lines are from a model calculation of the energy-modulated electron bunch distribution.

Publications

R.W. Schoenlein, S. Chattopadhyay, H.H.W. Chong, T.E. Glover, P.A. Heimann4, C.V. Shank, A.A. Zholents, and M.S. Zolotorev, "Femtosecond X-rays from a Synchrotron: A New Tool for Ultrafast Time-Resolved X-ray Spectroscopy," (submitted, to *Science* September 1999).

R.W. Schoenlein, S. Chattopadhyay, H.H.W. Chong, T.E. Glover, P.A. Heimann, W.P. Leemans, C.V. Shank, A.A. Zholents, and M.S. Zolotorev, "Generation of Femtosecond X-rays via Laser-Electron Beam Interaction," invited paper for *Applied Physics B* (in preparation).

R.W. Schoenlein, H.H.W. Chong, T.E. Glover, P.A. Heimann, C.V. Shank, A.A. Zholents, and M.S. Zolotorev, "Generation of 'Dark' Femtosecond Synchrotron Pulses from the Advanced Light Source," *Ultrafast Phenomena XI*, Springer-Verlag Series in Chemical Physics (December 1998).

R.W. Schoenlein, H.H.W. Chong, T.E. Glover, P.A. Heimann, C.V. Shank, A.A. Zholents, and M.S. Zolotorev, "Femtosecond Synchrotron Pulses Extracted from the Advanced Light Source," published in proceedings of OSA Annual Meeting 1999 (September 1999).

R.W. Schoenlein, H.H.W. Chong, T.E. Glover, P.A. Heimann, C.V. Shank, A.A. Zholents, and M.S. Zolotorev, "Generation of Femtosecond Synchrotron Pulses from the Advanced Light Source," published in proceedings of Conference on Lasers and Electro-Optics (May 1999).

Berkeley Experiments with Accelerated Radioactive Species at the 88-Inch Cyclotron

Principal Investigators: Joseph Cerny

Project No.: 98024

Project Description

The goal of the Berkeley Experiments with Accelerated Radioactive Species (BEARS) project is to study a radioactive ion beam (RIB) capability at Berkeley Lab's 88-Inch Cyclotron. Nuclear scientists around the world are greatly interested in the opportunities provided by RIBs. The 1996 Nuclear Science Advisory Committee (NSAC) long-range plan for nuclear physics lists the development of a national RIB facility as its highest priority after the completion of the Relativistic Heavy Ion Collider (RHIC) at Brookhaven National Laboratory. Aside from providing a new research tool at the 88-Inch Cyclotron, the work being done in the BEARS project may provide critical research and development proof-of-principle studies that will ultimately lead to such a national facility.

The BEARS project is made feasible by the presence of two existing cyclotrons at Berkeley Lab. The radioactive species to be accelerated are produced by the Biomedical Isotope Facility (BIF) cyclotron, a 10 MeV proton accelerator located approximately 300 meters uphill from the 88-Inch Cyclotron. Radioactive isotopes are produced from (p,n) and (p,α) reactions and are transported via a 300 meter capillary to the 88-Inch Cyclotron. There, the activity is separated from carrier gas, injected into an electron cyclotron resonance (ECR) ion source, and then accelerated by the 88-Inch Cyclotron. Beams of ^{11}C and ^{14}O will be made available using this technique.

All components of the BEARS system (for activity production, activity transport, gas removal, ionization, and acceleration) are based on established techniques. The challenge lies in combining these techniques with sufficient efficiency that radioactive beams of usable intensity and purity result. Additionally, safe transport of the radioactivity between the two cyclotrons is required.

Accomplishments

The past year has resulted in major achievements for BEARS. The entire system has been constructed, automated, and tested and is now fully operational, producing a radioactive ^{11}C beam of better than 1×10^8 atoms per second. This intensity exceeds the initial project goal by more than an order of magnitude. Three physics experiments have already been performed, two in collaboration with scientists external to Berkeley Lab.

Chemistry problems have delayed the successful production of a beam of ^{14}O. These are expected to be solved in the next few months, leading to additional experiments with this isotope.

BEARS has also met all its project goals as to safety in the handling of radioactivity. In particular, technological development of the transport system led to a reduction by a factor of three of the already small radiation levels present during operation.

The first experiment performed with BEARS, the measurement of the production of several different astatine isotopes by the bombardment of ^{11}C on gold, has been completed and a paper submitted to *Physical Review Letters*. The results from the radioactive beam were compared to those from a stable ^{12}C beam, providing a test of our understanding of fusion-evaporation reactions in this region.

Two experiments have begun in collaboration with outside scientists, both of which had successful data collection runs in late 1999. Fission following the bombardment of gold and platinum isotopes by ^{11}C has been measured in collaboration with Hope College, and elastic scattering of ^{11}C and protons, of nuclear-astrophysics interest, was measured using a detector system developed at Oak Ridge.

Publications

J. Powell, et al., "Berkeley Experiments with Accelerated Radioactive Species," (draft, to be submitted to *Nuclear Instruments and Methods*).

R. Joosten, et al., "Measurement of Excitation Functions in the Reactions $^{197}Au(^{11}C,xn)^{208-x}At$ using a Radioactive ^{11}C Beam," (draft, to be submitted to *Physical Review*).

Gamma Ray Studies using the 8-π Spectrometer

Principal Investigators: I-Yang Lee, Lee Schroeder, and David Ward

Project No.: 98025

Project Description

The 8-π Spectrometer, on loan from McMaster University, has been operating in Cave 4C at the 88-Inch Cyclotron since April 1998. The instrument is made up of a high-quality Bismuth-Germanate (BGO) spherical shell of 72 detectors and an array of twenty HPGe detectors with BGO Compton-suppressor shields. A number of auxiliary detectors and special equipment developed for the spectrometer have also been employed, including the computer-controlled recoil-distance apparatus. The combination of all these makes the 8-π a unique gamma-ray spectroscopy instrument for pursuing new studies of nuclear structure. This compliments the research program carried out at Gammasphere, currently sited at Argonne National Lab. In FY99, several experiments have been carried out with the 8-π array, using a total of 1463 hours of the 88-Inch Cyclotron beam time. In addition to Berkeley Lab staff, other users of the 8-π array included groups from three U.S. national laboratories, eight U.S. universities, and six foreign institutions.

Accomplishments

The following are highlights of the experiments:

Nuclear Collective Motion in the N=90 Isotones ^{152}Sm, ^{154}Gd, and ^{156}Dy

The N=90 isotones ^{152}Sm, ^{154}Gd, and ^{156}Dy fall at the onset of stable nuclear deformation and show remarkably similar structure in their low-lying excited states, which can be described either in terms of a deformed rotor or in terms of a mixed rotation-vibration configuration. Knowledge of the properties of the low-lying 0+ states is especially critical in achieving a coherent interpretation of the structure and to distinguish between competing interpretations. We have studied the excited states of ^{152}Sm, ^{154}Gd, and ^{156}Dy following the radioactive decays of ^{152}Eu, ^{154}Eu, ^{154}Tb and ^{156}Ho using the 8-π spectrometer. Spectroscopic information has been obtained based on gamma-ray singles and coincidence data along with gamma-gamma angular correlations. Results on ^{154}Gd indicate the 0+ excited band has the same moment of inertia as the ground state. A previous study based on lower statistical data has wrongly assigned a larger value for the moment of inertia.

Coulomb Excitation Studies of ^{235}U

We have studied the gamma rays of ^{235}U with the 8-π spectrometer following Coulomb excitation with ^{40}Ar and ^{136}Xe beams delivered by the Berkley Lab 88-Inch Cyclotron at energies of 182 MeV and 720 MeV, respectively. In addition to the rotational band built on the [743] 7/2 ground-state (seen to spin 5 1/2- in this experiment), we observe bands known from decay studies and previously assigned to the [631] 1/2 (up to spin 45/2+), and [622] 5/3 (up to 49/2+) configurations. Analysis of the intensity of these bands suggests enhanced octupole matrix elements to the ground-state band. We are currently examining whether such enhancements (about 12 Wu in the case of the [631] 1/2 band) can be understood within a deformed shell-model approach.

Fission Barriers, Coupled-Channel and Shell Effects, at the Coulomb Barrier in the A ~190 Mass Region

A study of the role of coupled-channel effects in the enhancement of the population of high-spin states was undertaken with the reactions $^{48}Ca+^{142}Nd$ and $^{80}Se+^{110}Pd$, near the Coulomb barrier, leading to the same compound nucleus, ^{190}Hg, at the same excitation energy. Statistical calculations with standard values for the level density parameters and fission barriers, predict an enhancement of the high-spin population for the more mass-symmetric system, brought about by the coupling to inelastic channels in the fusion process. No enhancement was observed, which we interpret as an inadequacy of the fission barriers used, and to the role of the shell corrections, in particular those at the saddle point.

Publications

C.M. Petrache, D. Bazzacco, T. Kroell, S. Lunardi, R. Menegazzo, C. Rossi Alvarez, G. Lo Bianco, G. Falconi, P. Spolaore, A.O. Macchiavelli, D. Ward,

R.M. Clark, M. Cromaz, P. Fallon, G.J. Lane, A. Galindo Uribarri, R.M. Lieder, W. Gast, I. Ragnarsson, and A.V. Afanasjev "Stable Triaxiality at the Highest Spins in ^{138}Nd and ^{139}Nd," (accepted for publication in *Physical Review C*).

B. Djerroud, B. Schaly, S. Flibotte, G.C. Ball, S. Courtin, M. Cromaz, D.S. Haslip, T. Lampman, A.O. Macchiavelli, J.M. Nieminen, C.E. Svensson, J.C. Waddington, D. Ward, and J.N. Wilson "Fission Barriers, Coupled-Channel and Shell Effects, at the Coulomb Barrier in the A ~190 Mass Region," (accepted for publication in *Physical Review C*).

I.Y. Lee, R.M.Clark, M. Cromaz, M.A. Deleplanque, R.M. Diamond, P. Fallon, G.J. Lan, A.O. Macchiavelli, F.S. Stephens, K. Vetter, and D. Ward "In Beam Gamma-ray Spectroscopy Using Target Fragmentation Reactions," APS Centennial Meeting, Atlanta (March 20-26, 1999).

N. Fotiades, J.A. Cizewski, K.Y. Ding, M. Cromaz, P. Fallon, I.Y. Lee, A.O. Macchiavelli, D. Ward, R.V.F. Janssens, J.A. Becker, L.A. Bernstein, K. Hauschild, D.P. McNabb, and A.G. Forgen "Entry Regions and Feeding Mechanisms of the Normal and M1 Bands in ^{196}Pb," APS Centennial Meeting, Atlanta (March 20-26, 1999).

I. Shestakova, P. Chowdhury, R. D'Alarcao, K. Krycka, E.H. Seabury R.M. Clark, M. Cromaz, P. Fallon, I.Y. Lee, A.O. Macchiavelli, C.E. Svensson, and D. Ward "Exploring the Dependence on Projectile Characteristics in Populating K-Isomers via Inelastic Excitation," 1999 Fall Meeting of the Division of Nuclear Physics of APS, Asilomar (October 20-23, 1999).

J.P. Zhang, W.C. Ma, R.B. Piercey, J.A. Winger, W. Liu, R.K. Vadapalli, P.G. Varmette, J.K. Hwang, C.J. Beyer, J.H. Hamilton, A.V. Ramayya, M.P. Carpenter, R.V.F. Janssens, and D. Ward "In-Beam Spectroscopy Study of Doubly-odd Nucleus ^{182}Au," 1999 Fall Meeting of the Division of Nuclear Physics of APS, Asilomar (October 20-23, 1999).

D. Ward, R.M. Clark, M. Cromaz, R.M. Diamond, M-A Deleplanque, P. Fallon, I.Y. Lee, A.O. Macchiavelli, F.S. Stephens, and K. Vetter, "Coulomb Excitation Studies of ^{235}U," 1999 Fall Meeting of the Division of Nuclear Physics of APS, Asilomar (October 20-23, 1999).

W.D. Kulp, B. MacDonald, J.L. Wood, M.R. Dragowsky, K.S. Krane, J. Loats, P. Schmelzenbach, C.J. Stapels, R.M. Larimer, E.B. Norman, and A. Piechaczek, "Nuclear Collective Motion in the N=90 Isotones ^{152}sm, ^{154}Gd, and ^{156}Dy," 1999 Fall Meeting of the Division of Nuclear Physics of APS, Asilomar (October 20-23, 1999).

Vacuum, RF, and Injection Systems for High-Intensity Stable Beams

Principal Investigators: Claude Lyneis and I-Yang Lee

Project No.: 99032

Project Description

The goal of this project was to identify and make an engineering evaluation of potential improvements and added capabilities to make the 88-Inch Cyclotron the Department of Energy (DOE)'s premier stable beam facility. A DOE decision to move forward with an advanced isotope separator on line (ISOL) facility follows the completion of the ISOL white papers, which identified several key research areas in nuclear physics. These include nuclear astrophysics, nuclear structure, exotic nuclei, and heavy elements, which will require both stable and radioactive beams. For that reason, we envision a need for a premier stable beam facility to complement the planned ISOL facility.

There are two major aspects to this proposal. First, is to study the re-engineering of the Cyclotron to modernize it and provide new capabilities and scientific opportunities. The second major aspect is to evaluate concepts for high-efficiency production and use of exotic stable beams from rare isotopes.

An engineering analysis of possible improvements to modernize the cyclotron will be done. Those improvements to be evaluated are listed below.

- Reconstruction of the vacuum system, including the vacuum enclosure, to produce very high vacuum for the transmission of very heavy ions made by the Advanced Electron-Cyclotron Resonance ion source (AECR-U) now, and in the future by the Third Generation electron-cyclotron resonance (ECR), which is under construction. Measurements of the transmission of high-charge-state ions coupled with an analysis of the cyclotron vacuum and losses due to charge pickup and charge

stripping indicate that significantly higher transmission could be achieved by improving the cyclotron vacuum to $1x10^{-7}$ Torr.

- Redesign of the center region geometry and improvement of the radio frequency (rf) system to provide single turn extraction and improved beam timing. Analysis and particle tracking need to be done to explore the possibility of achieving precise single turn extraction.
- Upgrade of the axial injection system to increase the transmission of high-intensity heavy-ion beams. Beam optics calculations including space charge can now be done to evaluate methods for compensating the space charge effects observed with high intensity beams.

The anticipated needs for exotic stable beams to complement the ISOL facility and the recent decision to end the production of stable isotopes at Oak Ridge National Laboratory make it essential to develop new, highly-efficient methods for separating and using rare isotopes. There are almost 300 stable isotopes and many of these have not been available due to their low abundance in nature.

Two approaches for the production of a wide range of exotic stable beams will be evaluated. First, by building a specialized hot liner, it may be possible to improve the efficiency of ionizing rare isotopes in the ECR ion sources by as much as 25 times. Second, a specialized on line separator, which directly injects 1+ ions of separated isotopes into the high charge ion source, could provide the capability to run rare stable isotopes.

Accomplishments

The LDRD effort during FY99 focused on the injection line and on efficient production of isotopically rare beams. Beam transport calculations using computer codes which include space charge effects have been done to analyze the existing system, and high-intensity beam tests were used to verify and fine tune the calculations. An emittance scanner was designed, constructed and installed to precisely measure the emittance of the AECR-U beam after it is sent through an analysis magnet. These measurements provide realistic input values for the beam transport codes. Initial results on the emittance showed that the ion source and the analysis magnet produce a good emittance beam, which indicates that the transport losses are due to emittance growth, which occurs in the horizontal and axial lines. One solution to the emittance growth may be to increase the injection voltage. This would require redesign of the inflector and center region. A preliminary analysis on use of a spiral inflector in place of the existing mirror inflector was done. This indicated that it would be possible after some modification of the cyclotron to use a spiral inflector and operate at injection voltages up to 30 kV.

Efficiency tests for calcium production in the AECR-U have been carried out. A new axial oven was constructed, installed, and tested. The detailed measurements will be carried out in FY00. An extensive set of measurements were made on the efficiency of the AECR-U with gases. These showed that the higher charge states are produced with greater efficiency, and that efficiencies up to 25% can be attained for the ionization of C^{4+} from CO_2.

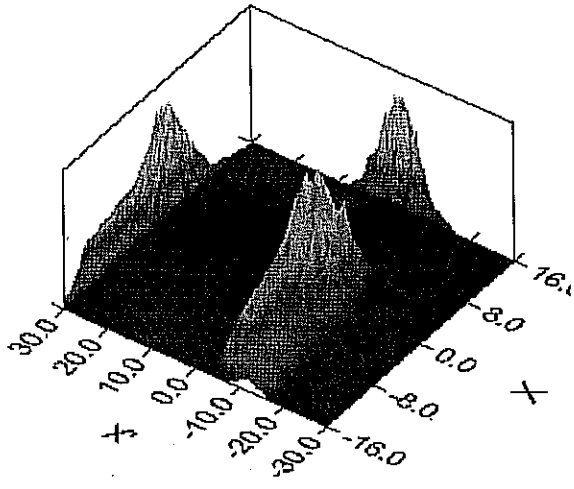

Figure 1. Plot of the emittance of a 520 μA $O6^+$ beam from the AECR-U ion source produced with the new emittance scanner.

Publications

D. Wutte, C.M. Lyneis, M.A. Leitner, and Z.Q. Xie, "Radioactive Ion Beam Development in Berkeley," published in proceedings of 14th Intl. Workshop on ECR Sources, CERN (May 1999).

M.A. Leitner, S.A. Lundgren, C.M. Lyneis, C.E. Taylor, and D.C. Wutte, "Progress Report of the 3rd Generation ECR Ion Source Fabrication," published in proceedings of 14th Intl. Workshop on ECR Sources, CERN (May 1999).

Z.Q. Xie, D. Wutte and C.M. Lyneis "Ionization Efficiencies for Highly Charged Stable and Radioactive Ions in the AECR-U Ion Source," submitted to *Nuclear Instruments and Methods* (July 99, in press).

First Chemical Study of Element 108, Hassium

Principal Investigators: Heino Nitsche and Uwe Kirbach

Project No.: 99033

Project Description

The purpose of this project is to develop the pre-requisites for and carry out a first-time study of the chemical properties of element 108, hassium, Hs. The major goals of the program are:

- Development, construction, and testing of the recoil product transfer chamber (RTC) interfaced to the Berkeley Gas-filled Separator (BGS) and a chemical reaction unit where the Hs undergoes chemical conversion.
- Development, construction, and testing of a cryo-thermochromatographic separator (CTS). The CTS separates the Hs reaction products from other actinide reaction products that are concurrently present in the BGS-interfaced recoil transfer chamber.
- Study for the first time the chemical properties of Hs and determine if it behaves in a similar manner as its chemical homologues ruthenium, Ru, and osmium, Os.

The chemical identification will be achieved by combining a novel chemical separation system with the advantages of the BGS. The BGS provides good and fast separation of transfer products stemming from impurities of the nuclear target and from long-lived spontaneous fission products. The novel chemical separator is based on the expected high volatility of the tetraoxides of Hs and consists of a chemical reaction chamber and the CTS. The development of the RTC and the interface to the BGS is an important part of this project and opens the possibility to directly couple the BGS with the chemical separation system, which will facilitate further separation from the actinides and detection by nuclear counting. In the chemical reaction chamber, the nuclear reaction products coming from the RTC via a gas jet are subjected to an oxygen/helium gas mixture at a reaction temperature of 900 °C to form volatile hassium oxides. The volatile oxides are then transported via the gas stream through a quartz capillary to the CTS, leaving behind non- and less-volatile compounds. The CTS consists of an assembly of two rows of 32 silicon PIN-diodes arranged opposite each other, forming a narrow rectangular channel through which the reaction gas flows. A decreasing thermal gradient ranging from room temperature to about –120 °C is applied to the PIN-diode assembly. This results in the deposition of the hassium oxide on one of the detectors, where it can be identified by alpha counting. We expect a separation factor of 10^7 to 10^9 for actinides from the combined BGS-CTS system.

For the production of hassium, which has an estimated half-life of about 9.3 s, we will use the reaction ^{26}Mg (^{248}Cm, 5n) ^{269}Hs. As model experiments, the chemical volatility and the chromatographic properties of the oxides of the lighter Hs-homologue Os (and possibly ruthenium, Ru) will be studied in off-line experiments using long-lived isotopes.

Accomplishments

The RTC was designed and constructed. It can be mounted on the existing BGS detector chamber to allow a fast transfer of pre-separated recoil nuclei from the BGS to the chemistry system. The RTC is interfaced to the BGS by a wire-grid-supported thin mylar foil with up to 200 $\mu g/cm^2$ thickness, thus enabling a pressure difference of 380 Torr between the BGS and the RTC. Thin windows are necessary to accommodate penetration of the recoil nuclei with relatively low kinetic energy. The energy of the

expected hassium recoil nucleus is about 13 MeV for the production reaction ^{26}Mg (^{248}Cm, 5n) ^{269}Hs. A sliding piston inside the RTC facilitates the change of the chamber's depth to accommodate different recoil stopping ranges for different recoil energies. This makes the RTC applicable for a wide range of nuclear reactions.

The RTC was tested in two initial experiments to determine the transfer efficiency. In the first experiment, the reaction ^{40}Ar (^{164}Dy, xn) $^{204-n}$Po was used to measure the efficiency at the high kinetic energy of the recoil nuclei of 43 MeV. The window material was an 800 μg/cm^2 aluminized mylar foil. The pressure inside the RTC and BGS was 760 and 1 Torr, respectively. The activity was transported through a polyethylene capillary 21 meters long via a KCl gas jet system to our rotating wheel alpha detection system. The total efficiency of the transport was about 25% compared to the activity measured in the BGS. In a second experiment, the reaction ^{22}Ne (^{197}Au, xn) $^{219-n}$Ac was used to measure the efficiency for 11 MeV recoil nuclei. The total transport efficiency was about 5% using a 340 μg/cm^2 mylar window and 760 Torr pressure inside the RTC. We calculated a stopping range of 370 μg/cm^2 in mylar for recoils, indicating that the actinium nuclei were stopped by the mylar foil used. We then used thinner mylar foils, which required reducing the pressure inside the RTC. First tests indicated a substantially decreased efficiency of the activity transport by the gas jet.

For the construction of the CTS, we tested the suitability of commercially produced silicon diodes as α-detectors for the strip detector. The detectors must be able to withstand temperatures from +20 to -120 °C, should have no protective window or coating on the silicon dioxide surface, and should be stackable in line very close to each other. We found one detector that worked well within the tested temperature range, and had an acceptable energy resolution of about 40 keV. Unfortunately, the geometric shape of the detector is not suitable for assembling the detector strip to the desired specifications. We are currently identifying other manufacturers of silicon diodes, and the possibility to have the detectors manufactured in-house.

To familiarize ourselves with the BGS, which will be used for producing the hassium for our chemical identification experiment, we participated in two series of experiments leading to the discovery of two new elements, elements 118 and 116. During the discovery of the new elements, a new hassium isotope was observed in the decay chain of element 118. Unfortunately, due to its short half-live of 1.2 (+1.7, -0.6) s, this isotope, ^{273}Hs, cannot be used for our first chemical identification study of hassium.

Publications

V. Ninov, K.E. Gregorich, W. Loveland, A. Ghiorso, D.C. Hoffman, D.M. Lee, H. Nitsche, W.J. Swiatecki, U.W. Kirbach, C.A. Laue, J.L. Adams, J.B. Patin, D.A. Shaughnessy, D.A. Strellis, and P.A. Wilk "Observation of Superheavy Nuclei Produced in the Reaction of ^{86}Kr with ^{208}Pb," *Phys. Rev. Lett.* **83**, 1104 (1999).

Stochastic Logic in Biochemical and Genetic Reaction Networks: Theory and Experiment with Application to Bacterial Pathogenesis

Principal Investigators: Adam Arkin

Project No.: 98026

Project Description

An organism's genome is commonly considered to be the program, executed by biochemistry, that defines the organism's behavior and development. It would be inaccurate, however, to attribute a computer-like "logic" to the decisions made by this program. In fact, the chemical reactions set off by this "computer" are highly nonlinear and do not obey the laws of Boolean logic. Qualitative analysis of their behavior as a network is made even more difficult because these reactions involve concentrations of molecules of less than 100 molecules per cell and share substrates, products, and effectors. This difficulty is exacerbated by the small numbers of molecules involved in these reactions. From physical first principles, thermal fluctuations in reaction rates are expected to become significant in comparison to average behavior at such low concentrations. Because reactions involving genetic control generally involve only one or two copies of the relevant promoters and genes per cell, these "noise" fluctuations are likely to be greater for these reactions.

In prior work, we have examined some detailed mechanisms of gene expression in prokaryotic systems and confirmed, theoretically, that the temporal pattern of protein production from a single gene in a growing cell is highly erratic for a wide range of experimentally observed kinetic parameters. If our theoretical analysis is correct, the immediate questions raised by this observation are: "How is the genetic program executed correctly if its elementary components are so noisy?" and "Are any organism's genetic programs set up to exploit this noise and achieve diversity in its behavior or the population as a whole?"

The developmental program encoded by the host's genome is designed, in large part, to throw the right set of genetic switches at the right times and places in order to produce particular cell types in an organism. To understand the common regulatory architectures that are used to construct these developmental switches, we have focused on the study of two genetic "switches": the bacteriophage lambda lysis/lysogeny decision and random phase variation of type-1 pili expression in *Escherichia coli*. The architecture of these two switches, one implemented by two antagonistic feedback loops and the other implemented by a DNA inversion reaction, is typical of a large class of developmental switches commonly found in pathogenic microorganisms (as well as in general developmental pathways). Our theories predict that the significant noise expected in the elementary genetic reactions will lead to a statistical divergence in cell fate even with identical initial conditions. We wish to experimentally confirm this prediction and explore the role of genetic noise in promoting the virulence of these particular organisms.

Our first goal is to build computational toolkits to (1) database the large amount of heterogeneous biological data necessary for building and validating the biological models needed to understand these systems; (2) create biologist-friendly model-building interfaces to this database; (3) design and build the tools for network analysis (e.g., stoichiometric network analysis, sensitivity analysis) and simulation (e.g., for hybrid stochastic, ordinary differential, algebraic, and spatially-dispersed systems); and (4) design and build visualization and reporting tools for digesting the complex time and space resolved output from the simulation programs. Our second goal is to apply these tools to the engineering analysis of the genetic switches described above.

Accomplishments

The expression of type-1 pili in *Escherichia coli*, adhesin-tipped molecules mediating attachment to the mannose-containing receptors found in many host tissue surfaces, is phase variable, meaning that individual cells in a population randomly alternate between a piliated state, in which pili are built densely on the outside of the cell, and a non-piliated state. This process of phase variation in *E. coli* presents a model of a random genetic switching

decision that increases the pathogenic potential of a population of infectious bacteria. The phase variation of type-1 fimbriae is controlled by the orientation of an invertible element known as the "*fim* switch," a 314 base pair length of DNA containing a promoter for the genes encoding the *fim* structural subunits. In one orientation (ON), this promoter directs transcription of the *fim* structural subunit genes (*fimA-fimH*), while in the other (OFF) orientation, the promoter is no longer adjacent to the structural subunit genes and transcription does not occur. Inversion of the *fim* switch is accomplished independently by two recombinases, the proteins FimE and FimB, and is affected by a number of global regulators including integration host factor (IHF), leucine-responsive regulatory protein (Lrp), and H-NS. Environmental conditions of media and temperature influence switching behavior as well.

In this project we developed single-cell and population level mathematical models of the gene network controlling phase variation in *E. coli*. These models, capable of reproducing observed type-1 pili phase variation behavior in *E. Coli* as a function of regulating protein concentrations and environmental factors, were then used to generate and test hypotheses on the mechanisms responsible for phase variation behavior. In particular, we applied nonlinear analysis and computer simulation techniques to our *fim* model to generate hypotheses on (1) the roles of [FimB], [FimE], their DNA binding affinities ΔG_i and switching efficiencies α_i in the observed switching behavior of a 'minimal' *fim* switch; (2) the source of the observed ON-to-OFF specificity of FimE; (3) the observed high ON-to-OFF switching speed; (4) why there are two recombinases when one would seem to suffice; (5) the role of the *fimE* orientational control, a phenomenon in switch dynamics, whereby *fimE* is significantly expressed if the *fim* switch is in the ON position, and nearly undetectable if the switch is in the OFF position, and (6) how temperature control of piliation is achieved.

Our analysis reveals intriguing differences between the mechanisms responsible for controlling P_{on}*, the percentage of piliated *E. Coli* in a population that has reached equilibrium, and τ the response speed of the system (the amount of time it takes to reach this equilibrium). The control mechanisms for P_{on}* and τ are coupled by their dependence on the ratio γ=[FimE]/[FimB]. Just as switching from a weakly ON population to a strongly OFF population and vice versa is accomplished via changes in the recombinase ratio γ=[FimE]/[FimB] from one regime, across γ=1, to another, as determined by switching efficiencies, a corresponding switch in the speed of response is achieved by the same control input γ. However, these mechanisms are decoupled by the differing nature of their dependencies on [FimB] and [FimE], associated switching efficiencies α_i and binding ΔG_i. While equilibrium P_{on}* depends only on relative concentrations and parameter values (ratios and differences), response speed τ depends on absolute concentrations and parameter values. One consequence of this surprising decoupling of response time and equilibrium %ON control mechanisms, is that response time can be varied without changing the equilibrium %ON. Any change in environment or growth phase affecting the expression levels of both genes equally will have no effect on the equilibrium value of P_{on} but will affect the amount of time it takes to reach this equilibrium.

On the question (4) above, a single recombinase model does not show the above described decoupling. It could be that whatever evolutionary advantage is conferred by a decoupling of response speed and equilibrium %ON mechanisms, played a role in shaping the two-recombinase *fim* gene network design.

Another feature of the *fim* network, intriguing from an evolutionary perspective, is that of the observed ON-to-OFF switching specificity of FimE, as opposed to the relatively unbiased switching of FimB. The results of our analysis indicate that there has been a concept missing from the discussion in the literature: that of switching efficiency. We show that it is differences in the switching efficiencies of FimB and FimE that are primarily responsible for the observed FimE specificity rather than, as previously hypothesized, differences in DNA binding affinity between FimE and FimB or the recently discovered orientational control of *fimE*. Not only does the orientational control of *fimE* not appear to contribute to FimE ON-to-OFF specificity, it actively works against it. Our analysis shows that the orientational control of *fimE* allows pili turn-ON to go higher and happen faster than it would without the presence of orientational control.

Finally, we examine the observed "temperature tuning" of pili expression to mammalian body temperature. Temperature tuning of bacterial gene expression is believed to be an important component of bacterial pathogenicity. An example of this temperature-tuning can be found in an *E. Coli* $fimB^+fimE^-$ mutant known to have a local maximum switching rate near 37° C. Our model provides a plausible hypothesis for a Lrp-mediated mechanism

responsible for the observed temperature tuning. This mechanism seems to be an example of a larger class of novel mechanisms responsible for phenotype "tuning" of bacteria to the environment.

Publications

D. Wolf and A.P. Arkin, "Mathematical Modeling, Analysis, and Simulation of *E. Coli* Piliation Switch Dynamics," (draft, in preparation).

X-Ray Microscopy of Multicomponent Biomolecular Machines

Principal Investigators: James Bartholomew

Project No.: 99034

Project Description

Most of the information we have on how biomolecular structures carry out their functions comes from indirect observations. We probe these structures using biochemical techniques, or alter them via mutagenesis, and look to see what changes occur in their functions. We have the tools for the direct observation of macromolecular structures, but these tools generally require the objects of interest to be in an environment that is not physiological. X-ray microscopy has the advantage of looking at molecular components in an environment in which they can function. If the technique can be shown to work at the resolution near that of the electron microscope, we could see how these biomolecular machines work and be able to determine what goes wrong in various situations.

For this project, two approaches were outlined to enhance and identify the components in the DNA replication complex of the virus SV40. Although the proposal originally focused on DNA replication, the general approach could be applied to other biological complexes like DNA repair and transcription. All of these functions take place in complexes that are difficult to observe with current technologies.

Accomplishments

To test the resolution of the x-ray microscope at the Advanced Light Source (ALS) we began by looking at SV40 virus particles isolated from CV-1 monkey cells growing in culture. The SV40 virus particle is a highly condensed particle of DNA and proteins with an icosahedral structure and a diameter of approximately 45 nanometers. These parameters have been worked out in detail using electron microscopy. The size of SV40 is at the predicted limit of detection of the x-ray microscope and is also the size that we calculated for the replication complex at the origin of SV40 DNA replication.

Our original attempts were to look directly at lysates from the CV-1 monkey kidney cells harvested from cell culture. The monkey cells were infected with SV40 at a multiplicity of three. After the cells lysed, the cell debris was removed by centrifugation and the lysate was used without further manipulation as a sample for the x-ray microscope. Under these conditions, the titre of virus was approximately 10^7 infectious particles per milliliter (ml). Three µl of sample were placed in the sample holder and viewed. Although a lot of particles were seen in these samples, none of the particles had the shape characteristic of SV40 particles. We concluded that we were seeing mainly fragments of cells still in the samples from the lysate. Another difficulty we realized at this point was that the volume of the sample being observed was very small. We were looking through a column of liquid approximately 50 microns in diameter and 0.5 microns thick. This volume is about 1000 cubic microns. Since each cubic micron is 10^{-12} ml, each field of view represents 10^{-9} ml. Our titre of virus was 10^7 infectious units per ml, meaning we would have a virus particle about once in every 100 fields of view. These calculations suggest we need to concentrate our preparations at least 100 fold before we can expect to see a virus particle. One caveat on this calculation is that the virus assays were measuring viable virus particles, and generally there are many more defective virus particles than there are viable viruses in a preparation. Although this ratio is unknown in these preparations, we could expect to see particles representing SV40 with a fold concentration of less than 100.

To concentrate and clean up the virus preparations, we ran the lysate through a sucrose density gradient onto a cushion of 30% sucrose. Under these conditions, the cell membranes and debris should separate from the virus particles. The virus particles could be seen as a layer on the top of the sucrose cushion. The layer containing the virus was isolated, and the virus particles were washed several times with phosphor buffered saline (PBS) in a centricon tube to remove sucrose. The resulting preparation was titred using CV-1 cells and shown to have a titre

of 10^9 infectious units per ml. This sample was used for observation in the x-ray microscope. Using this sample we were able to observe particles that resembled the images of SV40 in the electron microscope, although the resolution was not nearly good enough to identify the particles.

Within the timeframe of this LDRD, we clearly began to outline the problems that need to be solved in order to make x-ray microscopy of biomolecular machines feasible. The SV40 virus particle is a good test system to work out these problems, since it is of about the right size to serve as a model for more complicated projects. It is relatively easy to grow and concentrate. It is clear from our work that sample preparation is a major area of concern. The objects being investigated need to be at a concentration of at least 10^9 per ml and preferably higher. If the material being investigated is less concentrated, it will be very difficult to find the particles. Secondly, the particles need to be free of other debris. Other debris makes both finding and identifying the objects of study difficult. The techniques outlined in the original proposal would help greatly in the identification process, but the concentration problem can only be addressed through good biochemical procedures designed for the complex of interest.

The instrumentation issues are also important in this study. Can the resolution of the x-ray microscope be improved? Clearly the x-ray microscope at the ALS is at the forefront of this technology, but decisions have to be made as to whether it is worth the effort to try to improve the resolution of the instrument to address the type of research problems discussed in this study.

The work carried out in this project was made possible because of both the technical expertise and the enthusiasm of the late Werner Myer-Ilse. Werner was very interested in using his x-ray microscope to solve important biological problems. He generously shared his thoughts and time to try to make each of these projects a success. He will be greatly missed!

GEOCORE: The Development of a Protein Folding Algorithm

Principal Investigators: Kenneth Dill

Project No.: 98042

Project Description

This project addresses the "protein folding problem" by developing GEOCORE, a new computer algorithm intended to predict the folded structures of proteins from their amino-acid sequences. During the past 30 years, dozens of computer algorithms have been designed that attempt to fold proteins. None has yet succeeded.

GEOCORE is a new approach to computational protein folding methods. It is based on a very extensive conformational sampling method, a branch-and-bound method, which explores essentially all the conformations that might include the global minimum in free energy. GEOCORE uses an energy function involving united atoms, steric repulsion, hydrophobic and hydrogen bonding interactions. Our aim in this project is to (1) refine the energy, (2) develop a "smart" search strategy to construct tertiary structures from secondary structures, and (3) test it on peptides and proteins.

Accomplishments

We have taken several steps forward:

Assembly of Tertiary Structures from Helices and Strands: GEOCORE 2

We have now extended GEOCORE (called G2), to better treat tertiary structures. G1 was a chain growth assembly process in which one monomer at a time was added to a chain, in various conformations.

This works well for proteins less than about 30 amino acids long, but does not assemble more complex structures well. In G2, we now add either a single monomer at each growth step, or a helix or strand. Secondary structures are used in canonical conformations and the search step involves attempted assembly of each secondary element into a canonical tertiary structure, with side chain readjustments. Tests show that this method can assemble structures at the 3-6 angstroms resolution level, including β-proteins. It takes about a week per processor to fold a 100-mer, but we have been streamlining the code and hope to speed this up.

ENPOP (Energy Parameter Optimization)

We have developed a systematic way to optimize the parameters in models, such as those in computational biology, that involve single optimal structures that minimize an energy function.

We find the global optimum structures with an initial parameter vector. Using the implicit function theorem, we then find a next set of parameters that reduce the prediction errors while forcing the energy to remain at a minimum. In two test problems, the ENPOP method has been shown to give optimal parameters.

We are now generalizing the method for GEOCORE and other more realistic potentials.

GEOCORE/CGU

We are developing a new underestimator-based search strategy to find low energy states of the GEOCORE model faster than before. It is based on a Convex Global Underestimator (CGU) method that we have recently found to be a more efficient search strategy than Monte Carlo or Simulated Annealing.

Publications

K. Yue and K.A. Dill, "Constraint-Based Assembly of Tertiary Protein Structures from Secondary Structure Elements," (in preparation).

J.B. Rosen, A.T. Phillips, S.Y. Oh, and K.A. Dill, "A Method for Parameter Optimization in Computational Biology," submitted to *Biophysical Journal.*

K.W. Foreman, A.T. Phillips, J.B. Rosen, and K.A. Dill, "Comparing Search Strategies for Finding Global Optima on Energy Landscapes," *Journal of Computational Chemistry* **20**, 1527-1532 (1999).

Structural Biology of Large Biomolecular Complexes

Principal Investigators: Thomas Earnest

Project No.: 99035

Project Description

This project seeks to understand how biomolecular assemblies are formed, and how complexes of proteins and nucleic acids activate and modulate biological function. This includes the transient recognition and assembly of these molecules to define their role in signal transduction, and the investigation of large permanent assemblies. This research depends on tools and methods from a number of disciplines—molecular biology, biochemistry, and cell biology—along with access to a bright, tunable synchrotron crystallography beamline. There are two main components that serve as the basis of this project.

Wnt Receptor Pathway Proteins and Protein Complexes

The *Wnt* gene products are a family of secreted glycoproteins, which bind to transmembrane receptors and transduce developmental signals. In the past few years, there has been extensive research into the role of the *Wnt* gene products in cellular proliferation and the establishment of cell fate in both invertebrates and vertebrates. There has been a concurrent identification of the role of several members of the *Wnt* signal transduction pathway in cellular development, and in certain cancers. The misregulation of members of cellular development pathways is commonly seen in several types of cancer.

Since a number of these proteins are involved in more than a single pathway, it is critical to study the interactions of the molecules, which lead to differential activation. The atomic-resolution structure of the biologically-relevant complexes will illuminate how the interactions of these proteins mediate the function of these pathways. Since these are typically weak, transient interactions among large molecules, structural studies of these proteins typically will require high-brightness synchrotron-radiation sources. The requirement of multiwavelength anomalous diffraction (MAD) for phase information requires the tunability that only bright synchrotron sources offer.

Members of the *Wnt* family bind to the membrane-bound receptor, *frizzled*, which appears to consist of seven transmembrane helices. The proposed extracellular region of *frizzled* contains a conserved cysteine-rich domain. An extracellular protein, *frzB*, contains a homologous cysteine-rich domain and acts as an endogenous antagonist of *Wnt* signalling. It is believed that *frzB* binds to *Wnt*, preventing binding of *Wnt* to *frizzled*. The binding of *Wnt* to *frizzled* activates *dishevelled*, which then negatively regulates glycogen synthase kinase (GSK-3). GSK-3, *dishevelled*, axin, beta-catenin, and adenomatous polyposis coli (APC) protein form an intracellular complex of more than 600,000 daltons which regulates beta-catenin levels. This regulation of beta-catenin, which later forms an

intranuclear complex with LEF/TCF proteins and other transcriptional co-activators to regulate transcriptional activity, is a key step in the development of the organism. The misregulation of beta-catenin has been definitively linked to various forms of cancer.

The 70S Ribosome and Functional Complexes

The ribosome is the machinery that translates information from the genome into the production of proteins. The 70S ribosome is a massively large complex of 3 RNA and 52 protein molecules with a total molecular weight of over 2.5 million daltons, and consists of two subunits, 30S and 50S. The 50S subunit contains the peptidyl transferase activity responsible for amino acid ligation, while the interaction between the messenger RNA template and the aminoacylated transfer RNAs is mediated by the 30S subunit. The determination of the atomic structure of the 70S ribosome will serve as a basis of understanding ribosomal function, as well as a broader understanding about how these complexes are assembled and stabilized. Thus the significance of elucidating the structure of the 70S ribosome, as well as the technical difficulties of this task, makes it an ideal target for a full-scale effort for structure determination by the Macromolecular Crystallography Facility at the Advanced Light Source (MCF/ALS).

In an effort led by Dr. Harry Noller at University of California at Santa Cruz—who has extensive experience in RNA and ribosomal molecular biology, biochemistry, and crystallization—we undertake the determination of the structure of the 70S ribosome at atomic resolution, along with the structure of its functional complexes. Dr. Noller's group has obtained crystals that yield native data to 6-angstrom resolution at the MCF/ALS. Electron density maps to 7.8-angstrom resolution have been calculated that reveal the structural arrangement of a number of components of the ribosome. One particularly useful approach, which is unique to the MCF/ALS, is the ability to perform MAD experiments around the absorption edges of several atoms, including the uranium Mv edge at 3.55 keV. This is useful since the anomalous signal at this energy is large enough to phase a complex as massive at the 70S ribosome. We will continue to develop methods and instrumentation to improve the quality of the data from the MCF/ALS for this project, which will be generalizable to other large complexes. Furthermore, we will develop computational methods for determining structures of this size and difficulty. This will include multi-solution phasing approaches to determining the structure of large macromolecules.

Accomplishments

Wnt Pathway and Complexes

Initial results have been obtained from the PDZ molecular recognition domain of *dishevelled*. *Dishevelled* is a multi-functional, multi-domain protein involved in at least two pathways. Native crystals of the 97 amino-acid PDZ domain have been obtained that diffract to 2.3-angstrom resolution. Crystals of selenomethionine-containing protein diffract to 2.5-angstrom. In addition, a complete MAD data set has been collected and the structure determination completed that suggests a novel PDZ/PDZ homodimer. Cellular assays on mutants are being pursued, based on the information of this structure. This has led to a model of interaction between *dishevelled* and the proteins that it interacts with that suggests a mechanism for mediating multiple functions.

We have recently expressed and purified to homogeneity a number of other members of the *Wnt* pathway. Characterization and crystallization trials for these molecules, and their complexes are currently underway.

70S Ribosome

The contributions made by this program to the ribosome project led by Harry Noller helped lead to the structure determination of the 70S ribosome, along with a number of functional complexes. This has allowed for the development of a fuller understanding of the large molecular machinery involved in protein biosynthesis.

Publications

J. Cate, M. Yusupov, G. Yusupova, T. Earnest, and H. Noller, "X-ray Crystal Structures of 70S Ribosome Functional Complexes," *Science* **285:** 2095 (September 24, 1999).

N. Khlebtsova, L.-W. Hung, K. Henderson, R. Moon, and T. Earnest, "Expression, Crystallization, and Initial X-ray Characterization of the PDZ Domain of *Dishevelled* Protein," *Acta Crystallographica* **D56:** 212-214 (February 2000).

N. Khlebtsova, L.-W. Hung, K. Henderson, J. Miller, R. Moon, and T. Earnest, "Structure of the PDZ Domain of *Dishevelled* Protein," *Nature Structural Biology* (in preparation).

Primary Steps of Photosynthesis

Principal Investigators: Graham Fleming

Project No.: 99043

Project Description

The subtle interplay between electronic coupling, electron-phonon coupling, and disorder that makes natural photosynthetic systems so astoundingly efficient remains imperfectly understood. Indeed, the properties of photosynthetic antennas and reaction centers differ significantly from the simple sum of their components. The primary processes of photosynthesis occur on the $10^{-14} - 10^{-11}$ s timescale and thus require ultrafast spectroscopy for their investigation. We propose to apply novel nonlinear optical techniques in combination with theory and electronic structure calculations to determine the design principles of these exquisite devices.

We have developed the photon echo peak shift into a powerful tool to study energy and electron transfer in disordered systems. We will apply this technique, along with the new two-color, three-pulse echo peak shift technique, to the bacterial reaction center, the photosystem II reaction center of green plants, and the combined antenna/reaction center system of green plants—photosystem I. Combining these measurements with *ab initio* and density functional electronic structure calculations will produce a complete picture of the quantum dynamics of photosynthesis.

Accomplishments

Carotenoid molecules play a vital role as light harvesters, damage protectors and regulators in photosynthetic light harvesting complexes. These molecules possess an optical dark first excited singlet state (S1) that is implicated in both light harvesting and its regulation. The location of these states is unknown. We used femtosecond two-photon spectroscopy to determine the spectrum of S1 states in plant and bacterial carotenoids in the actual photosynthetic complexes themselves.

Photosynthetic light harvesting complexes are truly complex in the sense that their properties cannot be understood when the entire system is included in the model. We demonstrated this point on bacterial light harvesting complex LH2, where photon echo measurements and electronic structure calculations were used as input to a model incorporating disorder excitonic couplings and spectral overlaps. We showed that B800-B850 energy transfer can only be understood in the context of the complete model.

Preliminary photon echo studies were made in the major light harvesting complex LHCII, revealing the importance of chlorophyll b to chlorophyll b transfer for the first time.

Publications

P.J. Walla, J. Yom, B.P. Krueger, and G.R. Fleming, "Two-photon Excitation Spectrum of LHC II and Fluorescence Upconversion after One- and Two-photon Excitation of the Carotenoids," (submitted to *The Journal of Physical Chemistry B).*

XAFS of Bifunctional Transition Metal Molecular Sieves for Artificial Photosynthesis

Principal Investigators: Heinz Frei

Project No.: 99036

Project Description

Photochemical synthesis of a fuel by direct reduction of CO_2 using visible light and H_2O as an electron source is one of the most attractive, yet unrealized, goals in solar energy-to-fuel conversion. Photosynthesis of methanol for large-scale use in fuel cells is considered a promising option for replacement of fossil fuel combustion as a means of power generation. We propose to explore transition metal framework substituted microporous solids containing two different metals as a new type of photoreactor for CO_2 reduction by H_2O. The most critical and challenging aspect of this task is reliable characterization of such bifunctional molecular sieves and the verification of their structural integrity under

use. X-ray absorption techniques, especially Extended X-ray Absorption Fine Structure (EXAFS) and X-ray Absorption Near Edge Structure (XANES), are the best tools for this type of solid. The purpose of this project is to explore the synthesis of bifunctional framework metal sieves; and to conduct EXAFS and XANES studies at the Advanced Light Source (ALS), in order to establish an efficient approach for the characterization and screening of these new materials.

The project consists of XAFS experiments on two established microporous materials, $TiAlPO_4$-5 and Ti silicalite in order to elucidate the local structure of framework Ti centers. In parallel, the synthesis of novel mono-substituted sieves ($RuAlPO_4$) and bifunctional materials ($TiFeAlPO_4$) will be explored, and the samples characterized by XAFS measurements. The project involves the design and fabrication of an XAFS sample stage consisting of a cryostat (77 to 700° K), a holder for 12 samples, and detectors for measurement in transmission or fluorescence mode. Experiments will be conducted at beamline 9.3.1, whose energy range spans the K-edge of Ti and L-edge of Ru.

Accomplishments

A sample holder featuring 12 sample positions and variable temperature option (77 to 700° K) was designed and fabricated. An XYZ manipulator allowed convenient alignment of each sample (pressed wafer of molecular sieve crystallites) in the x-ray beam. The sample holder was mounted on an XAFS endstation built by Dr. Melvin Klein at ALS Beamline 9.3.1, which covers the energy range 2 to 6 keV. Detection is done in either transmission or fluorescence mode by a retrievable Si photodiode, mounted at a right angle.

With this new setup, we have recorded XANES spectra of Ti substituted aluminophosphate (TAPO-5) and silicate (TS-1) sieves synthesized in our laboratory. A sharp A_1-T_2 pre-edge absorption at 4968 eV characteristic of Ti centers in tetrahedral framework sites was detected in transmission and fluorescence modes. Using samples with Ti concentrations varying between 0.5 and 3 percent, the width and intensity of the pre-edge band revealed that materials with Ti content of 1.5 percent or lower exhibit perfect framework substitution (no extra-framework Ti present). Characterization of these Ti substituted sieves by XAFS measurements furnished the basis for two mechanistic studies on CO_2 and CO photoreduction in our laboratory, both completed. In these experiments, the Ti centers are utilized as chromophores and excited redox sites. Direct evidence for the precise nature of these active sites by XAFS, combined with *in situ* infrared monitoring of the photochemistry, has furnished the first insight into the primary reaction steps of carbon oxide reduction in these nanoporous reactors.

We have accomplished hydrothermal synthesis of a microporous $RuAlPO_4$ material. The importance of such a material lies in the known role of Ru in CO_2 chemistry. Preliminary characterization by powder x-ray diffraction, scanning electron microscopy, and ultraviolet-visible spectroscopy indicates a sieve with unidimensional channel structure and reversibly reducible Ru sites. L-edge measurements in the 2800 to 3000 eV range revealed two sharp absorptions whose separation as a function of oxidative/reductive treatment will allow us to assign the oxidation states of the Ru in the material. Synthesis of bifunctional sieves $TiFeAlPO_4$ and TiFe silicalite was accomplished.

Publications

N. Ulagappan and H. Frei, "Mechanism of CO_2 Photoreduction in TS-1 Molecular Sieve," *J. Phys. Chem.* (in draft).

Y. H. Yeom and H. Frei, "Photoreaction of CO with CH_3OH in Microporous Ti Silicate," *J. Phys. Chem.* (in draft).

Novel Approaches to the Study of Molecular Organization in Living Cells

Principal Investigators: Jay Groves

Project No.: 99044

Project Description

The purpose of this project is to develop new strategies for imaging and studying the dynamic spatial organization of molecular components in living cells. In recent work, we have introduced the concept of using microfabricated substrates to impose patterns and structure on fluid lipid bilayer membranes. This is a fairly general technique that combines standard microfabrication processes with membrane self-assembly to produce lipid membranes with precisely defined patterns. The aim of the

current research is to develop micropatterned membranes, along with more general structures, as novel means of examining the role of dynamic organization in cell membranes on the micrometer and nanometer scale.

This project involves a cross section of several rather different technologies. Conventionally microfabricated substrates will be used to guide the assembly of membranes and proteins into desired geometries. These hybrid bio-solid-state structures will then be employed in various experiments with proteins and living cells. Information will be gathered largely by fluorescence microscopy.

Accomplishments

The first phase of this project has focused primarily on system development. Our initial efforts have been directed towards characterization of the influence of supported lipid membranes on the adhesion of cells to solid substrates. Two standard and naturally adherent cell lines, HeLa and NIH 3T3, were chosen for the test studies. Both of these cell lines readily adhere and proliferate on silica substrates. Their ability to recognize and adhere to silica substrates coated with a supported membrane was analyzed for a variety of membrane compositions. The primary goal of this study was to identify membrane compositions that effectively block cell adhesion. These then will form the background material for membrane-based display of biological ligands at a later stage in this work. General characterization of the stability and physical properties (fluidity, continuity, etc.) of supported membranes under cell growth conditions was also necessary. Membrane compositions which successfully block cell adhesion and withstand cell growth conditions have been found and will be disclosed at a later date.

The next phase of development of our membrane-mediated cell adhesion system involves display of specific biological ligands on the cell membrane. Several adhesion ligands involving lipid-linked peptide fragments and oligosaccharides are currently being synthesized. When the synthesis is complete, these will be incorporated into membranes, with the inert compositions we have identified, and their influence on adhesion will be studied.

The long-term goals of this work will require a sophisticated level of micro- and nanofabrication capabilities. Organization to meet these needs is underway. Our first round of photomasks have been designed and are currently being fabricated. Production of electron beam patterned nanostructures has also begun.

Global Optimization Approaches to Protein Structure Prediction

Principal Investigators: Teresa Head-Gordon

Project No.: 96038

Project Description

The protein structure prediction problem is to determine the three-dimensional arrangement of the protein molecule, given a protein-solvent potential or free energy surface in accord with the amino acid sequence. The "rugged landscape" topography of this surface defines the underlying difficulty in solving the protein structure prediction problem; the native structure minimum, presumably the global minimum, must be discriminated from other minima whose number rises exponentially with the number of amino acids in the sequence. Furthermore, this energy surface is difficult to model reliably in a global sense, i.e. to ensure that all protein misfolds are higher in energy than the correctly folded conformation.

For a sufficiently well-defined energy surface, mathematical optimization research for obtaining the global solution to a large nonlinear system with numerous local minima can be broadly categorized into two approaches. Constrained optimization methods rely on the availability of sufficiently well-defined constraints so that the desired solution is the only available solution, and local optimization algorithms can be applied. However, the necessary set of biophysical constraints needed for robust protein structure determination cannot be unambiguously predicted at this time. Global optimization techniques, in principle, avoid this predictive capacity problem by systematically searching the potential energy surface to find all low-lying minima including the global energy minimum. In collaboration with computer science researchers at the University of Colorado, we have developed a global optimization approach based on both local and global sampling, perturbation, smoothing, and

biasing (soft constraints) that has been quite successful in the prediction of alpha-helical proteins.

Global optimization methods only make sense in the context of an objective function whose global minimum is actually the desired minimum sought. While in principal the protein structure prediction problem seeks the global free energy minimum, the modeling of an energy function that guarantees the native structure as the global minimum relative to all conceivable misfolded structures is a formidable task. It is well appreciated that so-called "gas phase" protein molecular mechanics force fields do not differentiate well between folded and misfolded energy conformation. Qualitative improvement in lowering the energy of correctly folded structures relative to non-native structures is to incorporate a description of aqueous solvation. We have developed an atomic pairwise additive solvation term that stabilizes the burial of hydrophobic groups as well as spatially longer-ranged stabilization of hydrophobic groups. When this solvation potential is combined with the AMBER95 protein force field, the total function gives the crystal structure of four different α-helical proteins as the lowest energy structure relative to other conformations.

The work is computationally demanding and requires a commitment of high performance computing resources, such as massively parallel platforms, to realize its full potential. The developed global optimization strategy was parallelized and run on the T3E at National Energy Research Scientific Computing (NERSC) using from 16 to 256 processors. A new dynamic load balancing strategy, broadly applicable to tree search problems in general, has been used to generate our most recent results on a four-helix bundle DNA binding protein.

Accomplishments

This project is a collaboration between leading research groups in numerical optimization and computational biochemistry to pursue a computational solution to the protein folding problem. The research has resulted in advances in both large-scale and parallel numerical computation, and in models and prediction methods for computational biology. To succeed in solving the protein structure prediction problem by optimization approaches, we have focused on the following four areas:

- Large-scale global optimization algorithms
- Construction of accurate energy models of proteins
- Prediction of protein secondary structure constraints
- Large-scale parallel computation

The research project involves a symbiotic relationship between these computational and scientific research topics. Key features of our research include new approaches to "smoothing" the energy model in order to increase the efficiency of the global optimization, incorporation of secondary structure prediction information as non-binding constraints in the global optimization process, and a novel representation of aqueous solvent that energetically differentiates the desired structure as the lowest energy conformer relative to other misfolds. Our global optimization methods require use of parallel computation, and we have explored scheduling, task migration, and load balancing to increase efficiency.

Researchers at Berkeley Lab and University of Colorado have actively collaborated on this effort. We have obtained state-of-the-art results in predicting helical proteins of about 70 amino acids, and have developed robust energy models involving solvation. Future work involves extending the research to more general proteins and larger targets. We will need to develop improved methods of secondary structure prediction using neural networks, and further improved energy models. This will result in the distribution of new algorithms, models, and software.

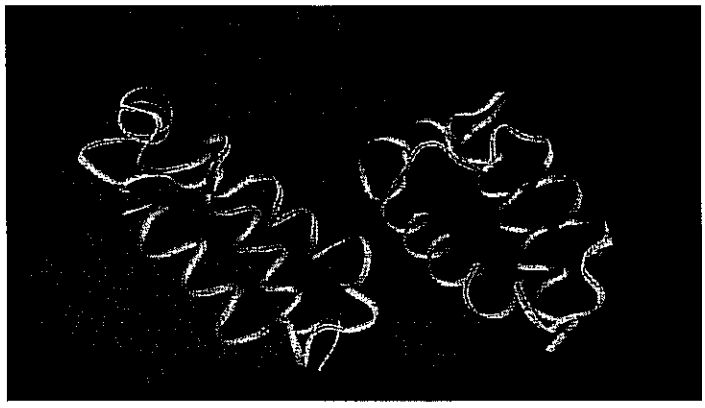

Figure 1. A ribbon diagram comparison between the nuclear magnetic resonance (NMR) structure of a four helix bundle DNA binding protein (1pou) (right) and the outcome of our global optimization algorithm (left)

Publications

S. Crivelli, T. Head-Gordon, R. H. Byrd, E. Eskow, and R. Schnabel , "A Hierarchical Approach for Parallelization of a Global Optimization Method for Protein Structure Prediction," lecture notes in *Computer Science*, Euro-Par '99, P. Amestoy, P. Berger, M. Dayde, I. Duff, V. Fraysse, L. Giraud, D. Ruiz (Eds.), Pg. 578-585 (1999).

A. Azmi, R. H. Byrd, E. Eskow, R. Schnabel, S. Crivelli, T. M. Philip, and T. Head-Gordon, "Predicting Protein Tertiary Structure Using A Global Optimization Algorithm With Smoothing," to be published in proceeding of International Conference on Optimization in Computational Chemistry and Molecular Biology: Local and Global Approaches (in press, 1999).

S. Crivelli, T. M. Philip, R. Byrd, E. Eskow, R. Schnabel, and T. Head-Gordon, "A Global Optimization Strategy For Predicting Protein Tertiary Structure: α-Helical Proteins," to be published in Computers & Chemistry, Conference Proceedings For New Trends In Computational Methods For Large Molecular Systems (in press, 1999).

S. Crivelli , T. Head-Gordon, "Parallelization of A Global Optimization Method for Protein Structure Prediction," (submitted to *J. Parallel & Distributed Computing* November 1999).

T. Head-Gordon, (Editor), "Genomic-Scale Modeling of Biological Systems," by invitation From Marcel Dekker, Inc. (accepted book proposal, November 1999).

Invited Presentations

T. Head-Gordon, "Computational Challenges in Structural and Functional Genomics," presented at NERSC Scientific Computing Group, Berkeley Lab (April 1999).

T. Head-Gordon, "Computational Challenges in Structural and Functional Genomics," presented at DOE Computational Sciences seminar series, Washington D. C. (April 1999).

T. Head-Gordon, "Lectures on Structural Genomics, Protein Folding and Prediction, and Hydration Forces," presented at National Center for Theoretical Sciences, Advanced School on Proteins, National Tsing Hua University in Hsinchu, Taiwan (June 1999).

T. Head-Gordon, "Global Optimization Approaches to Protein Structure Prediction: α-Helical Proteins," presented at Polish-American Workshop on Theoretical Chemistry and Molecular Modeling, Wroclaw, Poland (July 1999).

T. Head-Gordon, "Overview of Computational Biology," presented at Workshop on Computational Biology. Supercomputing '99, Portland, Oregon (November 1999).

T. Head-Gordon, "Protein Structure Prediction and Folding," presented at Workshop on Computational Biology, Supercomputing '99, Portland, Oregon (November 1999).

T. Head-Gordon, "Computational Biology, Protein Structure Prediction, and Folding," to be presented at Symposium on the 21st Century: How Far Can Computation Go with the Hardest Problems,

American Chemical Society, San Francisco (March 2000).

S. Crivelli, "A Hierarchical Approach for Parallelization of a Global Optimization Method for Protein Structure Prediction," presented at EuroBar '99, Toulouse, France (August 1999).

Identification of Novel Functional RNA Genes in Genomic DNA Sequences

Principal Investigators: Stephen Holbrook and Inna Dubchak

Project No.: 99037

Project Description

The goal of this project is to identify novel, functional RNA genes within genomic DNA sequences. Computational algorithms will be developed to assign putative RNA genes, the products of which can be verified and characterized by biochemical methods. Current programs for gene assignment are based largely on characteristics of protein sequences such as start and stop codons, ribosome binding site, and amino acid coding biases which are not applicable to RNA coding regions. We will, therefore, create an automated computer program that specifically recognizes sequences found predominantly in stable RNA structures. The computational methods we develop will be applied to current genome sequences (including *E. coli* and yeast) and partial genome sequences (i.e., human) and made publicly available to those involved in genome sequencing and analysis.

An automated method will be developed for the identification of putative genes coding for functional RNAs that are not homologous to previously characterized RNA molecules. The approach is based on the observation that all known functional RNAs share a small set of common structural elements. Sequences corresponding to these structural elements were shown to occur with a higher frequency in known RNA genes when compared to protein genes or non-coding regions. These frequencies, as well as the calculated free energies and base pairing of the predicted secondary structures, are being incorporated into computer-simulated neural networks for the prediction of novel RNA gene sequences in genomic DNA. Prediction of RNA gene promoters using hidden Markov models may be coupled with predictions of the RNA coding regions to define the gene structures. We will then test these predictions by biochemical and genetic methods, first by checking for the presence of a stable RNA transcript, and then for phenotypic consequences of gene deletion or disruption.

Accomplishments

Our initial approach to locating novel RNA genes was based on the premise that all stable, functional RNAs share common structural elements and that sequences corresponding to these elements occur preferentially in RNA genes.

Thus, we have used sequences characteristic of RNA structure such as GNRA tetraloops, uridine turns, UNCG tetraloops, tetraloop receptors, and adenosine platforms that are expected to occur in higher frequency in RNA genes, as well as the sequence CTAG that occurs rarely in *E. coli* protein genes compared to RNA genes. We have demonstrated a statistical preference for these structural elements in RNA genes from several genomes. We have also used the free energy of folding as a structural parameter representing double helicity in RNA sequences.

Since the frequency of occurrence of RNA structural elements cannot be expected to identify non-RNA sequences in a positive manner, we identified additional sequence preferences based on global sequence descriptors (previously applied to protein fold prediction) to discriminate RNA genes from non-RNA genes. These descriptors include 4 composition (C), 16 distribution (D), and 20 transition (T) parameters, for a total of 40 parameters (C+D+T). Alternatively, if only the composition and transition parameters are used (C+T), the total is 24 parameters.

From the known RNA genes in *E. coli*, we selected 305 sequence windows of 80 residues including examples from tRNAs, ribosomal RNAs, and miscellaneous RNAs in approximately equal ratios. We also selected 305 sequence windows from non-annotated regions of the genome. Neural networks were trained on these 610 examples to predict whether or not the sequence window was from an RNA gene. They were tested by the jackknife

method of removing one sequence at a time from the training set for testing and then averaging the predictions from all 610 trained networks. The testing results are shown in Table 1 at various strengths of prediction. The final neural network weights were obtained by training on the entire set of examples and stored for later use in prediction.

RNA GENE PREDICTION - Jackknife Testing of Computational Neural Networks

	Structure (6 parameter)		Sequence (C+T+D)		Sequence (C+T)		Voting (Structure, C+T)	
Threshold	% Correct	% Predicted	% Correct	% Predicted	% Correct	% Predicted	% Correct	% Predicted
10%	84.3	93.8	89.8	99.7	89.8	99.8	94.0	78.7
20%	84.3	89.7	89.8	99.7	90.0	98.7	90.5	78.0
40%	86.2	78.2	90.2	98.2	90.6	97.2	95.1	66.6
60%	88.6	57.7	91.9	89.2	91.4	88.2	95.4	46.6
70%	93.5	35.2	92.2	46.2	91.6	46.9	97.2	17.7
80%	97.8	22.1	86.4	9.7	83.6	9.0	100.0	1.5

*Table 1. All networks used 2 hidden nodes. Threshold=(pred1-pred2)*100./(pred1+pred2) - pred1 and pred2 are activities of 2 neural network outputs. C=%A,G,C,T; T=%Dinucleotides (i.e. AC,TG); D=Distribution in sequence (i.e. %A in first 1/4 sequence); Stucture=#UNCG, #GNRA, #CTAG, #Tetraloop receptor, #Uridine turns, Free energy of folding*10.0*

The structure-based and sequence-based neural networks are trained on very different parameters and therefore can be expected to be complimentary in their predictions. In order to optimize prediction, we used a voting procedure in which predictions were accepted only when predicted by both types of networks. The results of the voting predictions are summarized in Table 1. For the structure and voting based predictions, Table 1 shows that as the threshold of prediction is increased (strength of prediction), the number of predictions above this threshold decreases (% predicted), but the accuracy of prediction increases (% correct) toward 100% correct.

After the networks were trained, the next step was to parse the *E. coli* genome so as to remove the known RNA and protein gene sequences (including 50 residues upstream as promoters) and then divide the remaining intergenic sequences into windows of 80 residues overlapping by 40 residues. This resulted in 6,108 windows from each strand (only sequences without genes on either strand were considered). The free energy, structural parameters, and sequence parameters used as input to the neural nets were calculated for each of these windows. Structure-based, sequence-based, and voting predictions were made for each window and the strongest predictions chosen for further analysis. A total of 230 moderately strong (60% compositional/70% structural threshold) predictions were made by voting, while 9 windows were identified as potential RNA gene coding regions at the strongest level (70% compositonal/80% structural).

As a further indicator of RNA genes, we have searched for potential RNA promoters. New RNA genes can occur either in existing operons or with their own promoters. We used known promoters for 22 rRNA and tRNA genes to make a hidden Markov model of RNA gene promoters. This model was used to search the intergenic sequence windows for RNA promoters. In strand one, 19 potential promoters were identified along with 21 in strand two. Five examples of putative RNA promoters followed by strongly predicted RNA gene sequences were observed in strand one. An example is shown below (Figure 2) along with its predicted fold (predicted promoter underlined). One additional intergenic region containing both a predicted promoter and an RNA gene occurs in strand two.

A first step toward confirmation of a putative RNA gene is to see whether a sequence homologue appears in a closely related organism. We therefore searched the available genome sequence from *Salmonella typhimurium* using the sequences described above as probes and found strong sequence analogs (>90% identity) in Salmonella.

We have now reproduced the experiments described above for *E. coli* using genomes from several other organisms. These include *Mycoplasma genitalium, Mycoplasma pneumoniae, and Pyrococcus horikoshii.* These weights from the trained neural networks will be used in a public web server to allow users to make predictions using their sequences. We will be enlarging the number of organisms present in the database of our server, including other bacteria, lower eukaryotes such as yeast, and ultimately human.

Finally, we will require experimental verification of predicted RNA genes. The most direct approach initially is to probe total RNA using Northern blots. These experiments are currently underway.

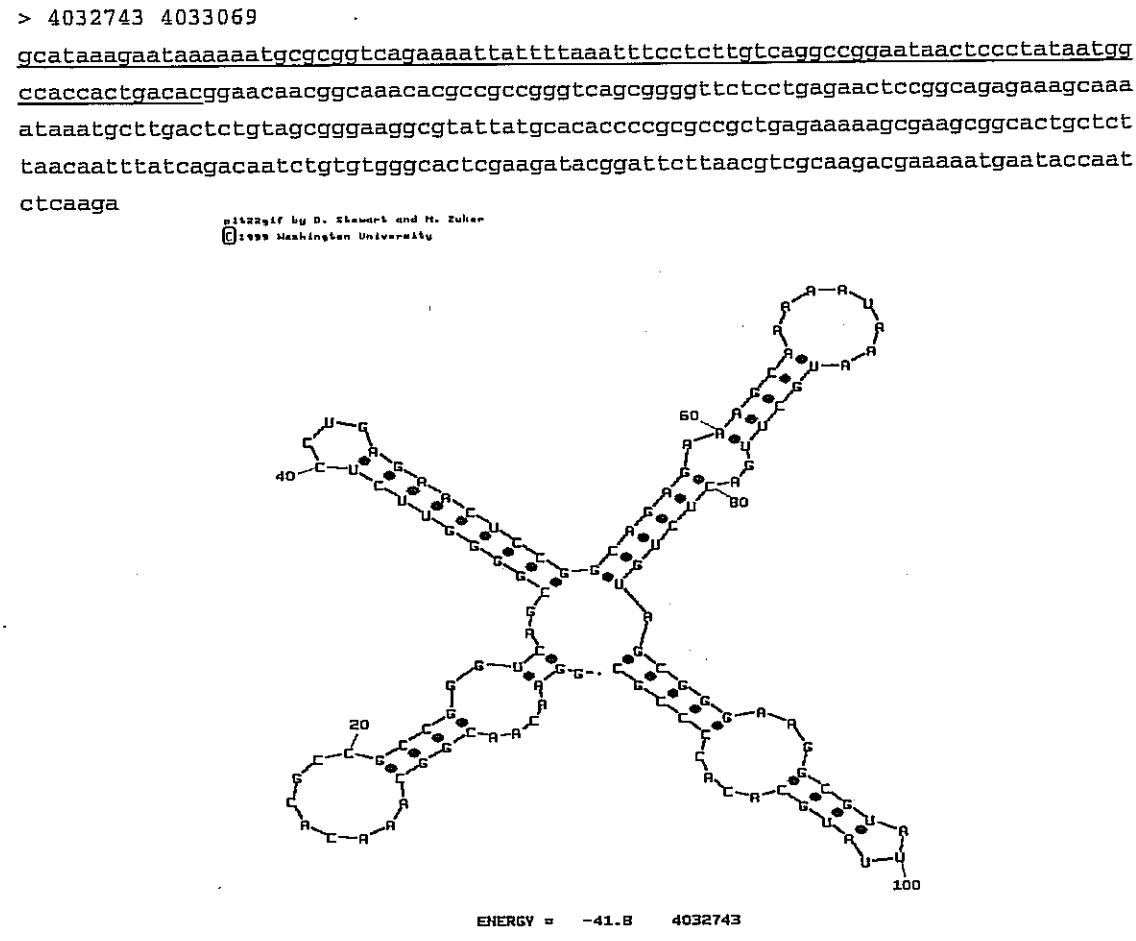

Figure 2. Intergenic region of E. Coli containing both a predicted promoter (underlined) and an RNA gene occurs in strand one as shown above. The predicted secondary structure of the RNA as calculated by MFold is shown below the sequence.

Publications

I. Dubchak, S.R. Holbrook, and I. Muchnik, "Global Description of Amino Acid & Nucleotide Sequences: Application to Predicting Protein Folds, Intron-Exon Discrimination, & RNA Gene Identification," Proceedings of the International Conference on Modeling and Simulation of Microsystems (1999).

I. Dubchak and S.R. Holbrook, "Identification of Novel RNA Genes in Genomic DNA Sequences" (draft).

Basis Set of Protein Folding: a Computational Taxonomy of Protein Folding Families

Principal Investigators: Sung-Hou Kim

Project No.: 98027

Project Description

An examination of genomic DNA sequences reveals that a majority of genes have no known functions as judged by sequence similarities. However, an increasing number of proteins with weak sequence similarity have been found to assume similar three-dimensional fold, and often have similar or related biochemical or biophysical functions. The objective of the project was to develop a computational method, based on amino acid properties alone, for detecting the fold similarity between two proteins with low sequence similarity.

Accomplishments

We have developed the proximity correlation matrix (PCM) method. This computational method is built on the observation that neighboring amino acid residues in sequence at structurally equivalent positions of two proteins of similar fold have physical properties that are often correlated, even when amino acid sequences are different. Hydrophobicity is shown to be the most strongly correlated property for all protein fold classes. The PCM method was tested on 420 proteins belonging to 64 different known folds, each having at least three proteins with little sequence similarity. The method detected fold similarities for 40% of the 420 sequences. Compared with sequence comparison and several fold recognition methods, the PCM method demonstrates good performance in detecting fold similarities among the proteins with low sequence identity. Applied to the complete genome of *Methanococcus jannaschii* this method recognized the folds for 22 hypothetical proteins.

Publications

I.V. Grigoriev and S.-H. Kim, "Detection of Protein Fold Similarity Based on Correlation of Amino Acid Properties," *PNAS* 96, 14318-14323 (1999).

Controlled Environment X-Ray Absorption Spectroscopy Studies at 2 to 5 KeV at the ALS

Principal Investigators: Vittal Yachandra and Melvin Klein

Project No.: 98043

Project Description

The purpose of this proposal is to provide a capability for performing x-ray absorption spectroscopy (XAS) of lower-Z elements at the Advanced Light Source (ALS). Elements from P through Ca have K-absorption edge energies between 1.8 and 4.9 keV, whereas the L-edges of most second-row elements fall in this range. The XAS, especially the near edge spectra of the lower Z elements, is extremely rich and can provide detailed chemical and structural information (especially chemical speciation) on samples as diverse as biological cells and geological samples. Such measurements can be performed on any state of matter at selected temperature and environment. The setup we propose will provide an enclosure with provisions for sample containment in an environment of the experimenter's choice (vacuum or specific atmosphere, elevated or reduced temperature, absorption or fluorescence detection).

We will construct a "mini-hutch" to safely contain general and specific components for XAS. Required components include detectors to monitor incident and transmitted photon flux, fluorescence, sample mounting, cryostat and other enclosures for achieving low or elevated temperatures, vacuum or other ambient gases, sample positioning, and alignment. Longitudinal positioning along the beam direction will provide for operation at or displaced from the beam focal position to permit examining a small or distributed fraction of a large sample.

Accomplishments

An endstation designed to achieve the goals stated in the project description has been designed, fabricated, installed on Beamline 9.3.1 at the ALS, tested, and placed in operation. First light was observed in the endstation exactly one year after the original proposal was submitted.

The endstation incorporates a number of useful features. It permits samples to be observed while in either vacuum or a gas of the experimenter's choosing. The temperature may range from ambient to 10° K. To minimize attenuation of the incoming soft x-rays it may be operated with a single thin window between the beamline vacuum and the sample. As most soft x-ray absorption spectra, XAS, are observed by fluorescence detection of x-rays characteristic of the element under study, we have incorporated a detector inside the sample chamber, thus avoiding another exit window. Provisions have been made to use detectors externally with only one window between sample and detector. Sample changes can be performed in minutes.

Incident beam intensity is measured either by photoemission from a metal mesh or by creating a small ionization chamber between two Be windows that can be inserted into the incident beam path. Spectra have been obtained at the P, S, Cl, Ar and Ca K-edges, at several second row transition element L-edges, and the three L-edges of Xe.

Because small shifts in the precise energy of features in the x-ray absorption near edge structure (XANES) often reveal significant chemical information, precise energy referencing from scan-to-scan and from run-to-run is required. For low-resolution studies, observation of an internal standard compound suffices. For more exacting studies, we have incorporated a Si crystal at fixed angle relative to both the incident beam and to a detector. The diffraction "glitches," which occur as the beamline monochromater scans energy, provide very sharp energy markers.

The endstation has been used by two groups from Physical Biosciences Division, one from Earth Sciences and one from Chemical Sciences. A number of investigators from outside Berkeley Lab have expressed interest in using the setup.

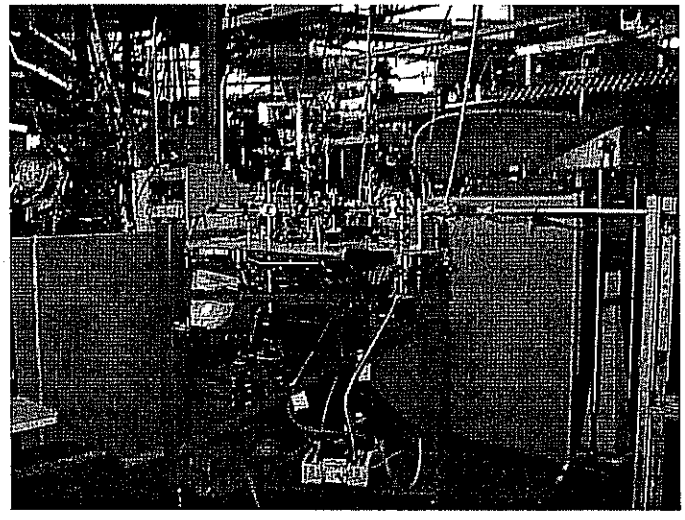

Figure 3. Arbitrary environment endstation for performing x-ray absorption spectroscopy in the energy range of 2 to 5 keV installed at Beamline 9.3.1 at the ALS.

Publications

K L. McFarlane, Z. Hussain, M.P. Klein, and V.K. Yachandra, "A Non-Vacuum End Station for Intermediate-Energy XAS and the ALS.," ALS Users Meeting, October 1999, in draft for *Review of Scientific Instruments.*

K.L. McFarlane, M.J. Latimer, M.P. Klein and V.K. Yachandra," Cryostat for XAS at Low Energy with Internal Fluorescence Detection," in draft for *Review of Scientific Instruments.*

Computational Modeling of Protein Folding and Unfolding Using Lattice Models and All-Atom Molecular Dynamics

Principal Investigators: Daniel Rokhsar

Project No.: 98044

Project Description

The goal of this project is the construction of quantitative theoretical models of biological materials and systems. Our primary focus is two-fold: (1) the thermodynamic and kinetic properties of proteins and (2) the development and organization of neuronal networks in the mammalian visual system.

Studies of protein folding require extensive Monte Carlo simulation for thermodynamic properties and molecular dynamics and Langevin analysis for kinetics. Because all-atom calculations are limited to nanoseconds of real time (while real proteins fold in milliseconds), progress demands the construction of faithful, yet tractable, models to make the best use of available computational resources. We use lattice models, simplified representations of proteins, and all-atom molecular dynamics with solvent to study the nature of folding and unfolding pathways.

Simulation and analysis of retinal and cortical patterns and their projections requires both image processing and dynamical simulations. Parallel simulations of a range of control parameters for these realistic networks is the best way to accumulate sufficient data to understand these complex dynamical systems. The goal of this effort is (1) a quantitative model of the developing mammalian retina and (2) the ability to make specific predictions for the behavior of this network under various conditions.

This computational effort relies heavily on the computational resources of National Energy Research Scientific Computing (NERSC), specifically the Cray T3E.

Accomplishments

Unfolding and Refolding a Beta Hairpin

Using molecular dynamics, we have studied the unfolding and refolding pathway of a beta-hairpin fragment of protein G. While this fragment is small, it possesses several of the qualities ascribed to small proteins: cooperatively formed beta-sheet secondary structure and a hydrophobic cluster of packed side chains. At high temperatures, we find that the hairpin unfolds through a series of sudden, discrete conformational changes. The discrete states are identified with the folded state, a pair of partially unfolded kinetic intermediates, and the unfolded state. To study refolding at low temperatures, we perform a series of short simulations, starting from the putative transition states of the discrete transition seen in unfolding. These simulations show that refolding at low temperatures can proceed by reversing the unfolding pathway at high temperatures.

Unfolding a Beta Hairpin by Mechanical Forces

Single-molecule mechanical unfolding experiments have the potential to provide insights into the details of protein folding pathways. To investigate the relationship between force-extension unfolding curves and microscopic events, we performed molecular dynamics simulations of the mechanical unfolding of the C-terminal hairpin of protein G. We have studied the dependence of the unfolding pathway on pulling speed, cantilever stiffness, and attachment points. Under conditions that generate low forces, the unfolding trajectory mimics the untethered, thermally accessible pathway previously proposed based on high-temperature studies. In this stepwise pathway, complete breakdown of the backbone hydrogen bonds precedes dissociation of the hydrophobic cluster. Under more extreme conditions, the cluster and hydrogen bonds break simultaneously. Transitions between folding intermediates can be identified in our simulations as features of the calculated force-extension curves.

Retinal Waves and Collective Network Properties

Propagating neural activity in the developing mammalian retina is required for the normal patterning of retinothalamic connections. This activity exhibits a complex spatiotemporal pattern of initiation, propagation, and termination. We have introduced a model of the developing retina using a

combination of simulation and analytic calculation. Our model produces spatially and temporally restricted waves without requiring inhibition, consistent with the early depolarizing activity of neurotransmitters in the retina. We find that highly correlated, temporally regular, spatially restricted activity occurs over a range of network parameters; this ensures that such spatiotemporal patterns can be produced robustly by immature neural networks in which synaptic transmission by individual neurons may be unreliable. Wider variation of these parameters results in several different regimes of behavior. We also find that wave properties are locally determined by a single mesoscopic parameter, the fraction of recruitable cells. From this perspective, a given area's local ability to support waves with a wide range of propagation speeds—as observed in experiment—reflects the variability in the local state of excitability of that area. These predictions are supported by whole-cell voltage-clamp recordings. Our approach to describing the developing retina provides new insight into how the organization of a neural circuit can lead to the generation of patterns of complex correlated activity.

DNA Microarray Analysis

We are developing GUACAMOLE, a comprehensive software package for the analysis of DNA microarray data. This integrated package combines image analysis and quantification; graphically oriented, user-guided sorting; classification and visualization of single microarray datasets; and higher-level analyses across multiple experiments, including complex queries, sorting, clustering, pattern recognition, etc. The package provides a single, user-friendly platform for navigation and exploration across single and multiple experiments. Results are stored in a relational database, BEANDIP, with a database schema that has been designed to be compatible with a wide range of other analysis tools, including especially the SCANALYZE series, and Laboratory Information Management Systems (LIMS)—including Stanford, Berkeley, and Berkley Lab versions. The implementation of a relational database permits high-level statistical analyses to be performed across multiple experiments. A simple web interface allows multiple users (with suitable identification/passwords) to access and search large collections of microarray data.

GUACAMOLE is in a beta-testing stage, with several groups at UC Berkeley and Berkeley Lab currently testing it using microbial, fly, mouse, and human arrays.

Bose-Einstein Condensation

Although not within the scope of the original proposal, some local computational resources were used to develop the theory of rotating Bose-Einstein condensates. Specifically, the steadily rotating states of the dilute Bose gas were determined exactly using a combination of analytical and computational methods. The result is stable rafts of quantized vortices. A single vortex was recently observed by the Joint Institute for Laboratory Astrophysics (JILA) group in Colorado.

Publications

Z. Bryant, V.S. Pande, and D.S. Rokhsar, "Pulling Apart a Beta Hairpin," to appear, *Biophysical Journal* **78** (2) (2000).

V.S. Pande and D.S. Rokhsar, "Molecular Dynamics Simulations of the Unfolding and Refolding of a Beta-Hairpin Fragment of Protein G," *Proceedings of the National Academy of Sciences* **96**, 9062-9067 (1999).

D.A. Butts, M.B. Feller, C.J. Shatz, and D.S. Rokhsar, "Retinal Waves are Governed by Collective Network Properties." *Journal of Neuroscience* **19**, 3580-3593 (1999).

V.S. Pande and D.S. Rokhsar, "Folding Pathway of a Lattice Model for Proteins," *Proceedings of the National Academy of Sciences* **96**, 1273-1278 (1999).

D.S. Rokhsar, "Condensates in a Twist." *Nature* (News and Views) (1999).

D.A. Butts and D.S. Rokhsar, "Predicted Signatures of Rotating Bose-Einstein Condensates," *Nature* **397**, 327-329 (1999).

Protein Microcrystallization and Structure Determination

Principal Investigators: Joseph Jaklevic, Peter Schultz, Jian Jin, and Raymond Stevens

Project No.: 98045

Project Description

The difficulty in producing quality crystals is a major bottleneck for protein molecular structure determination using x-ray crystallography. Typically, to obtain a single, high-quality protein crystal, it is necessary to screen the protein sample against a multi-dimensional array of variables (e.g. reagents, salt concentrations, pH levels), or "mother liquids," comprising hundreds of crystallization trials. Done manually, these trials are so labor intensive and tedious that it is not practical to set up enough trials to ensure success. Another limiting factor is the scarcity of highly purified protein samples, with the typical current protein yield ≈1 ml, which can limit the total number of trials.

The development of the robotic systems for protein crystallization studies began in FY98. A robotic system was conceptualized that automates the protein crystallization processes, synthesizes the necessary reagents, and optically screens the individual trials. The robotic system allows the user to vastly expand the number of possible reagents used to attempt crystallization. Compared to current state-of-the-art commercial systems, the first goal of this project is to achieve an order-of-magnitude increase in throughput of crystallization trials. The second goal is to reduce the amount of protein sample used in a single trial to one tenth of a microliter to vastly expand the number of trials per protein.

The goal of the entire system is to generate and detect high-quality protein crystals. Every protein sample will first be screened against a coarse array of 480 standard mother liquids that can be purchased in bulk from an outside vendor. An optical system will automatically monitor the individual trials for crystallization. As a crystal grows, repeated imaging will track its size, shape, and structure. If the crystal is of sufficient quality, the user will be alerted and the crystal removed for evaluation. If the crystal is suboptimal, two-dimensional arrays of new mother liquids will be automatically synthesized based on the identified mother liquid, and new crystallization trials will be created and monitored. Three discrete subsystems will perform the functions of 1) setting up a protein crystal growth plate; 2) optically monitoring the crystal growth trials; and 3) synthesizing the fine grid screening reagents. Through the use of unique barcodes on each microtiter plate, a single database is used to communicate and store information among the three subsystems.

Accomplishments

Crystallization Subsystem

By the end of FY98 the entire crystallization subsystem had been designed with detail drawings for each subcomponent complete and in the process of being fabricated. The early months of FY99 were spent testing subcomponents (e.g. greaser), designing and building the electronic control system, and assembling the complete system. Preliminary testing of the full system began in January. Following a delay in delivery of custom-designed and molded microtiter plates, full testing of the system with reagents was begun. The first crystals to be grown using the crystallization subsystem without manual intervention were done with drop volumes as low as 250 nl. By the end of April, lysozyme crystals were regularly being grown in total drop volumes as low as 40 nl and at a rate of 8 seconds/trial (6 minutes/microtiter plate). By early summer, effort was mainly directed into research issues surrounding dispensing of high-viscosity liquids, accuracy and repeatability of such liquids at low volume, investigating drop size versus crystallization rates, and designing test protocols for the end user. Effort was also spent on improving the control software for the client's use as well as creating an extensive operating manual.

Synthesizer

The second subsystem developed for the project is designed to provide a finer mesh of growth conditions following a successful (yet sub-optimal) identification of crystal growth conditions from the primary combinatorial robotic system. The synthesizer is based on a commercial Tecan robot modified with custom hardware fixtures and extensive software improvements. Development efforts were directed toward optimization of liquid level sensing of PEG solutions, as well as the initial construction of a database to allow for the creation of

the fine grid solutions based upon the 480 coarse solutions used in the crystallization subsystem. The early months of calendar 1999 saw the construction and assembly of the electrical control box, the necessary hardware to supply the stock solutions, and fixtures to adapt the Tecan deck plate to our use. Preliminary testing of single buffer pH gradients for the fine grid synthesizing showed the need to purchase the small volume pipetting option for accurate results. Time trials using multiple stock solutions and viscosities were begun in May, followed by work on the necessary refinements to the liquid handling protocols and database. June and July were spent on polishing GUI software for the client's use as well as creating an extensive operating manual.

Optical Station

The plan for the automated optical station for monitoring the crystal growth trials called for the station to be developed in two stages. During the first stage, a commercial *CrystalScore* system from Diversified Scientific, Inc. was bought to image the preliminary trials from the crystallization subsystem. Based on images collected by the *CrystalScore* system, software continued to be written for crystal recognition and analysis. This software is to be used in the second phase when a new, fully automated imaging station is built. This subsystem was conceptualized and optical specifications drawn up with detail drawings completed by early summer. Due to financial considerations, construction of this subsystem was put on hold while the clients continue to use the *CrystalScore* system to manually capture images of the crystal growth trials

Summary

The project has been successful in demonstrating the capability for large-scale combinatorial growth of protein crystals using very small volumes of purified reagents. This is an important breakthrough in the emerging area of genomics-based protein structure characterization since small crystals appropriate for synchrotron-based analysis can be rapidly prepared from small volumes of expressed purified proteins The automated approach also lends itself to scale-up to accommodate the large numbers of samples anticipated in planned studies. The project has also served as a lead-in to an additional instrumentation effort devoted to the automaton of x-ray crystal analysis at the Advanced Light Source (ALS) synchrotron facility.

These results demonstrate conclusively the validity of this approach. Continuing work will be required to demonstrate its applicability to the detection of specific targets. There is a *Science* article planned with our collaborators at NIFG. We are also presenting the results at an international automation conference in January.

Silicon-on-Insulator Technology for Ultra-Radiation Hard Sensors

Principal Investigators: Kevin Einsweiler, Naimisaranya Busek, Roberto Marchesini, Gerrit Meddeler, Oren Milgrome, Helmuth Spieler, George Zizka

Project No.: 99038

Project Description

Readout electronics for vertex detectors in high-luminosity colliders are becoming increasingly complex. One design for the ATLAS pixel readout integrated circuit (IC), for example, includes about 106 transistors. Consequently, assessing the suitability of a process for future detectors must go beyond merely determining whether devices "die" or not. Instead, a detailed evaluation of many electrical parameters is necessary to determine how the individual device parameters can be balanced against one another to mitigate the effects of radiation damage. Furthermore, a systematic procedure to compare the agreement between simulation parameters and actual device characteristics is necessary to allow reliable design of radiation-tolerant circuitry.

Accomplishments

Much of the effort in FY99 concentrated on detailed characterizations of devices before irradiation. We focussed on two processes:

- Honeywell 0.8 μm bulk CMOS, as used in the vertex detectors for BaBar at Stanford Linear Accelerator Center (SLAC), the Collider Detector at Fermilab (CDF) and DØ, also at Fermilab.
- Taiwan Semiconductor (TSMC) 0.25 μm CMOS, available through MOSIS.

The 0.25 μm process is especially interesting, as its gate oxide thickness approaches the regime where electron tunneling should substantially neutralize radiation-induced charge buildup.

Results from the measurements taken on the Honeywell process were used to develop an expanded set of test devices to allow a more reliable extraction of SPICE parameters. The enhanced device set was used for the TSMC 0.25 μm submission and for an additional submission using the DMILL process.

Extensive comparisons between measurements and simulations were conducted using Honeywell devices. There were several problems encountered in modeling MOS transistors, even with an advanced model such as BSIM3.2, used in this work. One factor is the dependence of drain current I_D vs. gate voltage V_{GS} for simulation and experiment of a device with 0.8 μm channel length. At gate voltages $V_{GS} > 1.5$ V the agreement is quite good. This is the strong inversion regime. At lower gate voltages the operating point moves into moderate and then weak inversion. Here the discrepancy is quite pronounced. Both the transition from strong to weak inversion and the subthreshold slope (i.e. weak inversion) are poorly reproduced. This discrepancy is critical in our designs, as the moderate and weak inversion are especially important in circuitry optimized for low power.

We also determined that at larger channel lengths the subthreshold slope is better reproduced, although the transition is shifted

A useful measure of the transition from strong to weak inversion is the current at which the normalized transconductance g_m/I_D is 50% of the weak inversion value. The comparison between experiment and simulation of this current vs. channel length is shown in Figure 1. Long channel devices show a factor-of-two discrepancy, whereas with decreasing channel length the disagreement between simulation and experiment approaches a factor of seven for the minimum channel length.

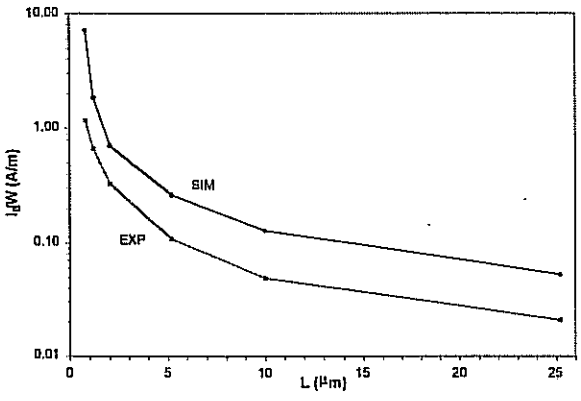

Figure 1. Current at which the normalized transconductance g_m/I_D attains half the weak inversion value vs. channel length

Clearly, the model parameters must be treated with care, especially since radiation damage will shift the transition point.

Deep submicron devices introduce additional features that complicate the models. Since the local fields in the channel are high, the carrier velocity saturates. This changes the drain current vs. gate voltage characteristics significantly, as shown in Figure 2 for the 0.25 μm process investigated in our work. Rather than showing the linear increase of transconductance with drain current typical of conventional devices, the transconductance saturates. This is indicative of velocity saturation of the carriers in the channel. This phenomenon allows a direct determination of the carrier density in the channel, which provides an important cross-check of post-radiation device physics.

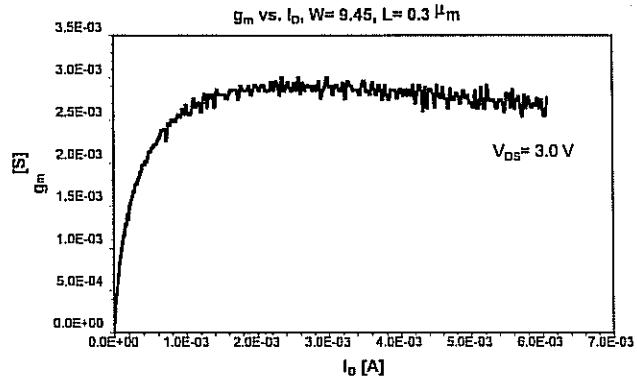

Figure 2. Transconductance vs. drain current, 0.3 μm channel length

On the other hand, saturation of transconductance also imposes an upper limit on the gain-bandwidth product obtainable with a given device. Specifically, this implies a maximum device size, which optimizes g_m/C. A drawback of the high fields in the deep submicron structures is increased susceptibility to impact ionization. Turn-on of the parasitic bipolar transistor associated with CMOS structures has been observed in many of the short-channel devices and considerable effort was expended to determine proper operating conditions and obtain valid device characteristics.

In summary, thorough analysis of device characteristics over a wide range of device geometries has been performed for both the 0.8 μm Honeywell and the 0.25 μm TSMC processes. Results have been used to develop a comprehensive framework for testing the reliability of simulation parameters and defining expanded sets of test structures for parameter extraction before and after radiation damage. Deep submicron devices show qualitatively different behavior in some respects, which poses additional difficulties for the models. The preparatory work necessary for a meaningful evaluation of post-radiation characteristics has been completed and the techniques can be applied to other processes.

Computational Innovations to Measure the Parameters of the Universe

Principal Investigators: Saul Perlmutter, Peter Nugent, Gerson Goldhaber, Donald Groom, and Gregory Aldering

Project No.: 96044

Project Description

In the next few years, we will measure the fundamental parameters of cosmology, using astrophysics techniques developed in the Supernova Cosmology Group. This project already requires

unusual computational environments and capabilities. The future, larger amount of data will need innovations for near-real-time computation, fast access to large data sets, and tools for scientific visualization, networking, and "collaboratory" environments—all of which are research interests of National Energy Research Scientific Computing (NERSC). As a first step in a collaboratory, we are using T3E calculations to interpret our supernova spectra. We have also begun studies of image processing with supercomputers.

The key to successful cosmological measurements is to attack statistical and systematic error. This current project aims to reduce the systematic error associated with the minor variation in intrinsic brightness among Type Ia Supernovae (SNe Ia) by calibrating against features of the supernovae spectrum (spectral work that involves supercomputer simulations of supernovae atmospheres to produce "synthetic spectra"). This theoretical and phenomenological research will make it possible to prepare simulated spectra that will enable us to understand the distant supernova spectra and thus calibrate the supernova's brightness.

Accomplishments

Using astrophysics techniques developed in the Berkeley Lab Physics Division's Supernova Cosmology Group and extensive use of the NERSC facilities and expertise, we have begun to measure the fundamental parameters of cosmology that shape our current understanding of particle physics through the observation of very distant Type Ia Supernovae (SNe Ia). Our results indicate that the universe does not contain enough matter to stop the expansion that began with the Big Bang and, more surprisingly, that the expansion is speeding up.

At this point in time, our measurements are no longer limited by statistical uncertainties. Systematic uncertainties are the dominant source of error. These include the effects of evolution (As you look back further in time do the SNe Ia behave the same way?); the effect of intergalactic dust on the brightness of the SNe Ia; and a thorough knowledge of the spectral response of SNe Ia as a function of time, especially in the ultraviolet (UV), where our current data sets are quite limited.

In FY99, we were able to usefully complete a number of the computational modeling and analysis efforts discussed in last year's report. More specifically:

- Spectrum synthesis studies, particularly on the metallicity environment for SNe Ia progenitors, enabled conclusions to be drawn about the limits on systematic uncertainties for values of the mass and radiation densities of the universe, and the cosmological constant.
- For these same parameters, studies on reddening due to interstellar dust were important in constraining systematic uncertainties due to this cause.
- Modeling peak luminosity in light curves was important in concluding that rise times of high and low redshift SNe Ia are consistent.
- Data reduction and image deblurring and denoising techniques were important in studies of Hubble Deep Field SNe Ia.

A final effort was an additional modeling effort for improving the discovery of SNe Ia. This would significantly increase the number of calibrators used to set the zero point in the determination of the cosmological parameters, and would provide us with a large enough data set, which we could sample in different ways to test for systematics. We would also be able to get a much better hold on the relationship between stretch (the breadth or narrowness of the light curve) and the peak luminosity of the supernova.

The effort was a complete success with over 40 supernovae discovered to date. We have begun the process of reducing and analyzing these observations in order to constrain the aforementioned systematic errors in the high-redshift results.

This LDRD lead to a very competitive five-year NASA Long-Term Space Astrophysics Grant of $578,221 for Dr. Nugent, which will allow us to continue and expand this program. In addition we successfully proposed for 24 orbits of Hubble Space Telescope time to obtain further observations of nearby SNe Ia in the UV.

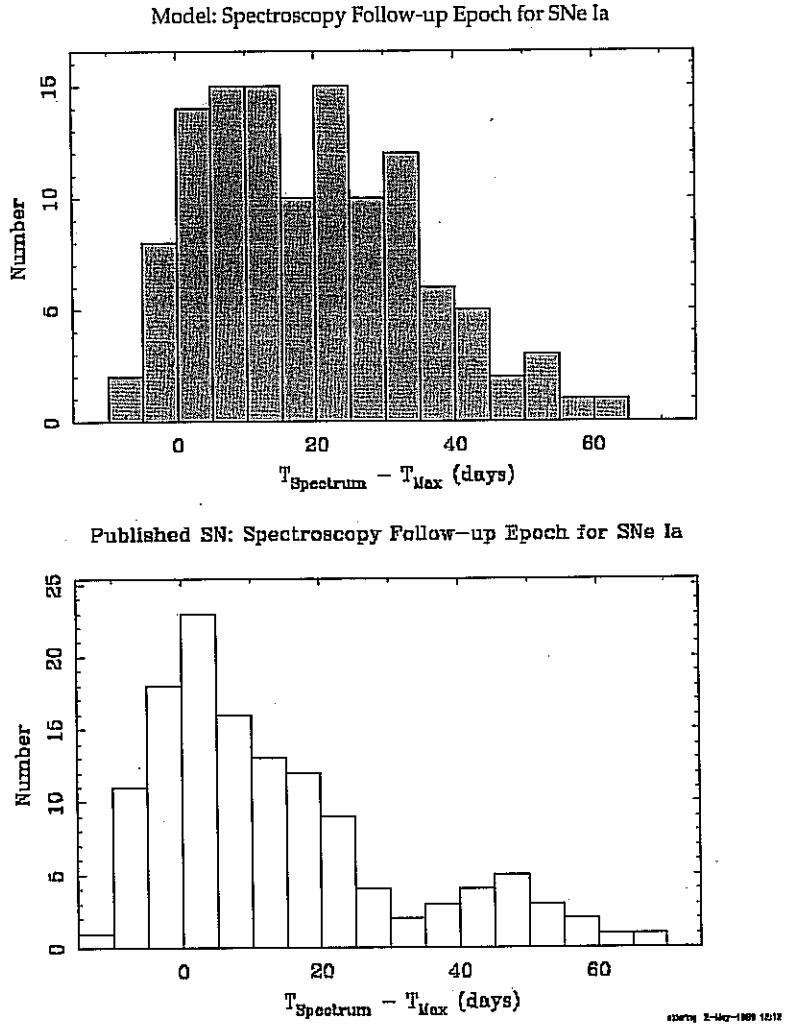

Figure 3. A comparison of the number of Type Ia Supernovae spectra observed (top) as a function of epoch with all of the previously published spectra (bottom).

Publications

R. Gilliland, P. Nugent, and M. Phillips, "High Redshift Supernovae in the Hubble Deep Field," *Ap. J.* **521**, 30 (April 1999).

S. Perlmutter, et al., "Measurements of Ω and Λ from 42 Supernova," *Ap. J.* **517**, 565-86 (June 1999).

Supernova Cosmology Project, "Supernovae *IAUC* 7117, 7118, 7122, 7125, 7128, 7130, 7131, 7133, 7134 and 7136," *International Astronomical Union Telegram* (March 1999).

G. Aldering, R. Knop, and P. Nugent, "The Risetimes of High and Low Redshift Type Ia Supernovae are Consistent," to be published in *A. J.* (April 2000).

E. Lentz, E. Baron, D. Branch, P. Hauschildt, and P. Nugent, "Metallicity Effects in NLTE Model Atmospheres of Type IA Supernovae," submitted to *Ap. J.*

P. Nugent, et al., "Color-Based K-corrections for Type Ia Supernovae," to be submitted *Ap. J. (in preparation).*

P. Nugent et al., "Spectroscopic Correlations in Type Ia Supernovae," to be submitted to *Ap. J. (in preparation).*

Solutions to Data Handling Constraints for Large HENP Experiments

Principal Investigators: David Quarrie

Project No.: 99045

Project Description

The current generation of large-scale High Energy and Nuclear Physics (HENP) experiments are characterized by significant data management problems. This is because of the sheer quantity of the information (0.3-1.0 petabytes per year), as well as the large size and geographical dispersion of the collaborations. Current experiments such as BaBar at Stanford Linear Accelerator Center (SLAC) and the Solenoidal Tracker at Relativistic Heavy Ion Collider (STAR at RHIC) have 500 to 1000 physicists, spread across 80 to 100 institutions in eight to ten countries. The next generation of experiment at the Large Hadron Collider (LHC) (ATLAS, CMS) will require further scaling of five to ten. Thus the problems of data storage and more importantly data access, are scaling faster than those of processing needs, particularly when contrasted with the performance growth of commercial hardware. Processing speeds are increasing faster than network speeds, which in turn are increasing faster then the performance of rotating disks and lastly, tape storage media.

Since the days of the Superconducting Super Collider (SSC), Berkeley Lab scientists have been at the forefront of applying innovative techniques to these data management problems. These techniques include the use of object-oriented programming languages and database management systems, distributed object brokers and data indexing. These efforts have most recently focussed on the BaBar and STAR experiments. This LDRD is designed to build upon the experience gained from these projects, to generalize the solutions so they are applicable across a broader range of experiments, and to address scalability and distributed-access issues that remain to be solved before the advent of the LHC experiments.

The BaBar data management system is based upon a commercial object-oriented database, but has added significant domain-specific software. This not only deals with the complex data model of the experiment data, but also adds several security and data-protection tools. This also provides monitoring tools to allow re-optimization of the data placement across a hierarchy of data servers. The management system includes the ability to iterate across so-called collections of events in order to select candidate events of interest for a particular physics analysis. However, indexing techniques offer the potential for significant performance enhancements relative to conventional iteration, and these are being developed, but are not yet in production. In addition, a mixed language environment based on both Java and C++ is now feasible, and the implications of this are beginning to be understood.

The LDRD proposes, therefore, to continue the development of the BaBar data management system, but to review the techniques and lessons with a view for their adoption by other experiments.

Accomplishments

Work on this LDRD in FY 1999 covered several areas:

Wide Area Access to Distributed Data

The major focus for this year was the creation of production procedures for tape-based wide area distribution of data to remote sites. This included both the distribution procedures themselves, and the bookkeeping procedures to track the flow between sites. Given the state of the wide area networks between the United States and Europe, it was decided to defer development of a network-based distribution scheme until there were improvements in the reliability and bandwidth of the networks, and the synchronous nature of the present distribution transaction management environment had been replaced by an asynchronous one. This is an area of active discussion between ourselves and the object-oriented database management system (ODBMS) vendor, and it is hoped that a collaborative project will be forthcoming shortly.

Scaling to Multi-petabyte Data Sizes

This has been addressed by the development of a larger address space (to 128-bit from 64-bit) and a so-called long-reference allowing navigation through this larger address space. This is still in development within the vendor, but resulted from strenuous negotiations with the research team and

other high energy physics, research and development groups.

However, active development of a CORBA-based extension is underway. The main focus of this is to allow more transparent access to the conditions data—which describes the state (detector alignments, electronics calibrations, etc.) of the detector at the time at which physics events were taken—and to decouple this access from the primary event store. It also allows a decoupling of the detailed configuration of the now disjoint federations, which will allow for better performance optimizations based on an enlarged page size (the unit of transfer to the persistent store) for the primary event store.

Security

An abstract security application programming interface (API) has been designed that can support a number of different protocols. Support for this API has been adopted by the vendor, and a Kerberos-based implementation is being developed, for deployment during FY2000. This will overcome the present security concerns and allow for improvements in wide area access, since firewalls and gateways can be configured to allow the secure protocols to be transmitted between remote sites.

Indexing Techniques

Two prototype, multi-dimensional indexing techniques have been implemented. One is based on the use of multiple one-dimensional bit-mapped indices developed by the HENP Grand Challenge Project, whereas the other is based upon the use of multi-dimensional grid files. These are ready for deployment in FY2000, whereupon we will be able to embark upon the investigation of their advantages and disadvantages relative to conventional iterative techniques.

Schema Evolution and Transient/Persistent Separation

Extensive tests were made of a variety of schema-evolution approaches during the FY99 work. It was determined that the vendor-provided solution was inadequate since it caused existing executables, even those only accessing unevolved data, to fail. It was therefore decided to implement a schema-evolution mechanism that took advantage of the separation between the transient information, as seen by the application programmer, and the underlying persistent representation. This had been the source of much design discussion, since there are significant disadvantages to the approach. In particular, one disadvantage is that one of the main foreseen advantages of an ODBMS—its direct programming language interface—has effectively been negated using this approach.

As implemented, the schema-evolution strategy is based upon a cascade, where each persistent type only knows about its immediate predecessor in the evolution chain, and the conversion to or from the transient form is performed automatically by the appropriate type. This has been found to scale reasonably well to the level of evolution that has been encountered in the first nine months of production running.

Data Access Optimization

This has been one of the major focal points for FY99. Of particular note has been the optimization of the configurations, both hardware and software, for parallel loading of the database detector information, as well as ongoing studies of access performance.

The database design called for an input rate of 100Hz from a farm of 200 networked client machines. These clients run the full event reconstruction chain in pseudo real-time, with the design goal that 90% of the event data should have been processed within two hours of it being acquired. Several server machines support this activity, backed up by a hierarchical mass storage system (HPSS). At the time of turn-on of the experiment, the achieved rate was 8Hz, well below the design value, and much effort has been targeted at understanding this and improving it. As can be seen in the figure, the achieved rate has improved to about 130Hz using 200 client nodes. The sources of improvements have been many, including:

- A better matching of the number of file server machines, and the number of file systems and CPUs per file server
- Associating groups of client nodes to different groups of databases
- Minimizing federation catalog operations
- Changes to system configuration parameters, most particularly the file descriptor limit
- The use of multiple database server processes per database server machine

- The use of dedicated auxiliary servers for the federation catalog and journal files

In parallel with this work, another development has focused upon read access, in particular for making fast event selections based upon a small subset of summary information, the so-called event tag. As an example of such efforts, the performance for one particular benchmark has improved from 35Hz to 2000Hz through careful optimization of the application code. Independent of this improvement, the aggregate bandwidth of the computing infrastructure for such physics analysis activities has increased, through the availability of more database servers and file systems, by approximately a factor of 25 during FY99. Further improvements are being planned for FY2000. Currently such infrastructure improvements have been aimed towards the aggregate throughput, and any single job is bandwidth limited. Understanding the relationship between this improvement and the availability of multi-dimensional indexing, and the investigation of parallel iteration techniques are proposed for future development.

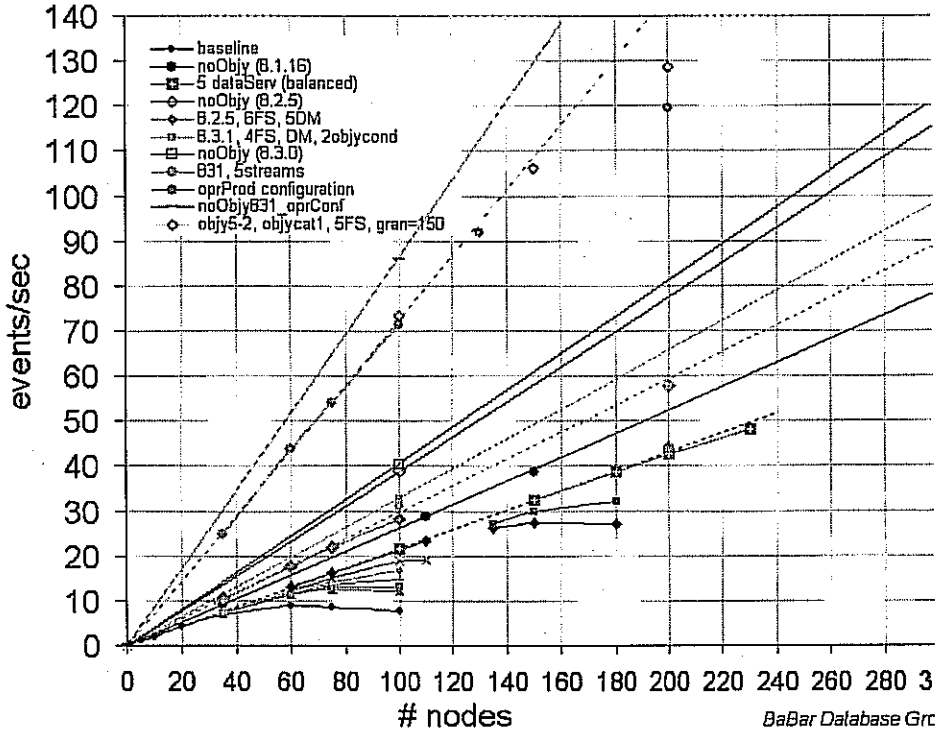

Figure 4. Plot of performance for reconstructing and storing high energy physics experiment data, measured as a rate in events/sec, achieved as a function of the number of client processing nodes and both software and hardware configuration improvements.

Publications

D. Quarrie, "First Experience with the BaBar Database," proceedings of Objectivity Worldview Conference (May 1999).

D. Quarrie, et al., "Operational Experience with the BaBar Database," submitted to *Computing in High Energy Physics* (February 2000).

J. Becla, et al., "Improving Performance of Object Oriented Databases, BaBar Case Studies," submitted to *Computing in High Energy Physics* (February 2000).

S. Patton, et al., "Schema Migration For BaBar Objectivity Federations," submitted to *Computing in High Energy Physics* (February 2000).

E. Leonardi, et al., "Distributing Data around the BaBar Collaboration's Objectivity Federations," submitted to *Computing in High Energy Physics* (February 2000).

Research on High-Luminosity Tracking Systems

Principal Investigators: James Siegrist

Project No.: 99039

Project Description

Charged particle tracking in high-luminosity experiments such as those planned for the Large Hadron Collider (LHC) depends heavily on measurements using pixel and silicon strip detector devices. The LHC groups, including the Berkeley Lab ATLAS group, have been developing such detectors for use at high-rate hadron colliders, but many of the components still need research and development to provide a tracker designed to run for many years at a luminosity of $10^{34}cm^{-2}sec^{-1}$. Silicon trackers, even at the LHC, cannot survive at full machine design luminosity at the innermost radii.

This project is to concentrate on some outstanding technical questions relating to silicon tracker development, both in the pixel system and the silicon strip systems. Not yet resolved, under the constraints noted above, is the comparison of measured signal development to simulated signal development in undamaged and radiation-damaged devices. Work on this project is to measure actual devices and compare the results with simulations. Various test devices excited by lasers, sources, and/or cosmic rays will be used in the measurements. Devices will be characterized, analyzed, and modeled after irradiation at the Berkeley Lab 88-Inch Cyclotron and with cobalt sources.

Accomplishments

Typical electrode structures in semiconductor vertex detectors have a pitch of 50 to 100 μm. To measure the signal pulse shape vs. the position of incidence relative to the electrode, the laser beam must be collimated to a spot diameter <10 μm, with a divergence sufficiently small to preserve this collimation throughout the thickness of the detector—typically 300 μm in readily available devices.

First, the spot size and the opening angle of the laser beam at the output of the optical fiber were measured to be 100 μm and 0.2 radians, somewhat larger than the manufacturer's estimates. We first investigated collimation using a pair of slits to provide a small spot size and divergence, but calculations indicated that fringing could be a problem. This was verified experimentally by scanning the beam across a strip detector. We then investigated a combination of collimation and focussing, where the collimation was performed at a rather large spot size to reduce the relative effect of fringing and a lens system focussed the beam. We compared a two-lens system with an intermediate iris collimator and a single lens preceded by the collimator. The latter was adopted and produced a spot size at the waist of 5 μm, which increased by 40% at ± 150 μm, i.e. the beam was smaller than 7 μm throughout the 300 μm thickness of the detector. Clearly, the use of a collimator to reduce the emittance also reduces the intensity, and measurements of the current pulse required averaging over many pulses to obtain an adequate signal-to-noise ratio.

The measurement system is shown in Figure 5. The optical fiber from the laser is coupled to the optical system, whose distance from the detector can be adjusted by a manual micrometer to 1 μm accuracy. This allows us to position the waist (i.e. focal plane) in the middle of the sensitive thickness and also to measure the divergence. A silicon strip detector with a 50 μm pitch is used as a sensor, mounted on a stage that can be positioned over a range of 25 mm to 1 μm accuracy. Since the 10 μm wide metal contacts on each strip are opaque to the laser beam, scanning the beam across the electrode edge allows the beam profile to be determined.

To determine the intensity distribution of the beam, we use charge-integrating preamps, feeding an amplifier and pulse shaper with 1 ms shaping time. For the measurement of the pulse shape, a system rise time < 1 ns is needed, so we use fast, low-noise preamps with a 50 ohm input impedance and 350 ps rise time. To maintain a small input time constant, the detector capacitance must be small, so we use short-strip detectors with 6 mm strip length fabricated some years ago in the Microsystems Lab for SSC detector R&D. This yields an input time constant of 100 ps, i.e. about 200 ps rise time. The strip detector is mounted on a detector board especially designed to provide low-inductance signal return paths and controlled impedance to the

preamp input. Signals from up to seven adjacent strips are brought out to measure the signal induced on the neighbor strips. The preamp signal is amplified in a subsequent wide band amplifier and viewed on an oscilloscope. The overall system rise time is 600 ps. Due to the large bandwidth, the signal-to-noise ratio is about unity, so about 100 pulses are averaged to extract the pulse shape. Currently, the measurement of the time structure is limited by the laser pulse width of 5 ns. Although this is adequate to determine gross features of the detector pulse shape, greater sensitivity is required to map the field profile. Modifications to the laser driver can reduce the pulse width to 1 ns, but at the expense of intensity. Some further optimization of the focussing optics may make up for this penalty, but ultimately a higher power laser coupled to a single-mode fiber will be necessary.

In summary, using existing equipment and inexpensive off-the-shelf optical and mechanical positioning components, a test system was assembled that allows measurement of the time structure of detector pulses. Initial results on strip detectors are in agreement with the simulations, but additional refinements to the measurement system and more detailed measurements are needed to test the code and proceed on the analysis of heavily radiation-damaged detectors.

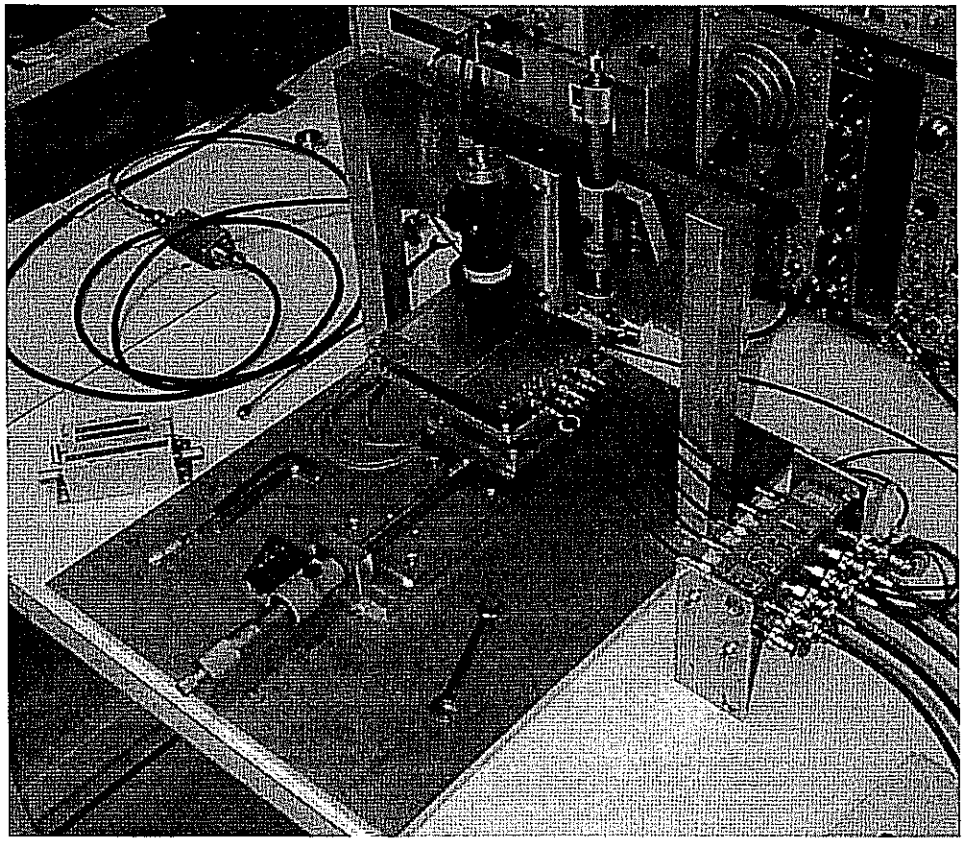

Figure 5. The detector mounting stage with micrometers for horizontal positioning of the detector and vertical adjustment of the optics. The fast (350 ps rise time) preamps are at the right.

Extraction of Fundamental Parameters from the Cosmic Microwave Background Data

Principal Investigators: George Smoot

Project No.: 97038

Project Description

The cosmic microwave background (CMB) is the universe's wallpaper. It is what is left over when all the radiation from astronomical objects is subtracted from what we observe. Theoretically, we understand it as the faintest echo of the Big Bang itself.

As the universe expands, the average energy of the matter and radiation drops. Today, it is three degrees above absolute zero, but 15 billion years ago—give or take five billion years—we think there was an arbitrarily hot Big Bang, when space and time came into being. Some 300,000 years later, the universe had cooled enough for the protons and electrons to stop bouncing off each other and electromagnetically couple to form neutral hydrogen atoms. In the absence of free electrons to scatter off, the photons simply continued in the direction they were last moving in until we detect them today. This collection of photons is what we call the Cosmic (because it fills the universe so completely and uniformly) Microwave (because of the frequency at which its spectrum peaks today) Background (because it originated further away from us than all other radiation we receive).

Despite its stunning uniformity—isotropic to a few parts in a million—it is the tiny perturbations in the CMB that contain its unprecedented view of the early universe. Already present before gravitationally bound objects had formed, these temperature differences are an imprint of the primordial density fluctuations that seeded everything from planets to galaxy clusters and superclusters. As such, they promise to be an exceptionally powerful discriminant between competing cosmological models.

Subtracting the foregrounds from what we measure at a particular frequency is a difficult job, often requiring us to extrapolate from a source's intensity at its characteristic frequency to the microwave frequencies at which the CMB is measured. The observational equipment itself—mirror, detectors, and electronics—also introduces significant noise into our measurements, even when cooled to a few degrees Kelvin. However, scanning each point in the sky many times allows us to distinguish between the signal and the noise components of the observations. Given a map of the sky temperature, and knowing something about the statistical properties of noise that went into it, we can now calculate the most likely underlying signal, and by how much it is the most likely.

Computing this maximum likelihood is now the limiting step in extracting cosmology from CMB observations. Recent successful flights of the MAXIMA and BOOMERANG balloon-borne detectors have produced the largest CMB data sets to date. Both experiments flew twice. They will be followed by the MAP and Planck satellites in 2001 and 2007. Over that time, the maps produced will grow from tens of thousands to millions of points, and, with the algorithms we currently use, the time needed to analyze them will correspondingly increase from hours to millions of years.

Accomplishments

Our work has continued to focus on the development and application of codes to obtain CMB angular power spectra from time-ordered observations of the sky temperature. Given the computational challenges inherent to this task, the majority of this work has continued to involve implementations for parallel architectures.

This year saw the release of MADCAP—the Microwave Anisotropy Dataset Computational Analysis Package—into the public domain. After a long period of testing the code and making it sufficiently robust for general release, a beta-version was made available in the early summer. Since then MADCAP has been taken up by a number of experiments. In addition to the original users, MAXIMA and BOOMERANG, new users include TopHat, BEAST, BOOST and Archeops. The MADCAP code has been ported to a number of locations in the United States, Canada, and Europe, and to a wide range of parallel architectures. Based on feedback from users and personal experience, MADCAP version 1.1 will be released early in 2000.

Our effort is guided by the notion that algorithmic development should be based on the problems encountered in handling actual data. We have therefore continued to apply MADCAP to the analysis of the MAXIMA and BOOMERANG data sets, with first results from each experiment being released in the winter of '99/'00. The BOOMERANG North American test flight preliminary results were posted to the preprint server and were featured in a front-page New York Times article the last week in November. The article included a preliminary map from MAXIMA [made using MADCAP on the National Energy Research Scientific Computing (NERSC) computers].

The MAXIMA-1 data are under intensive analysis. As soon as the preliminary results are released (and a Ph.D. thesis completed), attention will turn to the MAXIMA-2 flight data. The BOOMERANG Long Duration Balloon flight data is far along in its analysis and like MAXIMA-1 early results should become available early in 2000.

The primary focus has been to continue to develop MADCAP for ever larger and more complex data sets; we are now routinely handling data sets of up to 50,000,000 observations, resulting in maps with over 30,000 pixels.

Future work will focus on the next generation of algorithms, which will be necessary once the number of pixels exceeds 100,000. At that point, the memory and CPU-time scaling properties of MADCAP's direct approach will make it impractical as an analysis tool. However, it will continue to be useful as a tool to check the validity of the new algorithms we develop.

Large Astrophysical Data Sets

Principal Investigators: George Smoot

Project No.: 99040

Project Description

The purpose of this project is to develop an approach to handle the very large, complex astrophysical data sets now being generated by satellites and earth-based detectors. To accomplish this, we must provide a means for filtering these large data sets for events relevant to establishing the underlying astrophysical science and distributing these data sets to larger collaborations. This involves identifying extremely rare and unusual events and determining correlations among parameters in large databases, and coordinating collections of databases. These goals involve issues that are on the forefront of computer science and driving new statistical approaches to data handling.

More specifically, we chose an interesting and exciting astrophysical problem—the study of the supermassive black holes powering and disrupting active galactic nuclei which makes them visible across the entire universe—which has an appropriate and relevant data set available. We intend to use data generated in the array of sensors that comprise the AMANDA neutrino telescope operating at the South Pole. The detector transmits data now at a rate of ~1 Terabyte per year and will increase substantially during its further years of operation. This data set and collaboration serve as a pilot project to test: (a) the transmission of large amounts of data from a remote site to the mass storage at the National Energy Research Supercomputing Center (NERSC), (b) handling and processing of this data, and (c) the distribution of the filtered data sets to the collaboration members and eventually a wider audience.

Accomplishments

We have focused on organizing and processing several large astrophysical data sets collected by the AMANDA neutrino telescope, located at the South Pole. To date, the NERSC machines have filtered the 1997 data twice and we are in the process of filtering the 1998 data, which will be quickly followed by the filtering of the 1999 data. This effort required the development and testing of filter and reconstruction codes. In addition, we are analyzing the efficiency of the code and building tools to facilitate the organization and distribution of the data.

The 1997 data (0.9 Tbytes) was first processed in 1998 on the CRAY T3E using 1600 hours. After the detector was further calibrated, the data was refiltered in 1999 on 24 nodes of the PC Cluster Project belonging to the Future Technologies Group. This second processing included a full reconstruction of particle trajectories, and took 1100 CPU days. This data has been used by the collaboration to produce 10 papers presented at a Salt Lake City Conference in August 1999.

The 1998 data (1.8 Tbytes) are currently 10% processed on the Parallel Distributed Systems Facility (PDSF) cluster. The cumulative processing time is estimated to be 2900 CPU days. Increased resources are needed to sift through the larger data sample, as well as to split more complicated data streams. The new filter includes streams for time coincidences with the South Pole Air Shower Experiment (SPASE) array triggers, Gamma-Ray Bursts (GRB) triggers, weakly-interacting massive particle (WIMP)s, and cascades in addition to the particle trajectories filtered previously.

The 1999 data (~1 Tbyte) was delivered from the South Pole in November 1999. It will be transferred to HPSS and processed as soon as the 1998 data processing has been completed. A filter scheme similar to that currently being used on the 1998 data will be used to make multipurpose samples.

In addition to processing data, we have been working to organize the data. Web pages document the filters, and data samples stored in HPSS. A database of files has been created to facilitate data access, document file integrity, and keep track of detector live-time.

A web-based file distribution server has been under construction since early summer. With this facility, a user can download small filtered streams directly from HPSS or from our local cache disk. Any particular file from the raw or processed data is available. Limits have been established to ensure that users do not transfer more than a few Gbytes of data without contacting us for permission. In the future, we plan to include detector live-time calculations and filters in this product, so that while the data is streaming out to remote institutions, it can also be tailored to their particular requirements while providing them with the total detector live-time for their specific data sample.

Finally, we have been working with the collaboration on the reconstruction and simulation codes. These are fairly complex, and trade-offs between efficiency and multiple-data representations have been made. We are analyzing the code efficiency to improve future filter speed, and the reliability of the algorithms. We are investigating promising high-energy cascades, and rare-events mining.

Publications

R. Bay, et al., "AMANDA Search for High-Energy Neutrinos Accompanying Gamma Ray Bursts," presented at 1999 International Cosmic Ray Conference, Salt Lake City, Utah (August 1999).

A. Karle, et al., "Observation of Atmospheric Neutrino Events with AMANDA," presented at 1999 International Cosmic Ray Conference, Salt Lake City, Utah (August 1999).

J.H. Kim, et al., "A Search for Point Sources of High Energy Neutrinos with the AMANDA Neutrino Telescope," presented at 1999 International Cosmic Ray Conference, Salt Lake City, Utah (August 1999).

Computational Modeling of Turbulent Combustion Dynamics

Principal Investigators: John Bell, Nancy Brown, and Phillip Colella

Project No.: 99008

Project Description

The overall goal of this project is to develop a high fidelity numerical simulation capability for turbulent combustion processes such as those arising in natural gas burners, and spark-ignited and compression-ignited engines. The physical processes involved in engineering combustion are diverse. Our goal is to focus on the interaction of turbulent eddies in a reactive environment and to evaluate different subgrid models for representing this interaction.

Research aimed at understanding transient effects in turbulent flows has led investigators to study the interaction of a single vortical structure with a premixed flame. These flows offer advantages of being more repeatable and more amenable to analysis and experimental diagnostics than fully developed turbulent flow. Experimental studies typically consider either a planar vortex pair or an axisymmetric toroidal vortex.

Accomplishments

We conducted a DNS study of a vortex-flame interaction with premixed N_2-diluted methane flames having equivalence ratios in the range ϕ = 0.76 to1.28. The vortex was chosen to match that generated in an experiment by Nguyen and Paul. The numerical simulation used a parallel, adaptive low Mach number combustion algorithm developed by Day and Bell. All of the computations used chemistry, transport, and thermodynamic databases specified in GRI-Mech 1.2, a state-of-the-art chemical mechanism for natural gas combustion.

The computational study approximated the experimental conditions with a flat premixed flame oriented normal to the inlet flow, on which was superimposed the velocity field of a counter-rotating vortex pair. The vortex pair propagated upward with a self-induced velocity of 110 cm/s, the same as reported for the vortex pair in the experiment. Only the left vortex was numerically evolved, using a reflective boundary condition on the right boundary which became the line midway between the vortex pair. For the simulations, we chose five inlet stoichiometries: ϕ = 0.76, 1.01, 1.10, 1.19, and 1.28.

The vortex propagated upward and passed through the flame. Analysis showed that the vortex not only stretched and strained the flame, it also scoured material from the cold region in front of the flame and replenished the flow with inlet gases at early time. This scouring effect produced the dramatic decline in CH observed experimentally by Nguyen and Paul. The interactions showed a strong dependence of CH behavior on equivalence ratio. Additionally, the model predicted a measurable increase in C_2H_2 as a result of the vortex, and a marked increase in the low-temperature chemistry activity. The model failed to reproduce the enhancement of OH observed by Nguyen and Paul. One possibility is that some unknown chemistry or imprecise knowledge of thermochemistry in the model might lead to the discrepancy.

The use of an adaptive grid allows finer resolution and smaller time-steps where required, and permits us to count simulation time in days rather than months, which would be the case for traditional, static-grid DNS.

The dominant cost in combustion modeling with high fidelity chemical mechanisms is the time required to solve the ordinary differential equations associated with chemical kinetics. A class of methods to reduce the costs is to develop surrogates or models for the evolution of the chemical kinetics. These methods view the time evolution of chemical kinetics as a mapping from one chemical composition onto another. The methods then try to construct an approximation to that mapping that is inexpensive to evaluate. One such method, Piecewise Reusable Implementation of Solution Mapping (PRISM), was ported and interfaced with the adaptive grid computational fluid dynamics (CFD) code.

Because of the methodology used in PRISM, in addition to providing faster computing, it was realized that PRISM could serve as a tool to investigate the dimensional properties of the active portion of chemical composition space. In theory, the dimensionality of active chemical composition space at an instant of time cannot be more than the dimensionality of the physical space, which it represents. Adding time evolution to this can increase the dimensionality by at most one. In practice the issues are more complex. If the surface is sufficiently convoluted, it may appear to have a higher dimension than the theoretical bound when viewed with finite resolution. On the other extreme, it could be confined and localized sufficiently to appear to have lower dimensionality. PRISM's method of dividing chemical composition space into hypercubes makes it an ideal tool for looking at this space with varying degrees of resolution, thus allowing for the determination of the dimensionality.

We investigated the dimensionality for the two-dimensional case of a premixed hydrogen flame propagating through an unburned turbulent mixture. The turbulent intensity ranged from a weak case with little effect on the flame to strong turbulence-tearing pockets of burning fluid from the main flame.

The fractional dimensionality was determined as a function of turbulent intensity. In all the cases, it was found to be lower than the theoretical asymptote of 3 (which would occur at infinite resolution). We observed that fractional dimensionality was least in the weak turbulence case, highest for the intermediate case, and then decreased slightly again for the strong turbulence case.

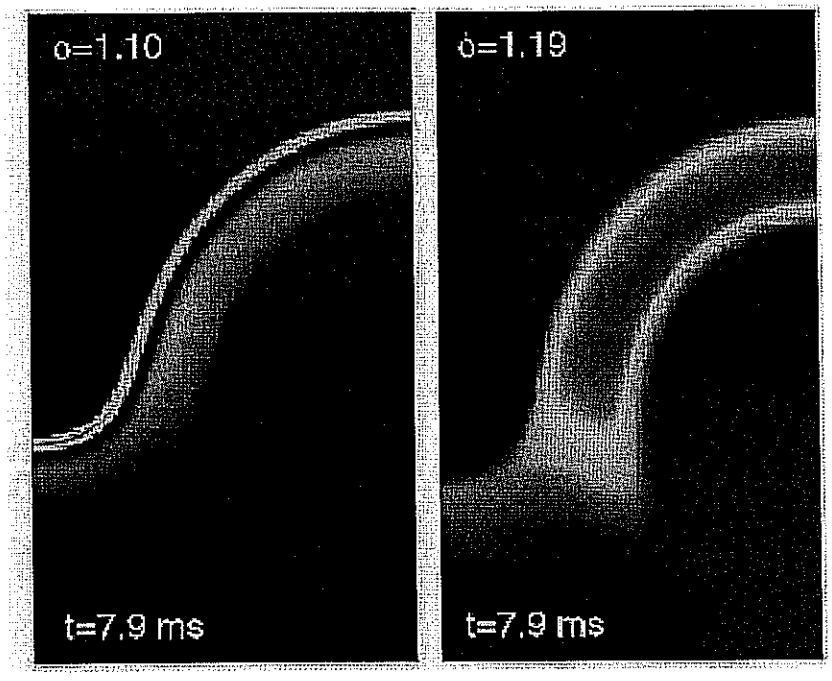

Figure 1. H_2 diffusion flux at the vortex-flame interface for stoichiometries ϕ= 1.10 and 1.19.

Publications

J.B. Bell, N.J. Brown, M.S. Day, M.J. Frenklach, F. Grcar, and S.R. Tonse, "The Effect of Stoichiometry on Vortex Flame Interactions," submitted to the 28th Symposium (Intl.) of The Combustion Institute, December 16, 1999 (in review).

J.B. Bell, N.J. Brown, M.S. Day, M. Frenklach, J.F. Grcar, R.M. Propp, and S.R. Tonse, "Scaling and Efficiency of PRISM in Adaptive Simulations of Turbulent Premixed Flames," submitted to the 28th Symposium (Intl.) of The Combustion Institute, December 16, 1999 (in review).

Research and Development for Kilometer-Scale Subsurface Neutrino Astrophysical Observatory

Principal Investigators: William Chinowsky, John Jacobsen, Douglas Lowder, Jozsef Ludvig, David Nygren, Gerald Przybylski, George Smoot, and Robert Stokstad

Project No.: 98029

Project Description

High-energy neutrino astronomy may allow earth-based instruments to detect and study some of the most energetic, violent, and bizarre processes in the universe.

The goal of this effort is to develop robust instrumentation for a kilometer (km)-scale high-energy neutrino detector, to be sited deep within the Antarctic icecap. Neutrino-induced reactions lead to extremely energetic muons and electrons, whose Cherenkov radiation may be detected at considerable distances from the origin. Muon trajectories retain most of the directional information of the incident neutrino, permitting a new form of astronomy if sufficient volume can be instrumented.

In FY99, LDRD supported electronic engineering activities for a specific Berkeley Lab system concept aimed at the realization of cost-effective, high-quality information capture, using modern digital system concepts and an innovative application-specific integrated circuit (ASIC), also developed at Berkeley Lab. Another major goal of this effort is to obtain the capability of completely remote set-up, control, calibration, operation, and monitoring, in order to realize a km-scale detector with limited personnel.

Accomplishments

During FY99, the original proposal components of conceptual design, detailed engineering, prototyping, software development, debugging, and testing were all successfully completed. The goals of the revised LDRD plan were entirely met, and the successful outcome of the LDRD project immediately led to its application as part of a Digital Optical Modules (DOM) activity in Antarctica. Consequently, this report will describe the overall specifications of the DOM activity, which applied the specific technical accomplishments of the LDRD project.

A single two-km-long twisted-pair connects each DOM to the surface. This ordinary twisted pair carries bi-directional communications and data, power, and timing signals for the establishment of a universal time-base with 1 nanosecond root-mean-square (rms) accuracy. A particularly successful part of this engineering effort was the development of ns timing accuracy and resolution, with such a modest communications link. A significant advantage of the DOM system concept is the total absence of fiber-optic links, which have not been consistently reliable in the deep ice environment, and which would add more than $10M to the km-scale detector system cost.

Inside each DOM is a complex electronic system. Functionality is controlled by a 32-bit low-power CPU, designed for hand-held applications, and a field-programmable Gate Array (FPGA). Signal capture is achieved with the Berkeley Lab ASIC "Analog Transient Waveform Digitizer" (ATWD). The ATWD can capture photomultiplier signals at sampling speeds up to 2 GHz (or as low as 0.2 GHz) and produce 10-bit digitized results. Simultaneous multichannel sampling permit dual- or triple-range signal capture to provide exceptional dynamic range for such rapid sampling. The excellent signal capture offered by the ATWD will provide data of superior quality for all classes of neutrino-induced events, the reconstruction of which is complicated by optical scattering of Cherenkov radiation in the deep ice.

Each DOM can store events for several minutes, facilitating relaxed triggering and event-building. In addition, each DOM communicates directly with its nearest neighbor, permitting the real-time implementation of a local coincidence.

Funds for the construction of a "Digital Test String" of 42 DOMs based on this engineering effort were separately obtained from the National Science Foundation (NSF) (G. Smoot–P.I.). In mid-January, 2000, as part of the Antarctic Muon and Neutrino Detector (AMANDA) collaboration, and in anticipation of an effort to reach the km-scale (IceCube proposal to NSF), the Digital Test String was deployed smoothly at the South Pole, to an operating depth of 2000 meters. Initial tests of the deployed string show that all but one DOM are responding properly. This outcome is a truly

spectacular achievement for such a short design-test-fabrication cycle.

The success of this effort places the DOM system concept, and Berkeley Lab, in a leading position to provide the technical and engineering basis for IceCube. This represents both an excellent opportunity to support the United States university community in an area which requires greater engineering strength than otherwise possible, and also to open a new frontier in science.

Synchrotron Radiation Research for Molecular Environmental Science

Principal Investigators: David Shuh, Neville Smith, Tetsu Tokunaga, Geraldine Lamble, Satish Myneni, and Glenn Waychunas

Project No.: 98030

Project Description

Molecular environmental science (MES) has emerged in the last few years in response to the need for basic research to underpin long-term solutions to environmental problems. The objectives of MES research are to provide information on the chemical and physical forms (speciation), spatial distribution, and reactivity of contaminants in natural materials and man-made waste forms; and to develop a fundamental understanding of the molecular-scale environmental processes, both chemical and biological, that affect the stability, transformations, mobility, and toxicity of contaminant species. Chemical reactions at the surface of natural solids play dominant roles in many environmental processes. Consequently, molecular-level studies of contaminant reactions at interfaces are an important focus of MES research. The vacuum ultraviolet (VUV)/soft x-ray synchrotron radiation (SR) region has traditionally been one of the domains of surface science research. However, experimental MES studies in this spectral region are complicated by the need for *in situ* studies with aqueous solutions, spatial and spectral resolution, and the ability to characterize the speciation of contaminants at very low concentrations. The combination of new technologies provided by third-generation, high-brightness SR sources, improved vacuum techniques, and improved detectors provide the opportunity for new applications of traditional VUV/soft x-ray surface science methods to MES issues.

Fundamental studies of several specific issues in MES have been initiated by techniques unique to the VUV/soft x-ray region. Well-developed techniques in the VUV/soft x-ray energy region have distinct advantages in surface sensitivity, spectral resolution, and spatial resolution when compared to techniques used for MES research in the x-ray region. The focus will be on fundamental spectroscopy/microscopy investigations of contaminant speciation in "wet" and model environmental systems at mineral interfaces, with organic materials, with microorganisms, and with solid state materials. This will include several key species containing C, N, Cr, Tc, Se, Mn, and selected actinides to provide molecular level information to explain macroscopic behavior. This is a coordinated environmental research effort to utilize the K-edges of the light elements, L-and K-edges of the transition metals, M-edges of the actinides, and low-lying core levels of other elements to obtain comprehensive chemical information. Many of these core level thresholds are exclusive to the VUV/soft x-ray spectral region and are optimal for investigation at the Advanced Light Source (ALS). The experimental studies will be complemented by a theoretical component extending existing spectral modeling into the VUV/soft x-ray region and will provide valuable data for computational efforts. Additionally, this research effort will develop specialized VUV/soft x-ray SR experimental instrumentation necessary for MES research. This research program will demonstrate the utility of VUV/soft x-ray SR methodologies for the investigation of a range of MES issues.

The MES research activities are a collaborative and multidisciplinary approach to utilizing VUV/soft x-ray SR techniques for MES research, involving scientists of the ALS, Chemical Sciences, and Earth Sciences Divisions, and external participants. The initial studies will make use of existing endstations, beamlines, and available beamtime at the ALS, while specialized instrumentation needed for future MES studies is developed.

Accomplishments

Correlation of 2p and 1s Absorption Edge Structure with Calcium Structural Sites

Ca is an important biochemical and environmental agent with rich and complex crystal chemistry. Both the 2p (L-edge) and 1s (K-edge) x-ray absorption near edge structure (XANES) spectra are amenable to simulation, particularly in the case of the 2p edge, due to the empty 3d shell. Initial efforts utilized a suite of well-characterized Ca minerals and model compounds to collect high quality spectra on both edges at the ALS. Subsequently, FEFF 8.0 has been used to calculate the 1s XANES with a self-consistent multiple scattering approach, and TTMultiplets to calculate the 2p XANES full multiplet structures. Results so far indicate that the XANES calculations can be used to determine the crystal field parameters and first interatomic shell distances in unknown Ca materials, which should allow good determinations of site geometries. Figure 2 shows the polarization dependent XANES and extended x-ray absorption fine structure (EXAFS) obtained from apophyllite. Related work has also proceeded to collect analogous Ca data from aqueous solutions and from sorption complexes on mineral surfaces. These experiments will help in the development of "wet" spectroscopy techniques at lower x-ray energies at the ALS.

Study of Sorption Properties and Structure of Schwertmannite

Schwertmannite is an important natural Fe oxyhydroxide found in acid-mine-drainage environments. It contains a large amount of supposedly structural sulfate, and can sorb high quantities of toxic heavy metal ions. However, the proposed structure for the mineral is problematic in view of infrared spectra of the bound sulfate groups, the type of x-ray diffraction patterns observed, and simulations that show large disparities in the interatomic distances from known stable structures. Wide-angle diffuse x-ray scattering and EXAFS analysis were used to characterize the structure and molecular topology about the sulfate site. Results showed that schwertmannite appears to be a disordered akaganeite with inner-sphere adsorbed sulfate that interrupts the growth process during formation. Measurements were also made on selenate-substituted schwertmannite that indicated an identical structural state for selenate in the structure. Electron diffraction studies to determine the exact nature of the defect arrangements are underway with colleagues at Ohio State University.

Structure of the Hydrated (0001) Surface of α-Al_2O_3

A thorough investigation of the hydrated (0001) face of a single crystal of sapphire was performed using surface x-ray diffraction at the CARS PRT (Beamline 13ID Advanced Photon Source (APS), Argonne National Laboratory). Crystal truncation rods of type (10L), (20L), (11L) and (20L) were collected. Refinement of the surface structure was done for a variety of models, with excellent agreement found for a geometry having relaxed oxygens in the termination surface, and an additional ordered oxygen overlayer. We intend to continue such studies with other metal oxides including quartz, hematite, magnetite, and manganese oxides, all important reactants in environmental systems. A new sample cell with attached ultra high vacuum (UHV) preparation chamber is being developed for this purpose for work both at the ALS (surface spectroscopy) and at the APS (surface scattering). This work was performed in conjunction with the Brown group at Stanford University, and the CARS PRT at the APS.

Zn Sorption on and Co-precipitation with Ferrihydrite

Zn aqueous complexes over a range of solution conditions have been sorbed onto ferrihydrite, and also prepared in a co-precipitation mode. The investigative parameters were chosen to study the sorption range where deviation from Langmuir behavior begins to occur. Considerable EXAFS analysis has been done on a wide range of sample compositions. Additional recent work has included FEFF 8.0 simulations of 1s XANES spectra. Results show that there is a continuous change in the nature of the average sorption complex as a function of sorption coverage. At low sorption density the aqueous Zn, found in solution only as a 6-coordinated complex, sorbs as a tetrahedral complex coupled to 3-4 or more edge-sharing Fe $(O,OH)_6$ octahedral units. With increasing sorption density, the number of attached Fe octahedral units decreases, and Zn-O-Zn polymerization begins to occur. At highest sorption density a well-defined Zn hydroxide precipitate with octahedral Zn $(O,OH)_6$ units is observed. Simulation of the XANES structure was essential in unraveling these changes, which could not be done with EXAFS alone, or via x-ray scattering methods. This work was done in collaboration with the U.S. Geological Survey, Menlo Park, California.

Spatially-resolved MES Studies of Speciation by Micro X-ray Absorption Spectroscopy

The combination of x-ray fluorescence microprobe (XRFM) and micro x-ray absorption spectroscopy (μ-XAS) techniques has been fully operational on a single beamline during the past year at the ALS. These techniques are powerful methods for investigating a range of issues pertinent to earth and environmental science. There has been continued development of the μ-XAS technique and improvement of the μ-XAS beamline instrumentation in collaboration with A. MacDowell, H. Padmore, and R. Celestre of the ALS. Recent spatially-resolved studies have examined mixed metal hydroxide formation on surfaces, zinc uptake in plant roots, and the speciation of both arsenic and zinc in soil materials.

Metal Ion Speciation Studies Utilizing X-ray Emission Spectroscopy

X-ray emission spectroscopy (XES) is important for MES studies since it yields valuable speciation information and is applicable to "wet" or other intractable sample environments such as those accompanying radioactive materials. In combination with photoemission and absorption spectroscopies, XES is able to determine the speciation of metal ions in complex environmental systems. Thus, XES furnishes a basis from which to characterize chemical bonding to develop an improved understanding of environmental systems. This knowledge is of particular importance for actinide species in which the behavior of the 5*f* electrons dictates chemical behavior and contrasts to that of the 4*f* lanthanide species. The first XES results from the simple uranium oxide series clearly distinguishes the common uranium oxides from one another. The most recent studies have extended the initial work to examine additional uranium materials series such as the fluorides, carbonates, and several uranates. The resonant inelastic x-ray scattering studies comparing the oxide to the fluoride spectra, establishes that *f-f* transitions are observed as in the corresponding optical spectra of these materials. This leads to the capability of identifying oxidation states in complex non-stoichiometic materials. Furthermore, the features in the spectra are easily distinguished. The spectra may be calculated within a fairly simple but meaningful theoretical framework that has confirmed the interpretation of the results. This work has been done in collaboration with S. Butorin, J. Guo, and J. Nordgren.

X-ray Photoemission and Near Edge Absorption Studies of Rhenium(VII) Absorption onto Fe-bearing Materials

Technetium (^{99}Tc) is a radioactive byproduct of nuclear fission, and its concentration in nuclear waste materials may set the regulatory limit for disposal. The high solubility and mobility of TcO_4^-, which can be present in both nuclear waste streams and waste forms, needs to be addressed. A solution is to reduce Tc^{7+} to Tc^{4+}, which is much less soluble and mobile. One method is by adsorbing Tc^{7+} onto surfaces of reducing agents. While previous experiments demonstrated that Tc^{7+} ions were sorbed on and reduced by some materials, the products and the mechanism of sorption and reduction are not fully characterized or understood. Re has similar redox properties as Tc and can be treated as a surrogate for Tc in selected systems. Rhenium sorption samples were prepared by immersing powders of Fe metal, FeO, FeS, and FeS_2, respectively, in a 0.010 M Re(VII) solution. The reacted powders were extracted after the mixtures were centrifuged and the liquid phase decanted. The photoemission of Re 4d and 4f core levels, and Near Edge X-ray Absorption Fine Structure (NEXAFS) of Re N_{III} experiments were performed at the ALS. The results reveal that the amount of absorbed Re decreases from Fe metal, through FeO, FeS, to FeS_2; and that different species of Re are sorbed on surfaces of different Fe-bearing materials, with more oxidized species tending to dominate on the less sorbed surfaces. This result is intriguing because the sulfides were thought to be more efficient than the oxide for reducing Re(VII) because the sulfide ion has higher reducing potential than the ferrous ion. The puzzle was solved after the pH values of the residual solutions were measured. The residual solutions of the sulfides have pH values of 2 to 4, while those of the Fe metal and FeO have pH values of 8 to 10. Low pH values made the sulfides less reducing and ReO_4^- chemisorb more easily to the surfaces, whereas high pH made the Fe and FeO more reducing and ReO_4^- does not readily chemisorb on the surfaces. Thus, the photoemission and NEXAFS results, together with the pH measurements of the residual solutions, suggest that the sorption and reduction of Re on the surfaces of Fe-bearing materials are at least partially controlled by the final pH of the solution-particle mixture.

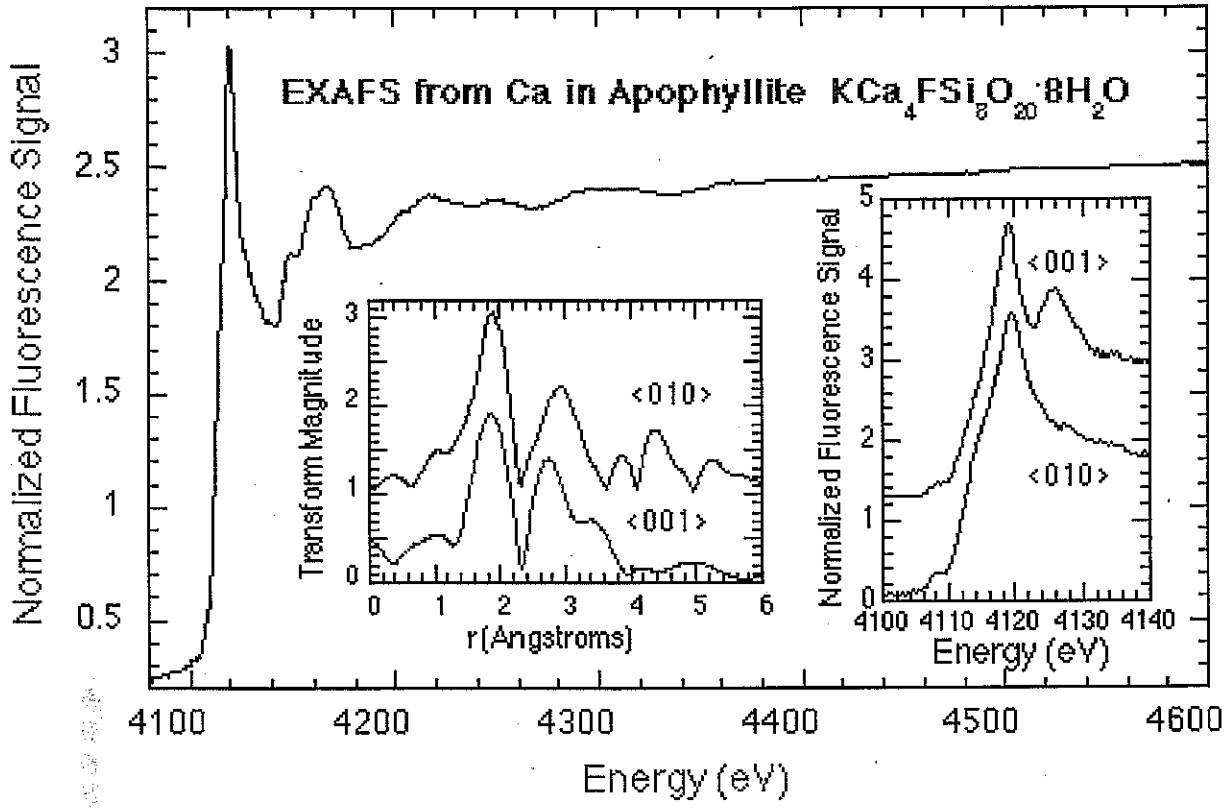

Figure 2. EXAFS scan from ALS Beamline 9.3.1 over Ca K edge for a single crystal of the mineral apophyllite. The electric vector is polarized in the crystallographic <010> direction. Right insert shows the polarization dependence of the near K-edge structure. Left insert shows the transformed EXAFS correlation functions for the two polarization directions. In the <001> orientation Ca-Ca and Ca-K correlations at distances from 4 to 5 Å (uncorrected for phase shifts) do not appear. Changes in contributions from Ca-Si correlations affect the second shell structure.

Publications

G.A. Waychunas, C.C. Fuller, and J.A. Davis, "EXAFS and XANES study of Zn Adsorption and Co-precipitation Geometry on Ferrihydrite: Detection of the Onset of Surface Precipitation," in preparation for *Geochimica et Cosmochimica Acta.*

G.A. Waychunas, S.C.B. Myneni, S.J. Traina, and J.M. Bigham, "EXAFS, XANES, and Simulation Study of AsO_4, SeO_4 and SO_4 Substituted Schwertmannites," in preparation for *Geochimica et Cosmochimica Acta.*

G.A. Waychunas, P. Liu, and D.K. Shuh, "Simulation of Ca^{2+} K- and L-edges via Multiple Scattering and Multiplet Calculations," in preparation for *Physical Review B.*

G.A. Waychunas, P. Liu, and D.K. Shuh, "Applications of Ca^{2+} X-ray Absorption Edge Structure for Molecular Speciation," in preparation for *Geochimica et Cosmochimica Acta.*

G.A. Waychunas, S.J. Traina, S.C.B. Myneni, and J.M. Bigham, "Wide Angle X-ray Scattering and Electron Diffraction Study of Substituted Schwertmannites," in preparation for *American Mineralogist.*

A. Moen, D. Nicholson, M. Ronning, G.M. Lamble, J.-F. Lee, and E. Hermann "X-ray Absorption Spectroscopic Study at the Cobalt K-edge on the Calcination and Reduction of the Microporous Cobalt Silicoaluminophosphate Catalyst CoSAPO-34, " *J. Chem. Soc., Faraday Trans.* 93, 4071 (1998).

A.M. Scheidegger, D.G. Strawn, G.M. Lamble and D.L. Sparks, "The Kinetics of Mixed Ni-Al Hydroxide Formation on Clay and Aluminum Oxide Minerals: A Time-resolved XAFS Study," *Geochimica et Cosmochimica Acta* **62**, 2233 (1998).

S.A. McHugo, A.C. Thompson, G.M. Lamble, A.A. MacDowell, R. Celestre, H. Padmore, M. Imaizumi, M. Yamaguchi, I. Perichaud, S. Martinuzzi, M. Werner, M. Rinio, H.J. Moller, B. Sopori, H. Hieslmair, C. Flink, A. Istratov, and E.R. Weber, "Direct Correlation of Solar Cell Performance with Metal Impurity Distributions in Polycrystalline Silicon Using Synchrotron-based X-ray Analysis," *Mat. Res. Soc. Symp. Proc.* **524**, 297 (1998).

R.J. Reeder, G.M. Lamble, and P.A. Northrup, "XAFS Study of the Coordination and Local Relaxation Around Co^{2+}, Zn^{2+}, Pb^{2+} and Ba^{2+} Trace Elements in Calcite," *Amer. Mineral.* **84**, 1049 (1999).

A. Manceau, J.-L. Hazemann, and G.M. Lamble, "Speciation of Zn in a Smelter-impacted Soil," to be published in *J. Clay Mineral Soc.* (1999).

H.-Y.N. Holman, D.L. Perry, M.C. Martin, G.M. Lamble, W.R. McKinney, and J.C. Hunter-Cevera, "Real-time Characterization of Biogeochemical Reduction of Cr(VI) on Basalt Surfaces by SR-FTIR Imaging," accepted, *J. Geomicrobiology* (October 1999).

R.J. Reeder, G.M. Lamble, *et al.*, "The Chemistry of the Uranyl Anion in Calcite and Aragonite," accepted by *Environ. Sci. Technol.*

A. Manceau, B. Lanson, M. Schlegel, M. Musso, L Eybert-Bérard, J.-L. Hazemann, D. Chateigner, and G.M. Lamble, "Chemical Forms of Trace Metals in Soils by XAFS Spectroscopy. I. Quantitative Zn Speciation in Smelter-contaminated Soils," accepted, *The American Journal of Science*, (1999).

A.A. MacDowell, C-H. Chang G.M. Lamble, R.S. Celestre, J.R. Patel, and H.A. Padmore, "Progress Towards Sub-micron Hard X-ray Imaging Using Elliptically Bent Mirrors and its Applications," "SPIE, X-Ray Microfocusing: Applications and Techniques, ed. I. McNulty **3449**, 137 (1998).

T. Warwick, S. Anders, Z. Hussain, G.M. Lamble, G.F. Lorusso, A.A. MacDowell, M.C. Martin, S.A. McHugo, W. R. McKinney, and H.A. Padmore, "Imaging Spectroscopic Analysis at the Advanced Light Source," *Synchrotron Radiation News* **11**, 5 (1998).

S. M. Butorin, M. Magnuson, K. Ivanov, D. K. Shuh, T. Takahashi, S. Kunii, J.-H. Guo, and J. Nordgren, "Resonant Inelastic Soft X-ray Scattering at the 4d Edge of Ce-based Heavy-Fermion Materials," *J. Electron Spectros.* **101-103**, 783 (1999).

P. Liu, E.J. Moler, G.A. Waychunas, and D.K. Shuh, "X-ray Photoemission and Near-edge Absorption Studies of Rhenium(VII) Adsorption onto Fe-bearing Materials," manuscript in preparation.

S. Butorin, J.-H. Guo, D. K. Shuh, and J. A. Nordgren, "Resonant Inelastic Soft X-ray Scattering as a Probe of Ground-state J-mixing in Rare-earth Compounds," submitted to *Phys. Rev. Letts.*

P.J. Eng, T.P. Trainor, G.E. Brown, Jr., G.A. Waychunas, M. Newville, S.R. Sutton, and M. Rivers, "Structure of the Hydrated α-Al_2O_3(0001) Surface: Crystal Truncation Rod X-ray Diffraction Results," submitted to *Science*.

Acronyms and Abbreviations

AECR-U	advanced electron-cyclotron resonance
AFM	atomic force microscopy
AFRD	Accelerator and Fusion Research Division
ALS	Advanced Light Source
AMR	adaptive mesh refinement
APE	apurinic/apyrimidinic endonuclease
API	application programming interface
ARPES	angle resolved photoemission spectroscopy
ASIC	application-specific integrated circuit
ATWD	analog transient waveform digitizer
AVHRR	advanced very high-resolution radiometry
BaBar	B/B-bar (system of mesons produced at SLAC)
BGO	Bismuth-Germanate
BGS	Berkeley Gas-filled Separator
BIF	Biomedical Isotope Facility
BNCT	Boron Neutron Capture Therapy
CCD	charge-coupled device
CDF	Collider Detector at Fermi Laboratory
CDMS	charge detection mass spectrometry
CFD	computational fluid dynamics
CGU	convex global underestimator
CI2	Chymotrypsin Inhibitor 2
CMB	cosmic microwave background
CMP	chemical mechanical polishing
CMR	colossal magnetoresistance
CPU	central processing unit
CS	Computing Sciences
CSD	Chemical Sciences Division
CTS	cryo-thermochromatographic separator
cw	continuous wave
DER	dispersed electricity resources
DFT	density functional theory
DIMS	dual inlet mass spectrometry
DNA	deoxyribonucleic acid
DOE	Department of Energy
DOM	digital optical modules
DOS	density of states
DSB	double strand break
DSP	Diesel particle scatterometer or digital signal processor
ECL	electrochemiluminescence
ECR	electron cyclotron resonance
ED	Engineering Division
EDTA	ethylenediaminetetra acetic acid
EETD	Environmental Energy Technologies Division
EM	electron microscopy
EMSA	electrophoretic mobility shift assays
ENPOP	Energy Parameter Optimization
EPA	Environmental Protection Agency
ERG	Energy Renormalization Group
ESA	electron spin analyzer
ESD	Earth Sciences Division
ESP	effective system performance
ESR	electrons in response
EST	expressed sequence tag
EXAFS	extended x-ray absorption fine structure
FA	factor analysis
FAA	Federal Aviation Administration
FABP	fatty acid-binding protein
FACTS	flexible alternating current transmission
FC	full configuration
FEL	free-electron-laser
FOD	foreign object damage
FPGA	field-programmable gate array
FRET	fluorescence-resonance-energy transfer

FROG	frequency resolved optical gating
fs	femtosecond
GC-IRMS	gas chromatograph-isotope ratio monitoring mass spectrometer
GCM	general circulation model
GRB	Gamma-Ray Bursts
HDAC	hydrothermal diamond anvil cell
HENP	High Energy and Nuclear Physics
HEP	High Energy Physics
HEPAP	High Energy Physics Advisory Panel
HERS	high-energy-resolution spectrometer
HID	high-intensity discharge
HL	hepatic lipase
HPSS	high performance storage system
HTS	high-temperature superconducting
IBAD	ion-beam assisted deposition
IC	integrated circuit
IHF	integration host factor
IPCC	Intergovernmental Panel on Climate Change
IR	infrared
IRMPD	infrared multiphoton dissociation
ISOL	isotope separator on line
ITEX	ion-beam thin film texturing
IVR	vibrational energy
JGI	Joint Genome Institute
LBNL	Ernest Orlando Lawrence Berkeley National Laboratory
LCP	liquid crystalline polymers
LDRD	Laboratory Directed Research and Development
LHC	Large Hadron Collider
LiF	Laser induced Fluorescence
LP	lean premixed
LPL	lipoprotein lipase
Lrp	leucine-responsive regulatory protein
LSD	Life Sciences Division
LSI	latent semantic indexing
MAD	methodical accelerator design or multiwavelength anomalous diffraction
MBE	molecular beam epitaxy
MBP	maltose binding protein
MCD	magnetic circular dichroism
MCF	Macromolecular Crystallography Facility
MEMS	microelectromechanical structures
MES	molecular environmental science
MEXH	multi-energy x-ray holography
μ-XAFS	micro x-ray absorption fine structure
MSD	Materials Sciences Division
NASA	National Aeronautics and Space Administration
NCEP	National Center for Environmental Prediction
NCSA	National Center for Supercomputing Applications
NERSC	National Energy Research Scientific Computing Center
NEXAFS	near edge x-ray absorption fine structure
NIH	National Institutes of Health
NIST	National Institute of Standards and Technology
NMR	nuclear magnetic resonance
NSAC	Nuclear Science Advisory Committee
NSD	Nuclear Science Division
NSF	National Science Foundation
ODBMS	object-oriented database management system
PBD	Physical Biosciences Division
PBS	phosphor buffered saline
PCM	proximity correlation matrix
PCR	polymerase chain reaction
PD	Physics Division
PDSF	Parallel Distributed Systems Facility
PE	processor element
PI	Principal Investigator

PIC	particulate inorganic matter or particle in cell
PLD	pulsed laser deposition
PM	particulate matter
POC	particulate organic carbon
ppb	parts-per-billion
PV	photovoltaic
QED	quantum electrodynamics
QSPR	Quasiparticle Scattering Resonances
QW	quantum well
QWS	quantum well states
R&D	research and development
RCSM	regional climate system model
RCSMhp	high-performance regional climate system model
REMPI	Resonance Enhanced MultiPhoton Ionization
rf	radio frequency
RHEED	reflection high energy electron diffraction
RHIC	Relativistic Heavy Ion Collider
RIB	radioactive ion beam
RNA	ribonucleic acid
RTC	recoil product transfer chamber
S&T	Science and Technology
SAGE	serial analysis of gene expression
SAXS	small angle x-ray scattering
SC/IVR	semiclassical initial value representation
SLAC	Stanford Linear Accelerator Center
SMOKE	Surface Magneto-Optic Kerr Effect
SMP	symmetric multiprocessor
spFRET	single-pair FRET
SQUID	Superconducting QUantum Interference Device
SR	synchrotron radiation
SSC	Superconducting Super Collider
ss-DNA	single stranded DNA
SSRL	Stanford Synchrotron Radiation Laboratory
SST	sea surface temperature
STAR	Solenoidal Tracker at RHIC
STM	scanning tunneling microscope or microscopy
SVD	singular value decomposition
TBP	TATA Binding Protein (TBP)
TCR	transcription-coupled repair
TEY	total electron yield
TGF	transforming growth factor
UC	University of California
UV	ultraviolet
VUV	vacuum ultraviolet
WIMP	weakly-interacting massive particle
XAFS	x-ray absorption fine structure
XANES	x-ray absorption near-edge structure spectroscopy
XAS	x-ray absorption spectroscopy
XES	x-ray emission spectroscopy
XFH	x-ray fluorescence holography
XMCD	x-ray magnetic circular dichroism
XPS	x-ray photoelectron spectrum
XRFM	x-ray fluorescence microprobe
YBCO	YBa2Cu3O7
YSZ	yttria-stabilized zirconia